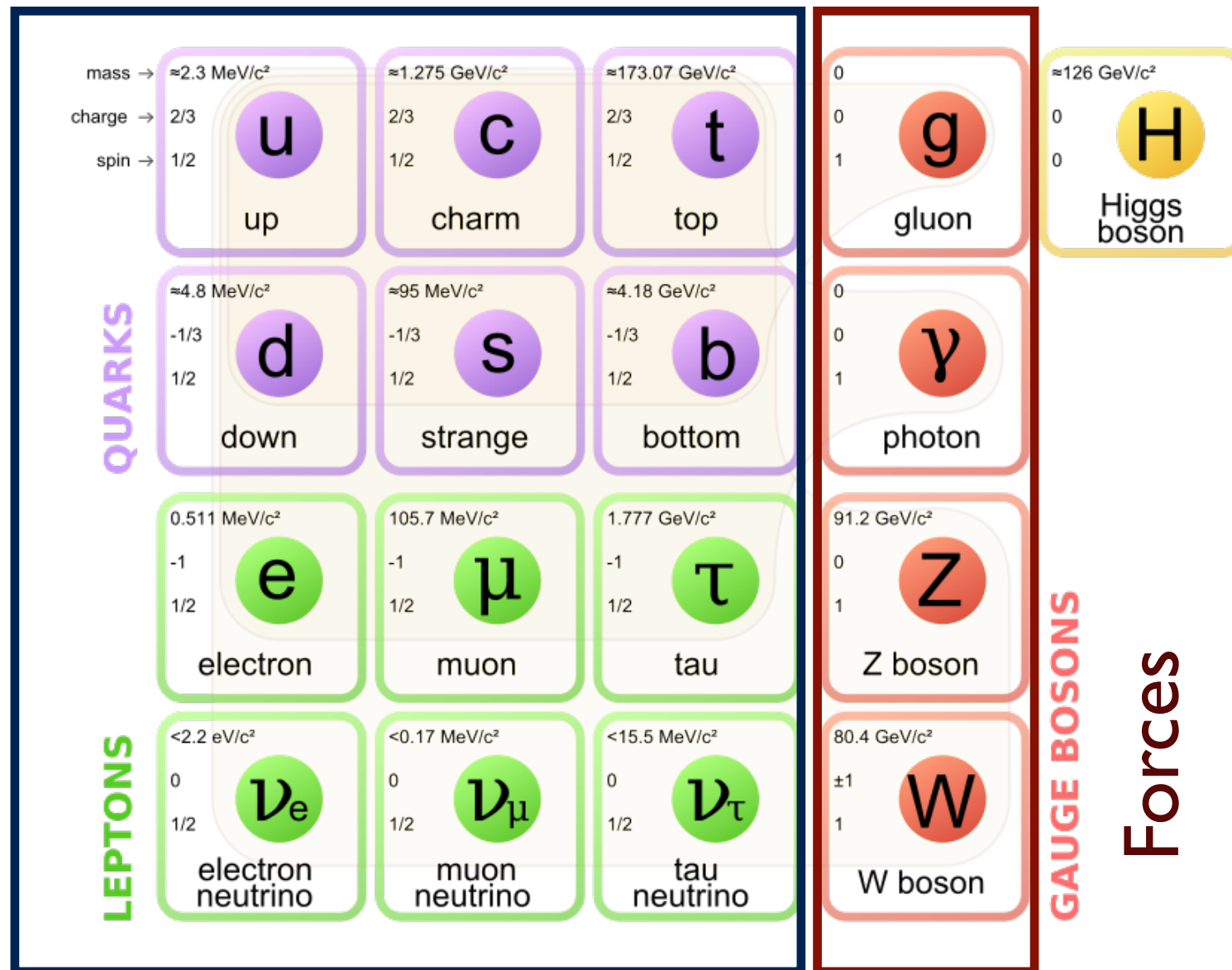


# Characterising experimentally the Higgs Boson and the Electroweak processes as a portal to new phenomena

Gaetano Αθανάσιος Barone  
*Brookhaven National Laboratory*

## Matter

Fermions  
 $s=1/2$



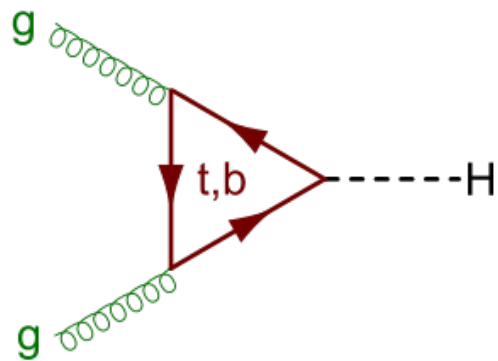
Forces

Fields

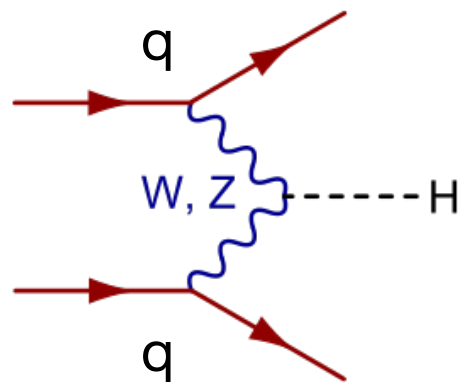
# Introduction

- Higgs boson ( $H$ ) main production in proton-proton collisions:

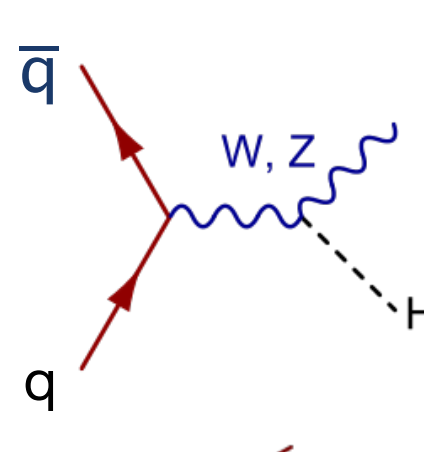
- ▶ Predominant production gluon-gluon fusion (87%) and VBF (6.8)
- ▶  $W, Z$  associated production (4%) and  $t\bar{t}H$  (<1%)



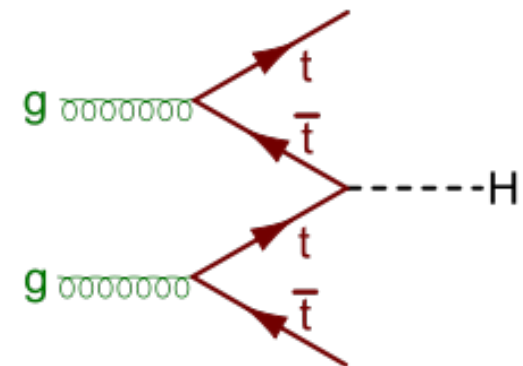
$ggF$



VBF

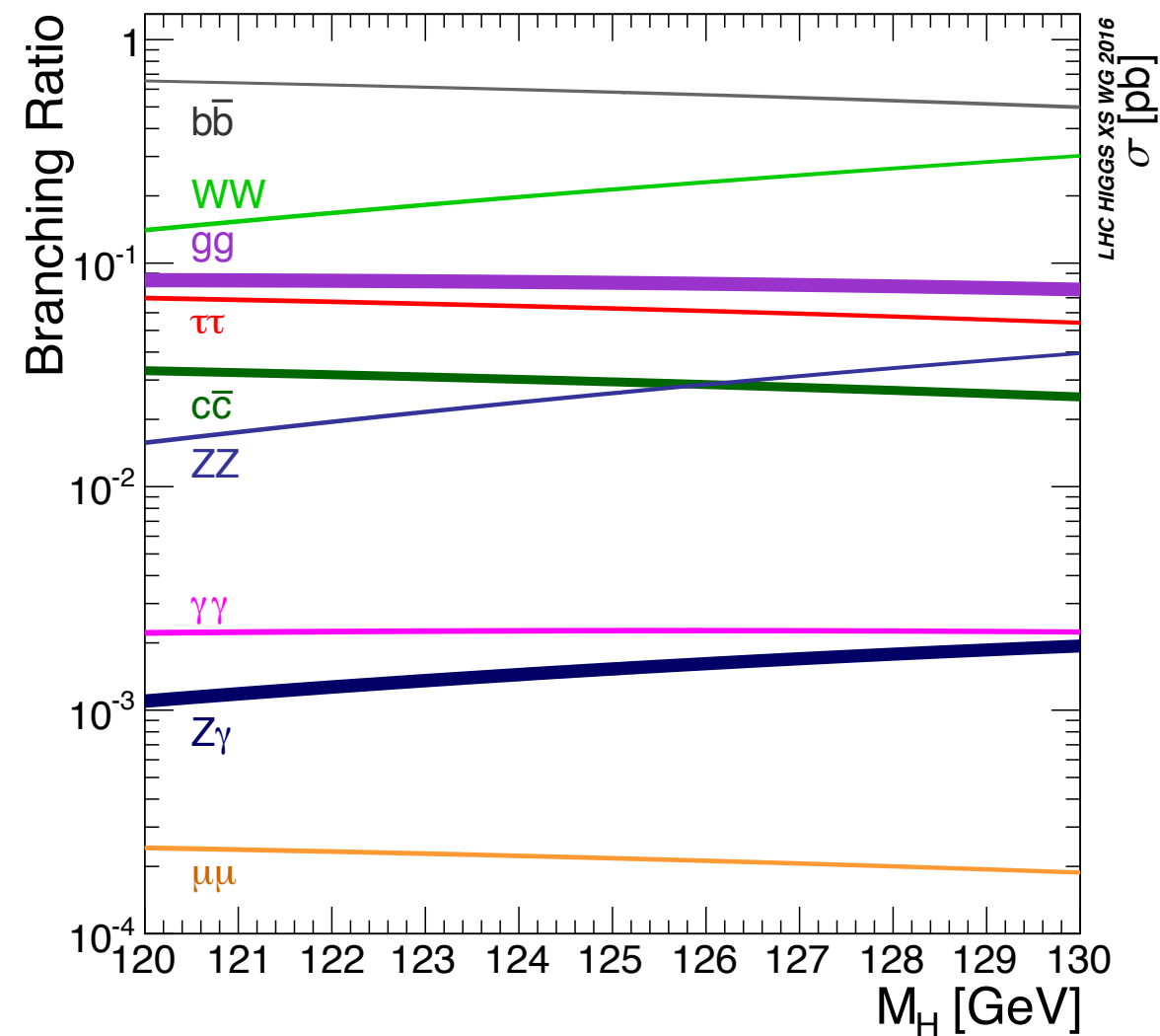


$WH, ZH$



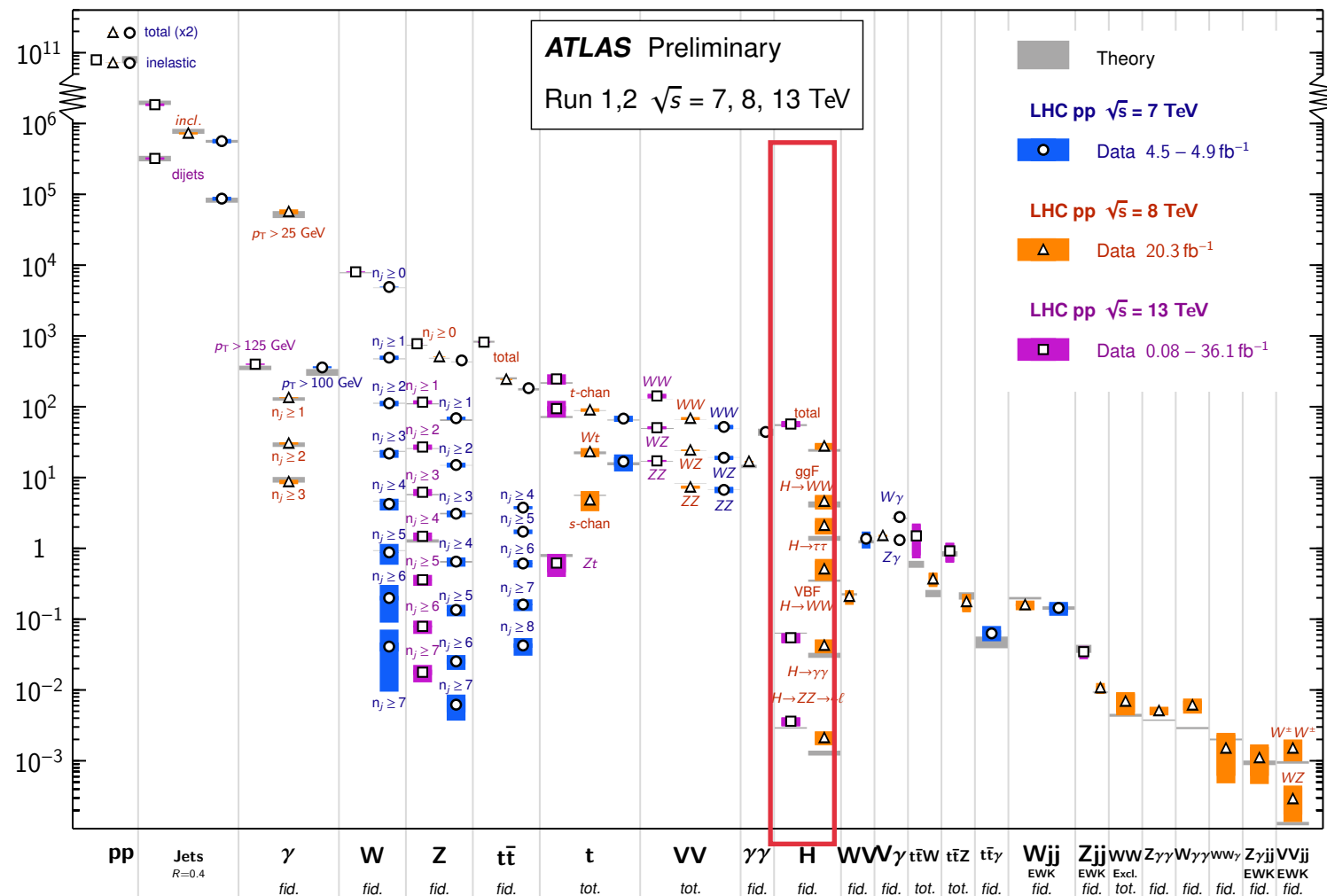
$t\bar{t}H$

# Introduction



## Standard Model Production Cross Section Measurements

Status: July 2017



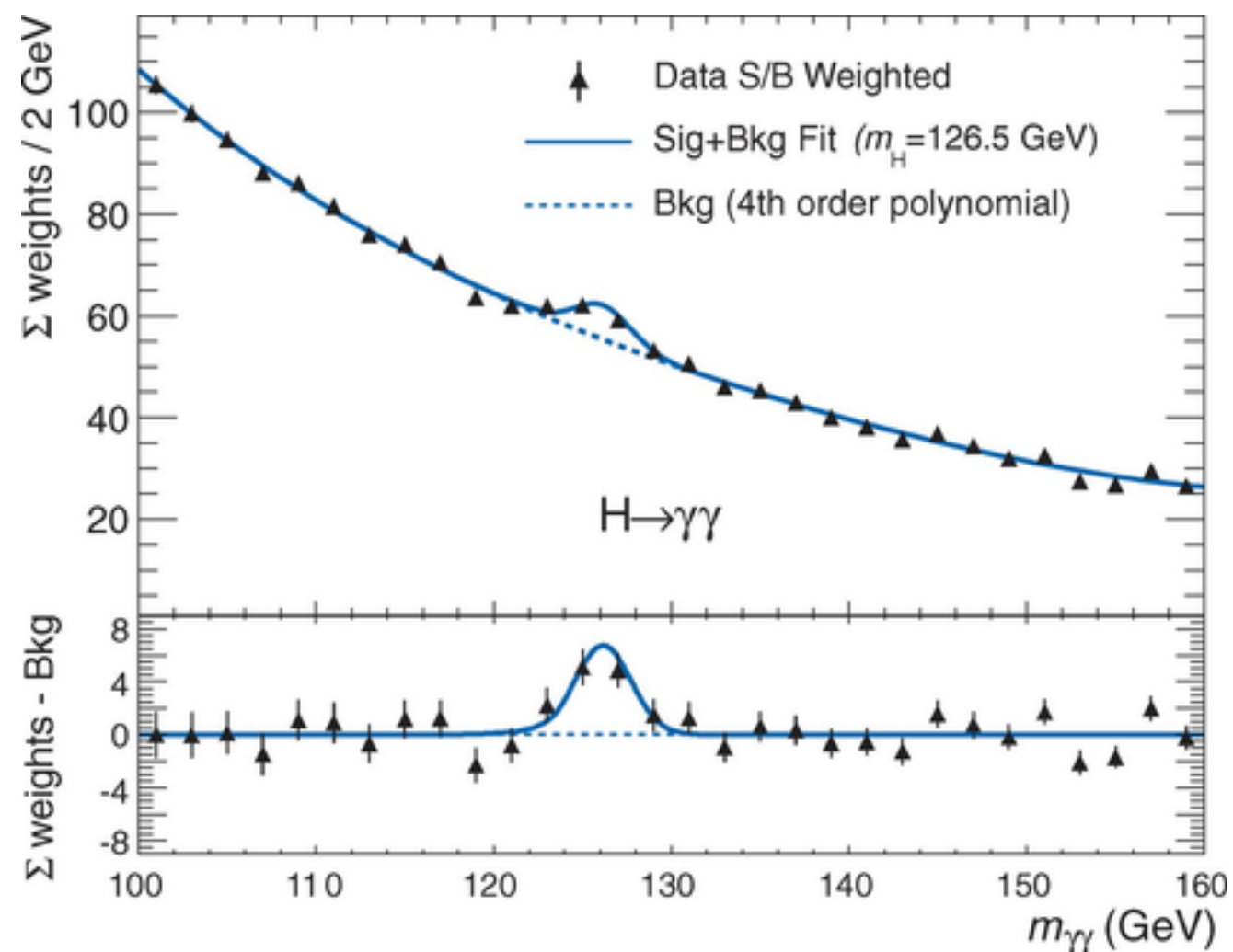
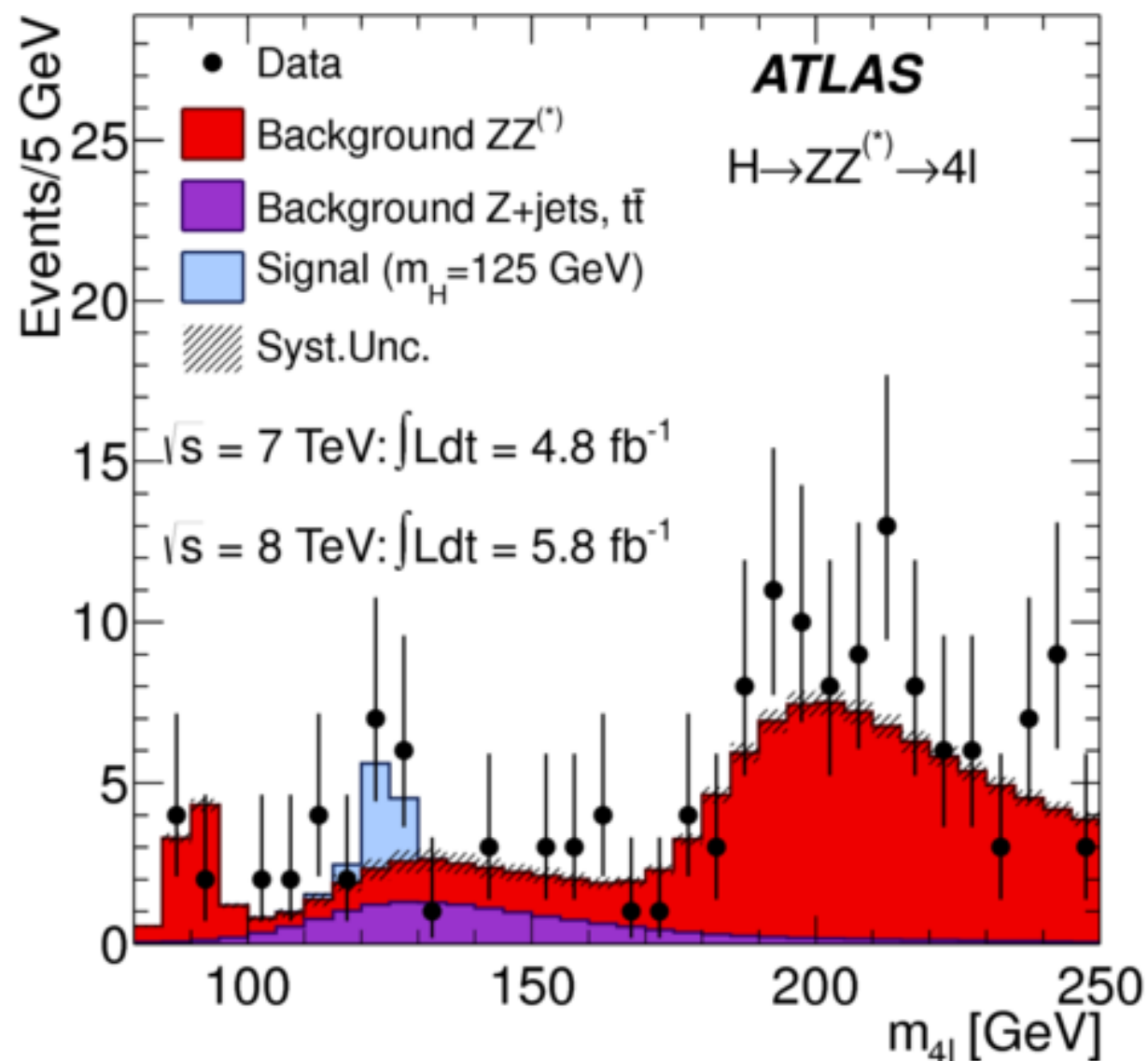
## Experimentally challenging final states

- ▶ In association with additional jets, same final state of many other processes
- ▶ forward jets with large rapidity gap, small rates



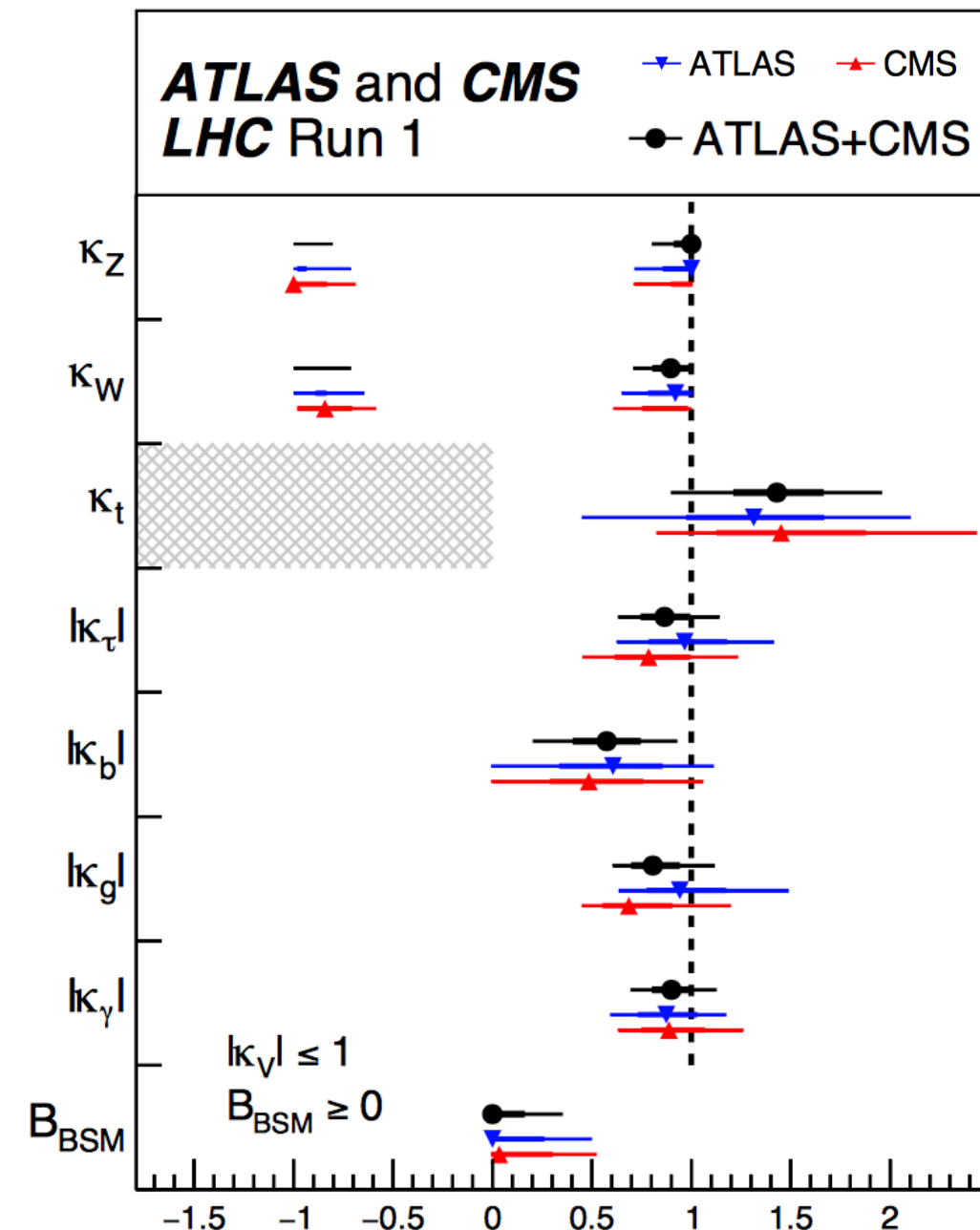
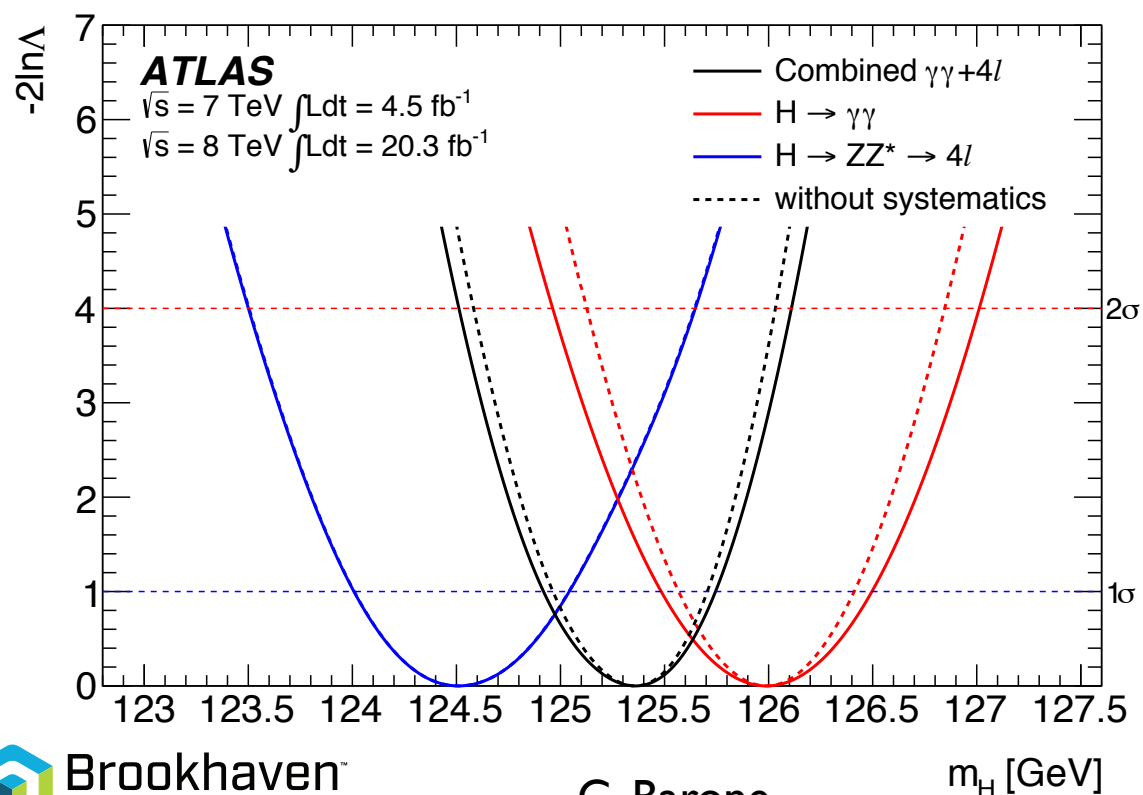
# Run I Discovery

- Run-I featured *in primis* the discovery in July 2012
  - First properties measurements
  - Programme largely limited by statistical accuracy.
- Where do we stand with our understanding of the Higgs 10 years later ?



# Run I Legacy

- Run-I featured *in primis* the discovery
  - First properties measurements
  - Programme largely limited by statistical accuracy.
- Properties:
  - ATLAS precision in  $m_H$  of 0.33%:
  - Couplings measured to 10% to 25% precision
  - $H \rightarrow \text{inv.}$  constrained to  $< 30\%$
  - First studies of  $J^{PC} = 0^{++}$ , (indirect) width  $\Gamma_H < 14.4$  MeV (15.2 MeV)



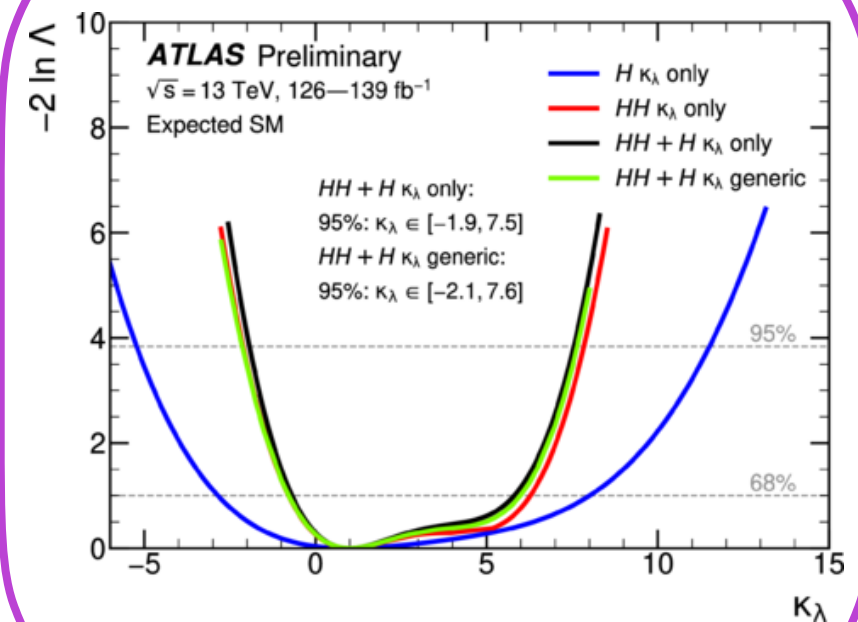
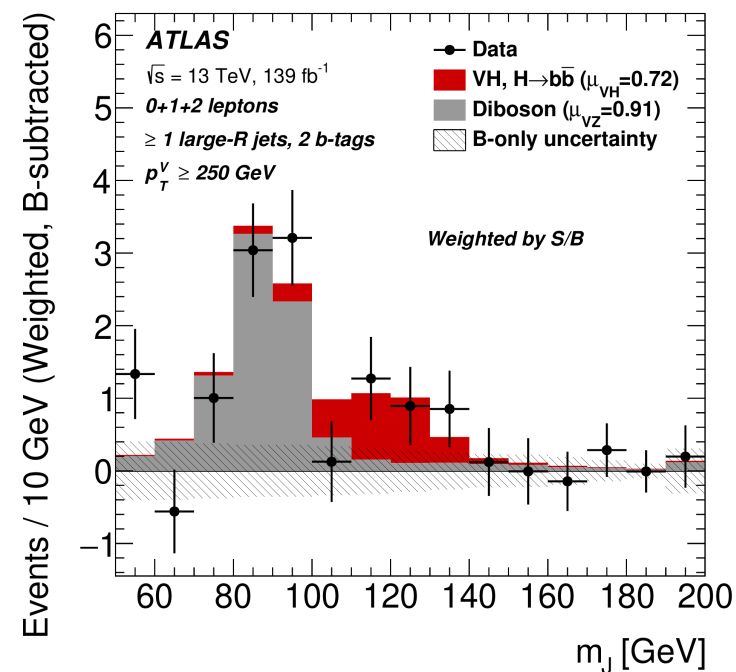
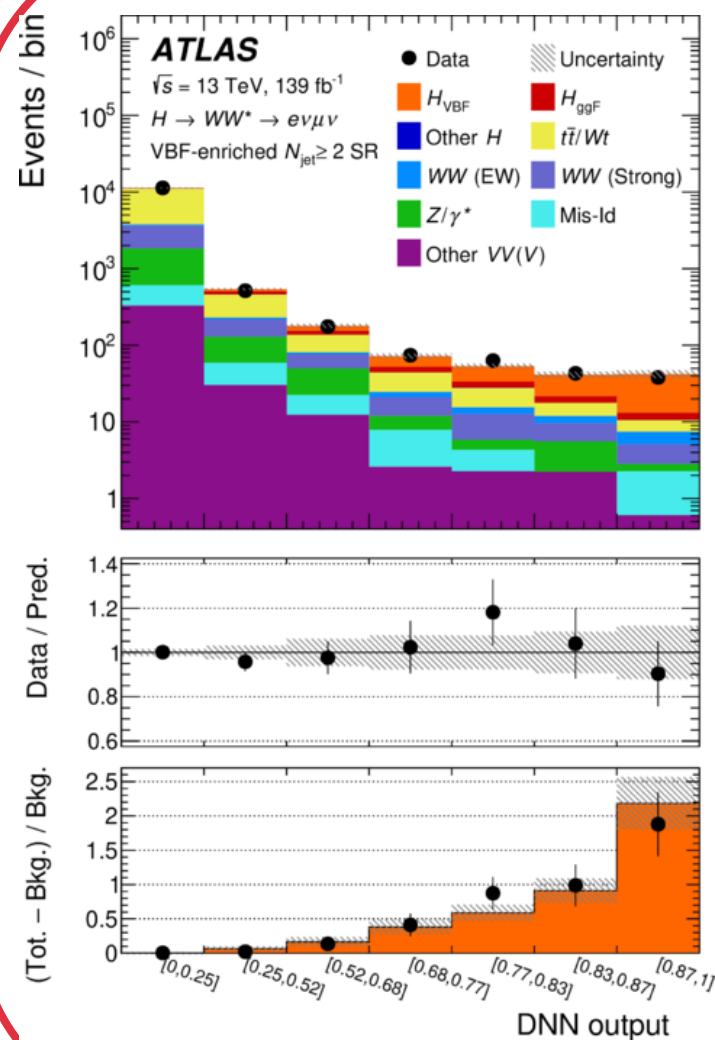
Channel	Mass measurement [GeV]
$H \rightarrow \gamma\gamma$	$125.98 \pm 0.42$ (stat) $\pm 0.28$ (syst) = $125.98 \pm 0.50$
$H \rightarrow ZZ^* \rightarrow 4\ell$	$124.51 \pm 0.52$ (stat) $\pm 0.06$ (syst) = $124.51 \pm 0.52$
Combined	$125.36 \pm 0.37$ (stat) $\pm 0.18$ (syst) = $125.36 \pm 0.41$

# Overview

- ATLAS collected 139 fb<sup>-1</sup> in Run 2

- ▶ Sufficient statistics for precision-level measurements.
- ▶ Path open to exploration of SM Lagrangian in the Electro-Weak symmetry breaking sector.
- ▶ Probe to couplings to **bosons** and **fermions**
- ▶ Understand structure of its **potential**.

$$\mathcal{L} = -\frac{1}{4}F_{\mu\nu}F^{\mu\nu} + i\bar{\Psi}\not{D}\psi + \boxed{D_{\mu}\Phi^{\dagger}D^{\mu}\Phi} - \boxed{V(\Phi)} + \boxed{\bar{\Psi}_L\hat{Y}\Phi\Psi_R + h.c.}$$



# Overview

- ATLAS collected 139 fb<sup>-1</sup> in Run 2

- ▶ Sufficient statistics for precision-level measurements.
- ▶ Path open to exploration of SM Lagrangian in the Electro-Weak symmetry breaking sector.
- ▶ Probe to couplings to **bosons** and **fermions**
- ▶ Understand structure of its **potential**.

$$\begin{aligned}\mathcal{L} = & -\frac{1}{4}F_{\mu\nu}F^{\mu\nu} \\ & + i\bar{\Psi}\not{D}\psi \\ & + \boxed{D_{\mu}\Phi^{\dagger}D^{\mu}\Phi} - \boxed{V(\Phi)} \\ & + \boxed{\bar{\Psi}_L\hat{Y}\Phi\Psi_R + h.c.}\end{aligned}$$

- In ten years from the discovery in July 2012:

1. Understanding of the  $H$  potential structure, through the measurement of its mass.
2. Advances in probes of Yukawa couplings to second and first generation fermions.
3. Production mode cross sections.
4. Differential cross sections.

## 2. Mass measurement

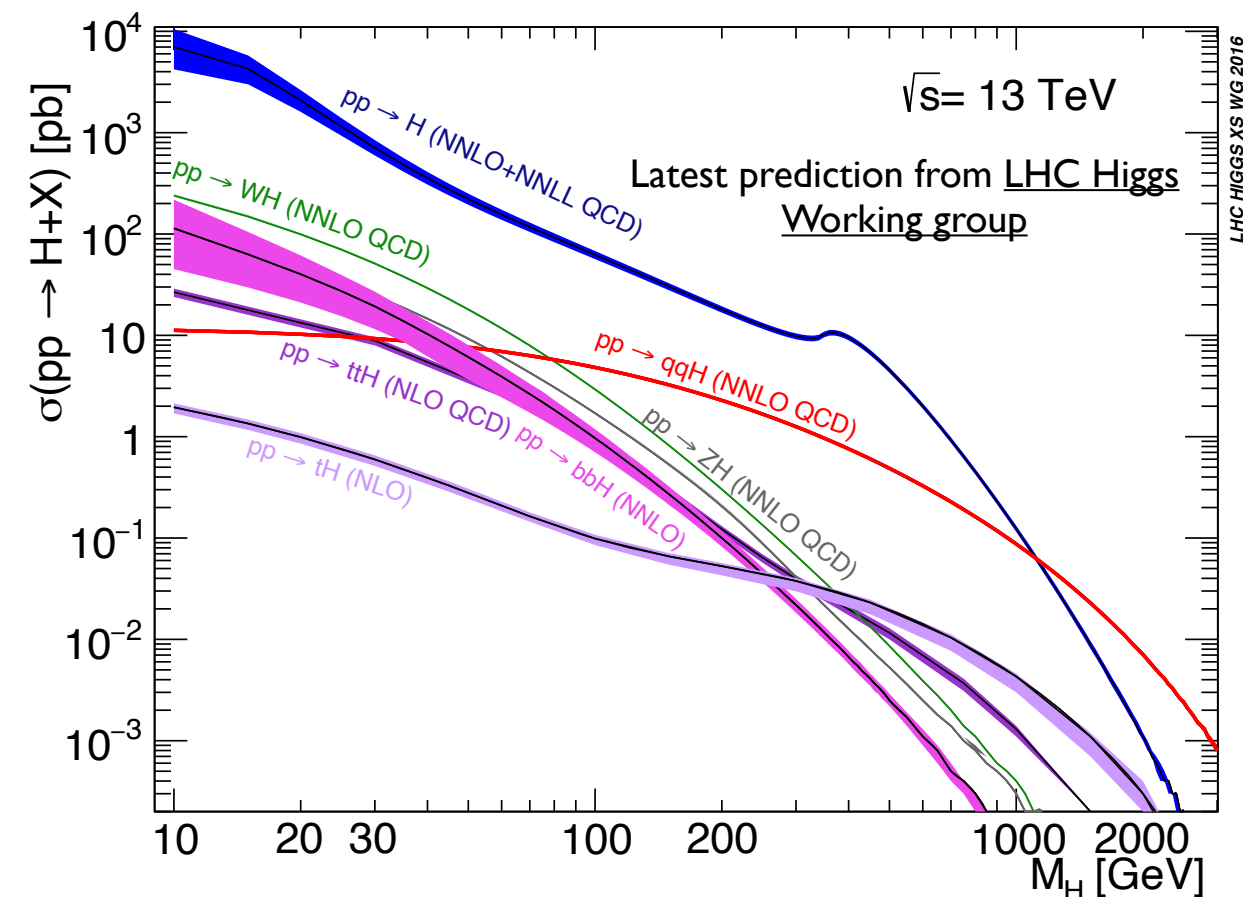
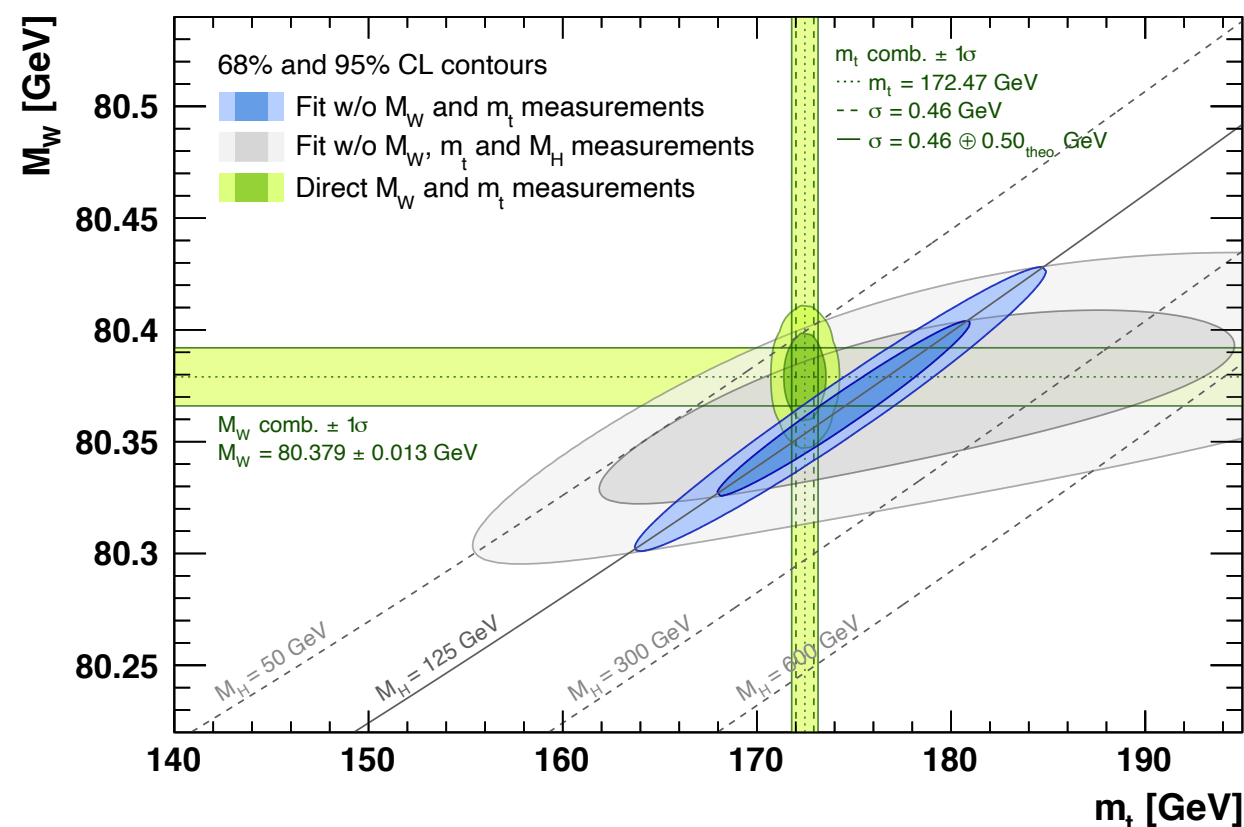
- Importance of  $m_H$  and  $\Gamma_H$  in several aspects of our understanding of fundamental physics.

Power law expansion of the potential

$$V(h) = \frac{1}{4}\lambda h^4 + \lambda v h^3 + \lambda v^2 h^2$$

- Understanding the perturbative expansion of its potential ( $\lambda v^2 h^2$ ).
- Higgs couplings defined by the value of  $m_H$ .
- Input to precision global fit of the Standard Model.

$$\begin{aligned} \mathcal{L} = & -\frac{1}{4}F_{\mu\nu}F^{\mu\nu} \\ & + i\bar{\Psi}\not{D}\psi \\ & + D_\mu\Phi^\dagger D^\mu\Phi - V(\Phi) \\ & + \bar{\Psi}_L\hat{Y}\Phi\Psi_R + h.c. \end{aligned}$$



Global Electroweak fits from the Gfitter Collaboration



# Run I status

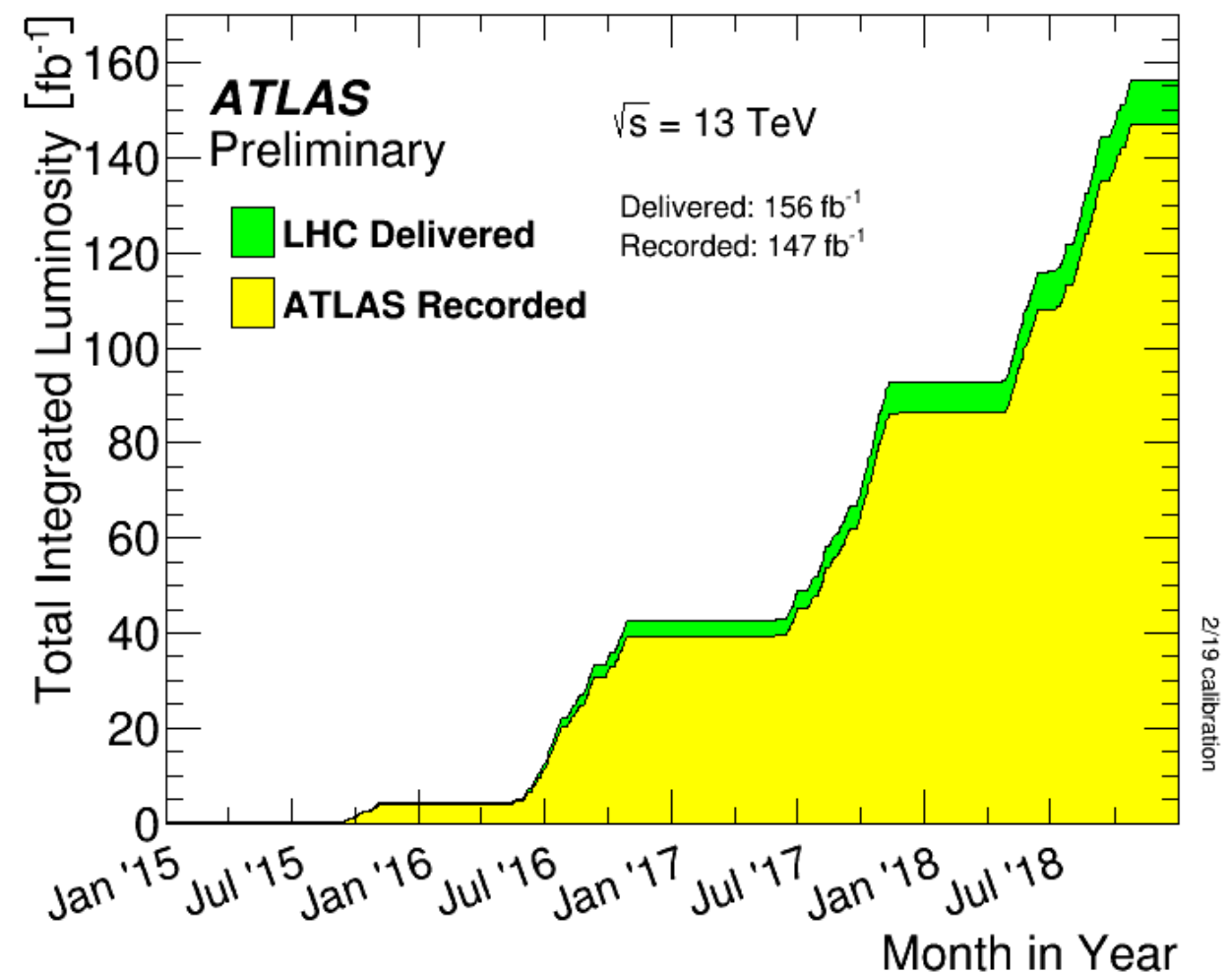
- ATLAS run I precision on  $m_H$  of 0.33%
  - ▶ combined measurement from  $H \rightarrow \gamma\gamma$  and  $H \rightarrow ZZ^* \rightarrow 4\ell$ .

Channel	Mass measurement [GeV]
$H \rightarrow \gamma\gamma$	$125.98 \pm 0.42$ (stat) $\pm 0.28$ (syst) = $125.98 \pm 0.50$
$H \rightarrow ZZ^* \rightarrow 4\ell$	$124.51 \pm 0.52$ (stat) $\pm 0.06$ (syst) = $124.51 \pm 0.52$
Combined	$125.36 \pm 0.37$ (stat) $\pm 0.18$ (syst) = $125.36 \pm 0.41$

- ▶ Both channels dominated by statistical uncertainty

- At Run2 aim in improving significantly the precision:

- ▶ Expect 7 times more candidates, with  $139 \text{ fb}^{-1}$  at  $\sqrt{s}=13 \text{ TeV}$
- ▶ Improve on the detector calibration.



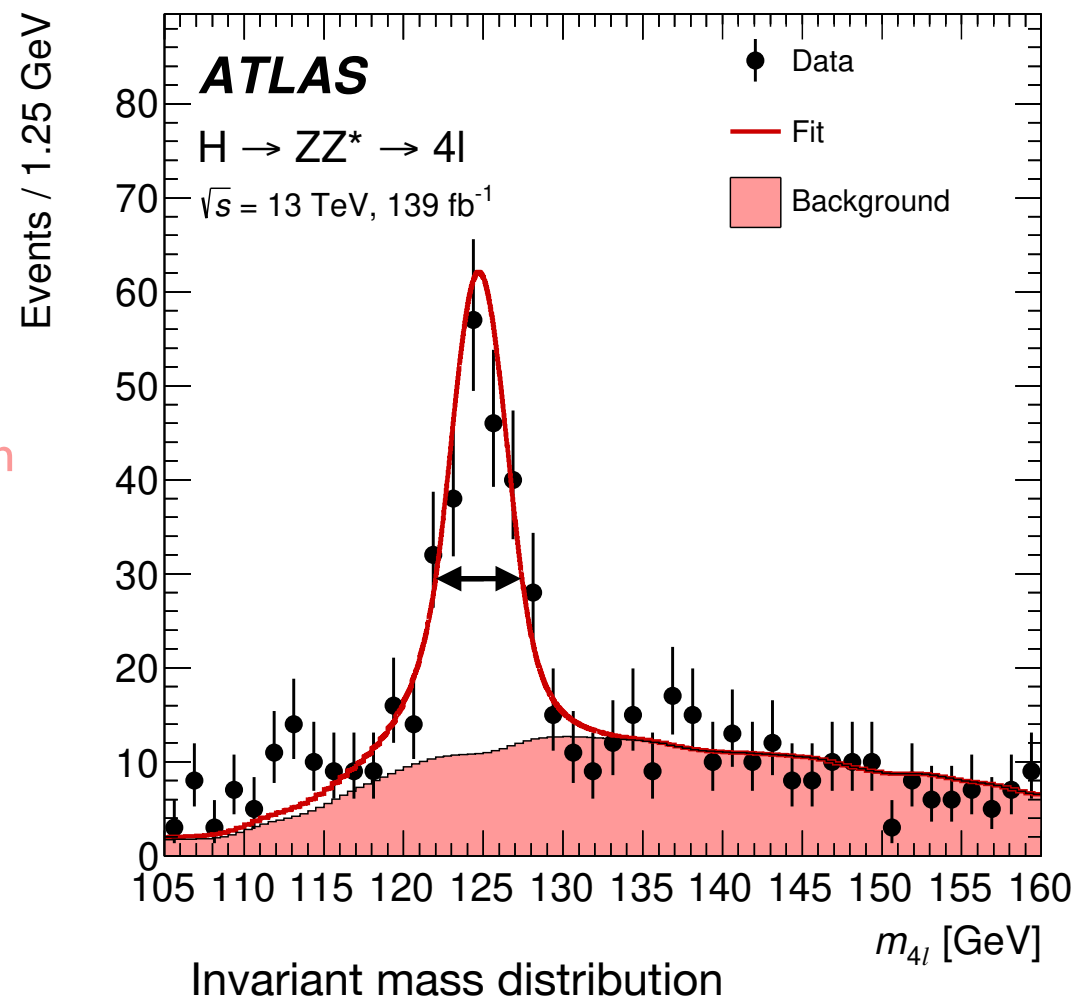
- In the  $H \rightarrow ZZ \rightarrow 4\ell$  the signal is a narrow resonant peak above a background continuum.

$\ell$  = electron or muon

- $4\ell$  final state forms  $4\mu$ ,  $4e$ ,  $2\mu 2e$ , and  $2e 2\mu$  channels.

Higgs signal,  
resonant at the  
value of  $m_H$

Non resonant  
background from non  
 $H$  production



$$\delta m_H \simeq \frac{\sigma(m_{4\ell}, \gamma\gamma)}{\sqrt{N - N_b}}$$

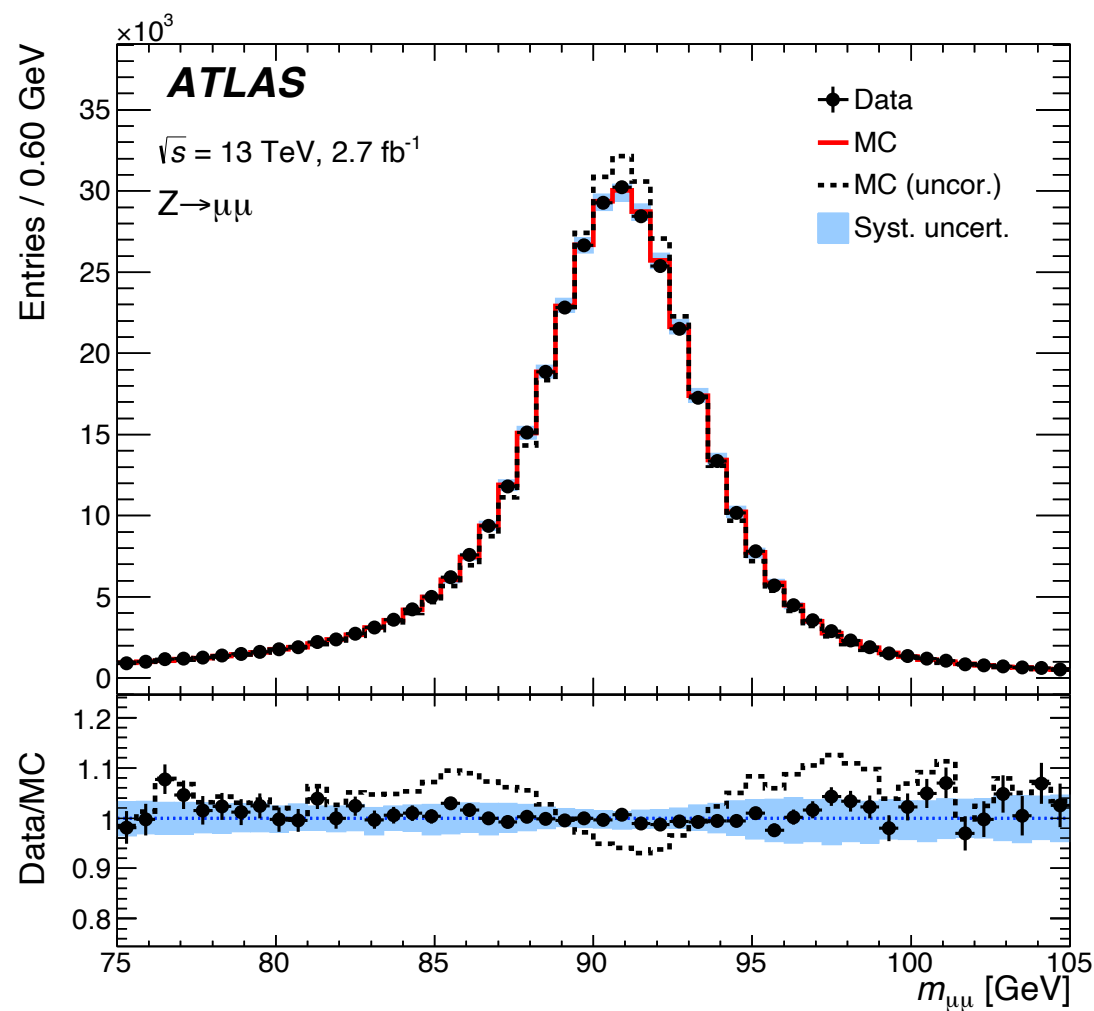
Statistical uncertainty on  $m_H$  approximated by the uncertainty on the mean of the mass distribution

- (I) **Statistical** precision depends upon:
  - resolution of the reconstructed final state and number of signal events.
- (II) **Systematic** uncertainty from understanding of detector performance.

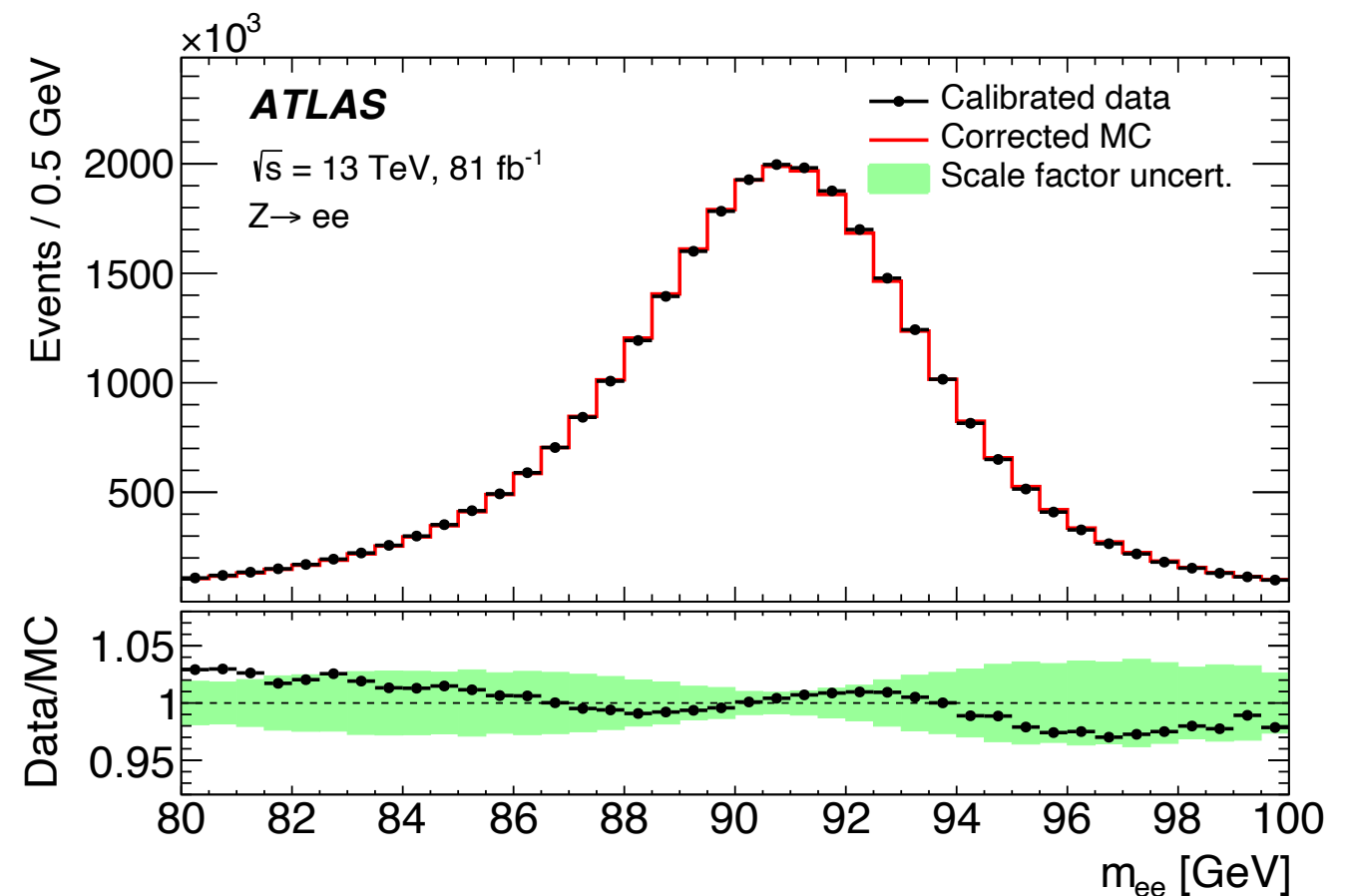
Addressing these from both improving the *detector performance* and novel *data analysis techniques*.



- Resolution in electron and muon reconstruction crucial for  $m_H$  uncertainty.
- We used well known processes to calibrate the detector response.
  - Resonant process of  $J/\psi$ ,  $\Upsilon$  and  $Z$ ,
  - for modelling of calorimeters deposits, alignment precision, etc.

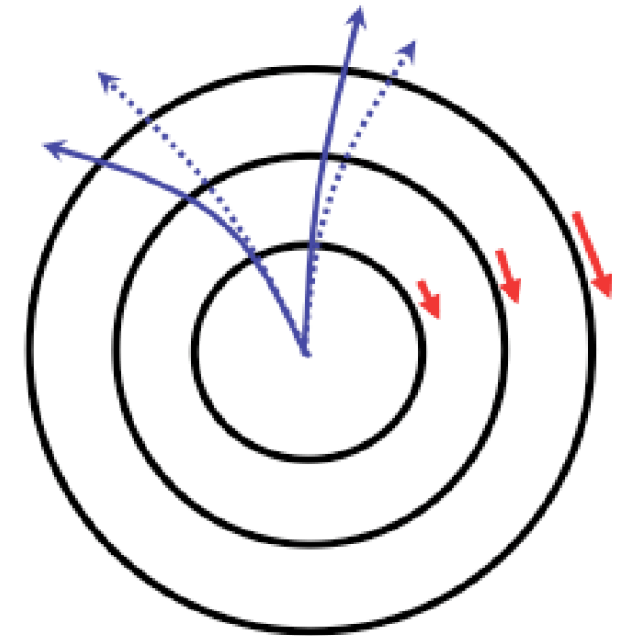


$Z \rightarrow \mu\mu$  resonant line shape for data and detector simulation



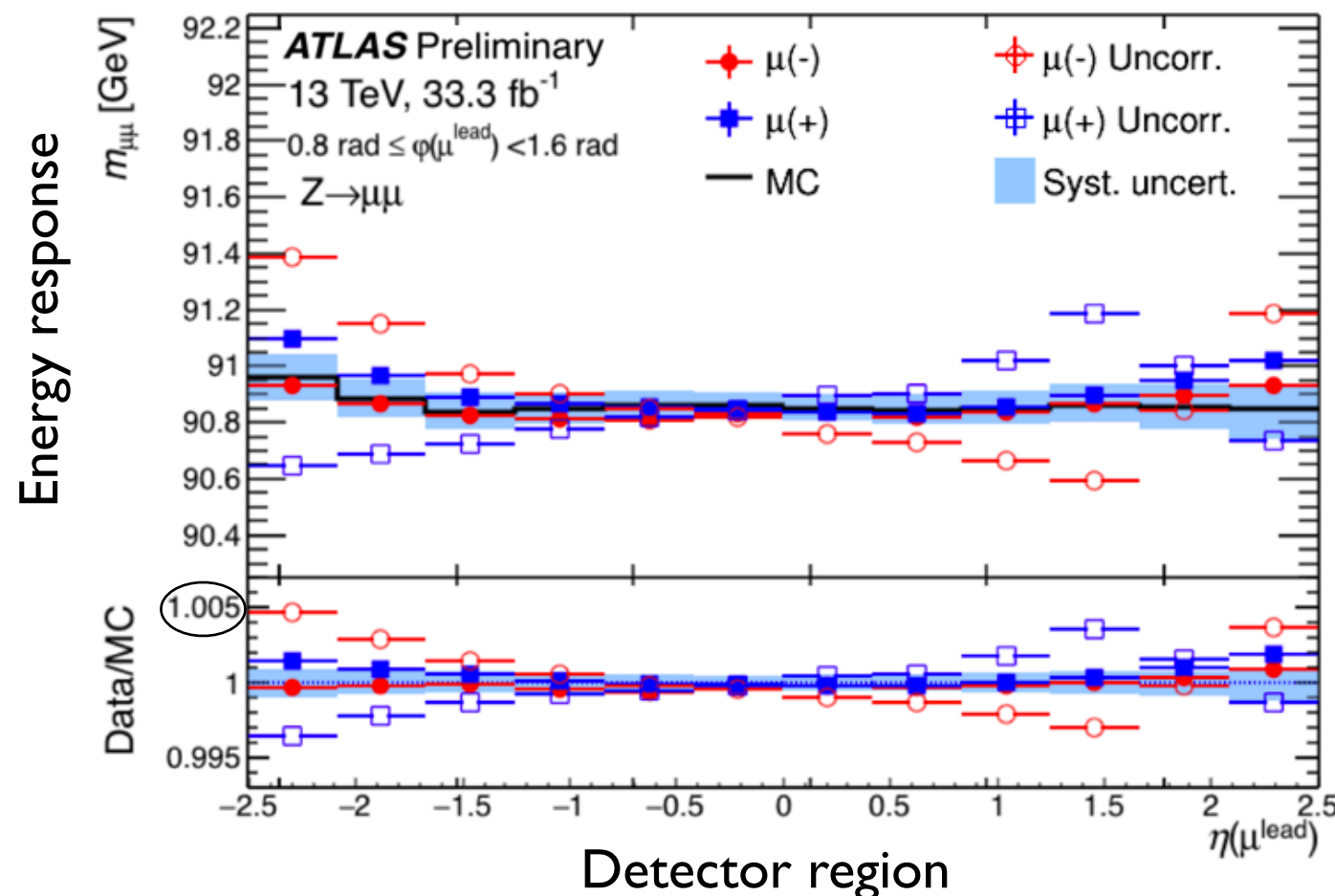
$Z \rightarrow ee$  resonant line shape for data and detector simulation

- High precision mandates for studying second order effects:
  - ▶ charge-dependent bias because of detector movements.
  - ▶ We created an innovative *ad-hoc* correction based on  $Z \rightarrow \mu\mu$ , **recovering up to 5% in precision.**
  - ▶ Allows for **per-mille level** understating of detector's systematic uncertainties.



- ✦ Biased **positive** and **negative** tracks
- ✦ Corrected **positive** and **negative** tracks

Detector layer movements biasing the measurement of the bending of the particle

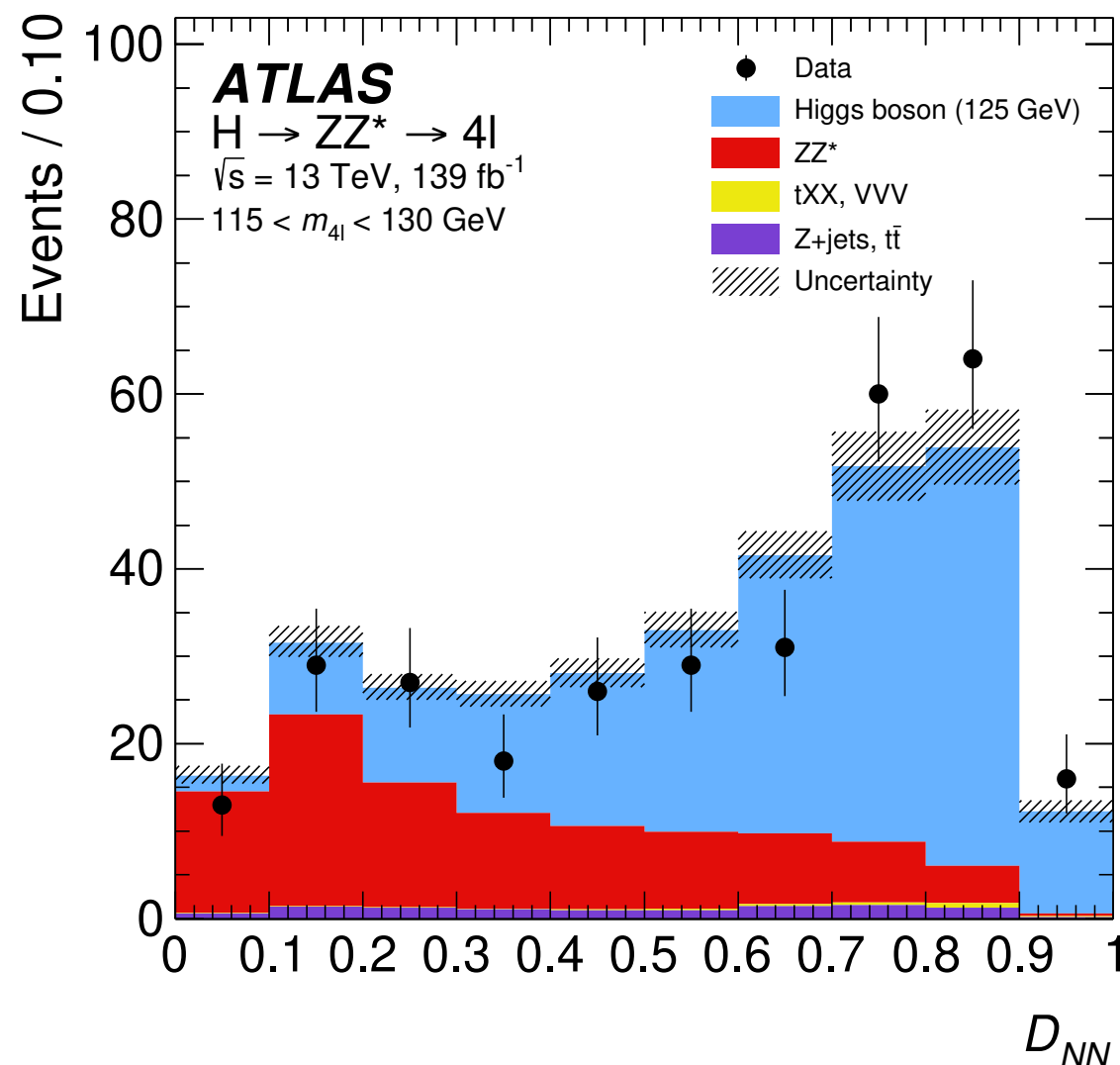


- Three-prong approach to reduce uncertainty at analysis level:

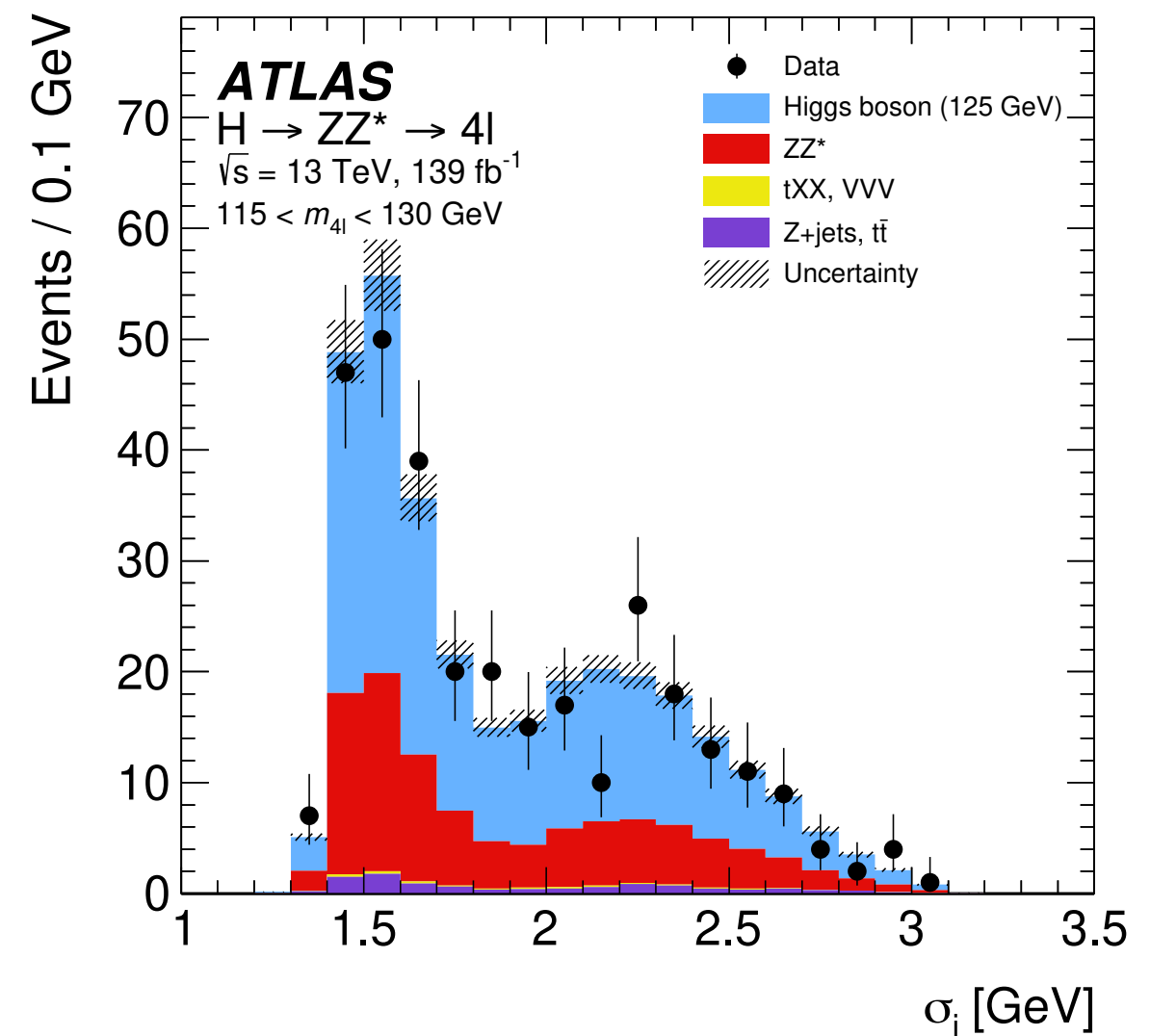
[arXiv:2207.00320](https://arxiv.org/abs/2207.00320)

- constraint to  $m_Z$**  with kinematic fit and second order detector effects.
- machine-learning **discriminant** selecting signal and background events
- Per-event resolution likelihood.**

◆ **Machine Learning** to target each event's unique characteristics

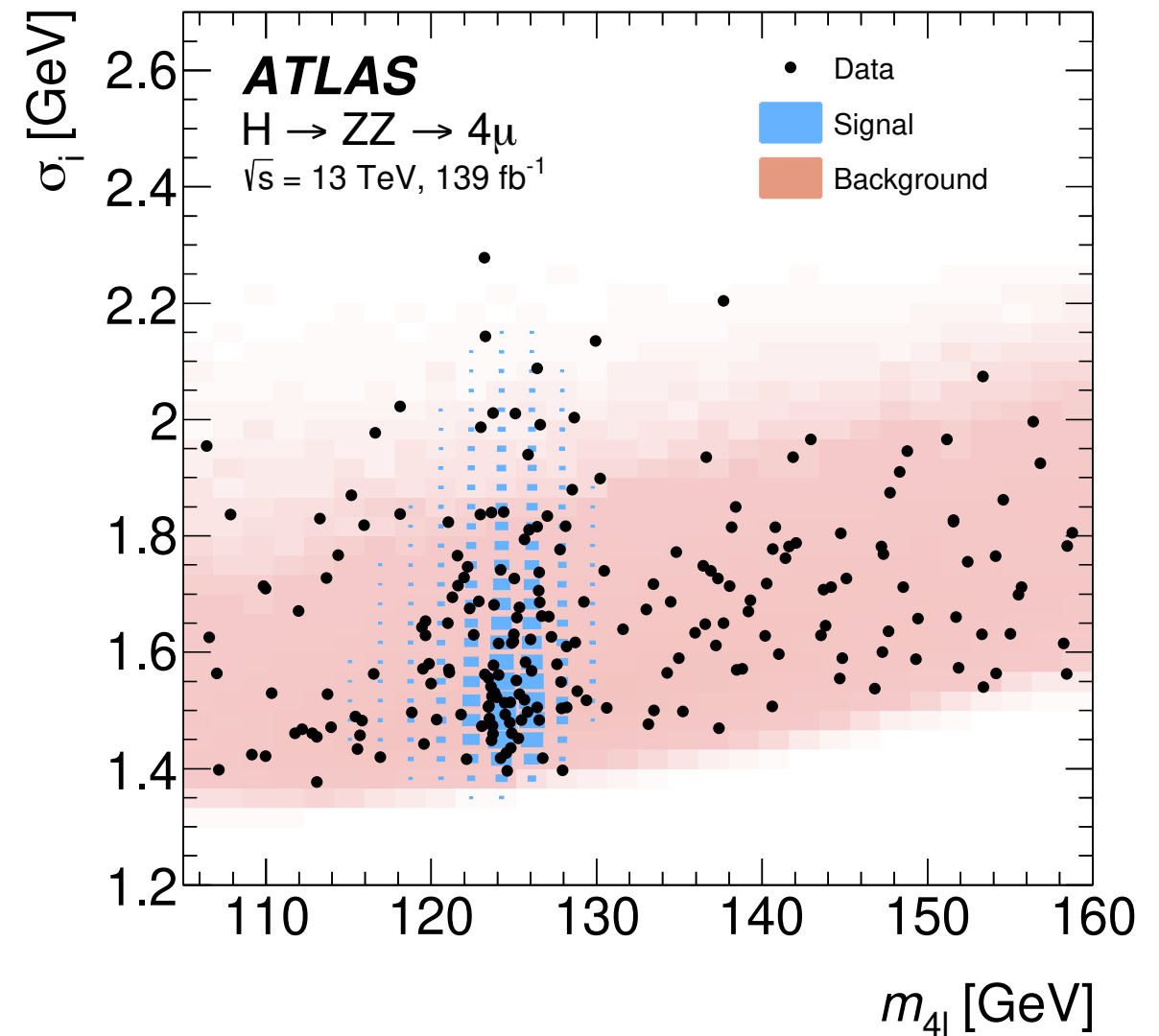
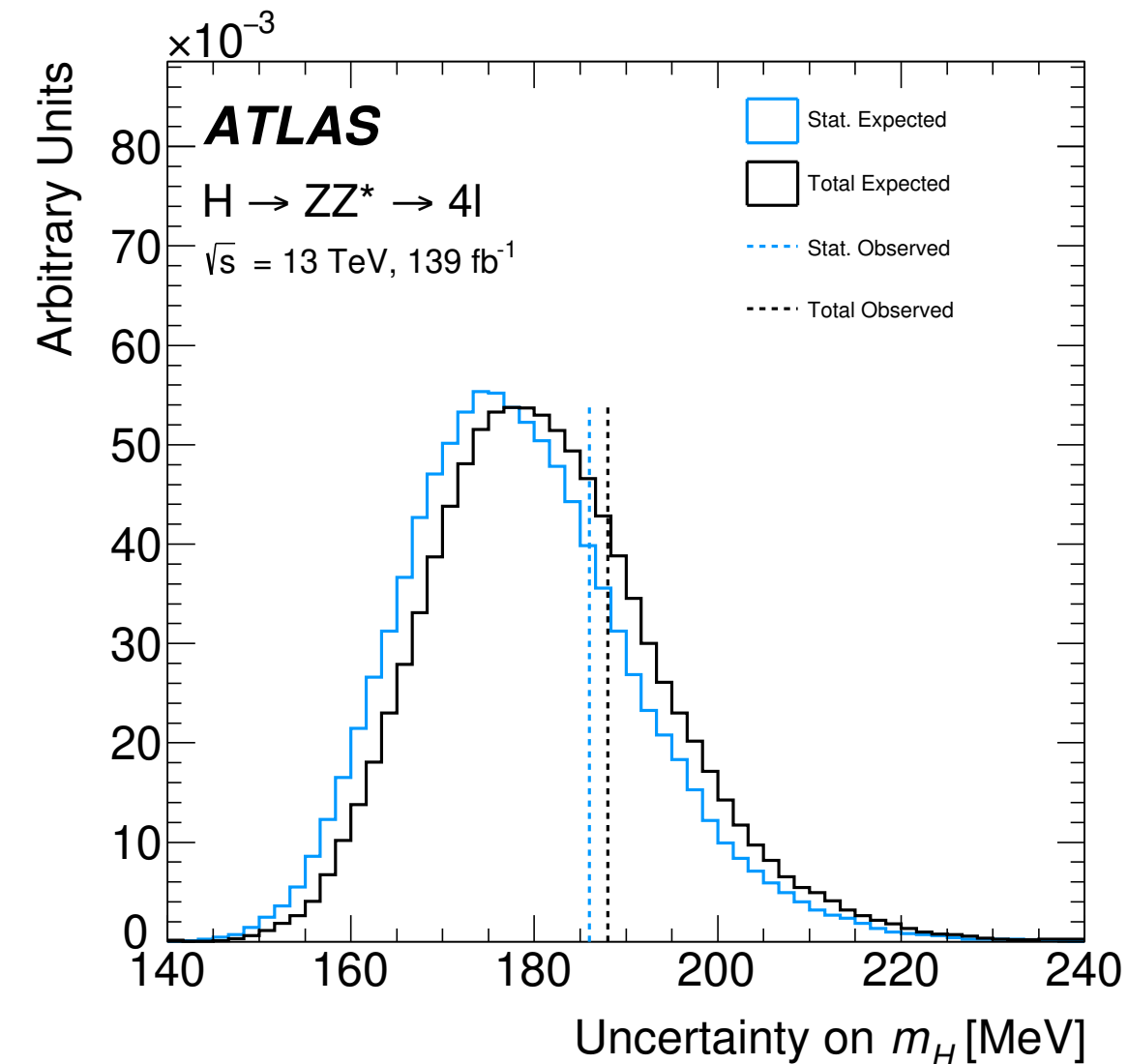


Neural network output of the event's resolution



ML output for **signal** and **background**

- Output used in **multidimensional fit**, improving with respect to average detector response.
  - Fit dimensions:  $m_{4\ell} \times D_{NN} \times \sigma_i$
  - Tailored resolution to each event's characteristics.
  - One-sided  $p$ -value for compatibility between the observed and expected total uncertainties is 0.28.



MC-based per-event pseudo experiments.

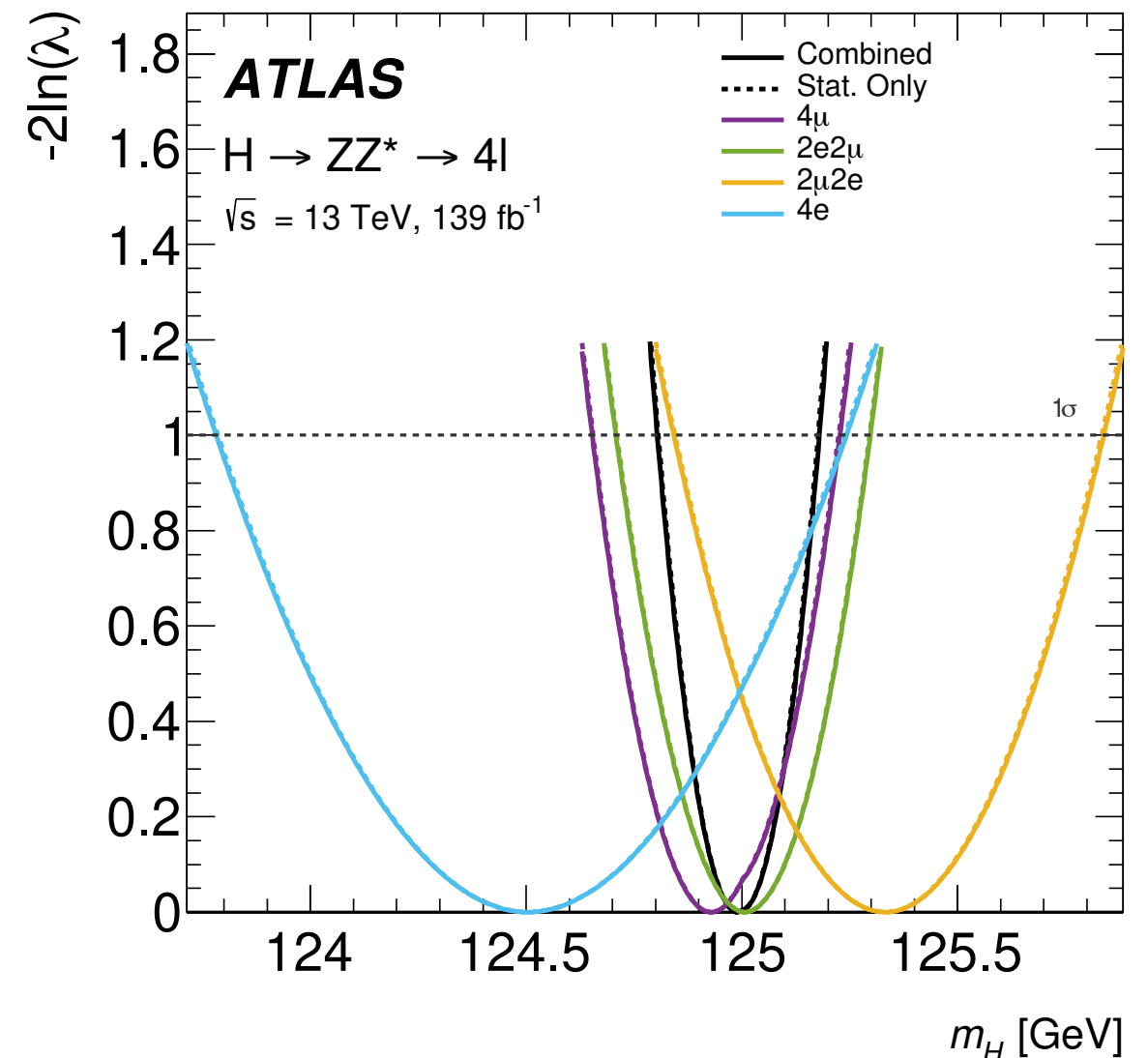
- Simultaneous fit for all channels over the **multidimensional model**

‣ Channel compatibility within a p-value of 0.8

- Systematic uncertainty of 40 MeV

- Result:

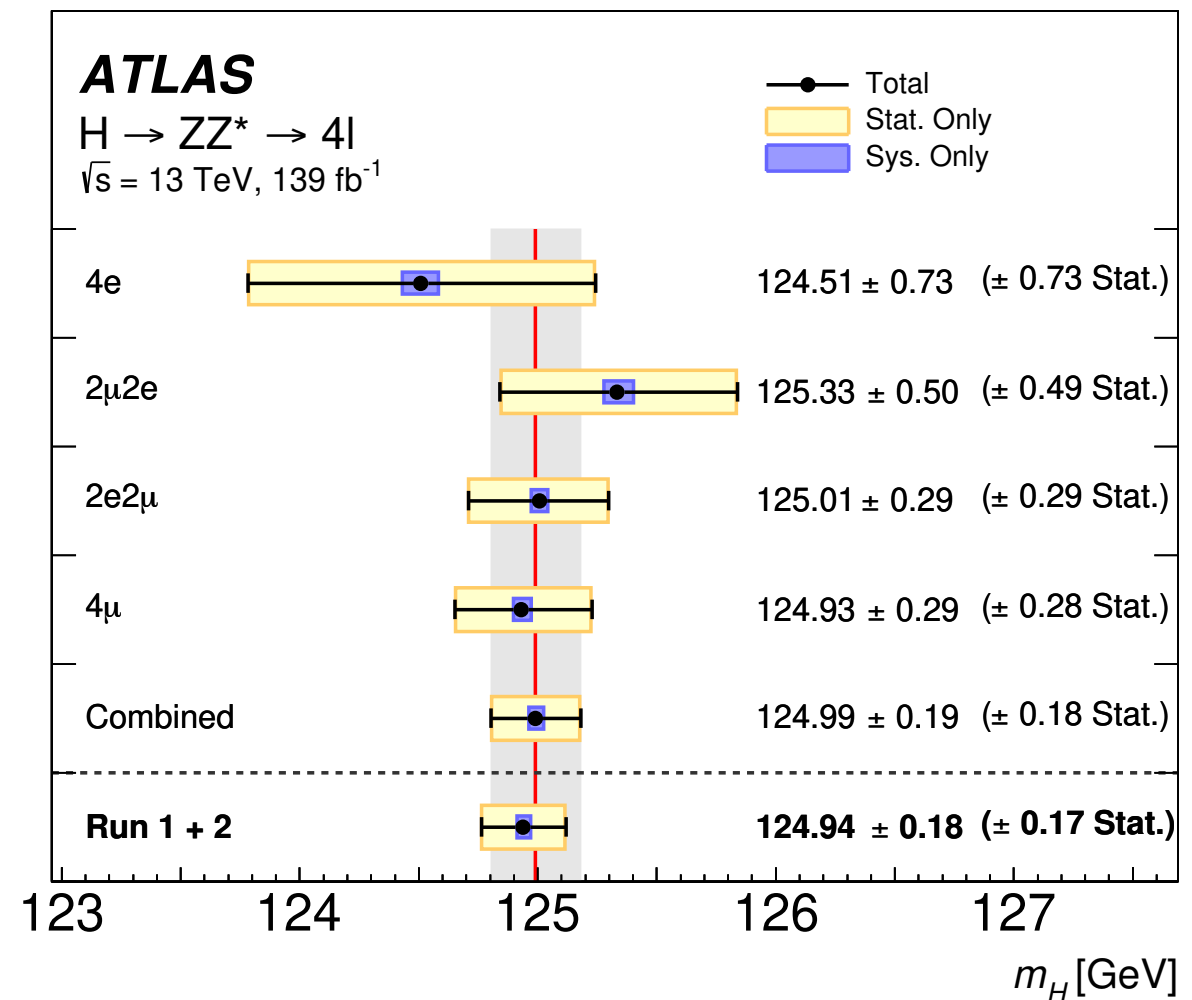
Systematic Uncertainty	Contribution [MeV]
Muon momentum scale	$\pm 28$
Electron energy scale	$\pm 19$
Signal-process theory	$\pm 14$



‣ 26% improved (total) precision with respect to Run I Combination.

$$m_H = 124.99 \pm 0.18(\text{stat.}) \pm 0.04(\text{syst.}) \text{ GeV}$$

- Combination with  $H \rightarrow ZZ \rightarrow 4\ell$  Run-I measurement.
  - ▶ New  $p_T$  calibration techniques  $\rightarrow$  uncorrelated  $p_T(\mu)$  systematics between Run I and Run2
- **Total uncertainty of 0.14%**
- **Systematic uncertainty of 0.02%**
  - ▶ **88% improvement** w.r.t  $m_H^{H \rightarrow ZZ, \text{Run I}}$
  - ▶ Momentum scale uncertainties reduced by a factor 2.
  - ▶ 33% improved precision w.r.t previous  $m_H^{\text{ATLAS, Run I+2}}$
  - ▶ **Most precise measurement by ATLAS, so far.**



Measured  $m_H$  for all channels and combined.

$$m_H = 124.94 \pm 0.17(\text{stat.}) \pm 0.03(\text{syst.}) \text{ GeV}$$

### 3. Elusive Yukawa couplings: light leptons

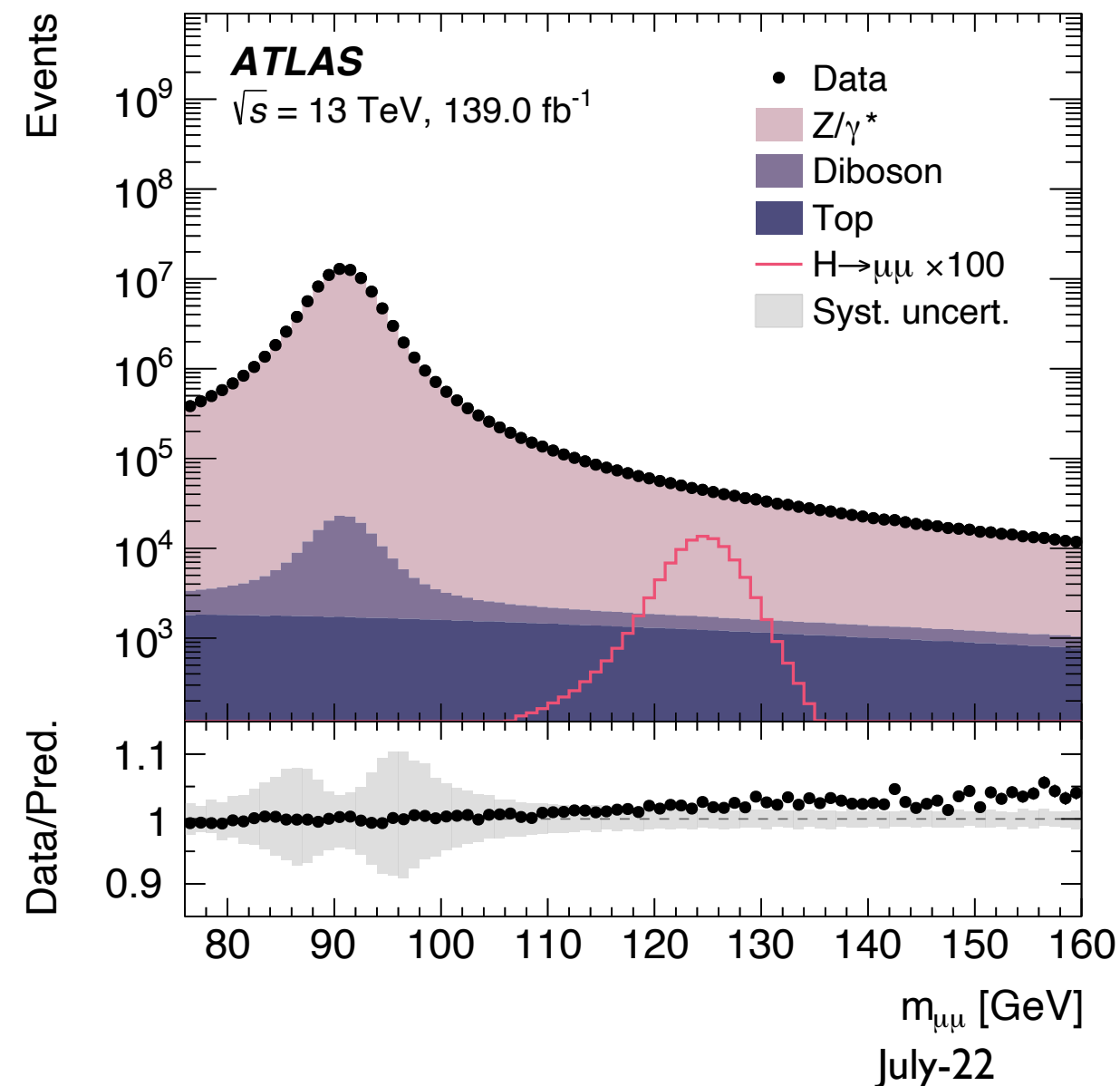
$$\mathcal{L} = -\frac{1}{4}F_{\mu\nu}F^{\mu\nu} + i\bar{\Psi}\not{D}\psi + D_{\mu}\Phi^{\dagger}D^{\mu}\Phi - V(\Phi) + \bar{\Psi}_L\hat{Y}\Phi\Psi_R + h.c.$$

- Fermions acquire mass through Yukawa interactions with the Higgs field.

- Remains an elusive sector not probed by EWK precision tests.
- LHC successfully probed couplings to third generation fermions ( $t\bar{t}H$ ,  $H\rightarrow\tau\tau$ )

- Next milestone, probe couplings to second and first generation fermions.

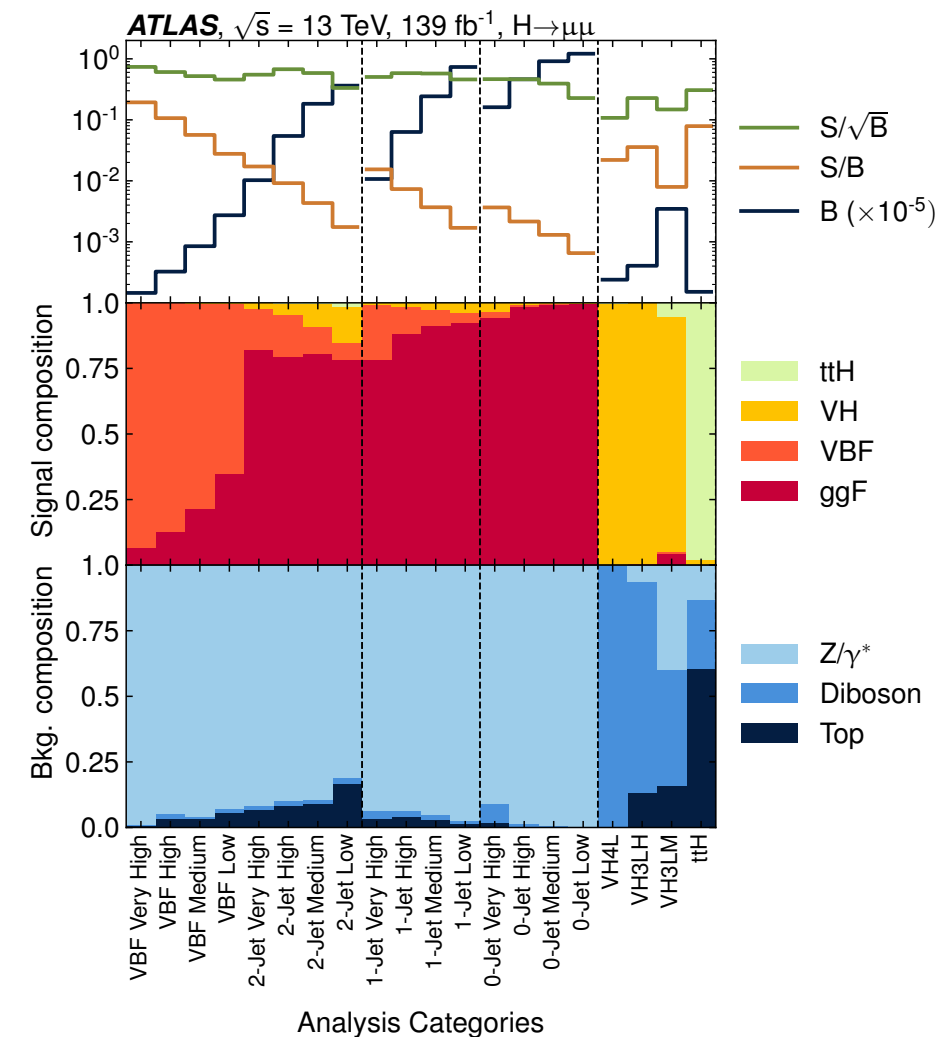
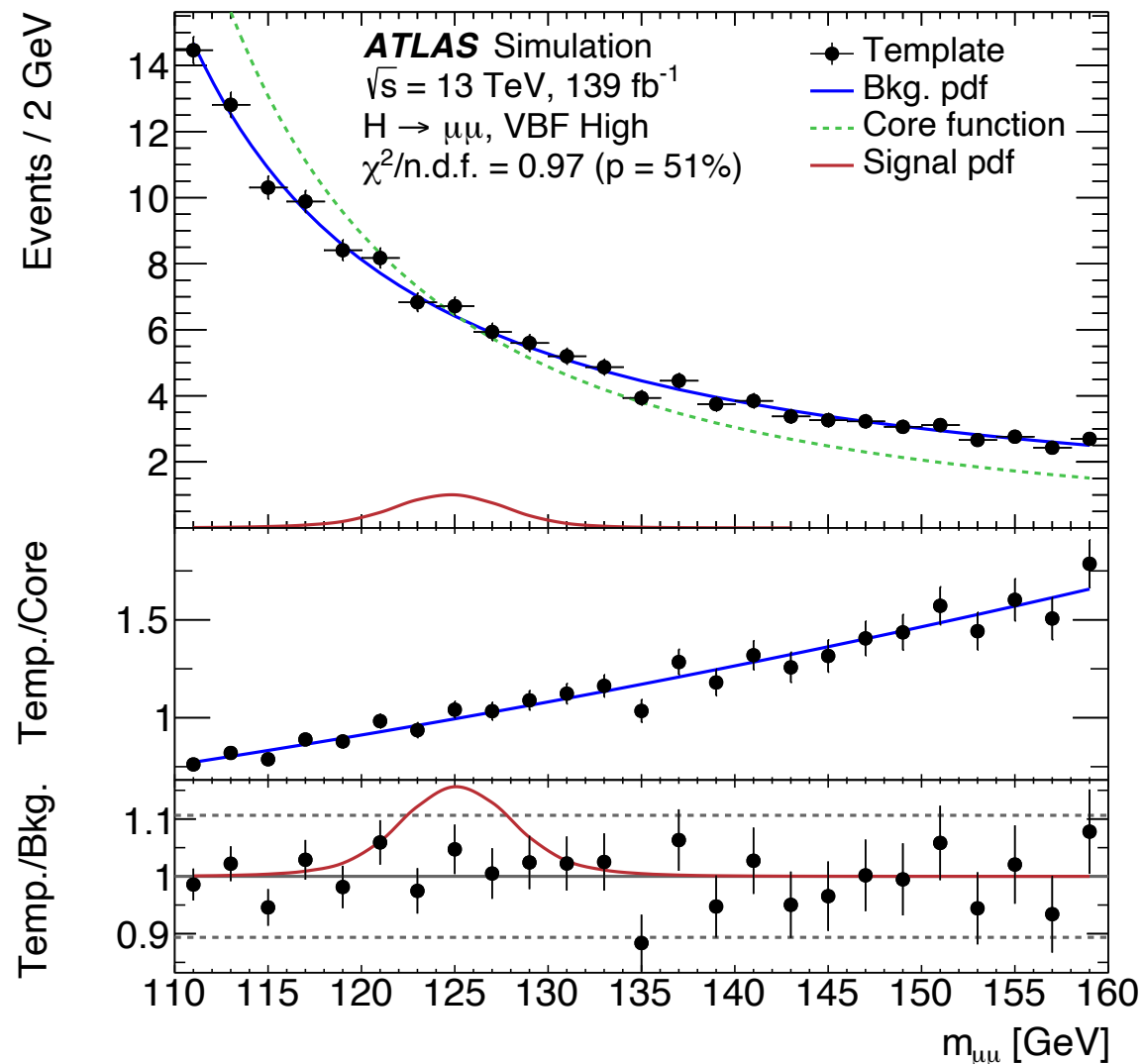
- $H\rightarrow\mu\mu$  and  $ee$  offer unique insight.
- Fully reconstructed final states with low hadronic activity.
- Very rare processes:
  - $\mathcal{B}(H\rightarrow\mu\mu) \sim (2.17 \pm 0.04) \times 10^{-4}$
  - Large backgrounds from Drell-Yann production  $Z\rightarrow\mu\mu, ee$





## ● Mutually exclusive categories

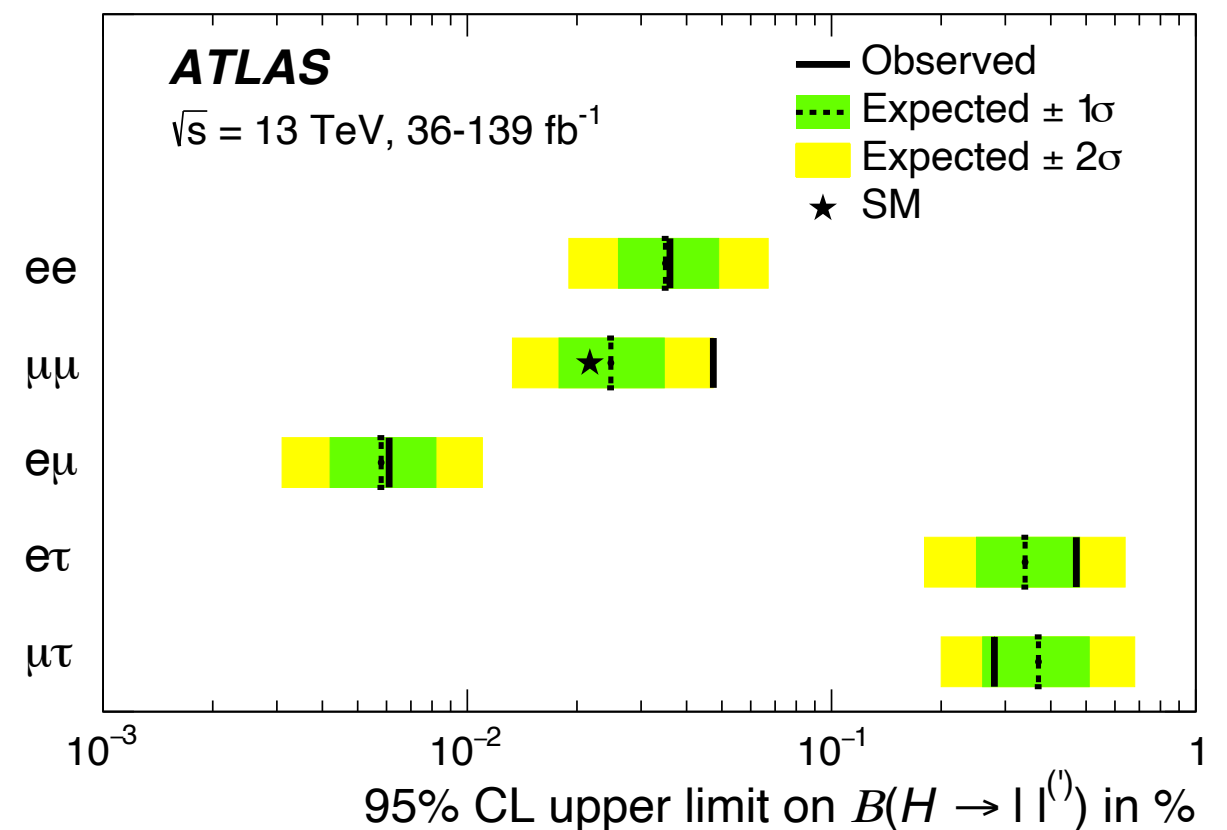
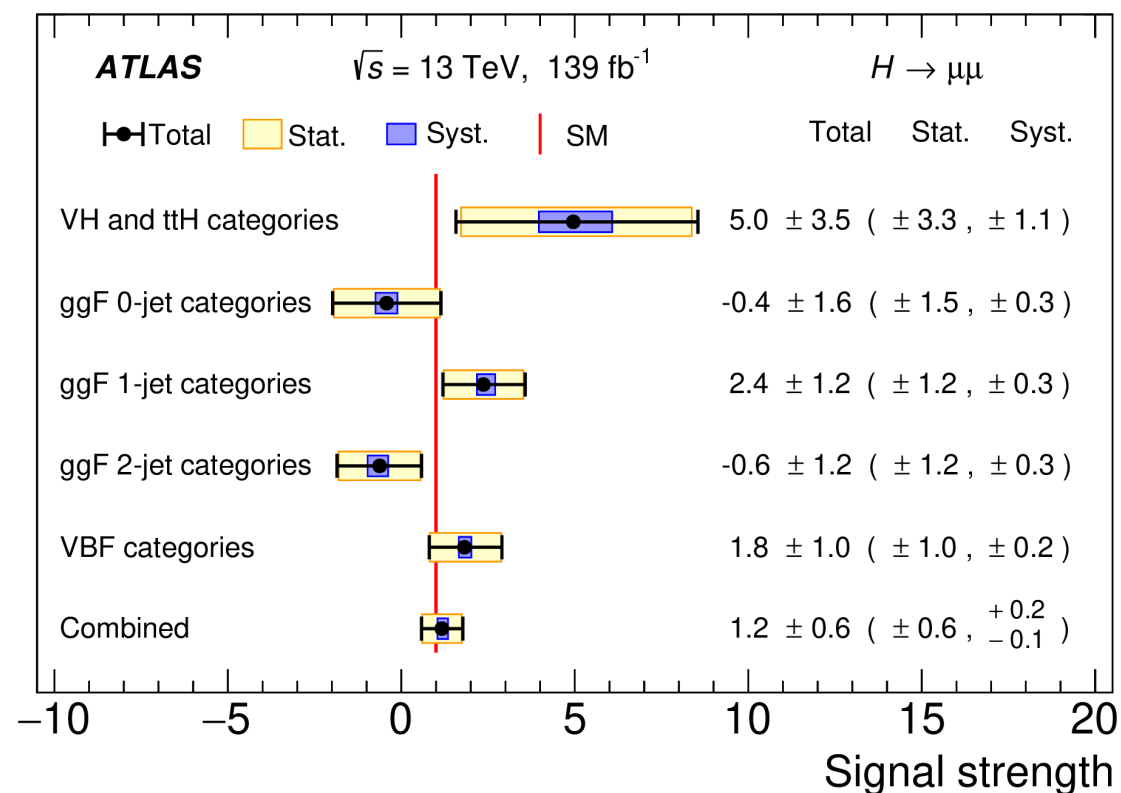
- ▶ Targeting the various Higgs production modes, to increase s/b.
- ▶  $H \rightarrow \mu\mu$ , further splitting according process-specific **multivariate boosted decision tree**.



## ● Empirical background modelling in both analyses.

- ▶  $F(m_{\mu\mu}) = \text{Rigid core}(m_{\mu\mu}) \times \text{Flexible Empirical}(m_{\mu\mu})$
- ▶ Per-mille precision reached

- $\mathcal{B}(H \rightarrow ee) < 3.6 \times 10^{-4}$  at 95%CL.
  - Expected limit at  $3.5 \times 10^{-4}$
  - Improvement of a **factor of 5 w.r.t** previous.
- $H \rightarrow \mu\mu$ : **observed significance  $2.0\sigma$** ,  $\mu = 1.2 \pm 0.5$ .
  - Expected  $1.7\sigma$ .
  - $\sigma(H \rightarrow \mu\mu) / \sigma^{\text{SM}}(H \rightarrow \mu\mu) < 2.2$  at 95%CL.
  - Improvement of a factor 2.5, with 25% from the methods used.

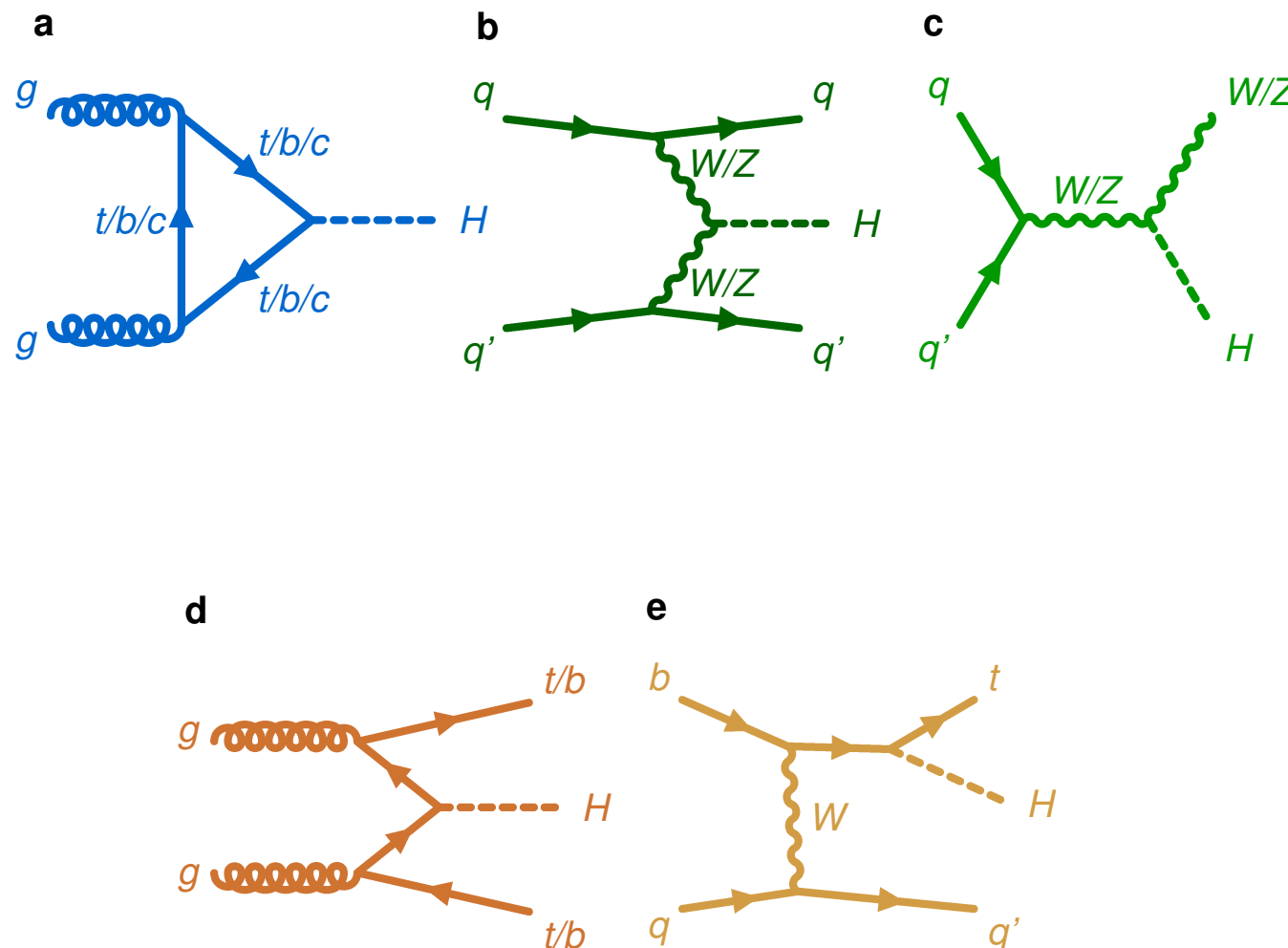


## 4. Production mode measurements

## ● ATLAS full Run-2 combination

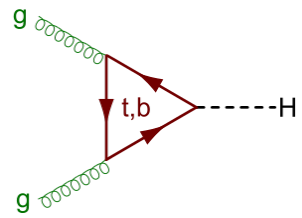
Nature 607, 52–59 (2022)

- Combined sensitivity of all channels to increase the precision of the Higgs productions.

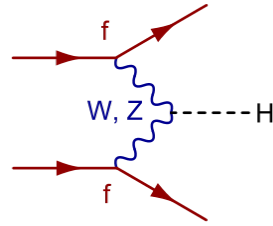


Decay mode	Targeted production processes	$\mathcal{L}$ [ $\text{fb}^{-1}$ ]
$H \rightarrow \gamma\gamma$	ggF, VBF, $WH$ , $ZH$ , $t\bar{t}H$ , $tH$	139
$H \rightarrow ZZ$	ggF, VBF, $WH + ZH$ , $t\bar{t}H + tH$	139
	$t\bar{t}H + tH$ (multilepton)	36.1
$H \rightarrow WW$	ggF, VBF	139
	$WH, ZH$	36.1
	$t\bar{t}H + tH$ (multilepton)	36.1
$H \rightarrow Z\gamma$	inclusive	139
$H \rightarrow b\bar{b}$	$WH, ZH$	139
	VBF	126
	$t\bar{t}H + tH$	139
	inclusive	139
$H \rightarrow \tau\tau$	ggF, VBF, $WH + ZH$ , $t\bar{t}H + tH$	139
	$t\bar{t}H + tH$ (multilepton)	36.1
$H \rightarrow \mu\mu$	ggF + $t\bar{t}H + tH$ , VBF + $WH + ZH$	139
$H \rightarrow c\bar{c}$	$WH + ZH$	139
$H \rightarrow \text{invisible}$	VBF	139
	$ZH$	139

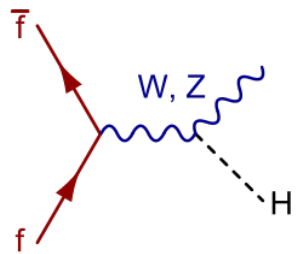
Nature 607, 52–59 (2022)



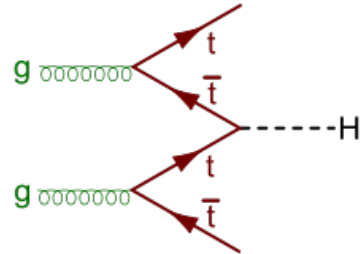
$ggF$



VBF:  $6.5 \sigma$

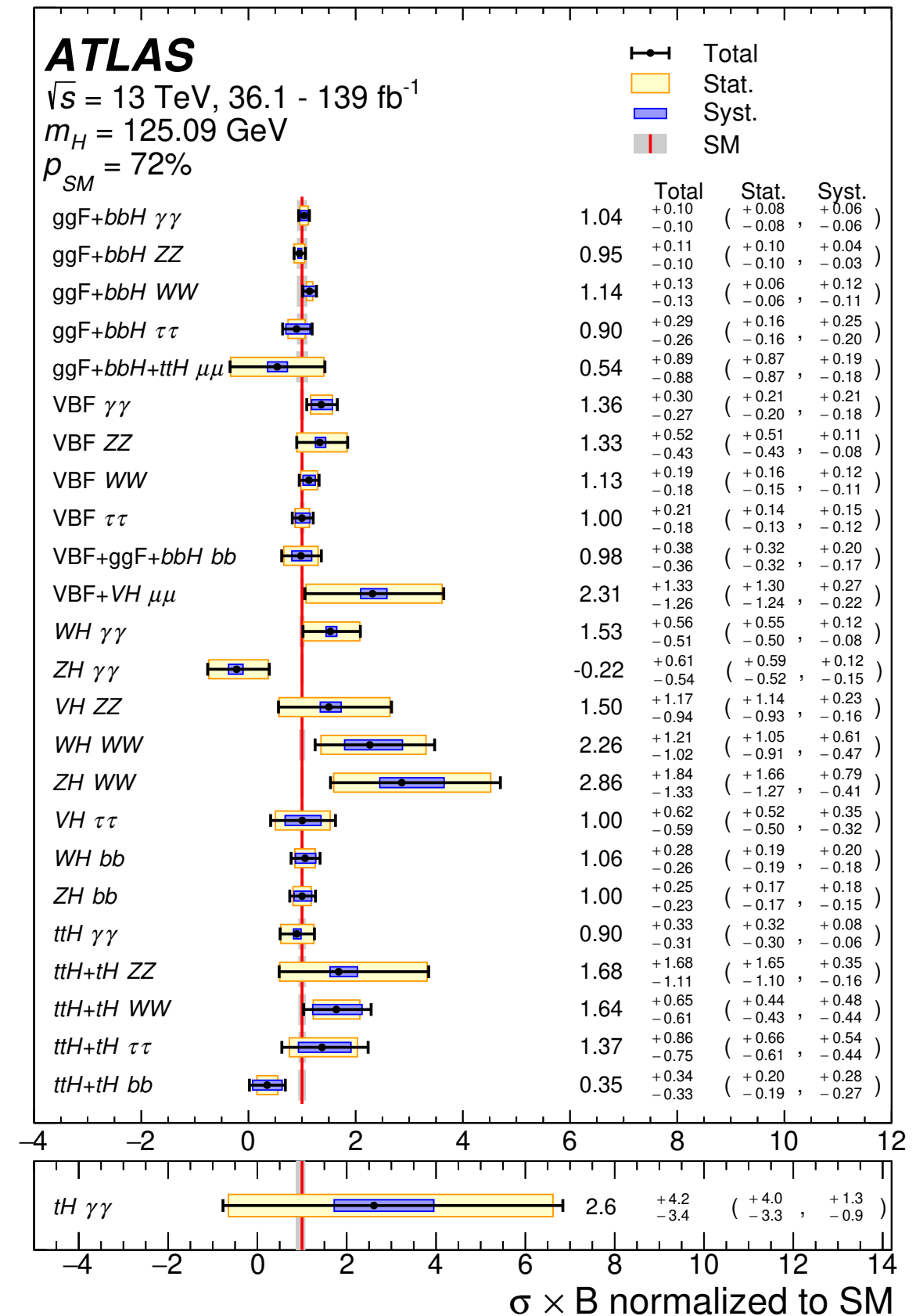


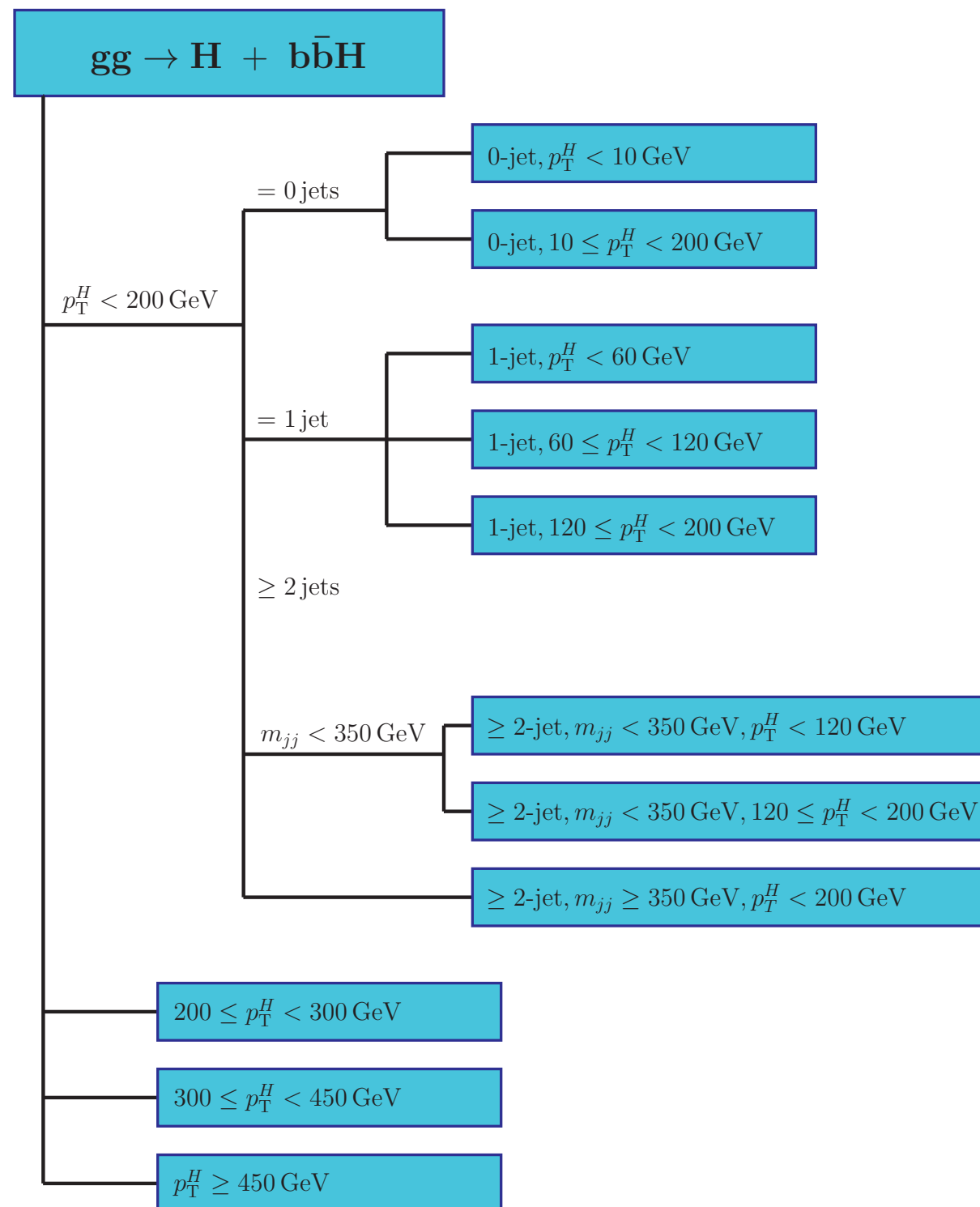
$VH: 5.3 \sigma$



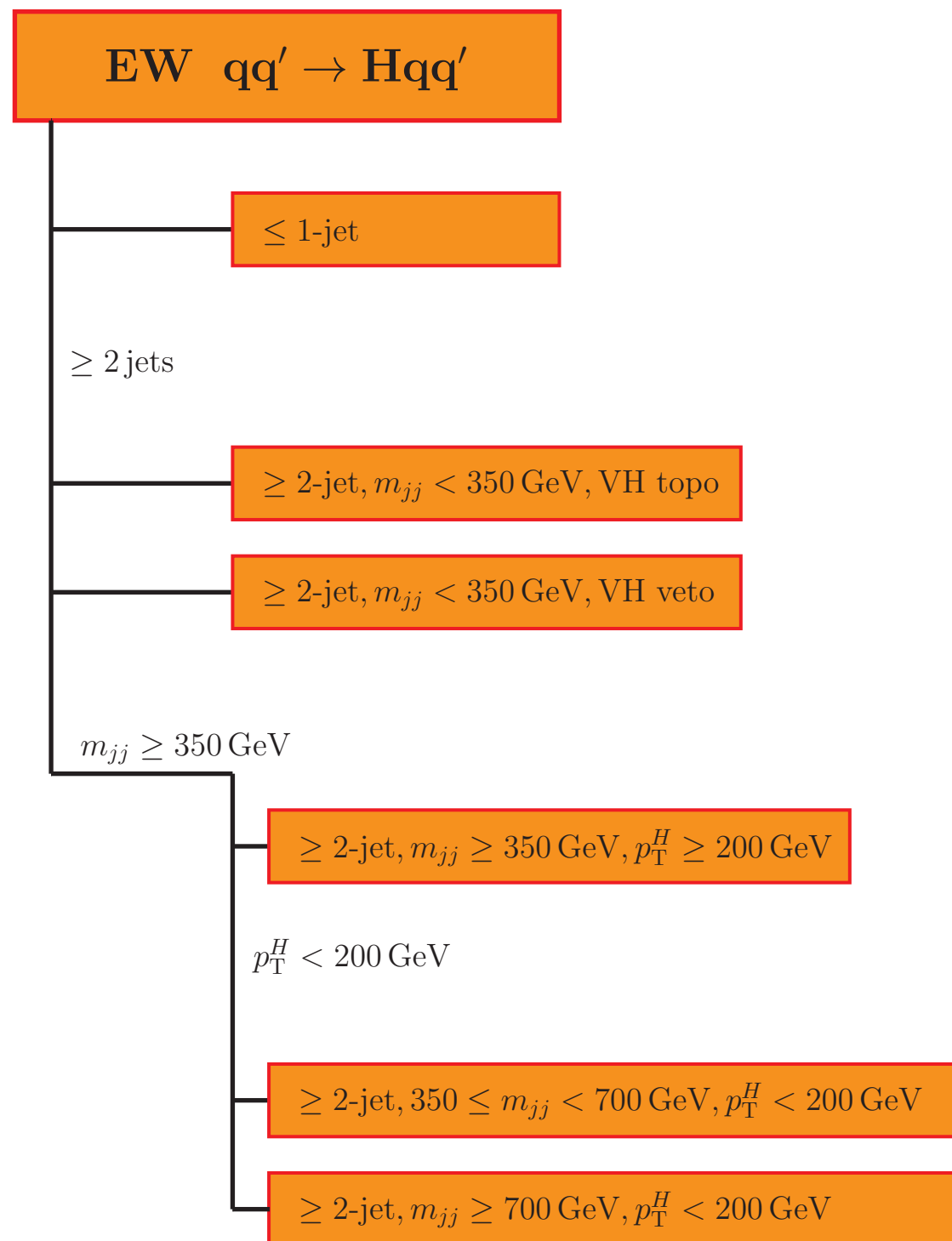
$t\bar{t}H: 5.8 \sigma$

- In the first Run-2 data observed all SM production modes at the LHC.
- ▶ With current precision uncertainties from 20% to 7% on production cross section.
- ▶ Sufficient for more in-depth investigations into the couplings



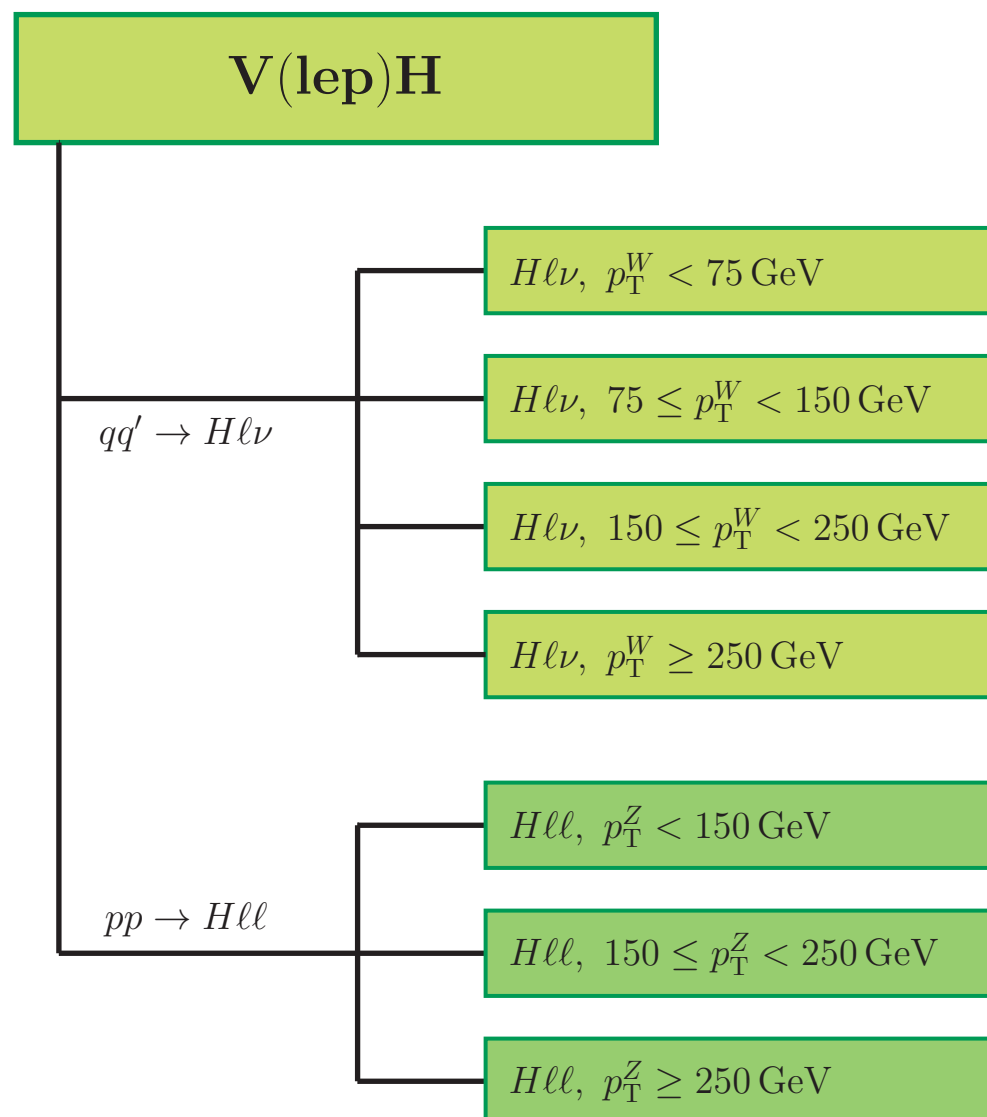


- Measure mutually exclusive phase-spaces
  - ▶ In terms of kinematics of the Higgs or associated objects in productions.
  - ▶ Sensitivity to deviations from SM.
  - ▶ Avoidance of large modelling uncertainties.
  - ▶ Approximate experimental sensitivity.
- Advantage of complementary sensitivity in production from different final states:
  - ▶  $m_{jj} > 450$  GeV from  $H \rightarrow WW^*$
  - ▶ High  $p_T^H$  from  $H \rightarrow bb$

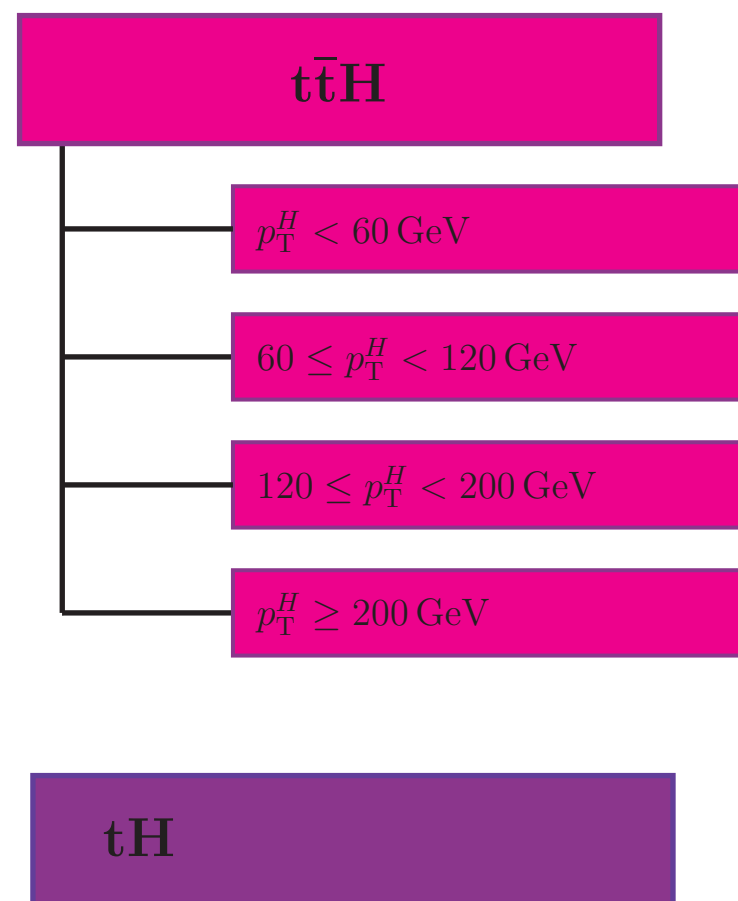


- Measure mutually exclusive phase-spaces
  - ▶ In terms of kinematics of the Higgs or associated objects in productions.
  - ▶ Sensitivity to deviations from SM.
  - ▶ Avoidance of large modelling uncertainties.
  - ▶ Approximate experimental sensitivity.
- Advantage of complementary sensitivity in production from different final states:
  - ▶  $m_{jj} > 450$  GeV from  $H \rightarrow WW^*$
  - ▶ High  $p_T^H$  from  $H \rightarrow bb$

- Measure mutually exclusive phase-spaces
  - ▶ In terms of kinematics of the Higgs or associated objects in productions.
  - ▶ Sensitivity to deviations from SM.
  - ▶ Avoidance of large modelling uncertainties.
  - ▶ Approximate experimental sensitivity.
- Advantage of complementary sensitivity in production from different final states:
  - ▶  $m_{jj} > 450 \text{ GeV}$  from  $H \rightarrow WW^*$
  - ▶ High  $p_T^H$  from  $H \rightarrow bb$

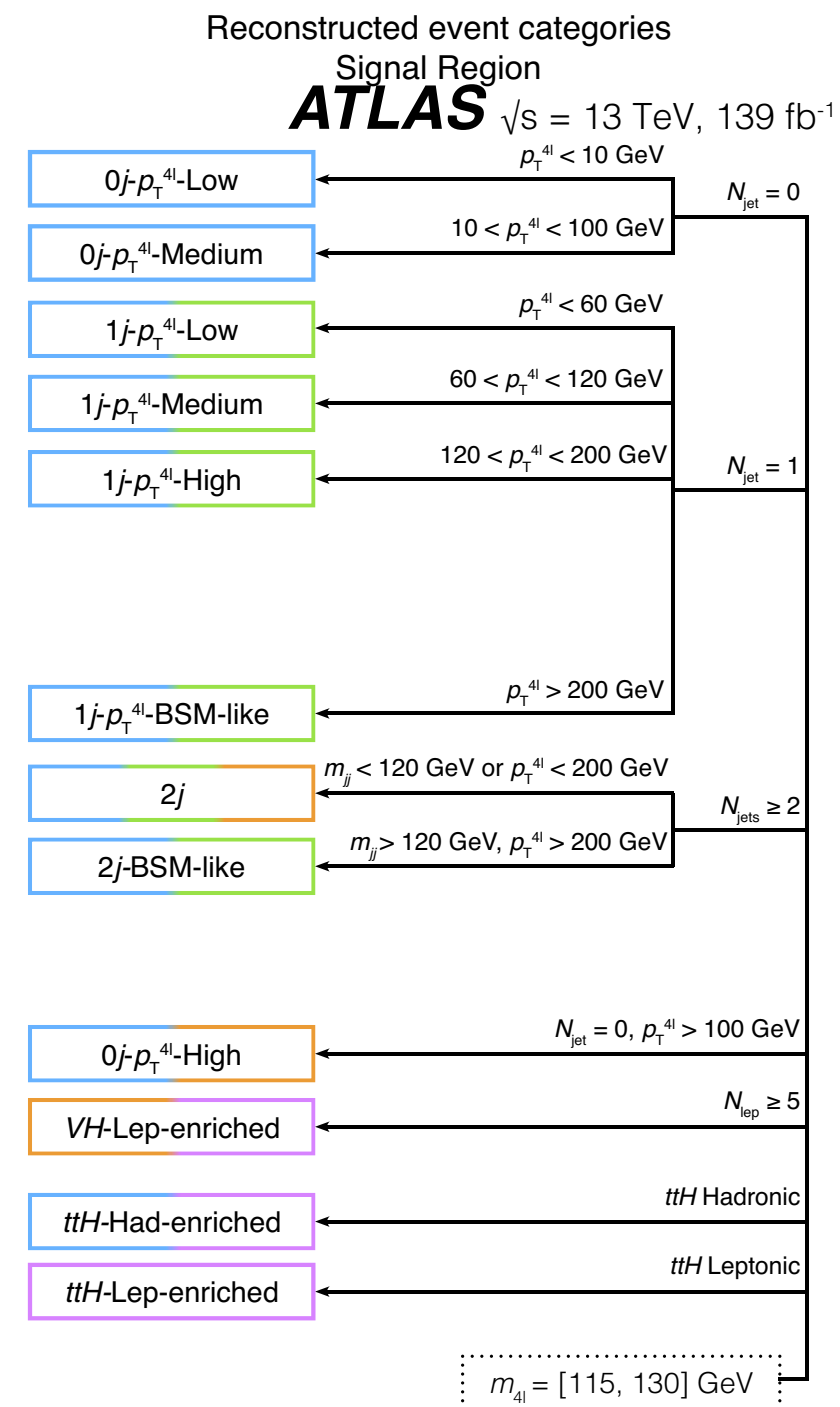
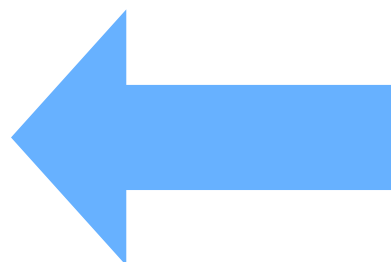
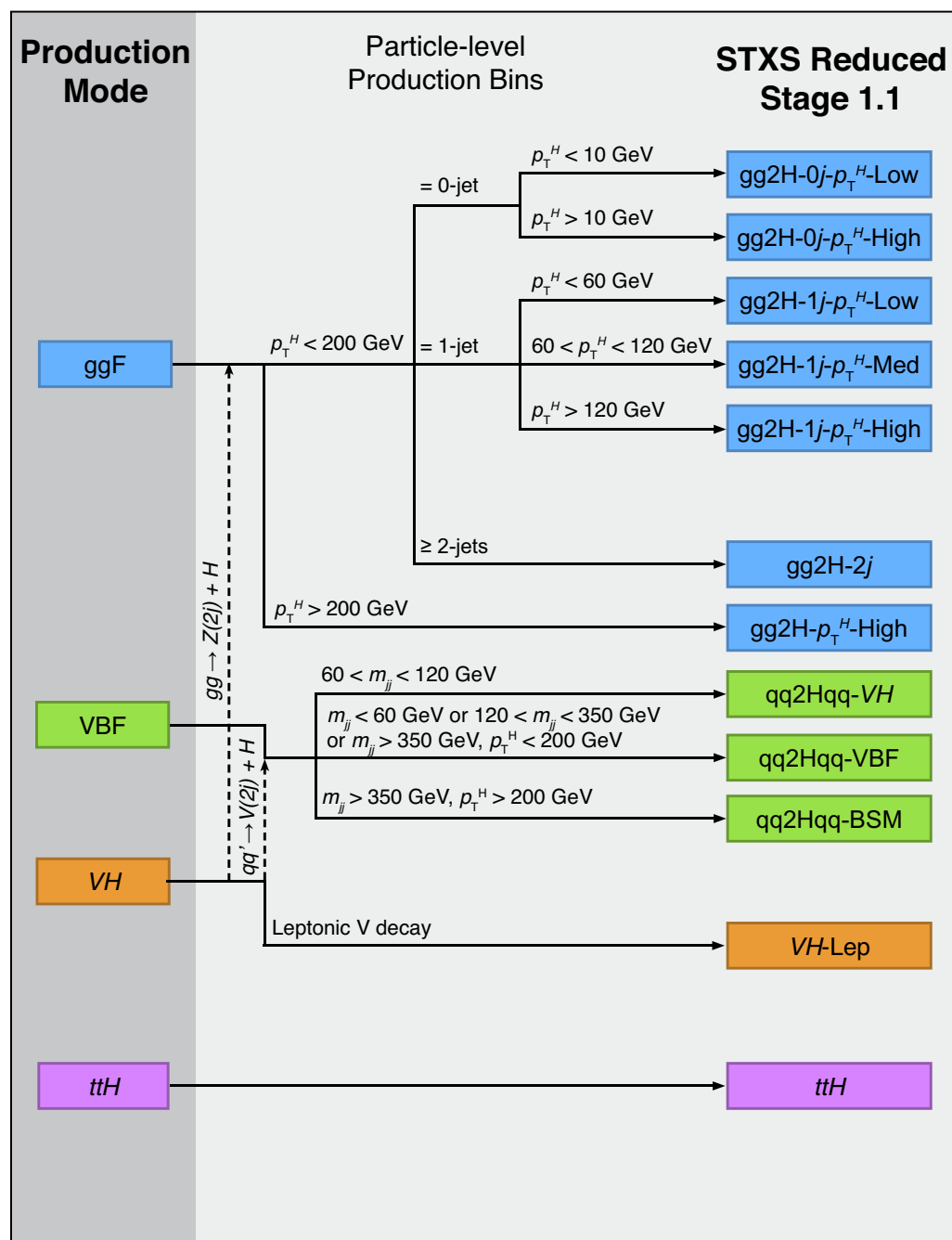






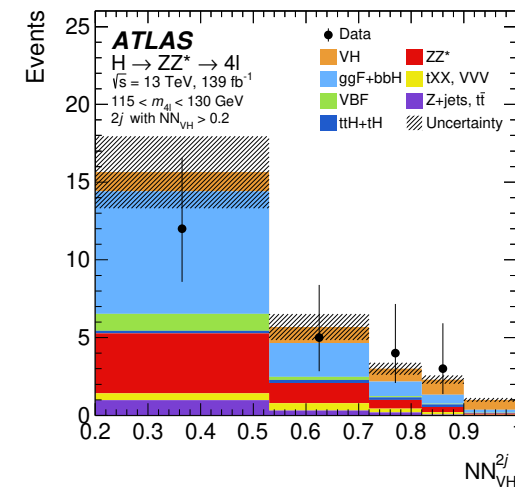
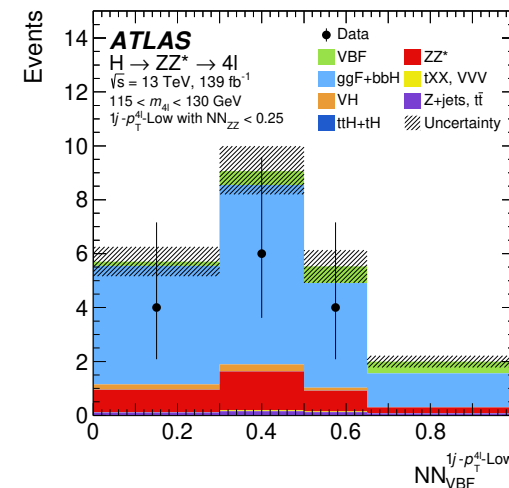
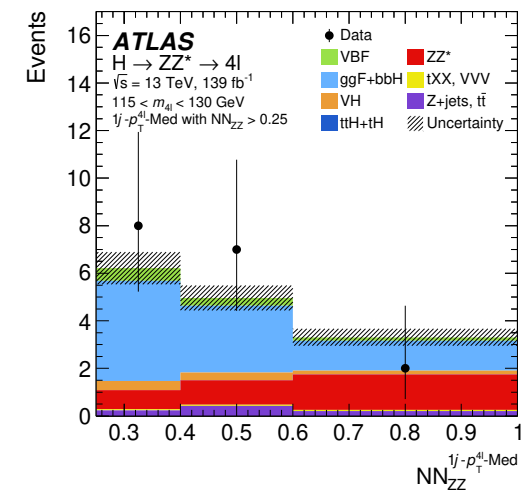
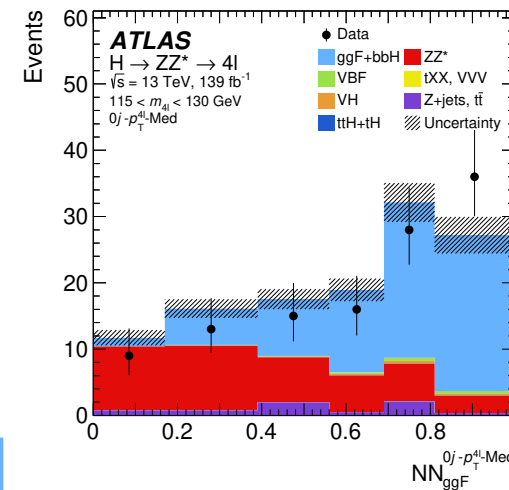
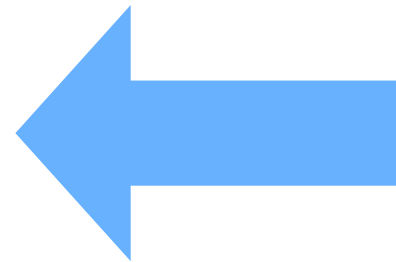
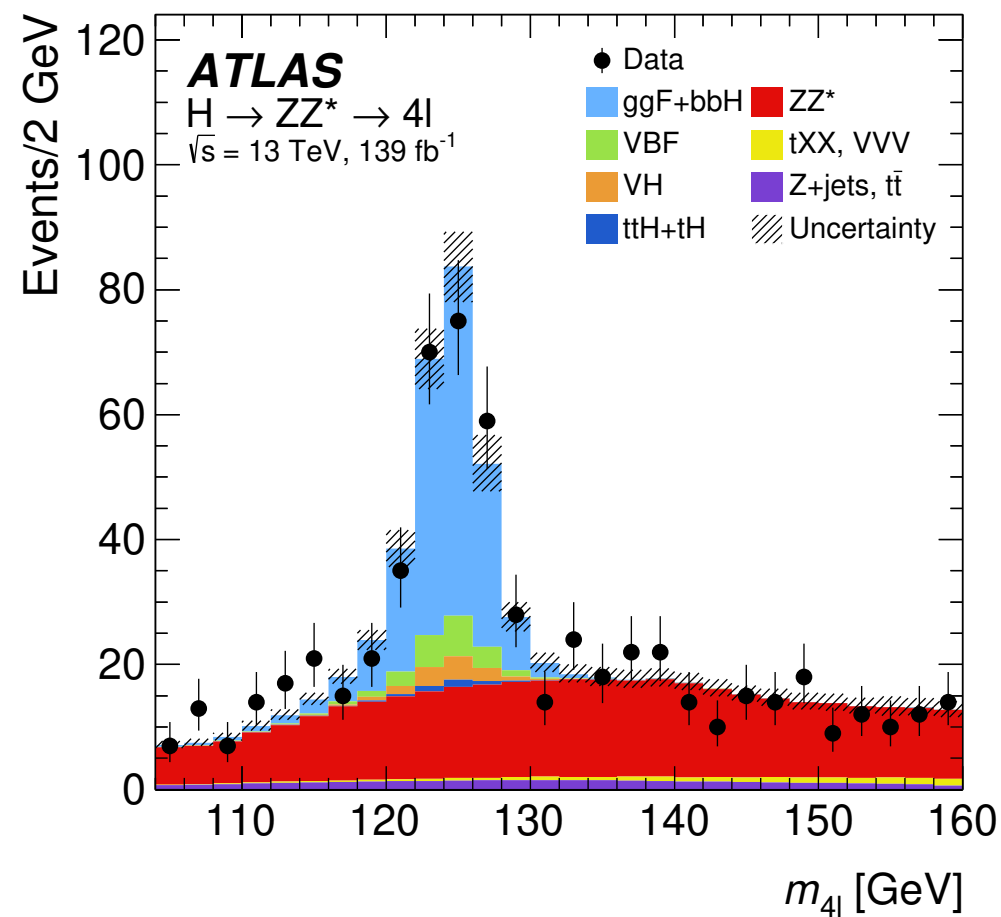
- Measure mutually exclusive phase-spaces
  - ▶ In terms of kinematics of the Higgs or associated objects in productions.
  - ▶ Sensitivity to deviations from SM.
  - ▶ Avoidance of large modelling uncertainties.
  - ▶ Approximate experimental sensitivity.
- Advantage of complementary sensitivity in production from different final states:
  - ▶  $m_{jj} > 450 \text{ GeV}$  from  $H \rightarrow WW^*$
  - ▶ High  $p_T^H$  from  $H \rightarrow bb$

- Strategy in measuring the cross section in these exclusive categories
  - Discussing here the example of the  $H \rightarrow ZZ^*$
- Cut-based reconstruction-level categories,
  - maximising purity and minimising extrapolation to true phase-spaces.

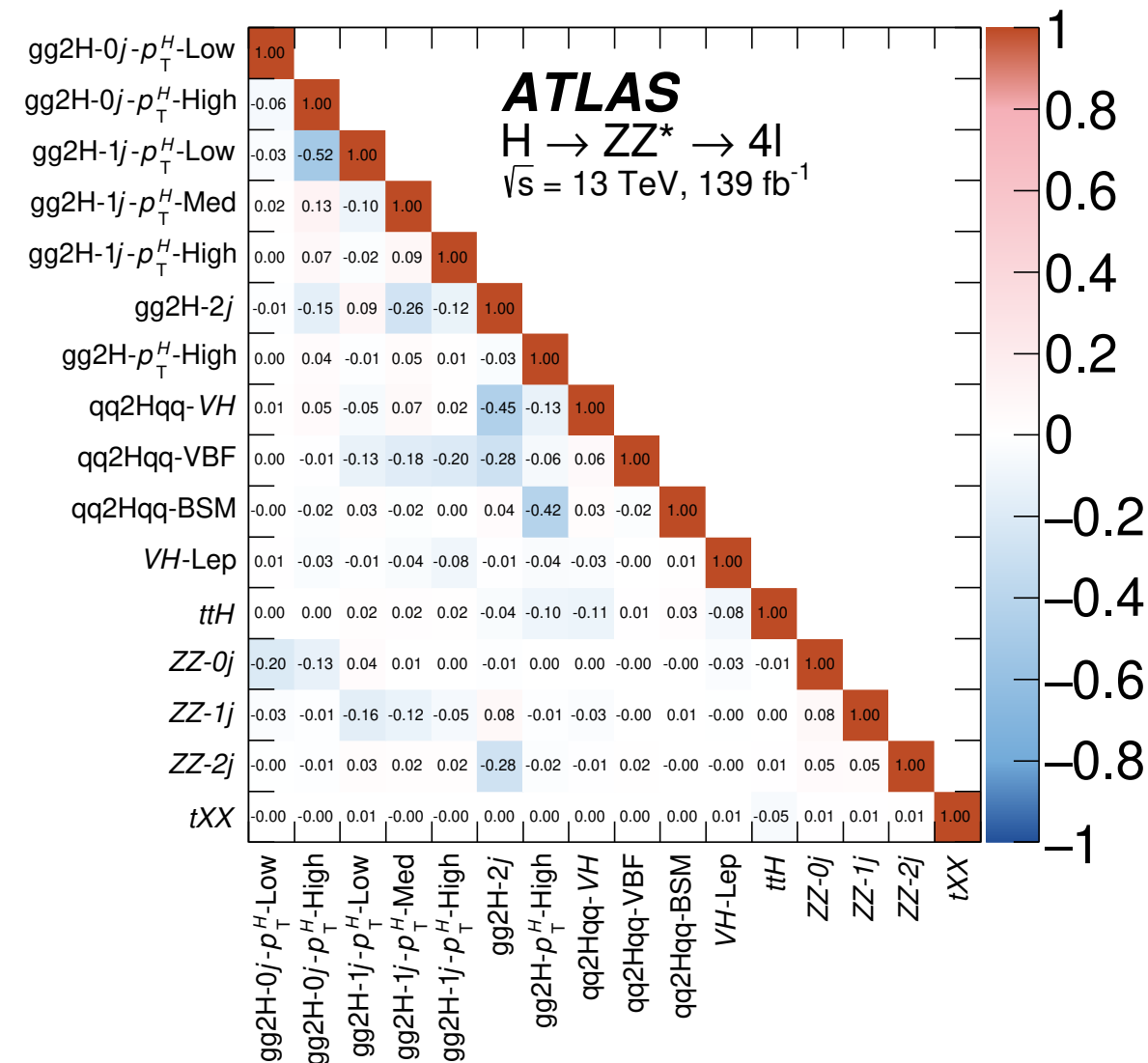
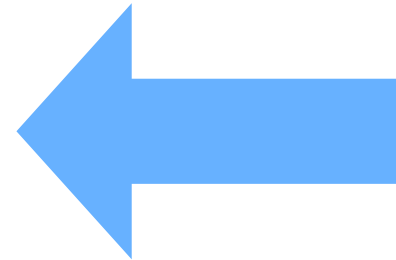
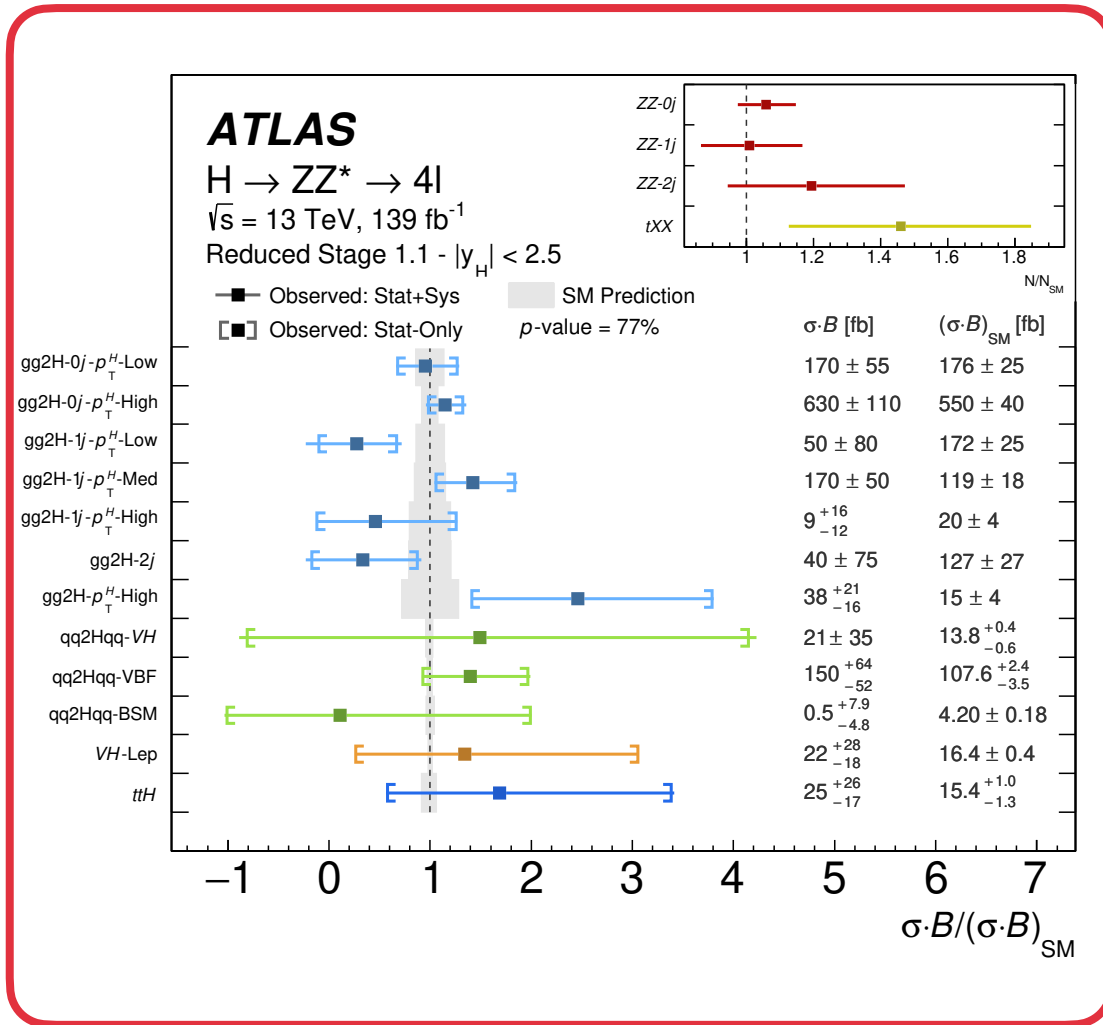


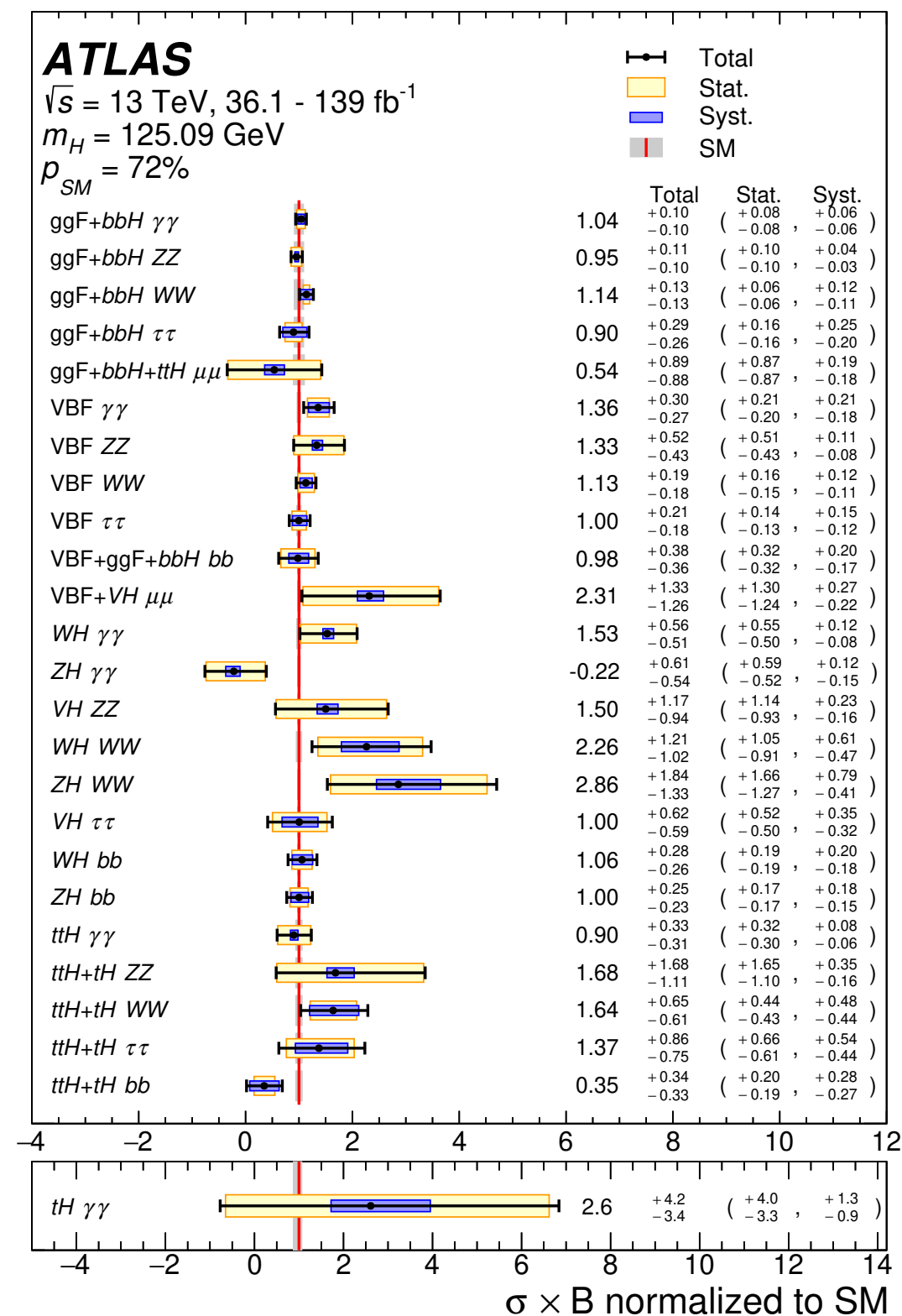
- Multi-output-node neural network discriminants in detector category.
  - Multidimensional fits on  $n$ -1 dimensions on  $n$  output nodes per category.
- Backgrounds from data sidebands on resonant signal.
  - Performed as a function of the jet multiplicity to reduce higher order correction uncertainties.

**ATLAS**  $\sqrt{s} = 13 \text{ TeV}, 139 \text{ fb}^{-1}$



- Multi-output-node neural network discriminants in detector category.
  - Multidimensional fits on  $n$ -1 dimensions on  $n$  output nodes per category.
- Backgrounds from data sidebands on resonant signal.
  - Performed as a function of the jet multiplicity to reduce higher order correction uncertainties.

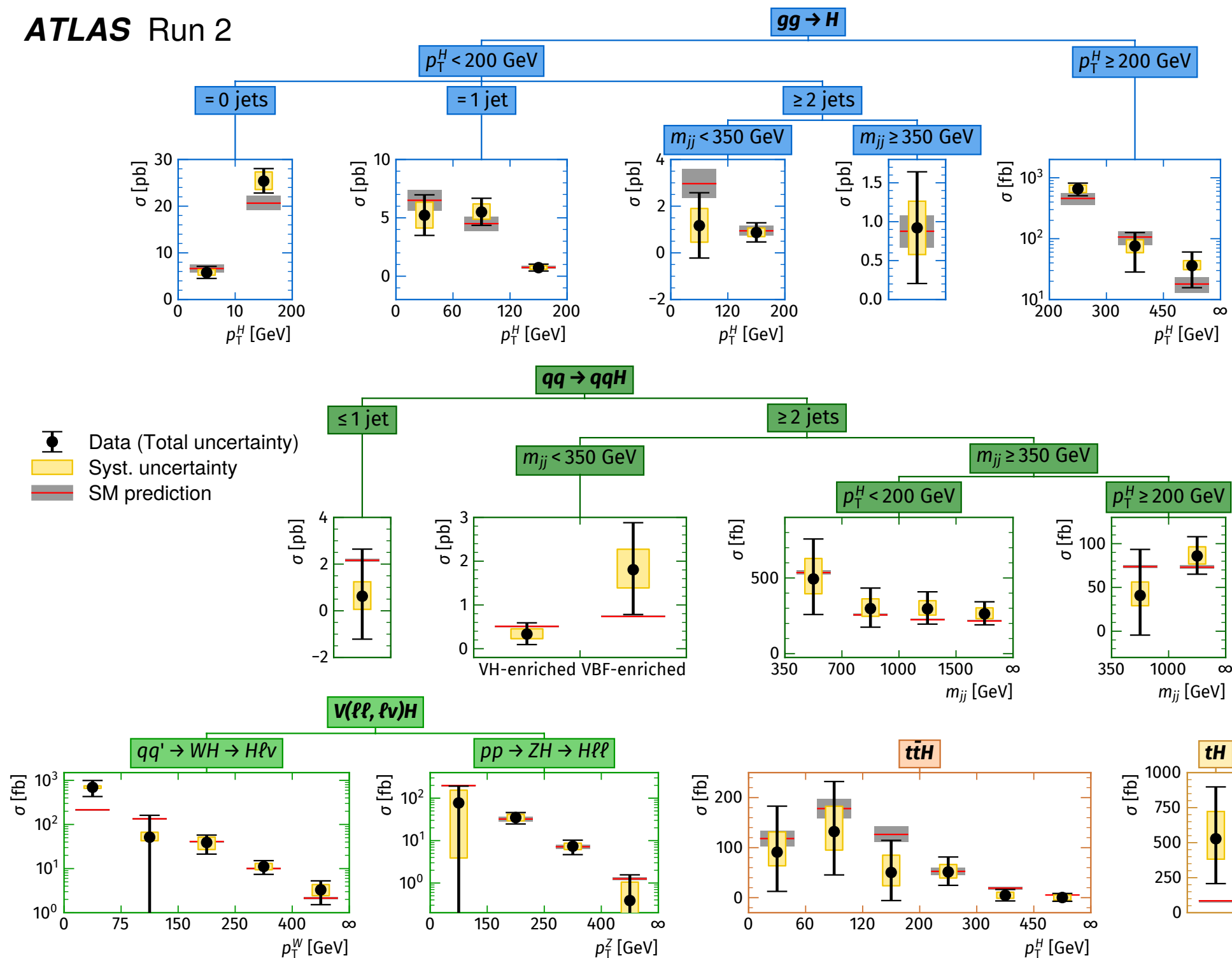




- Measure mutually exclusive phase-spaces
  - ▶ In terms of kinematics of the Higgs or associated objects in productions.
  - ▶ Sensitivity to deviations from SM.
  - ▶ Avoidance of large modelling uncertainties.
  - ▶ Approximate experimental sensitivity.
- Advantage of complementary sensitivity in production from different final states:
  - ▶  $m_{jj} > 450 \text{ GeV}$  from  $H \rightarrow WW^*$
  - ▶ High  $p_T^H$  from  $H \rightarrow bb$

- Measure mutually exclusive phase-spaces

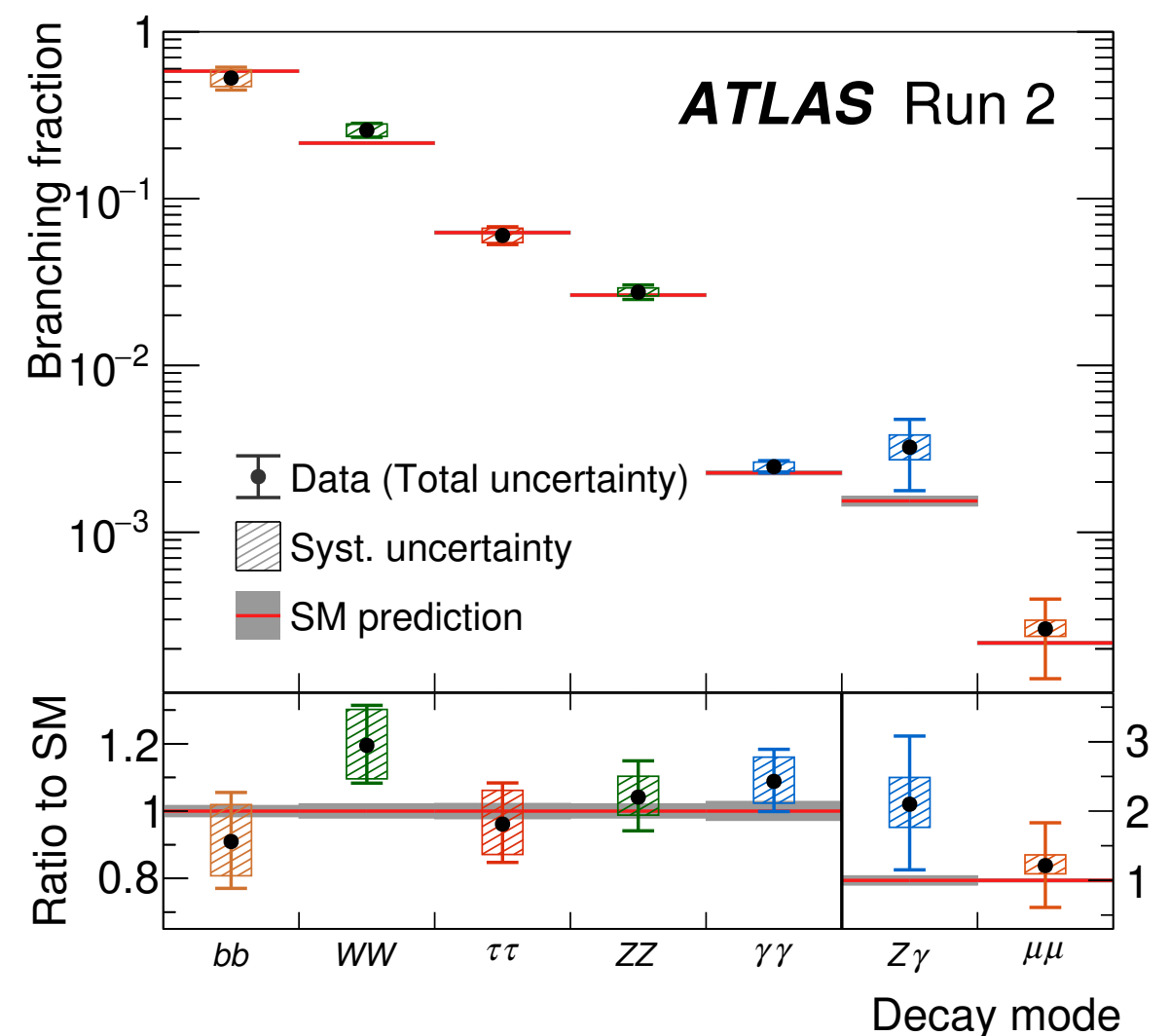
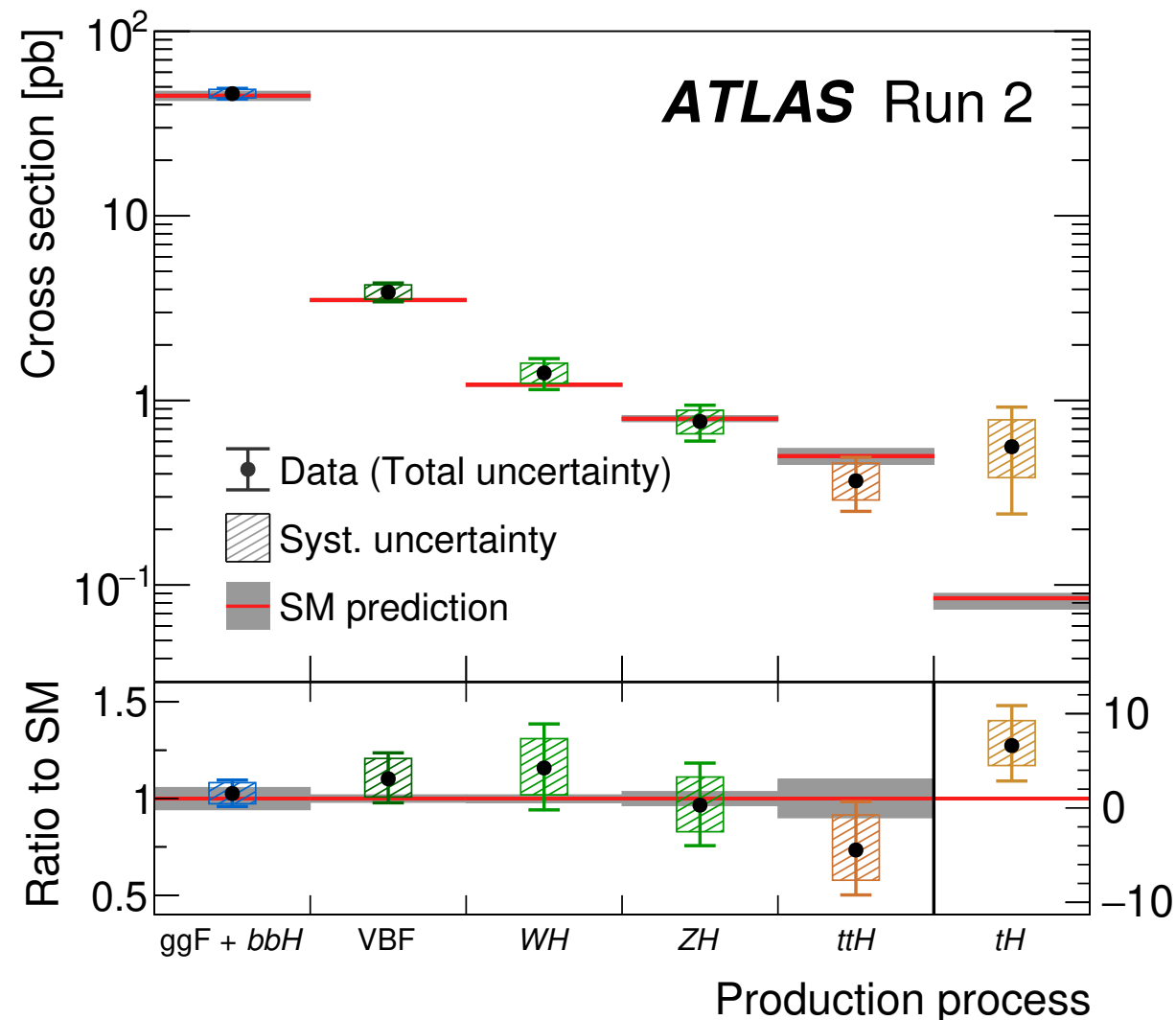
**ATLAS Run 2**



- Simultaneous fit to all template cross sections

- ▶ Extraction of global signal strength ( $\mu = \sigma^{\text{obs}} / \sigma^{\text{exp}}$ ).
- ▶ Experimental sensitivity of the same order as of theory (up to N<sup>3</sup>LO for ggF)

$$\mu = 1.05 \pm 0.06 = 1.05 \pm 0.03 \text{ (stat.)} \pm 0.03 \text{ (exp.)} \pm 0.04 \text{ (sig. th.)} \pm 0.02 \text{ (bkg. th.)}$$

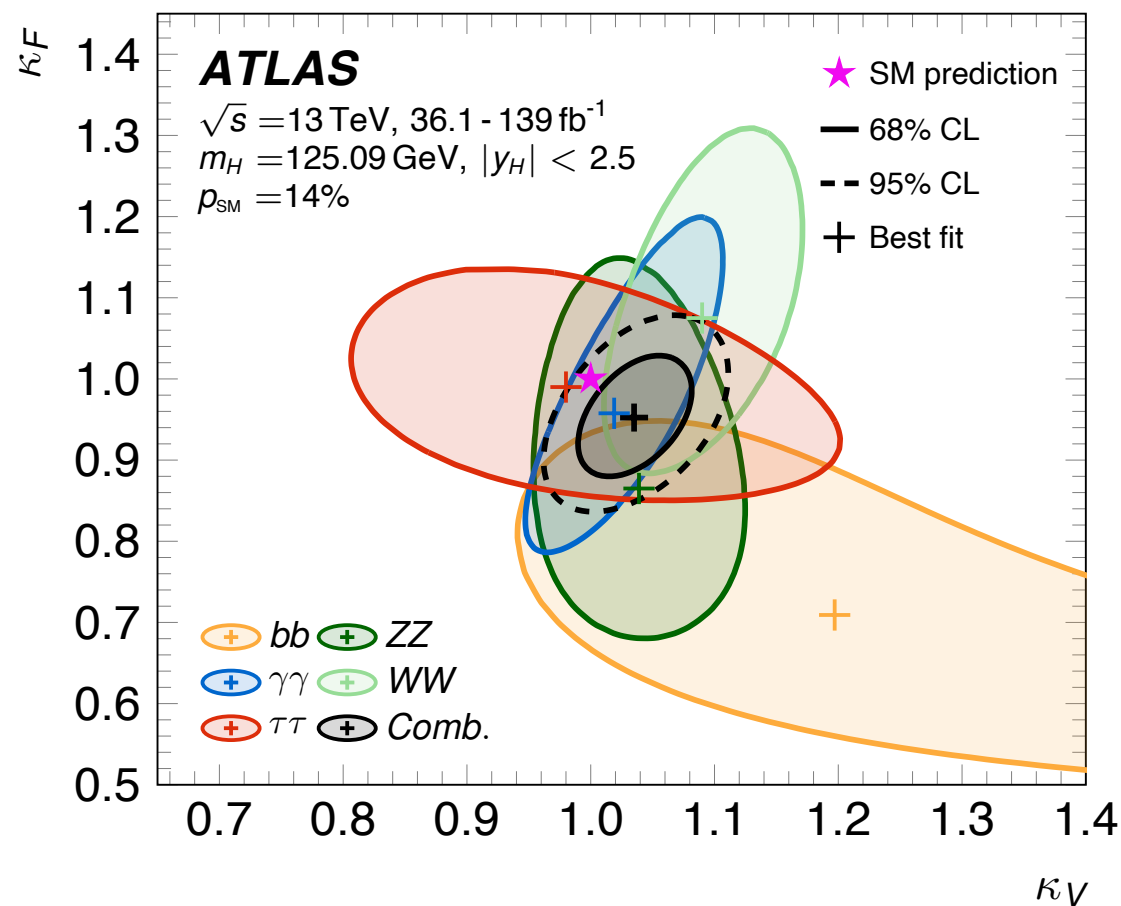


# Running couplings

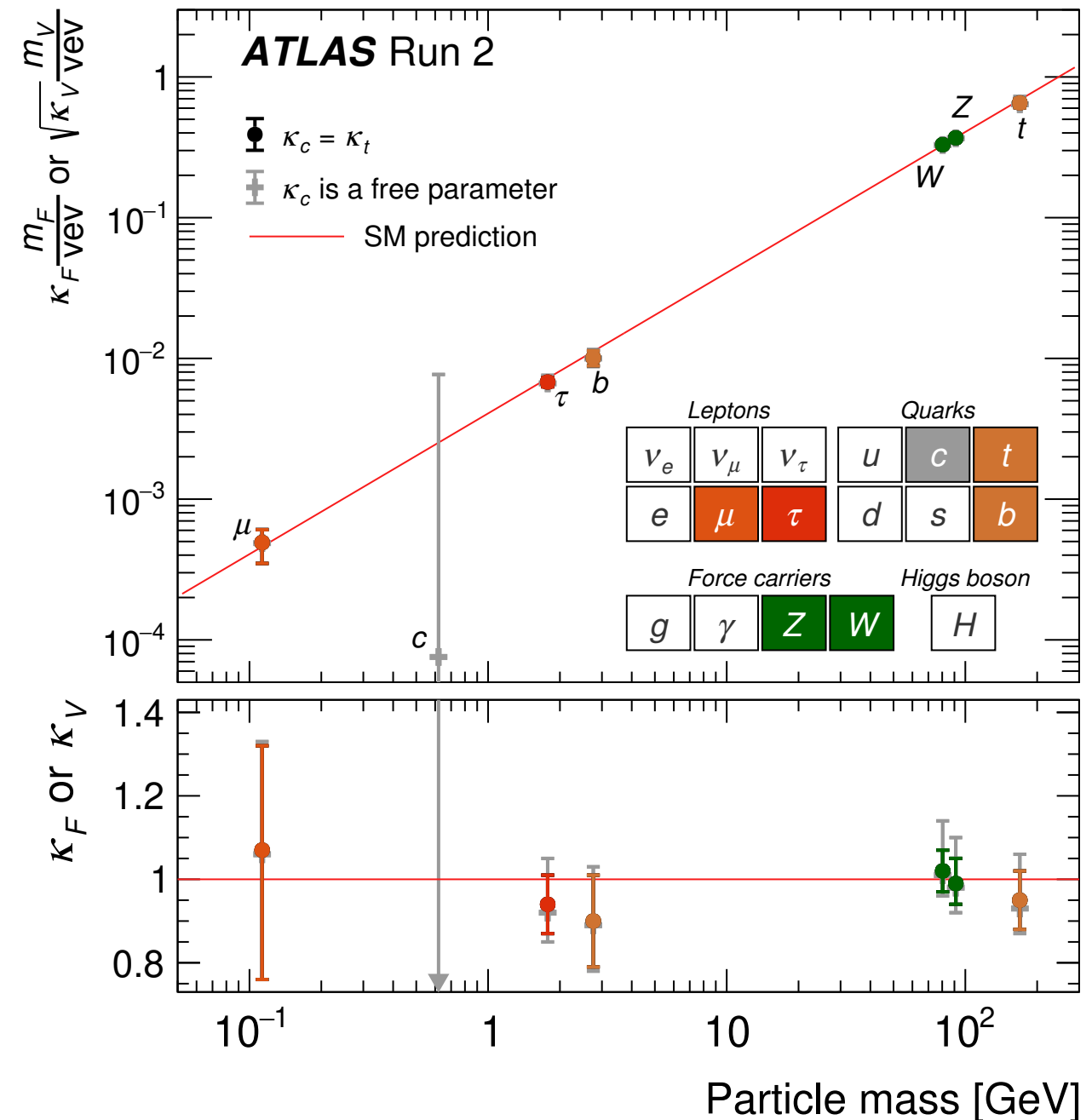
Nature 607, 52–59 (2022)

- Higgs boson couplings as a function of the particle's mass.
- Assuming production and decay are factorised
- Coupling strength modifiers

$$\sigma_i \times B_f = \frac{\sigma_i(\kappa) \times \Gamma_f(\kappa)}{\Gamma_H}$$



- Unprecedented agreement with SM Higgs.
- Yet, given  $m_H$ 's value new phenomena might stabilise the vacuum expectation ?





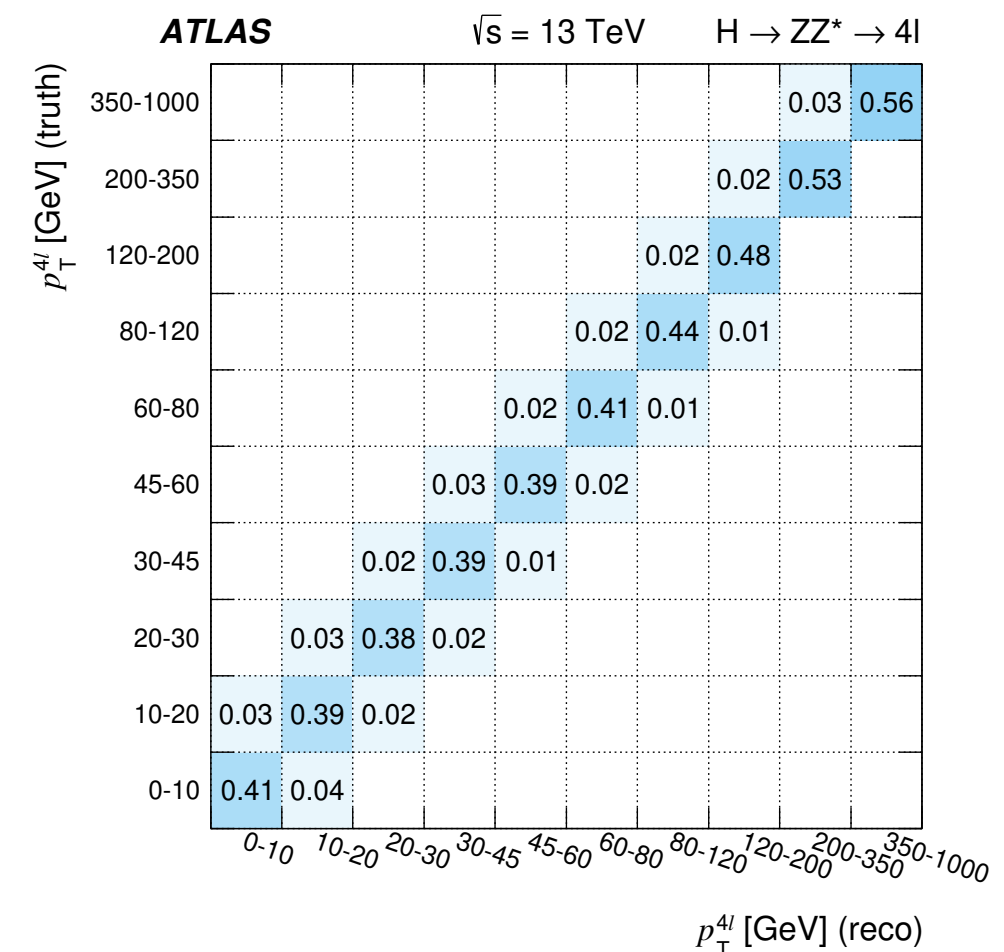
## 5. Differential cross section measurements

- At Run II sufficient statistics for constraining differential measurements
- Fiducial cross section definition
  - ▶ including detector efficiency ( $C$ ), detector acceptance ( $A$ ) and branching  $\mathcal{B}$

$$\sigma_{i,\text{fid}} = \sigma_i \times A_i \times \mathcal{B} = \frac{N_{i,\text{fit}}}{\mathcal{L} \times C_i}$$

- ▶ Cuts mimicking reconstruction selection:
  - (i) Model independent result.
  - (ii) No extrapolation beyond measurable phase-space

- In diboson channels, resonant peak over smooth background
  - ▶ Good resolution on final-state particles, in particular in  $H \rightarrow 4\ell, \gamma\gamma$
- *Unfolding* performed within the signal extraction fit

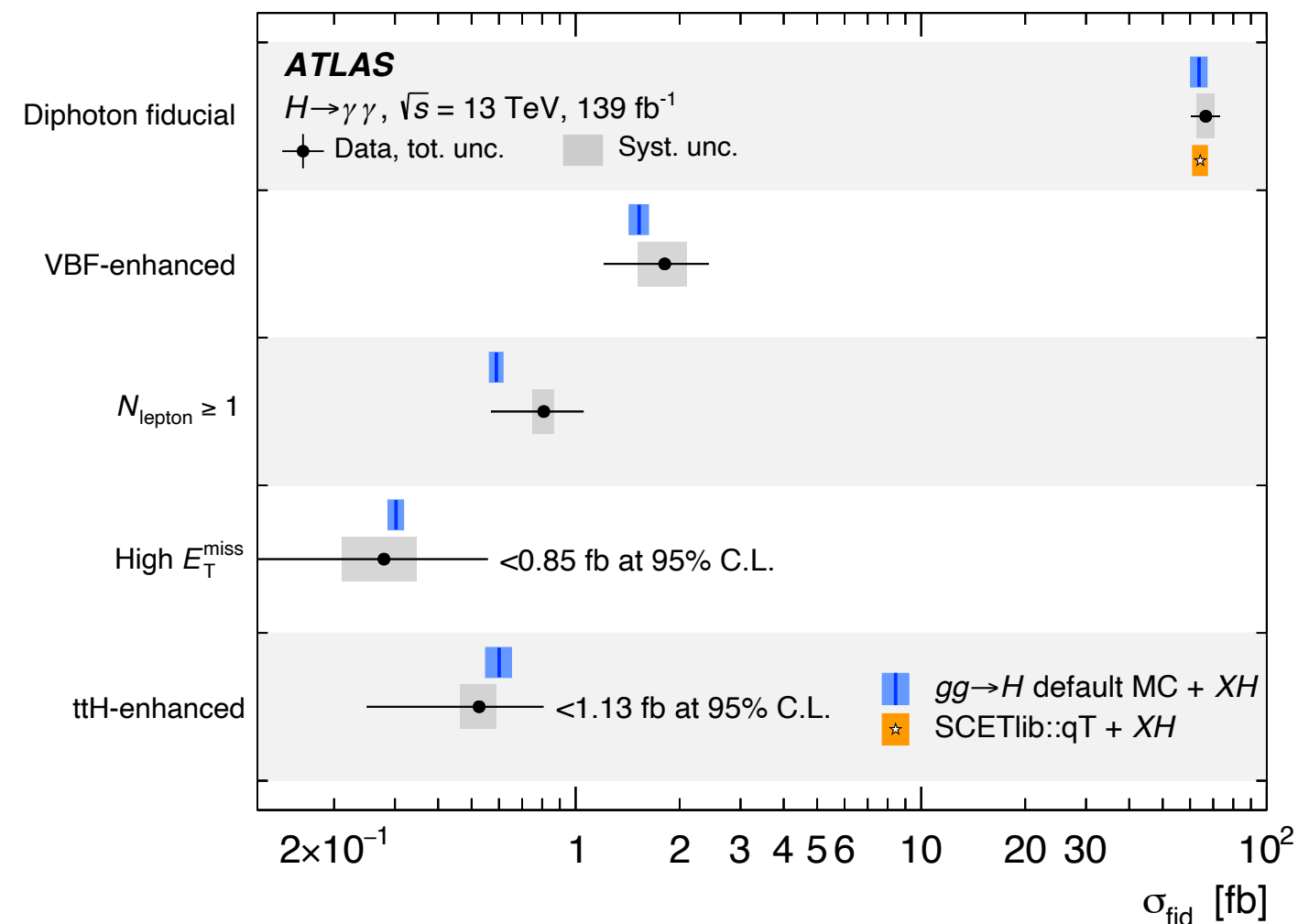
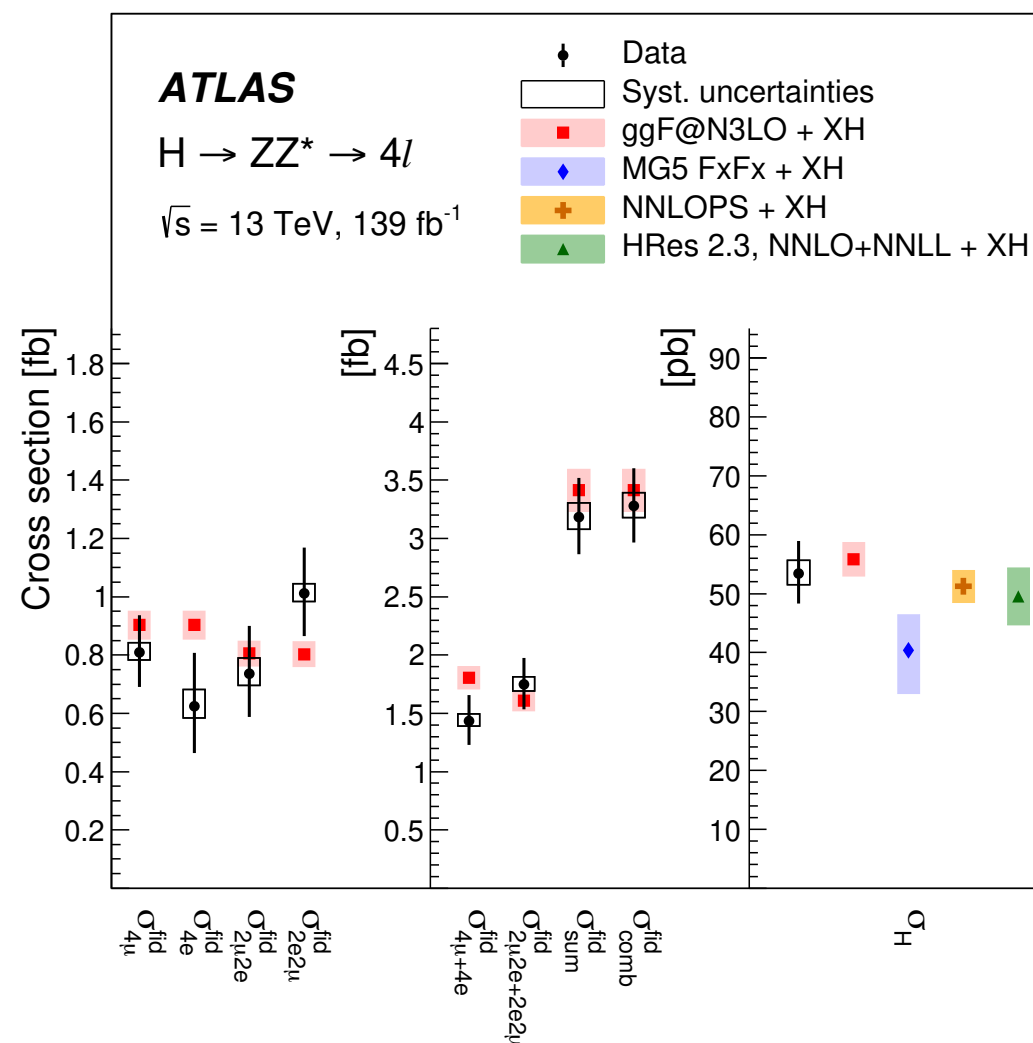


- Inclusive fiducial cross sections:

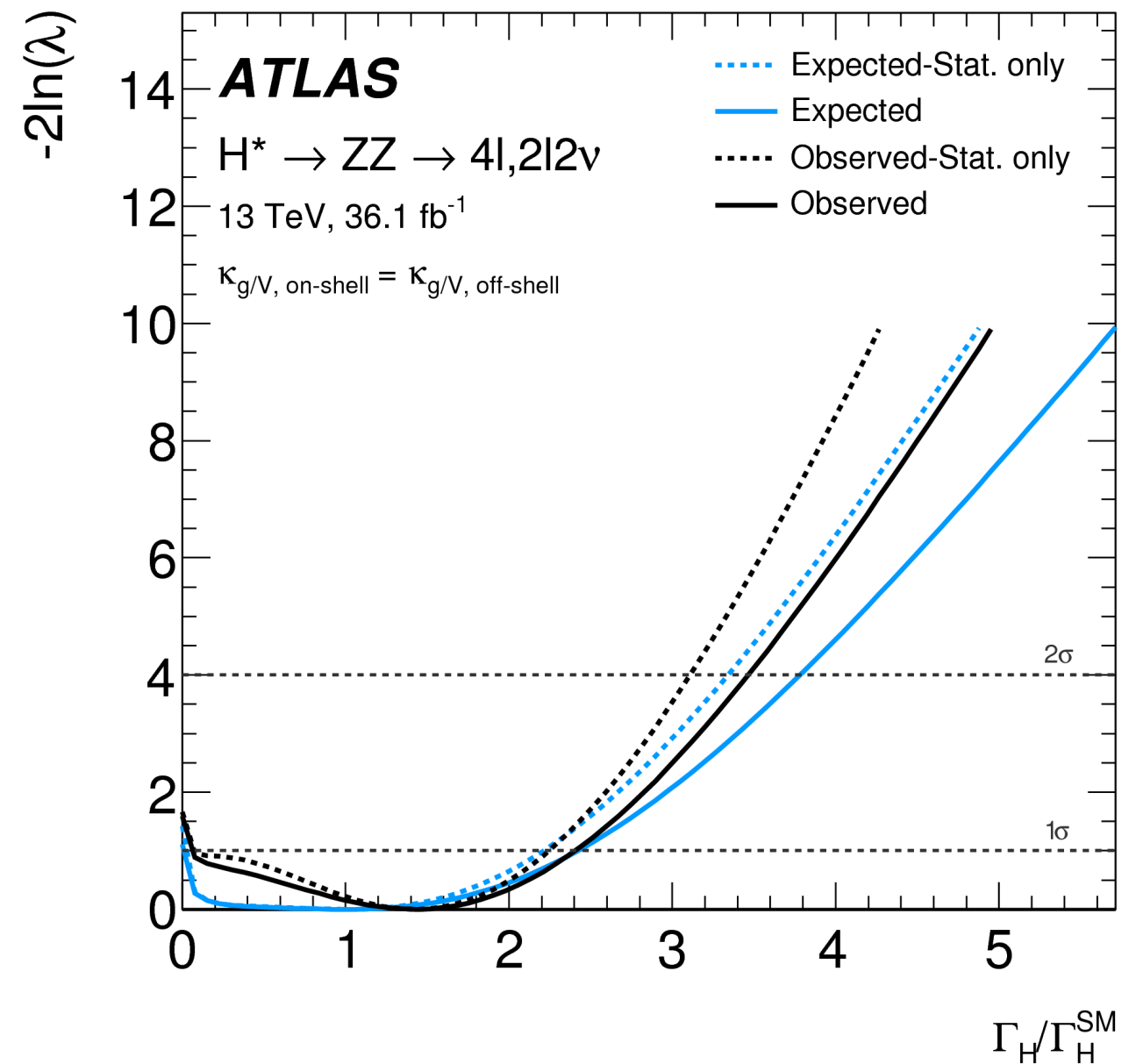
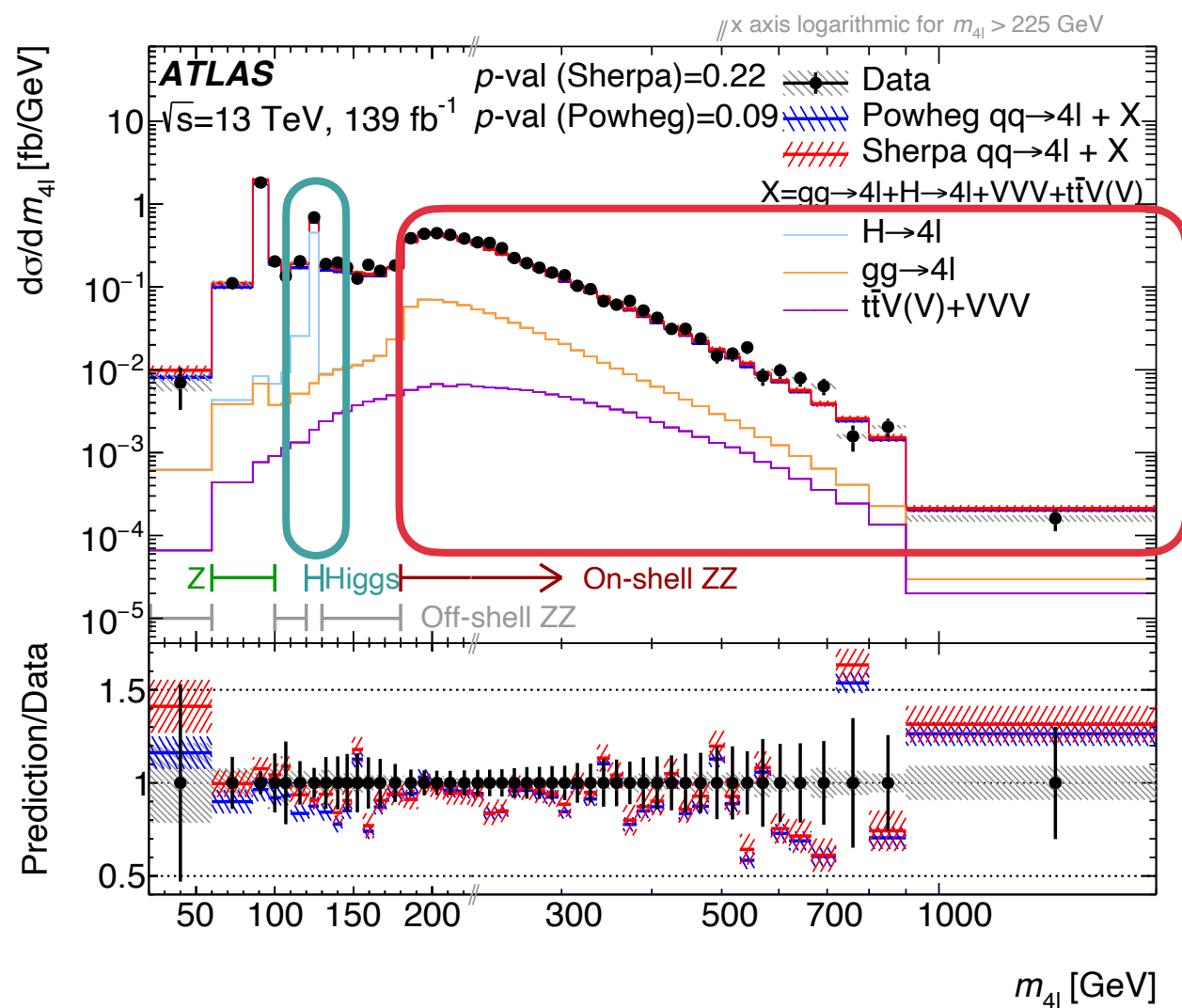
- ▶ SM predictions of  $3.33 \pm 0.15$  fb ( $H \rightarrow ZZ$ ) and  $63.5 \pm 3.3$  fb ( $H \rightarrow \gamma\gamma$ )

- For  $ZZ$  also cross section per final state

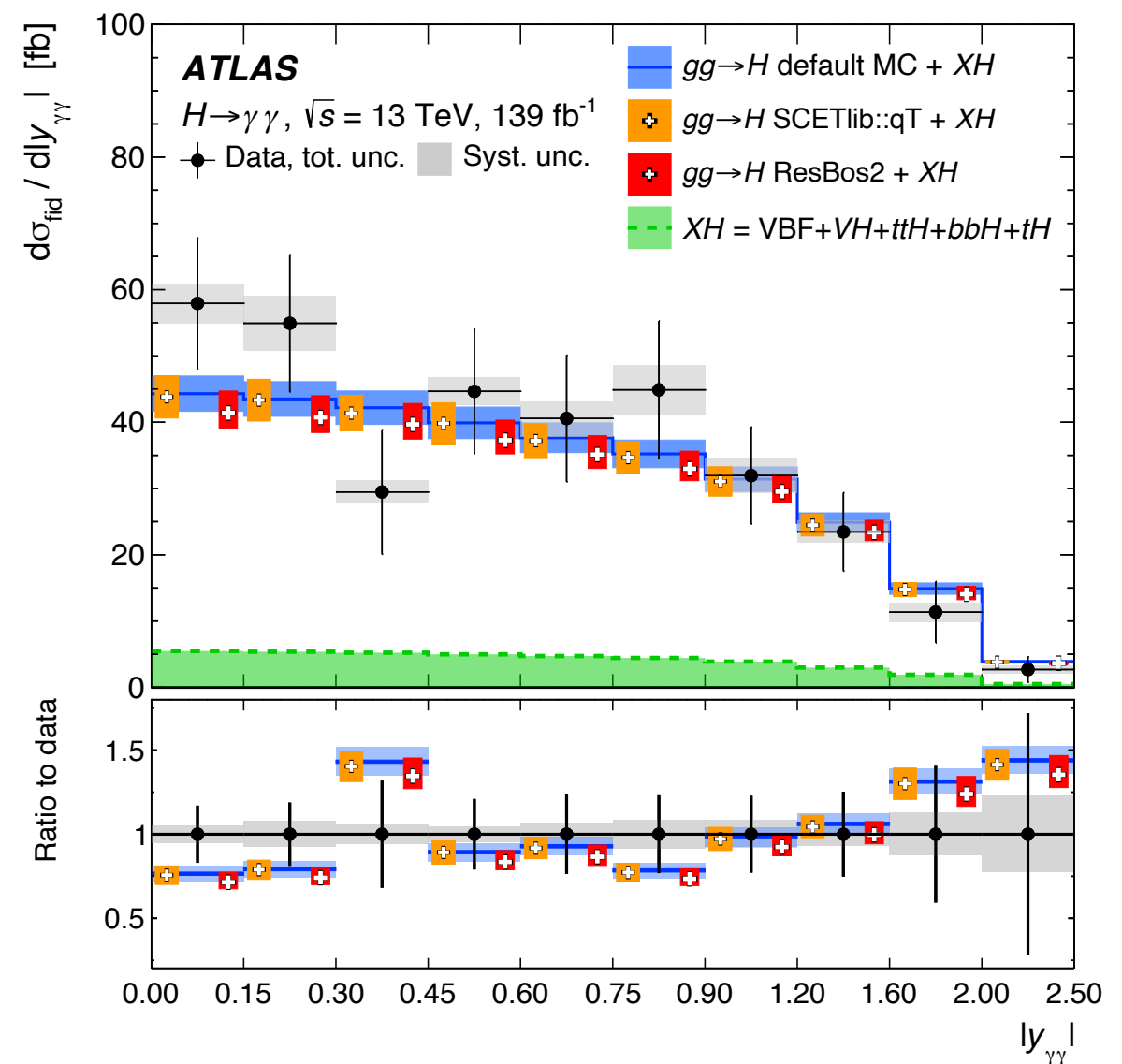
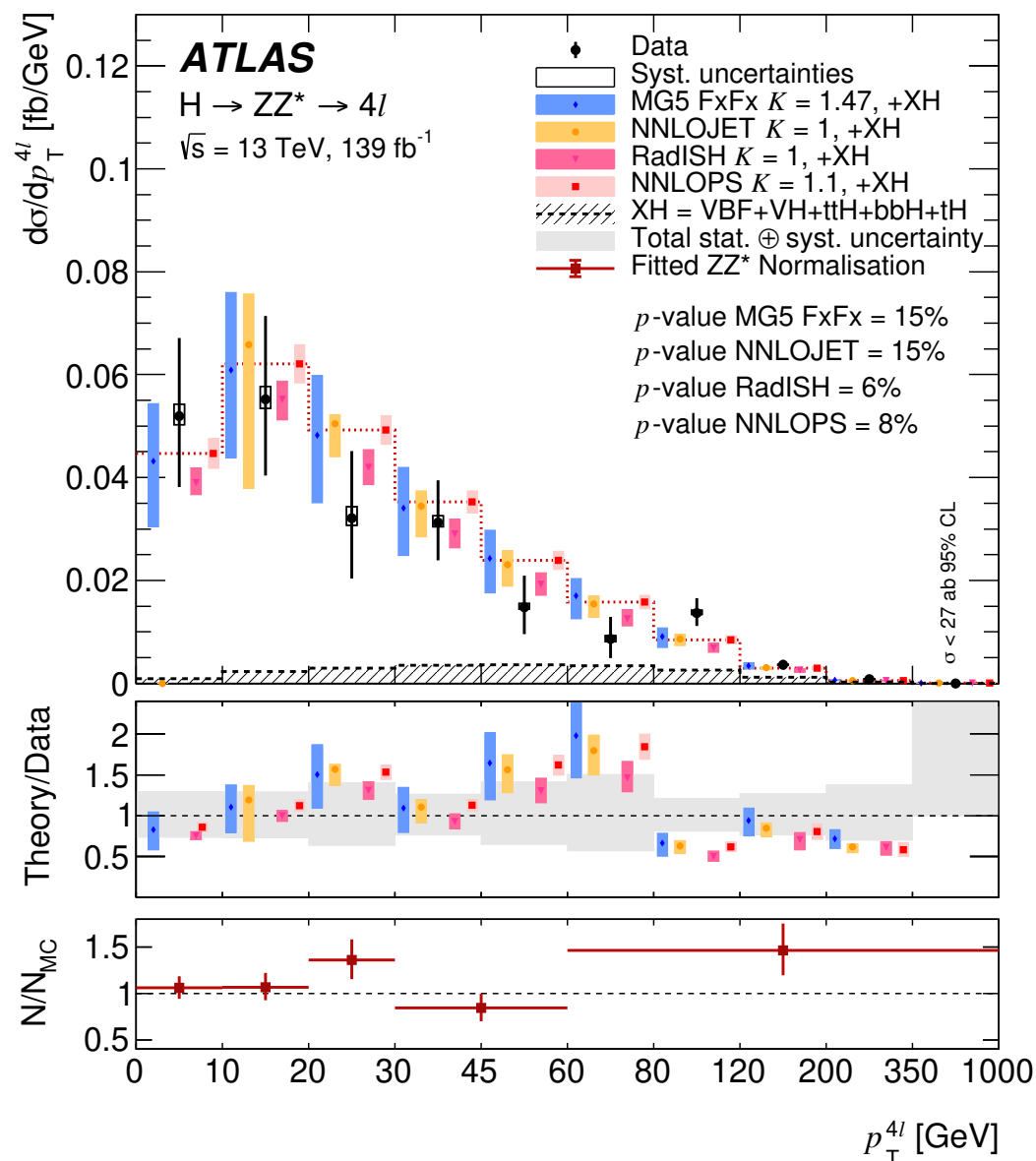
- ▶ Eventually sensitivity to final state interference (10%) in same flavour quadruplets



- Study of the the  $m_{4\ell}$  spectrum and off-shell  $H$  production
  - ▶ Offshell Higgs production, enhanced at 350 GeV because of top-quark loops in  $ggF$
  - ▶ Measured upper limit on width combining  $4\ell$  and  $\ell\bar{\ell}\nu\bar{\nu}$
  - ▶ Limit  $\Gamma_H$  possible from the off-shell to on-shell event yield ratio  $R_{gg}$ 
    - ◆ on-shell event yields  $\sim k_{g,\text{on-shell}}^2 / \Gamma_H$ , while off-shell  $\sim k_{g,\text{off-shell}}^2$

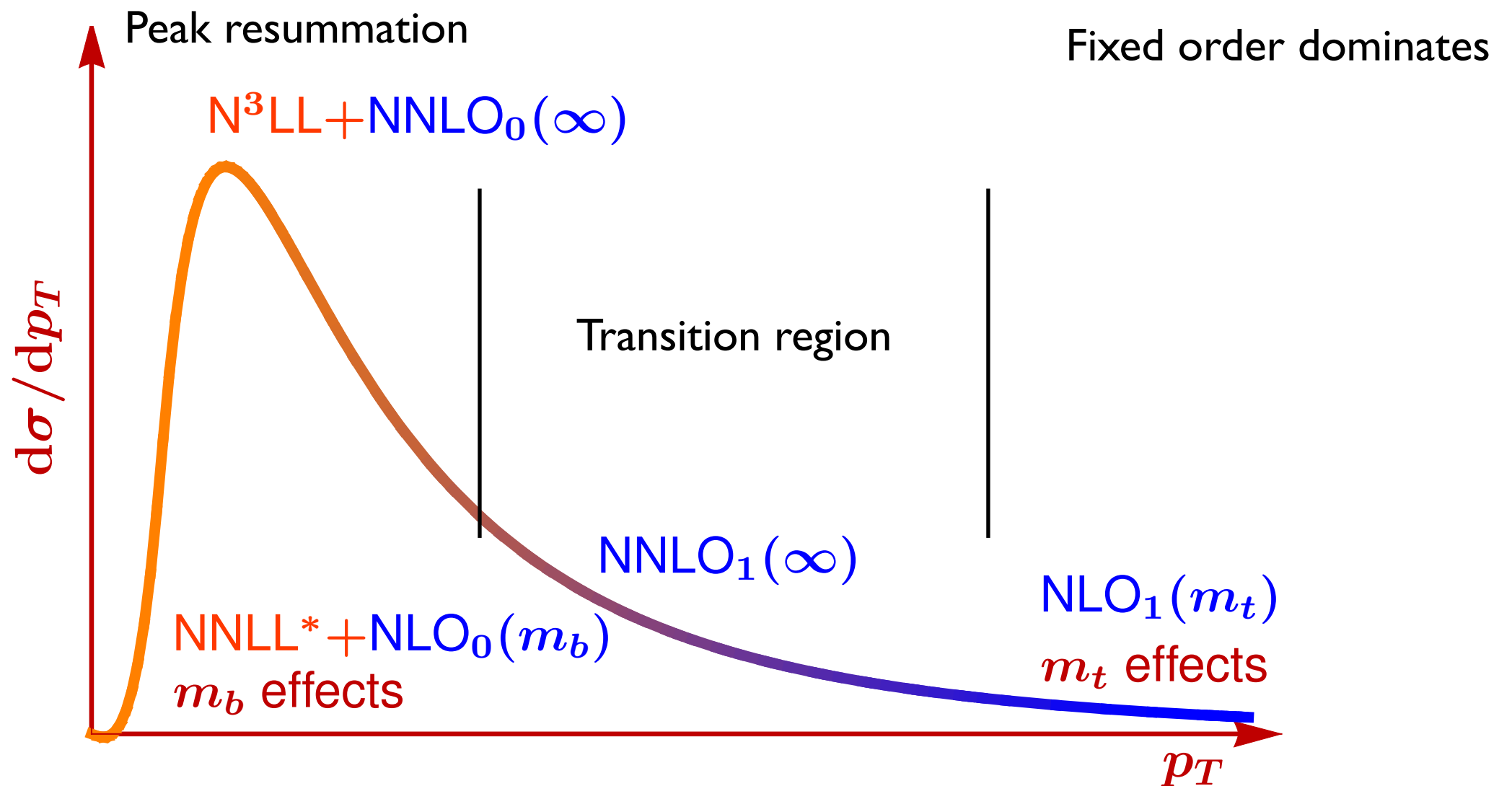


- $4\ell$ : isolate signal under the Higgs resonant peak.
- $\gamma\gamma$  cross section extracted from resonant peak over the  $\gamma\gamma$  continuum.
- Higgs boson  $p_{T,4\ell(\gamma\gamma)}$  and rapidity ( $y_{4\ell(\gamma\gamma)}$ ) probe.
  - ▶  $p_{T,4\ell(\gamma\gamma)}$ : Lagrangian structure of  $H$  interactions, Yukawa couplings
  - ▶  $y_{4\ell(\gamma\gamma)}$ : Sensitivity to proton's parton density functions.



- Transition region

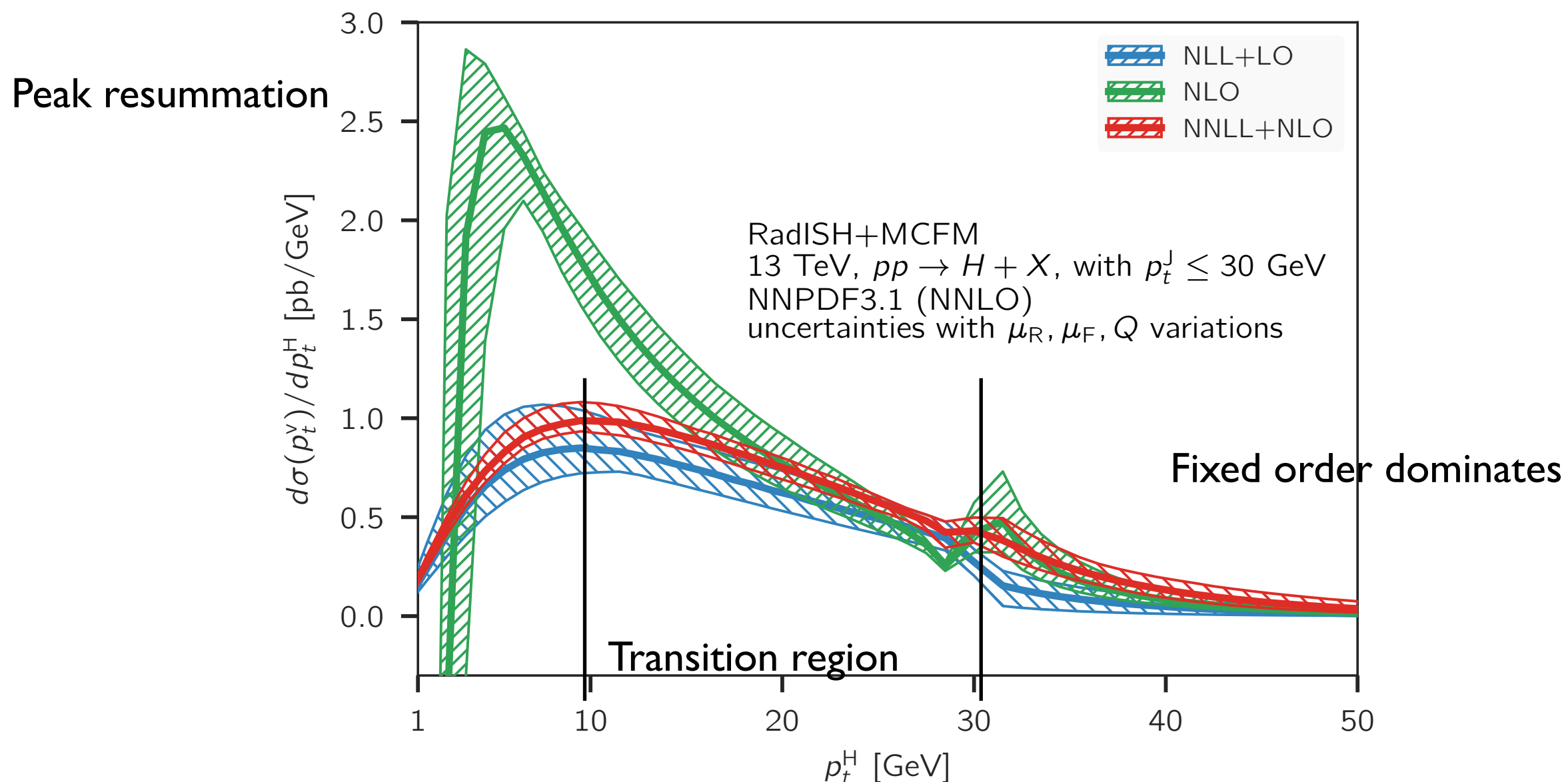
- ▶ Increased precision needed to disentangle effects from higher-order corrections from observables spectra:
  - ▶ Ex Higgs  $p_T$  as a function of jet vetos



Depiction adapted from F. Tackmann

## ● Transition region

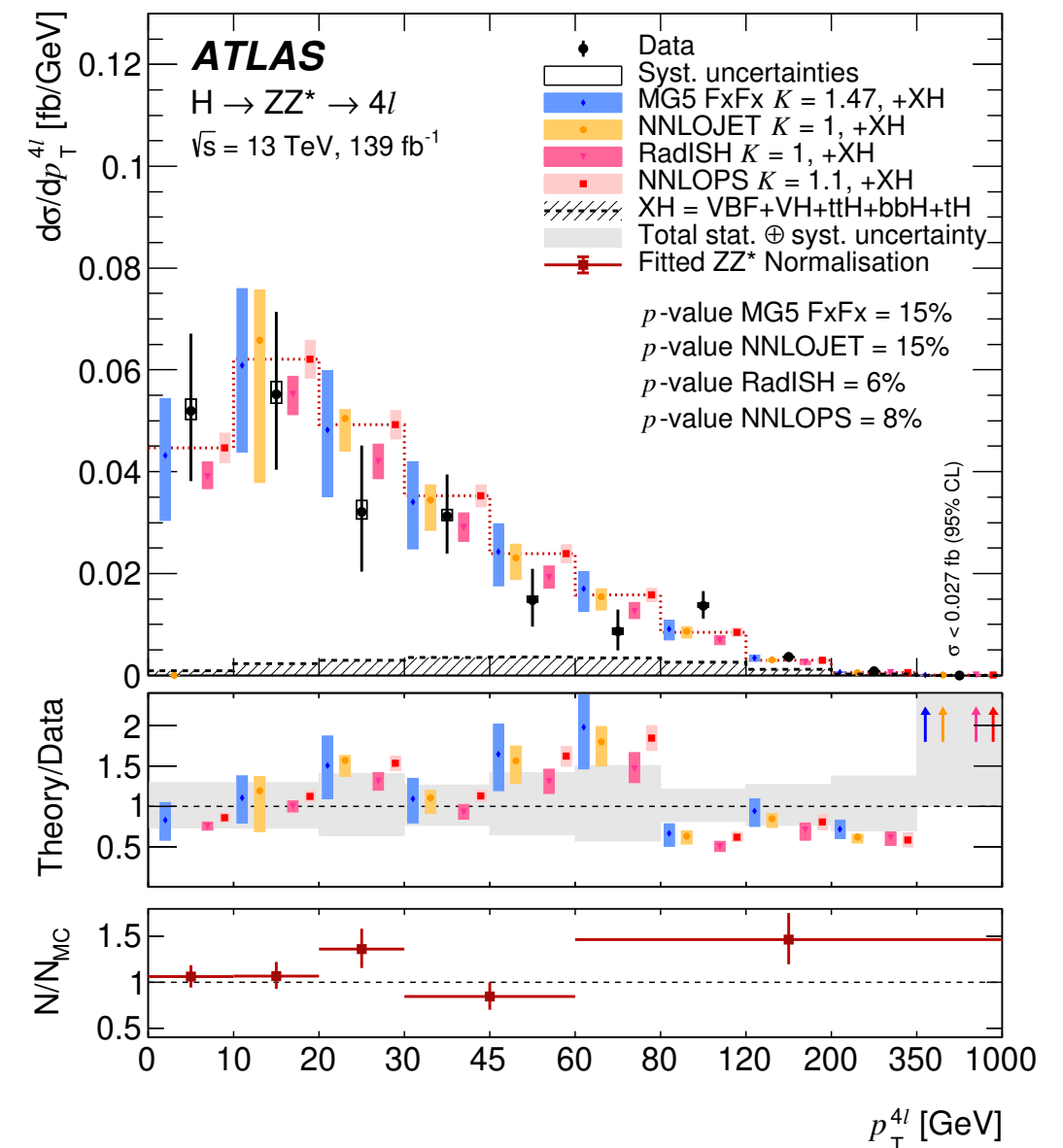
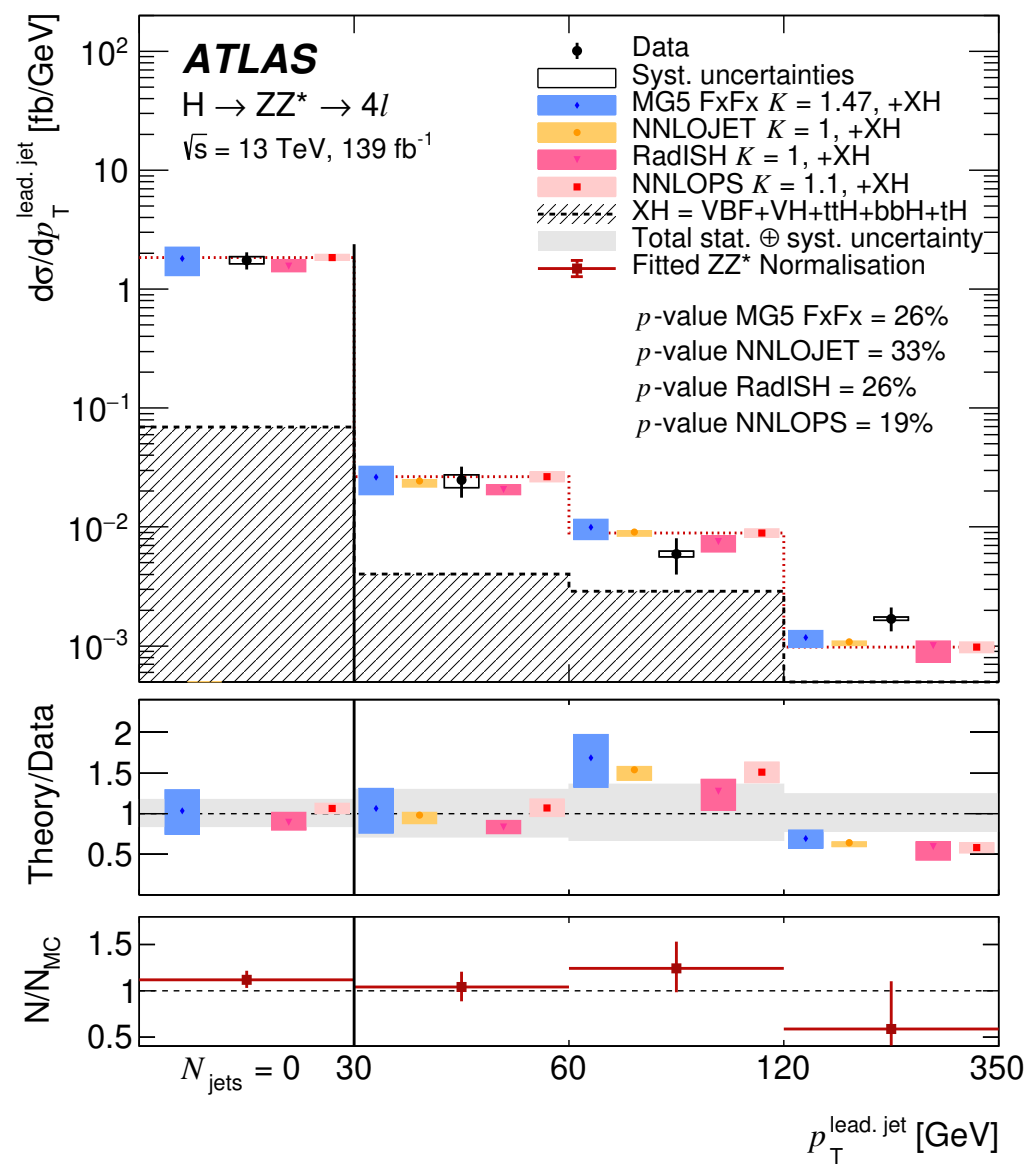
- ▶ Increased precision needed to disentangle effects from higher-order corrections from observables spectra:
  - ▶ Ex Higgs  $p_T$  as a function of jet vetos
  - ▶ State of the art predictions in these regions start being published.



# H and jets variables

# Differential cross section

- Increased precision needed to disentangle effects from higher-order corrections from observables spectra:
  - Measurements at Run-2 competitive on these state-of-the-art predictions

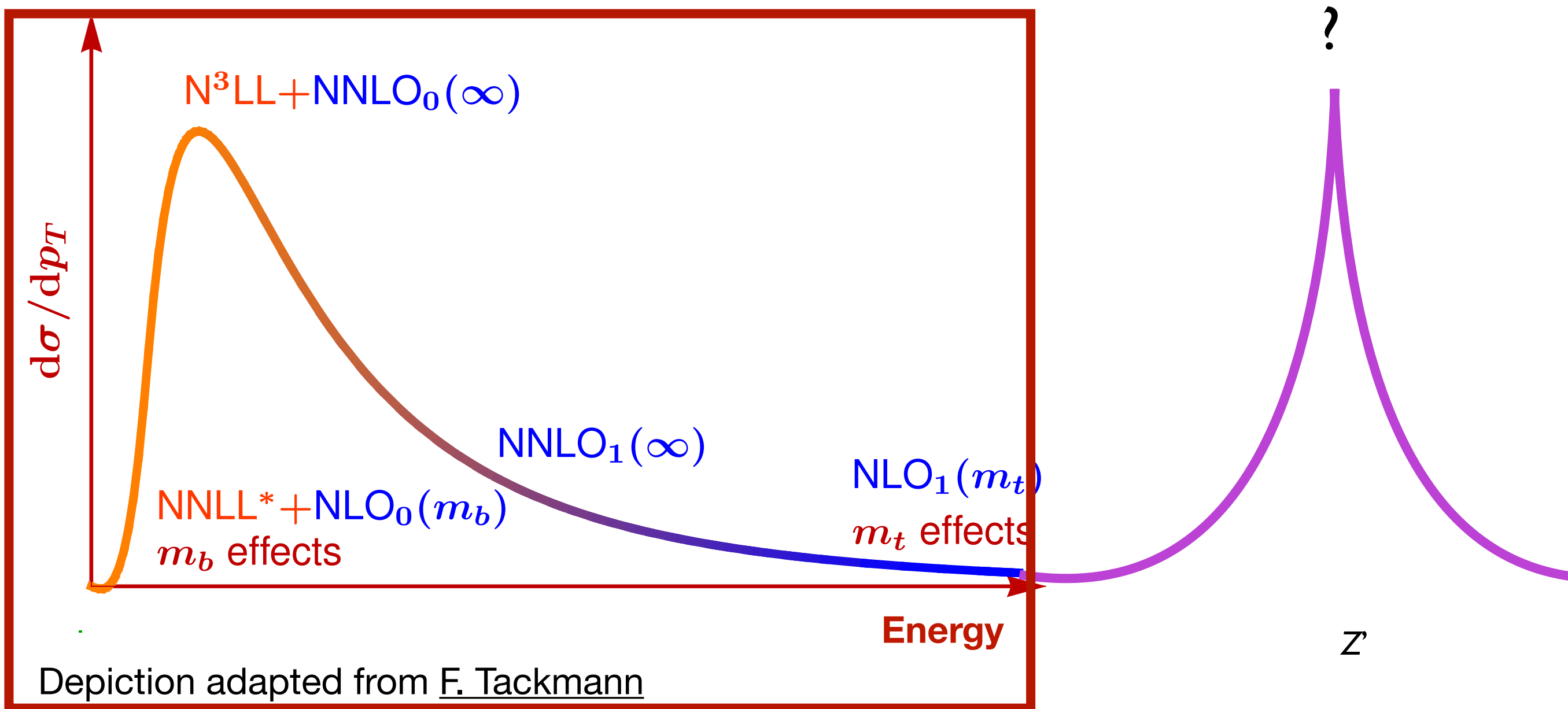




# Where is the new physics ?

- The LHC search programme did not identify yet New Physics.
- Hints for new physics in HEP:
  - ▶ Dark matter astronomy,  $g_\mu-2$ , gravitational waves, lepton universality in  $B^+ \rightarrow K^+ \ell \ell$ , CP anomalies in B-physics..., For  $m_H \sim 125$  GeV, vacuum metastable, mass unnatural  $\Lambda > 550$  GeV.
- What if New Physics is resonant outside our direct experimental reach ?

Energy boundaries of the experiment

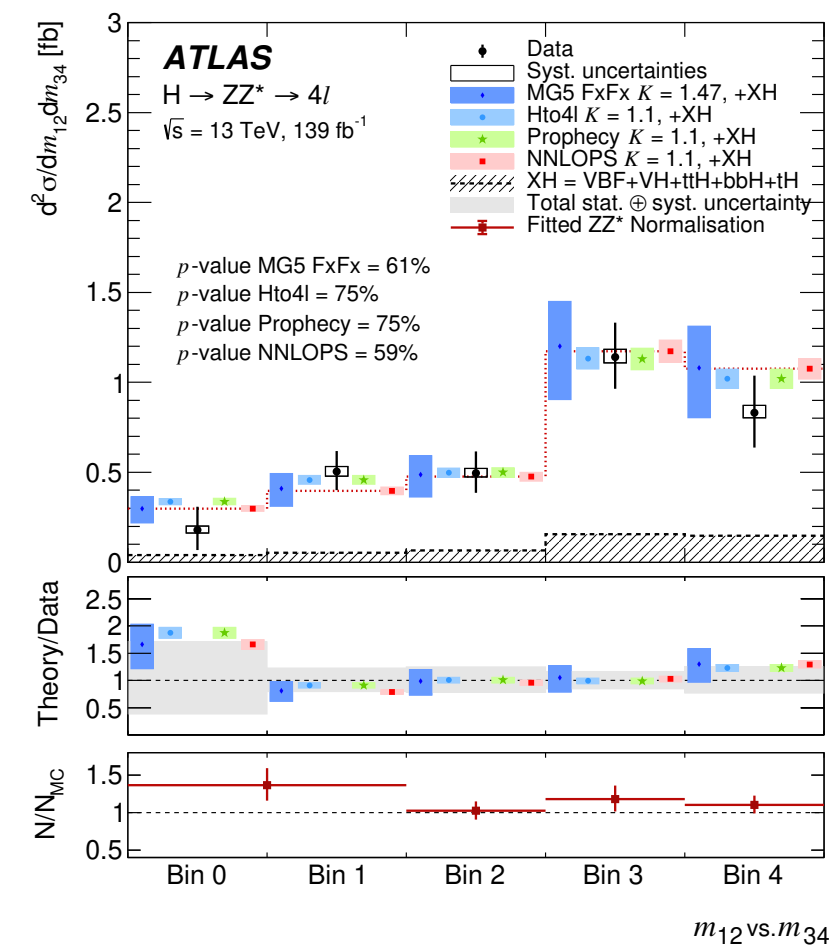
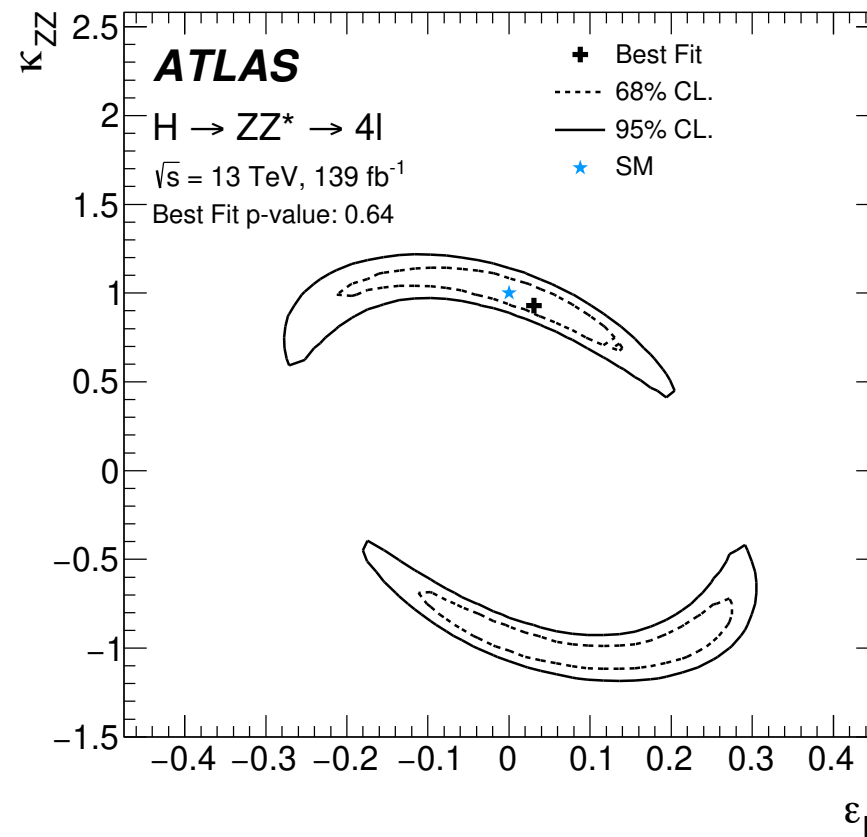
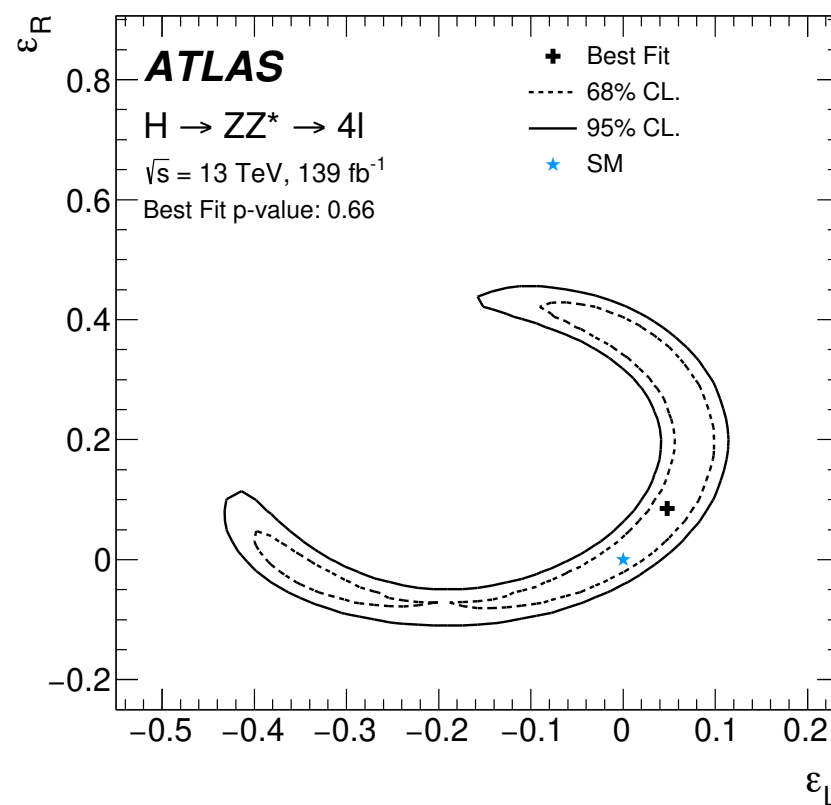
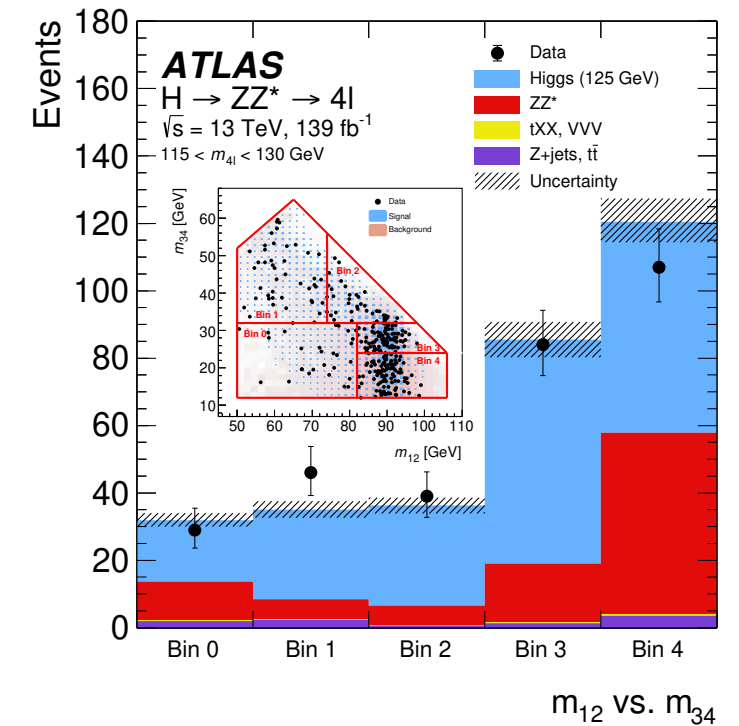


# Pseudo observables

- In  $H \rightarrow 4\ell$   $m_{12}$  vs  $m_{34}$ : sensitivity to contact interactions:

- ▶  $\varepsilon_R, \varepsilon_L$  and  $K$ : flavour universal modifiers of the contact terms between  $H, Z$  and leptons (arXiv:1504.04018)

♦ Angular distributions unaffected: same Lorentz structure as SM term.



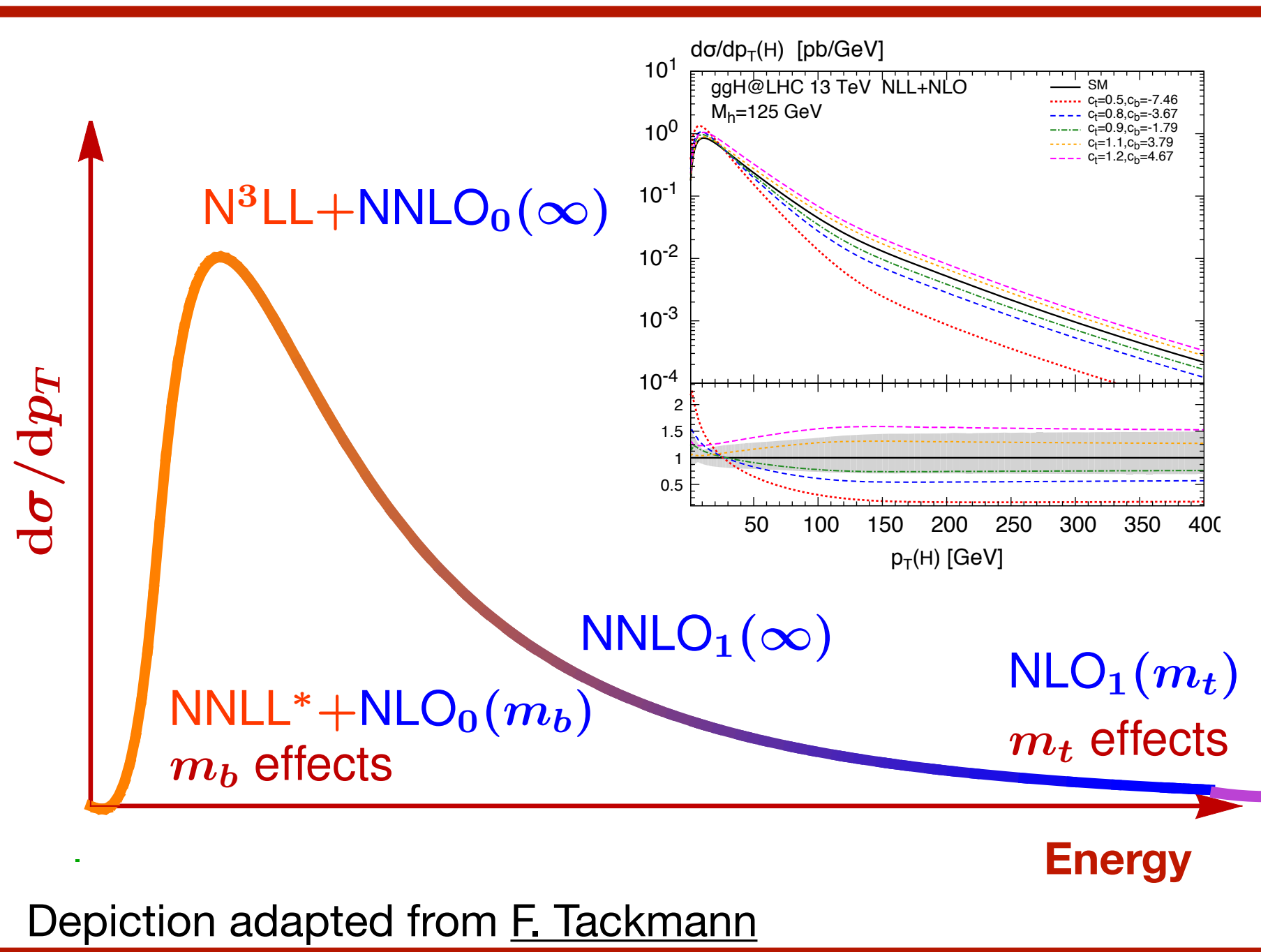
# Where is the new physics ?

- What if New Physics is resonant outside our direct experimental reach ?

- Systematic approach: Effective Field Theory

$$\mathcal{L}_{\text{SMEFT}} = \mathcal{L}_{\text{SM}} + \sum_i^{N_{d6}} \frac{c_i}{\Lambda^2} O_i^{(6)} + \sum_j^{N_{d8}} \frac{b_j}{\Lambda^4} O_j^{(8)} + \dots$$

Energy boundaries of the experiment



Depiction adapted from F. Tackmann

# Where is the new physics ?

- What if New Physics is resonant outside our direct experimental reach ?

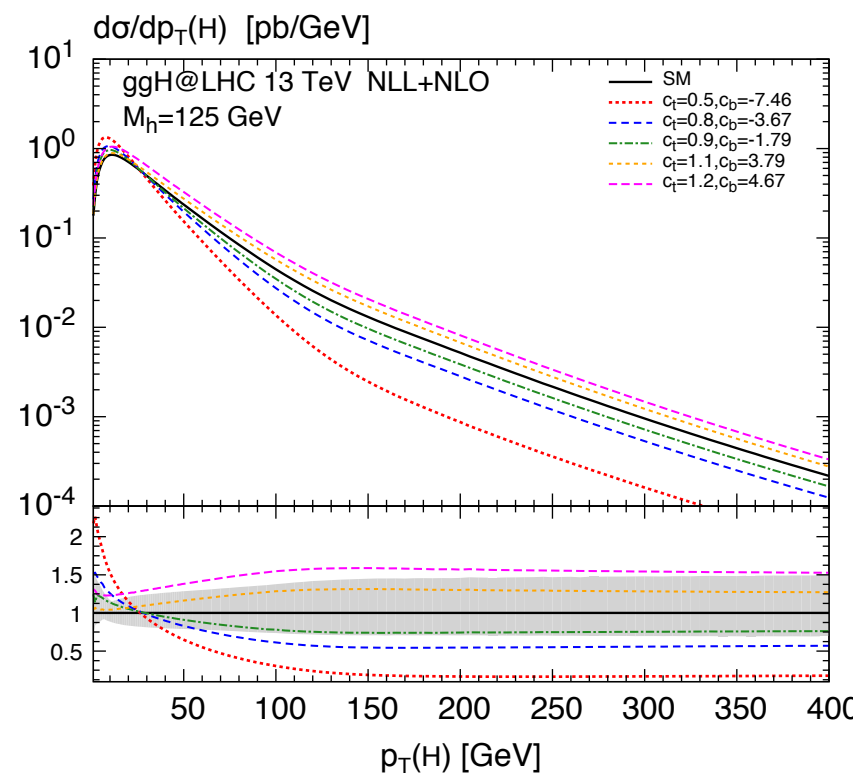
► Standard Model Effective Field Theory as the standard candle.

► Probe for non-SM contributions to the tensor structure of the Higgs boson.

$$\mathcal{L}_{\text{SMEFT}} = \mathcal{L}_{\text{SM}} + \sum_i^{N_{d6}} \frac{c_i}{\Lambda^2} \mathcal{O}_i^{(6)} + \sum_j^{N_{d8}} \frac{b_j}{\Lambda^4} \mathcal{O}_j^{(8)} + \dots$$

Energy boundaries of the experiment

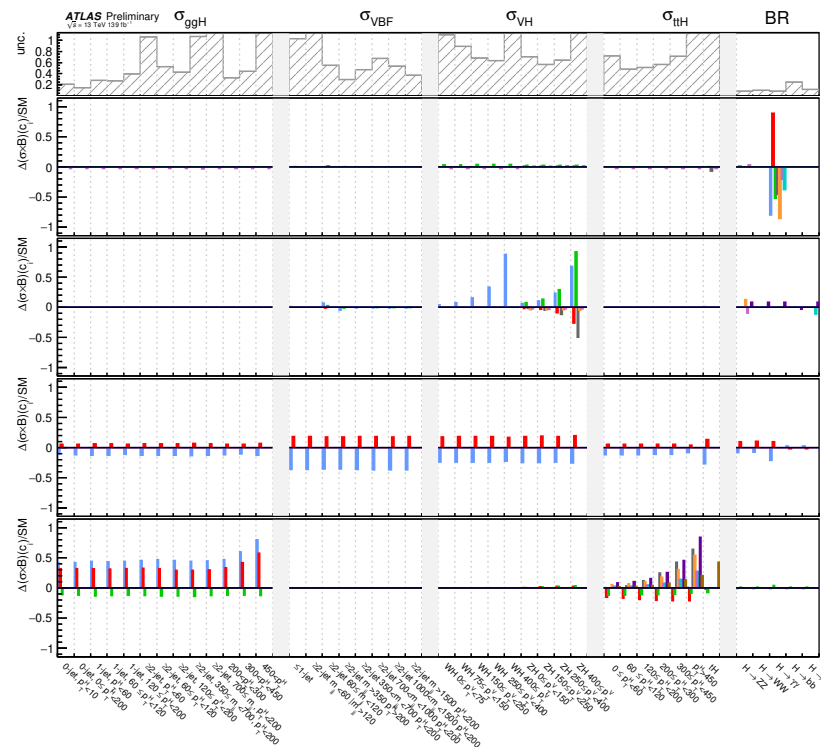
$$\left. \begin{aligned} \frac{c_1}{\Lambda^2} \mathcal{O}_1 &\rightarrow \frac{\alpha_S}{\pi v} c_g h G_{\mu\nu}^a G^{a,\mu\nu}, \\ \frac{c_2}{\Lambda^2} \mathcal{O}_2 &\rightarrow \frac{m_t}{v} c_t h \bar{t} t, \\ \frac{c_3}{\Lambda^2} \mathcal{O}_3 &\rightarrow \frac{m_b}{v} c_b h \bar{b} b, \\ \frac{c_4}{\Lambda^2} \mathcal{O}_4 &\rightarrow c_{tg} \frac{g_S m_t}{2v^3} (v + h) G_{\mu\nu}^a (\bar{t}_L \sigma^{\mu\nu} T^a t_R + h.c) \end{aligned} \right\} \begin{aligned} &c_g: ggH \text{ contact interaction} \\ &c_t: t \text{ and } b \text{ Yukawa couplings} \\ &c_{tg}: \text{dipole-moment, } g\text{-}t \text{ interaction} \end{aligned}$$



?

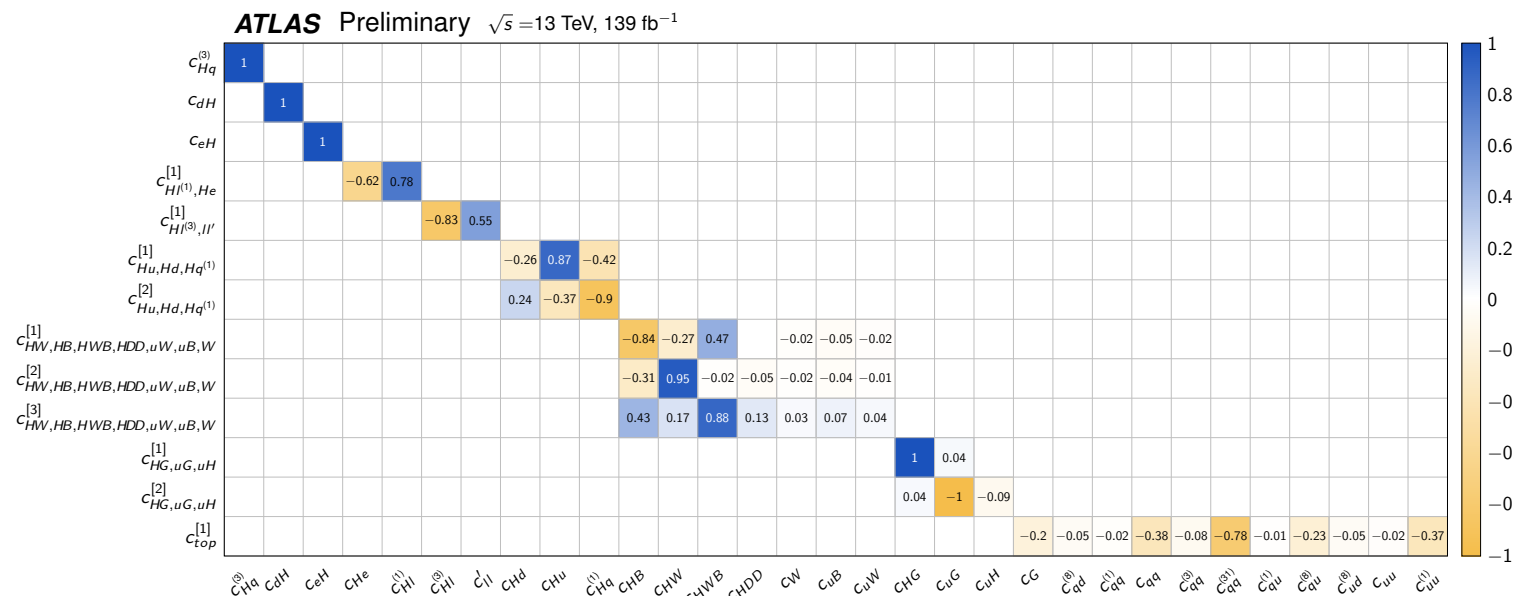
# Where is the new physics ?

- Sensitivity from a multitude of couplings in each measured quantity



- Enhance sensitivity

- by isolating dependencies in Wilson coefficients ( $c_i$ ) allowing for simultaneous extraction through eigenvector decomposition of the dependencies.

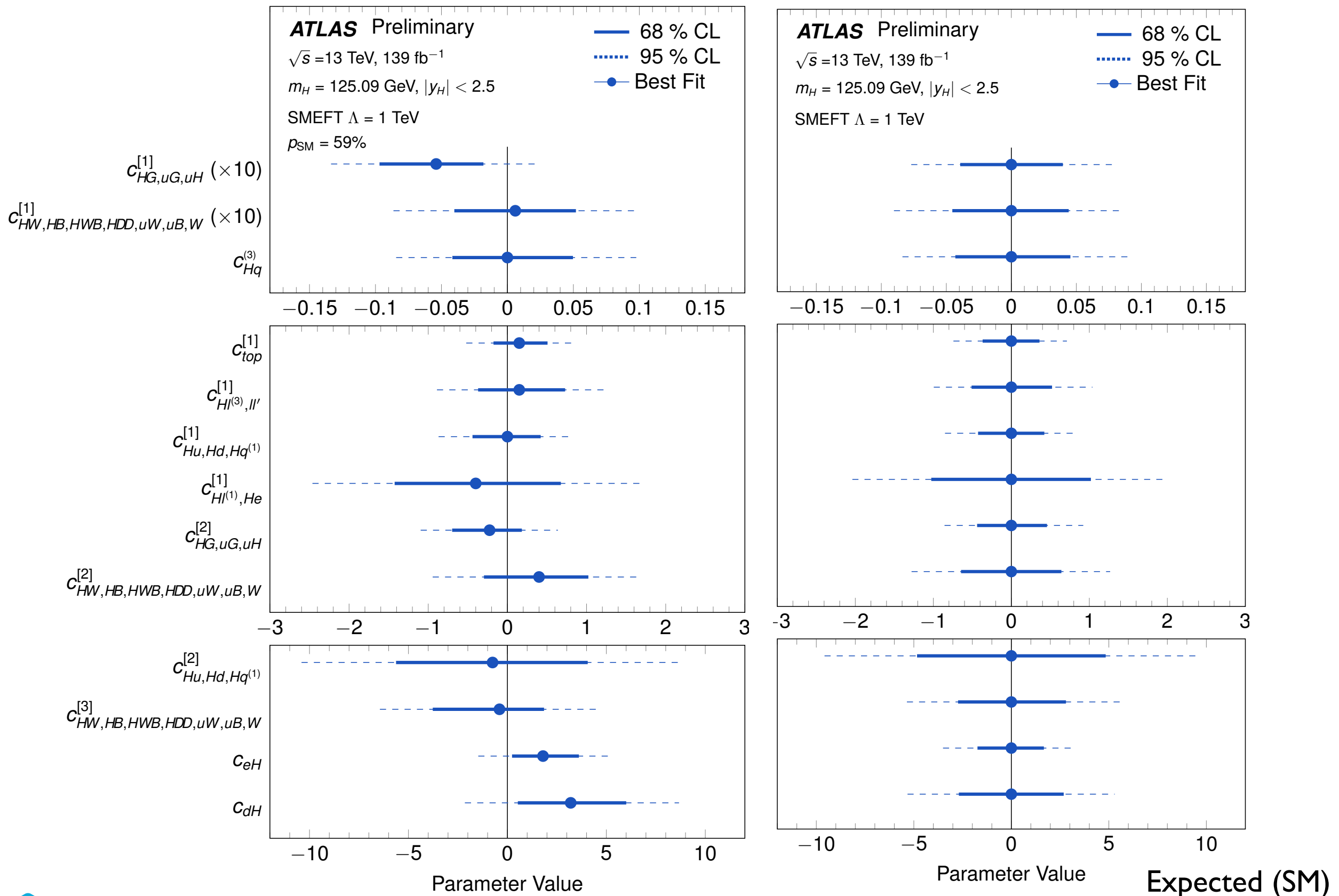


# Production mode

Coefficient	Operator	Example process
$c_{HDD}$	$(H^\dagger D^\mu H)^* (H^\dagger D_\mu H)$	
$c_{HG}$	$H^\dagger H G_{\mu\nu}^A G^{A\mu\nu}$	
$c_{HB}$	$H^\dagger H B_{\mu\nu} B^{\mu\nu}$	
$c_{HW}$	$H^\dagger H W_{\mu\nu}^I W^{I\mu\nu}$	
$c_{HWB}$	$H^\dagger \tau^I H W_{\mu\nu}^I B^{\mu\nu}$	
$c_{eH}$	$(H^\dagger H)(\bar{l}_p e_r H)$	
$c_{Hl}^{(1)}$	$(H^\dagger i \overleftrightarrow{D}_\mu H)(\bar{l}_p \gamma^\mu l_r)$	
$c_{Hl}^{(3)}$	$(H^\dagger i \overleftrightarrow{D}_\mu^I H)(\bar{l}_p \tau^I \gamma^\mu l_r)$	
$c_{He}$	$(H^\dagger i \overleftrightarrow{D}_\mu H)(\bar{e}_p \gamma^\mu e_r)$	
$c_{Hq}^{(1)}$	$(H^\dagger i \overleftrightarrow{D}_\mu H)(\bar{q}_p \gamma^\mu q_r)$	
$c_{Hq}^{(3)}$	$(H^\dagger i \overleftrightarrow{D}_\mu^I H)(\bar{q}_p \tau^I \gamma^\mu q_r)$	
$c_{Hu}$	$(H^\dagger i \overleftrightarrow{D}_\mu H)(\bar{u}_p \gamma^\mu u_r)$	
$c_{Hd}$	$(H^\dagger i \overleftrightarrow{D}_\mu H)(\bar{d}_p \gamma^\mu d_r)$	

# Where is the new physics ?

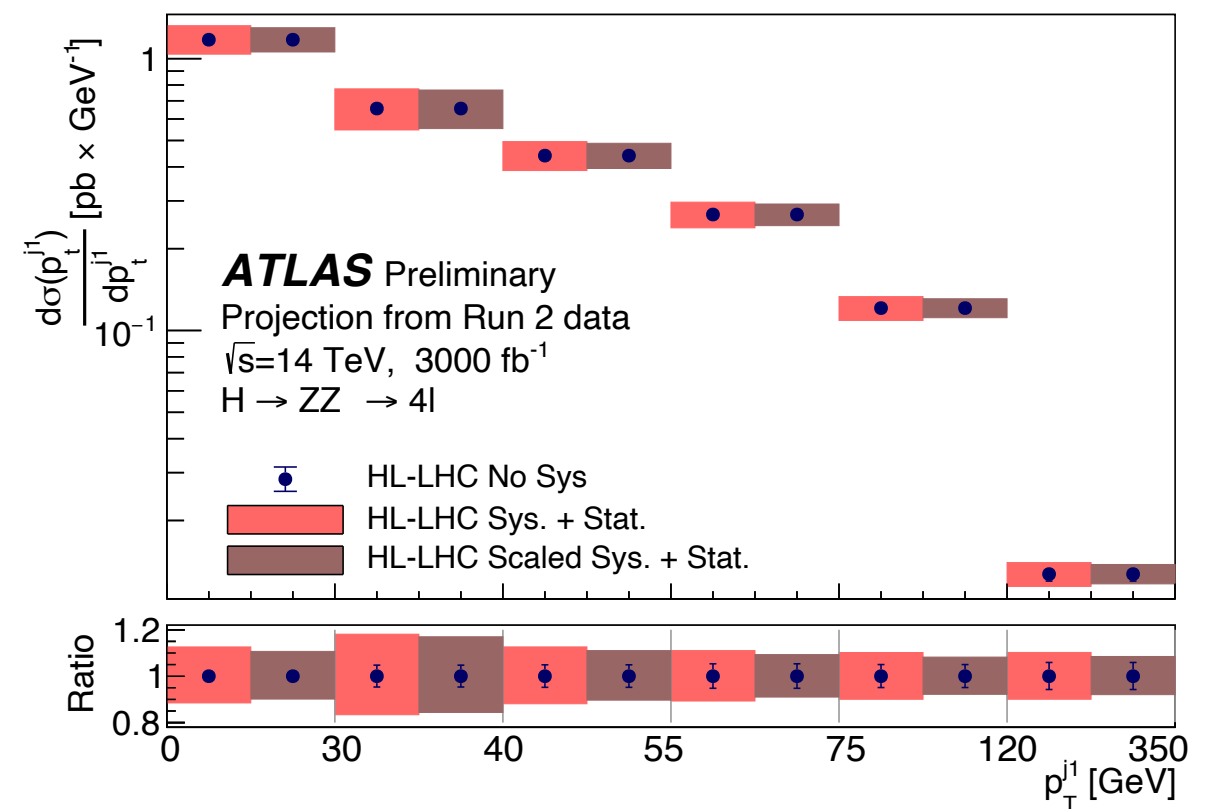
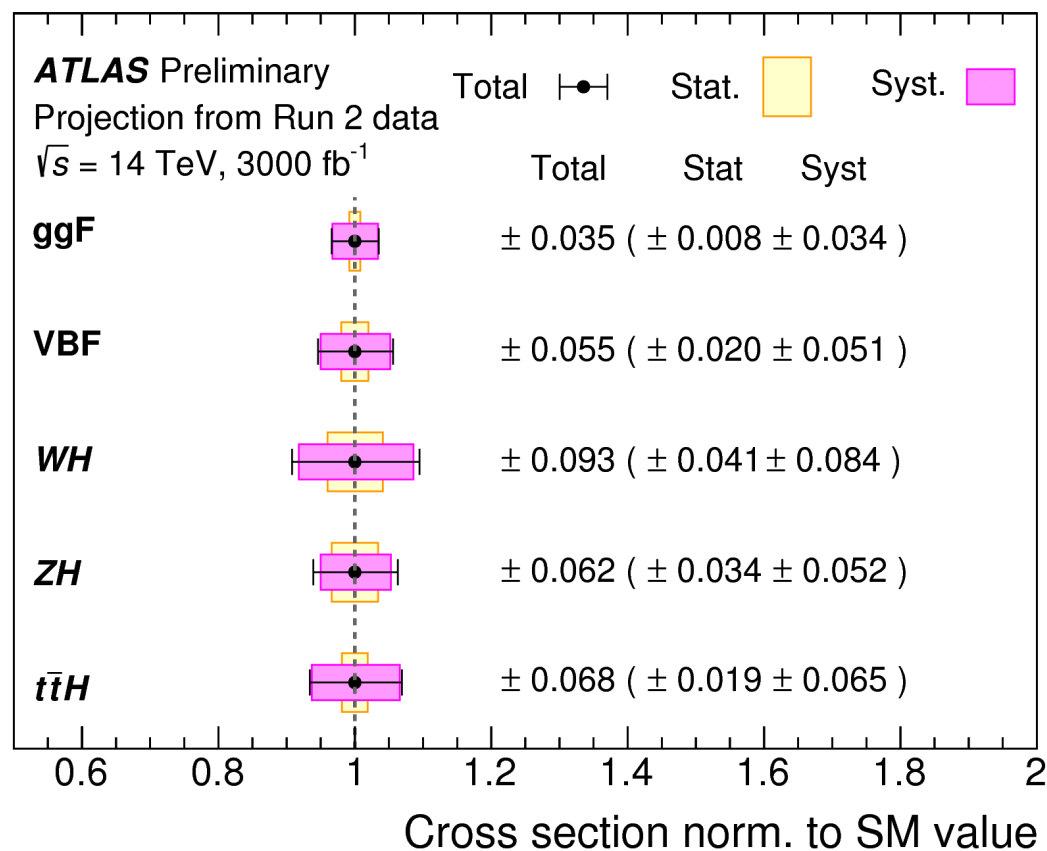
- Results interpreted in the context of new physics:



## 6. Conclusions

# Conclusion

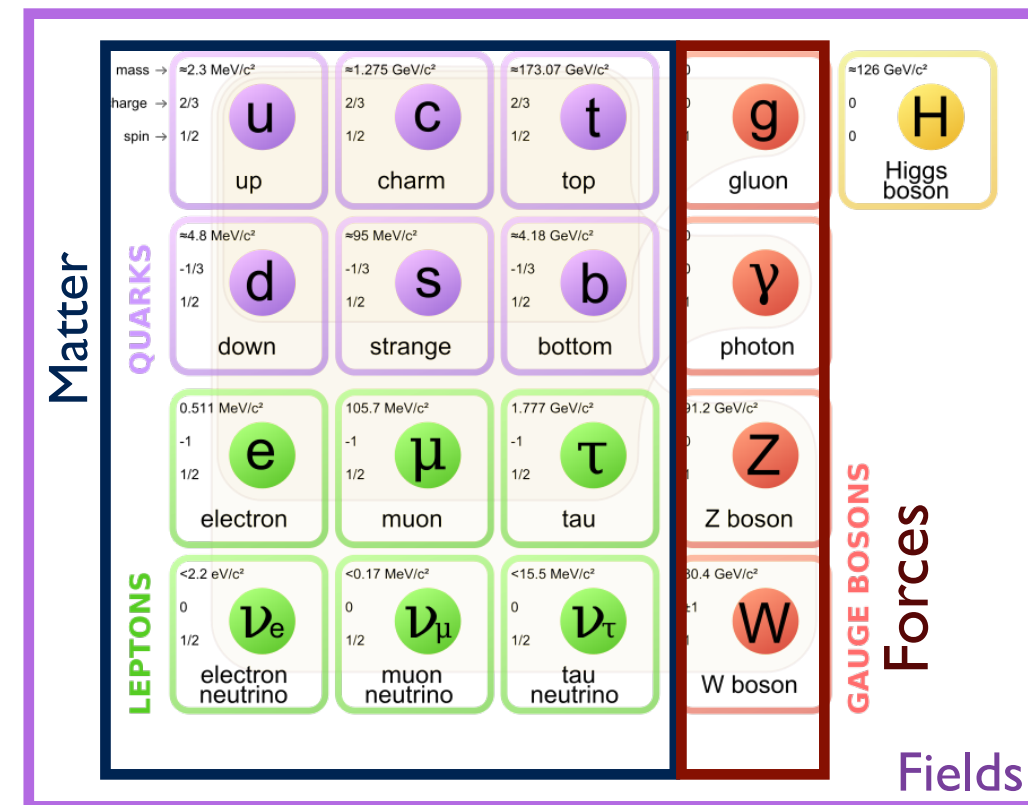
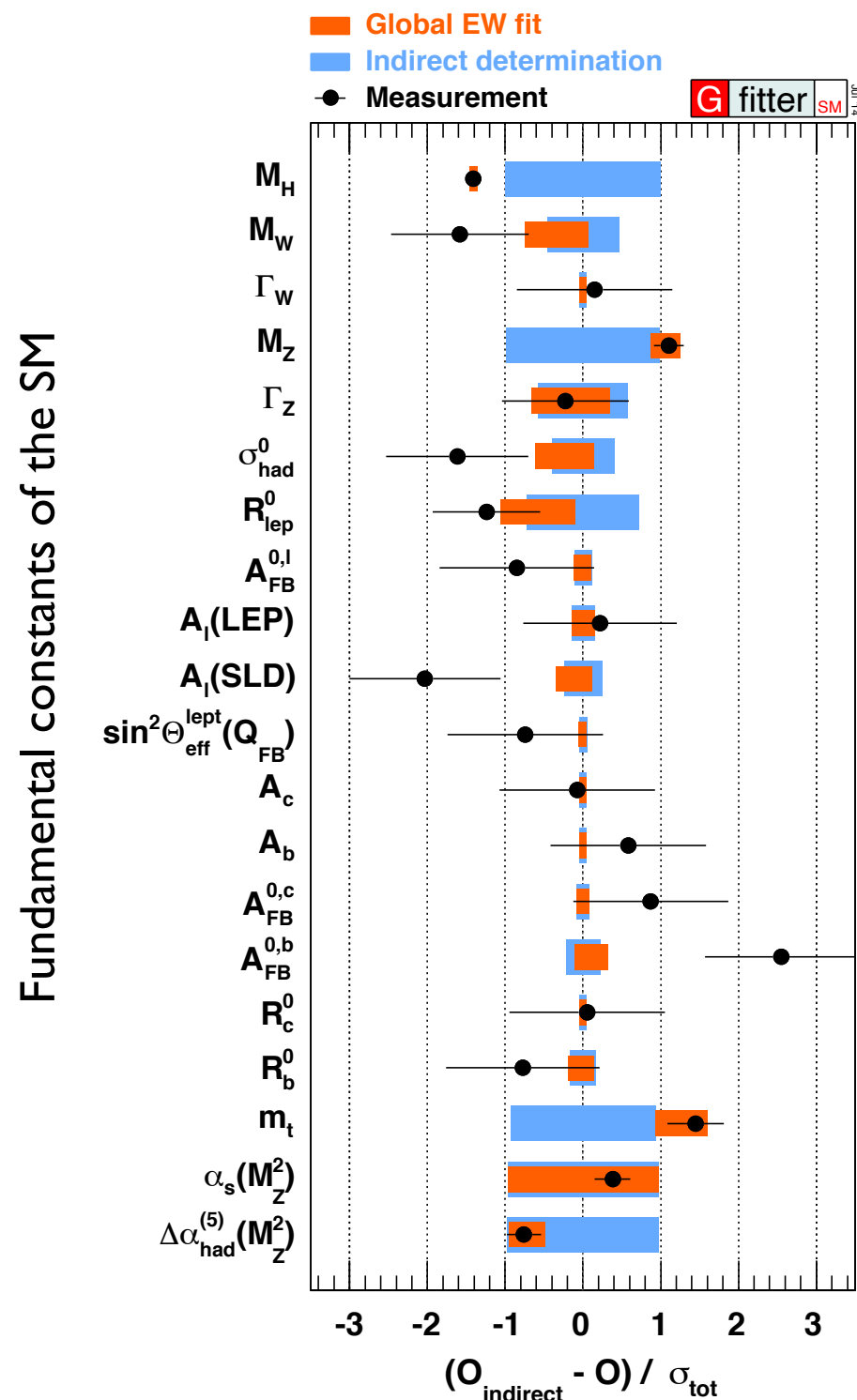
- Current reach same order of magnitude as that expected with 20 times the data.
  - ▶ Inclusive measurements at percent level
  - ▶ Double differential cross sections  $O(20\%)$
- Path for higher luminosities at the LHC:
  - ▶ Novel ideas in constraining (systematic) uncertainties at higher luminosities.





# Conclusion

- The Standard Model (SM) is our current understanding of the microcosm.



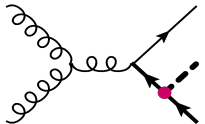

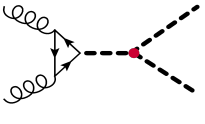
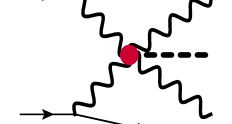
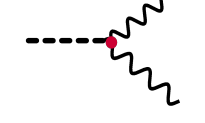

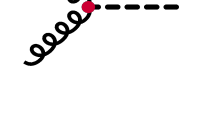

- Hints for new physics in HEP:
  - Dark matter astronomy,  $g_{\mu-2}$ , gravitational waves, lepton universality in  $B^+ \rightarrow K^+ \ell \ell$ , CP anomalies in B-physics...
- New phenomena hide:
  - In unexplored corners of the phase-space.
  - At energies beyond what's accessible by our colliders.
- Methodical study from current experimental picture.

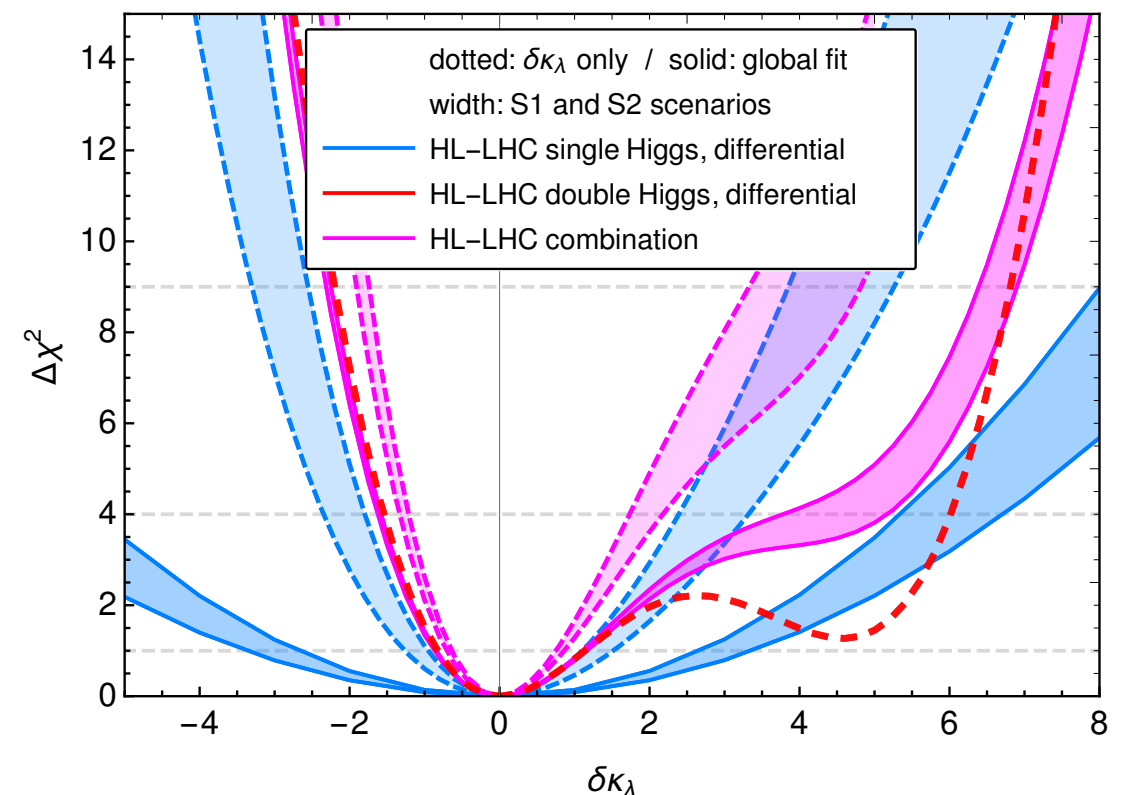
Global Electroweak fits from the Gfitter Collaboration

# Conclusion

- Current reach same order of magnitude as that expected with 20 times the data.
  - ▶ Inclusive measurements at percent level
  - ▶ Double differential cross sections  $O(20\%)$
- Path for higher luminosities at the LHC:
  - ▶ Novel ideas in constraining (systematic) uncertainties at higher luminosities.
    - ▶ Combination of direct and indirect constraints on  $K_\lambda$ .
    - ▶ Combination of processes linked to H production.

## Examples

		HC	HwH	Growth
$\kappa_t$	$\mathcal{O}_{yt}$			$\sim \frac{E^2}{\Lambda^2}$
$\kappa_\lambda$	$\mathcal{O}_6$			$\sim \frac{vE}{\Lambda^2}$
$\kappa_{Z\gamma}$ $\kappa_{\gamma\gamma}$ $\kappa_V$	$\mathcal{O}_{WW}$ $\mathcal{O}_{BB}$ $\mathcal{O}_r$			$\sim \frac{E^2}{\Lambda^2}$
$\kappa_g$	$\mathcal{O}_{gg}$			$\sim \frac{E^2}{\Lambda^2}$



Henning *et al* 10.1103/PhysRevLett.123.181801

# Roadmap ?

- Increase precision through novel techniques and analyses.

- ▶ VBF cross sections in  $H \rightarrow ZZ/WW$  channels (ongoing)
- ▶ 2D measurements of  $VV^*(+jj)$  and  $H(+jj)$  productions.

- ▶ ....

- Increase sensitivity in offshell Higgs couplings.

- Direct measurements of  $HH$  production.

- ▶ High precision Higgs properties measurements.

- Precision measurements of  $V_L V_L$

- ▶  $e^+e^-$  (FCC-ee/ILC) colliders in VBS  $VV \rightarrow gg$

LHC Run2 and Run3  
~300 fb<sup>-1</sup> pp collisions

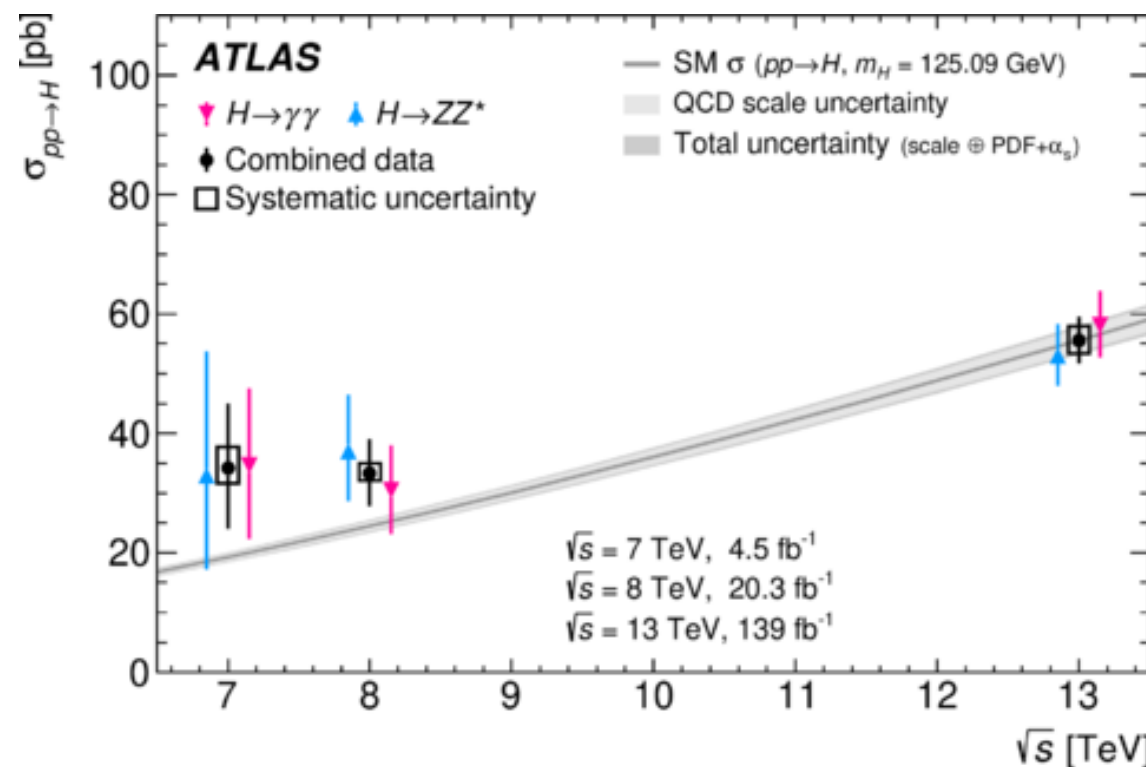
now

High Luminosity LHC  
~3000 fb<sup>-1</sup> pp collisions

time

# Conclusion

- Higgs physics provide an excellent picture for
  - Searches for new phenomena resonant at higher scales.
  - Searches for deviations to theory within the scales of the experiment.
- After a decade of cracking the mass problem:
  1. Measurement of  $m_H$  at 2 per mille precision level.
  2. Fiducial cross section measurements, sensitivity to several distributions
  3. Production mode analysis and template cross section measurements.



- Presented only a selection results full set

<https://twiki.cern.ch/twiki/bin/view/AtlasPublic/HiggsPublicResults>

Additional material

# Object selection

## ● Electrons ( $e$ ).

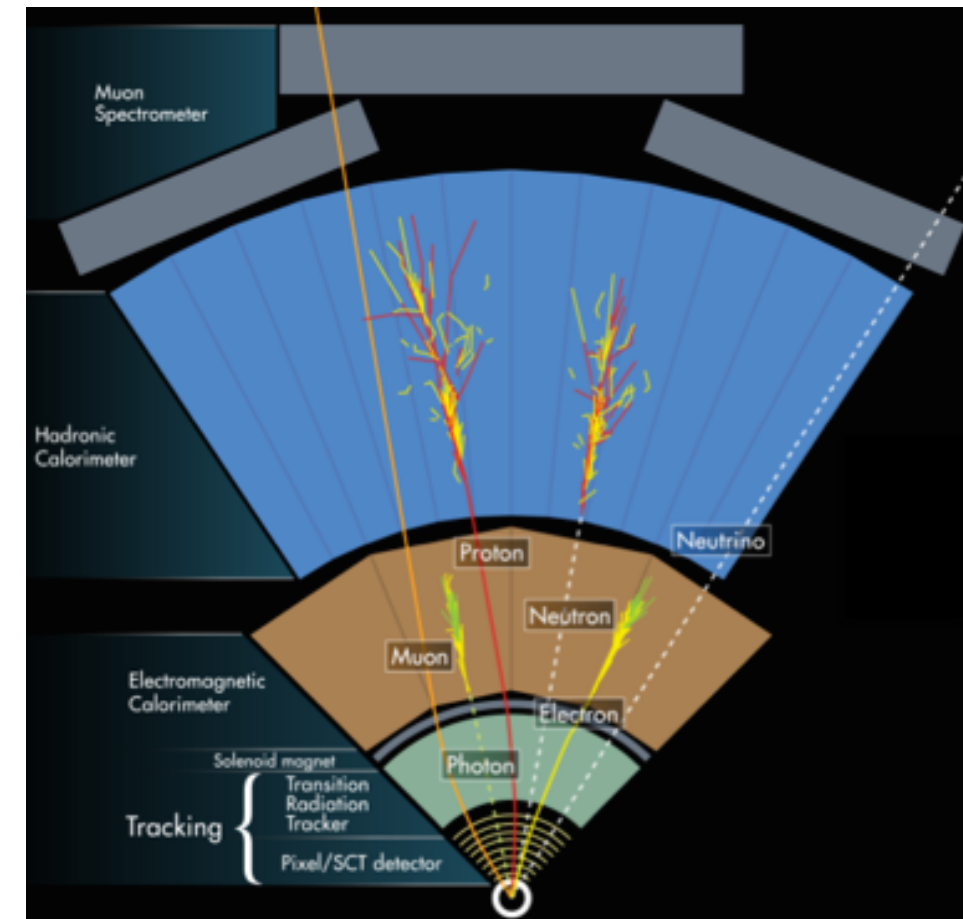
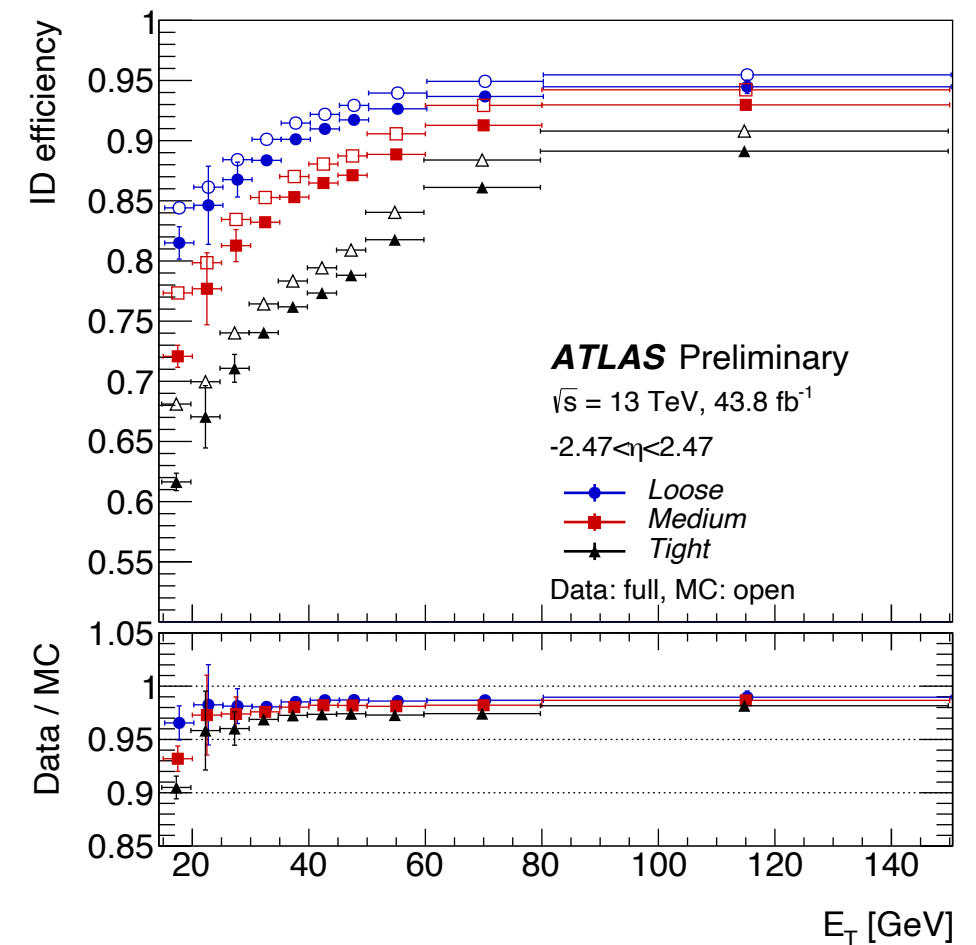
- ▶ Isolated objects clustered from calorimeter energy deposits with associated ID track.
- ▶  $E_T > 7 \text{ GeV}$ ,  $|\eta| < 2.47$  and  $|z_0 \sin(\vartheta)| < 0.5 \text{ mm}$

## ● Muons ( $\mu$ ).

- ▶ Combined track fit of Inner Detector and Muon Spectrometer hits,
- ▶  $p_T > 5 \text{ GeV}$ ,  $|\eta| < 2.7$   $|z_0 \sin(\vartheta)| < 0.5 \text{ mm}$  of “loose or medium quality”
- ▶ Isolated objects

## ● Missing transverse energy ( $E_T^{\text{miss}}$ ).

- ▶ Inferred from transverse momentum imbalance



# Object selection

## ● Electrons ( $e$ ).

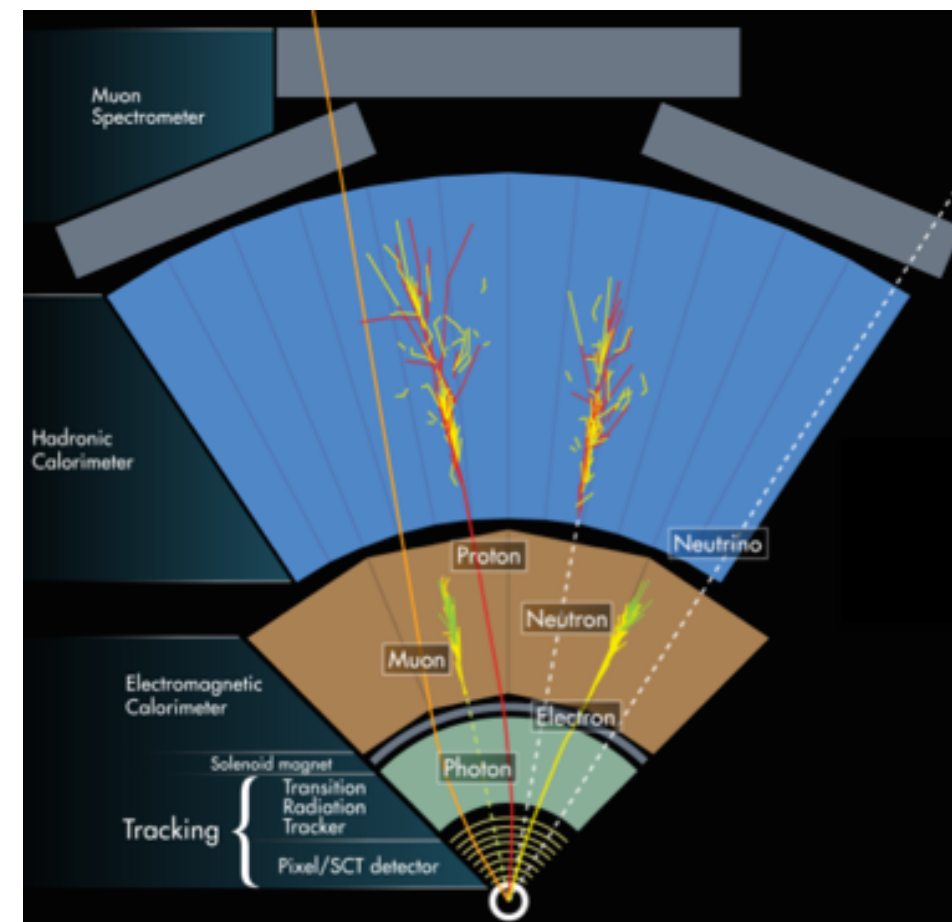
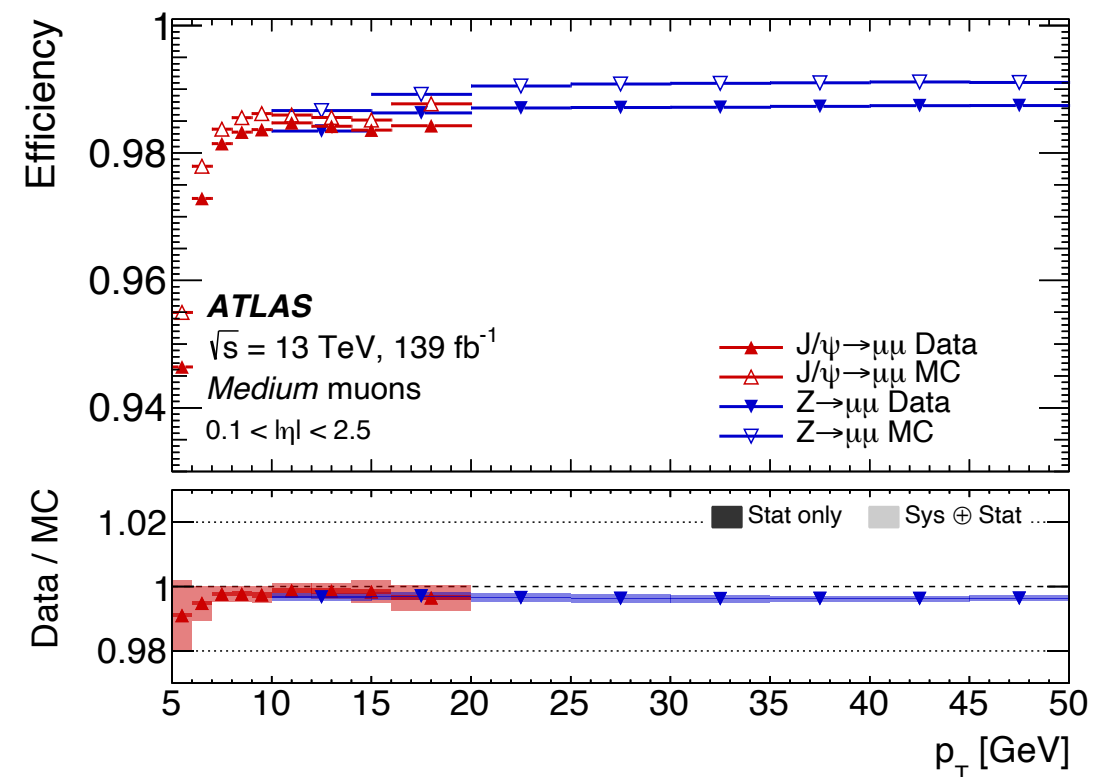
- ▶ Isolated objects clustered from calorimeter energy deposits with associated ID track.
- ▶  $E_T > 7$  GeV,  $|\eta| < 2.47$  and  $|z_0 \sin(\vartheta)| < 0.5$  mm

## ● Muons ( $\mu$ ).

- ▶ Combined track fit of Inner Detector and Muon Spectrometer hits,
- ▶  $p_T > 5$  GeV,  $|\eta| < 2.7$   $|z_0 \sin(\vartheta)| < 0.5$  mm of “loose or medium quality”
- ▶ Isolated objects

## ● Jets ( $j$ ).

- ▶ Energy deposit grouping with *infra*-red safe algorithm:
- ▶  $p_T > 25$  GeV and  $|\eta| < 4.5$ 
  - ◆ Clustering with anti- $k_T$ ,  $R=0.4$





# Object selection

## ● Electrons ( $e$ ).

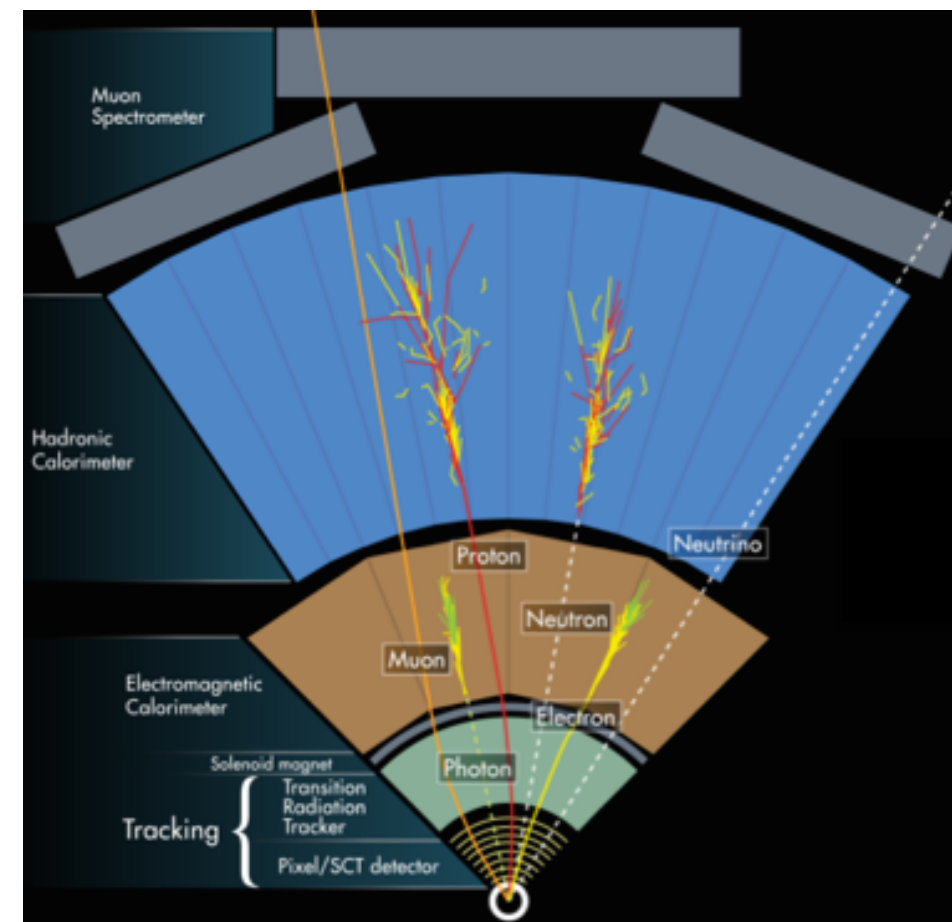
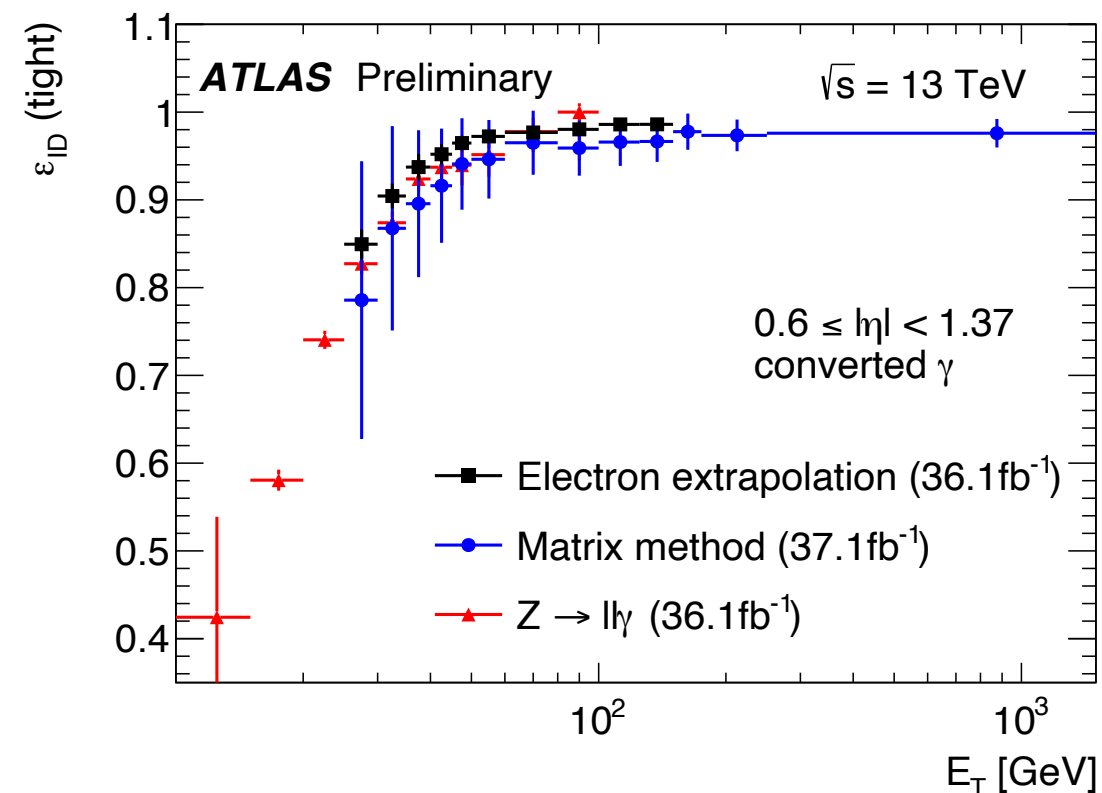
- ▶ Isolated objects clustered from calorimeter energy deposits with associated ID track.
- ▶  $E_T > 7 \text{ GeV}$ ,  $|\eta| < 2.47$  and  $|z_0 \sin(\vartheta)| < 0.5 \text{ mm}$

## ● Muons ( $\mu$ ).

- ▶ Combined track fit of Inner Detector and Muon Spectrometer hits,
- ▶  $p_T > 5 \text{ GeV}$ ,  $|\eta| < 2.7$   $|z_0 \sin(\vartheta)| < 0.5 \text{ mm}$  of “loose or medium quality”
- ▶ Isolated objects

## ● Photons ( $\gamma$ ).

- ▶ Clustering of calorimeter energy deposits.
- ▶ Identified with rectangular cuts on shower shapes.





# Object selection

## ● Electrons ( $e$ ).

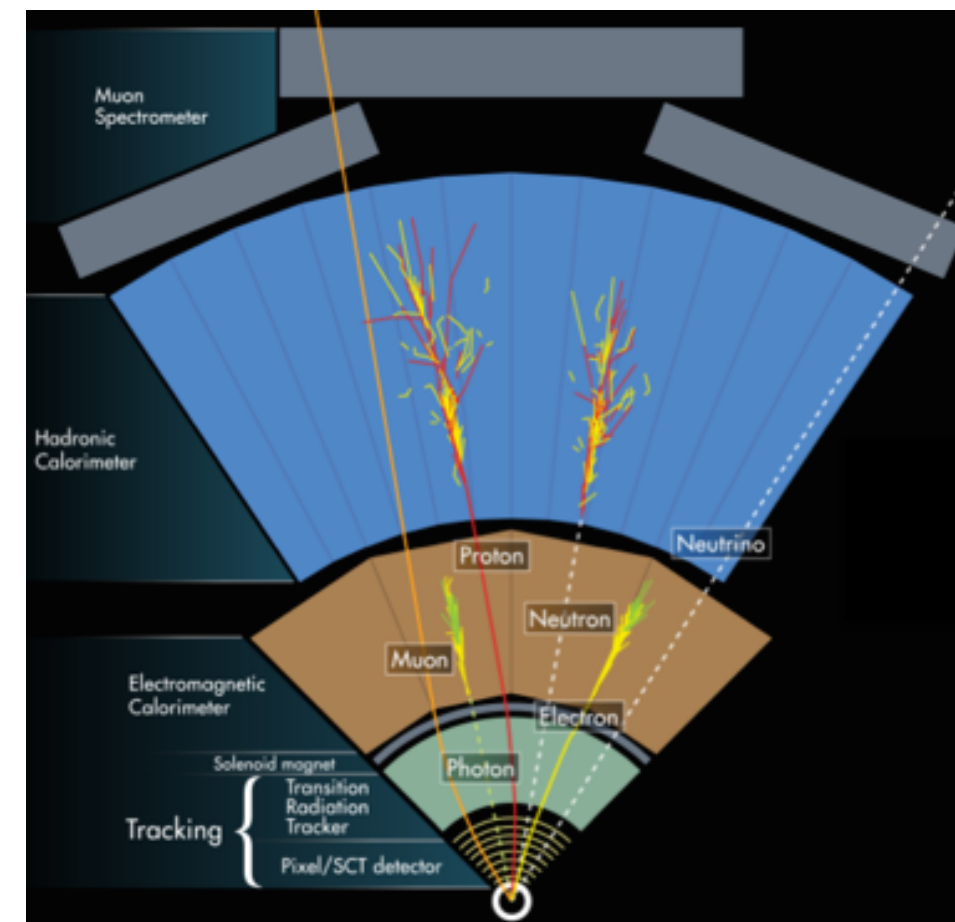
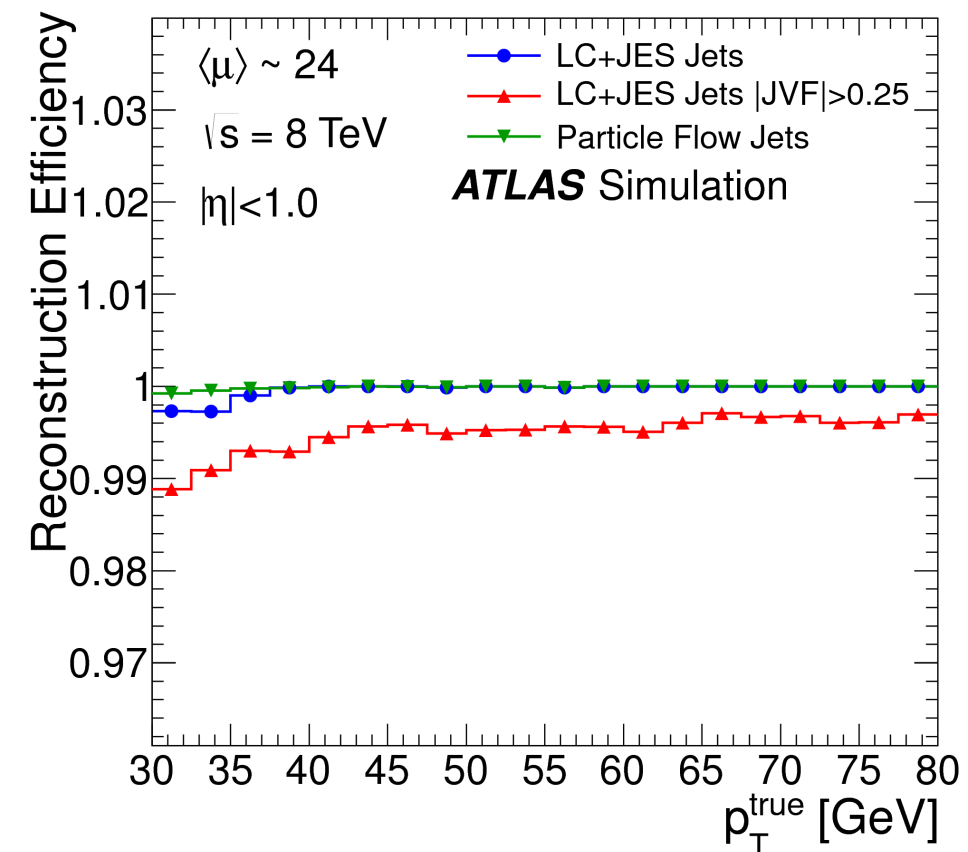
- ▶ Isolated objects clustered from calorimeter energy deposits with associated ID track.
- ▶  $E_T > 7 \text{ GeV}$ ,  $|\eta| < 2.47$  and  $|z_0 \sin(\vartheta)| < 0.5 \text{ mm}$

## ● Muons ( $\mu$ ).

- ▶ Combined track fit of Inner Detector and Muon Spectrometer hits,
- ▶  $p_T > 5 \text{ GeV}$ ,  $|\eta| < 2.7$   $|z_0 \sin(\vartheta)| < 0.5 \text{ mm}$  of “loose or medium quality”
- ▶ Isolated objects

## ● Jets ( $j$ ).

- ▶ Energy deposit grouping with *infra-red* safe algorithm:
- ▶  $p_T > 25 \text{ GeV}$  and  $|\eta| < 4.5$ 
  - ◆ Clustering with anti- $k_T$ ,  $R=0.4$



# Di-Higgs production

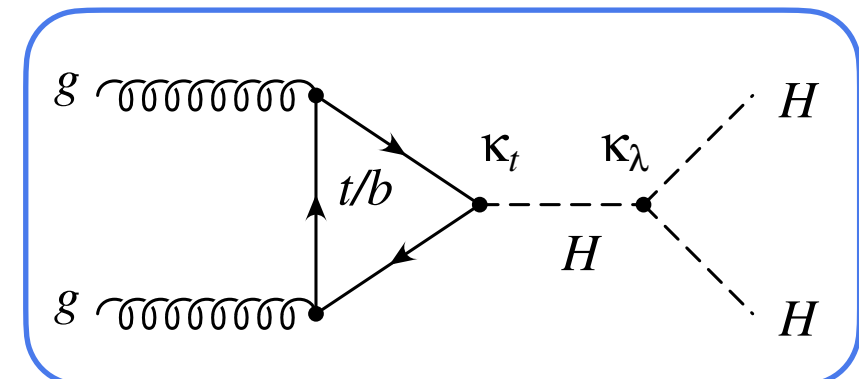
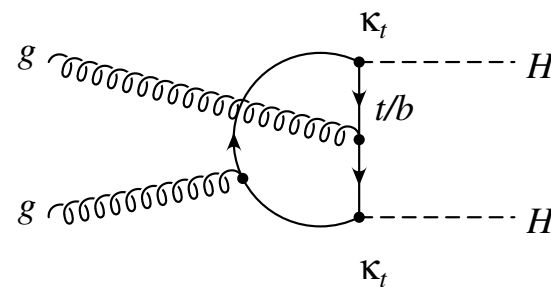
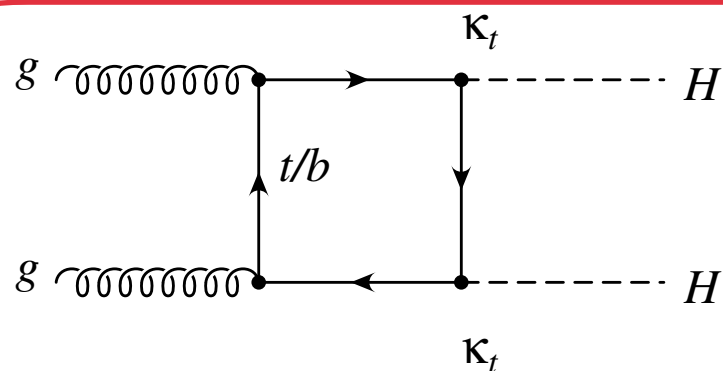
- The Higgs boson can interact with itself through quadratic terms in the Higgs potential

$$\mathcal{L} = -\frac{1}{4}F_{\mu\nu}F^{\mu\nu} + i\bar{\Psi}\not{D}\psi + D_{\mu}\Phi^{\dagger}D^{\mu}\Phi - \boxed{V(\Phi)} + \bar{\Psi}_L\hat{Y}\Phi\Psi_R + h.c.$$

➔

$$V(\Phi) \sim -\mu^2(\Phi^{\dagger}\Phi) + \boxed{\lambda}(\Phi^{\dagger}\Phi)^2$$

- ▶ About 500 times suppression of  $\sigma(gg \rightarrow H)$  (48.5 pb) /  $\sigma(gg \rightarrow HH)$  ( $\sim 33.4$  fb)
- ▶ Destructive interference between the terms proportional to the  $\kappa_t^2$  and the product of  $\kappa_t$  and  $\kappa_{\lambda}$



- ▶ Single Higgs process do not depend on the trilinear self ( $\lambda_{HHH}$ ) coupling at LO but are needed for the NLO EW corrections.

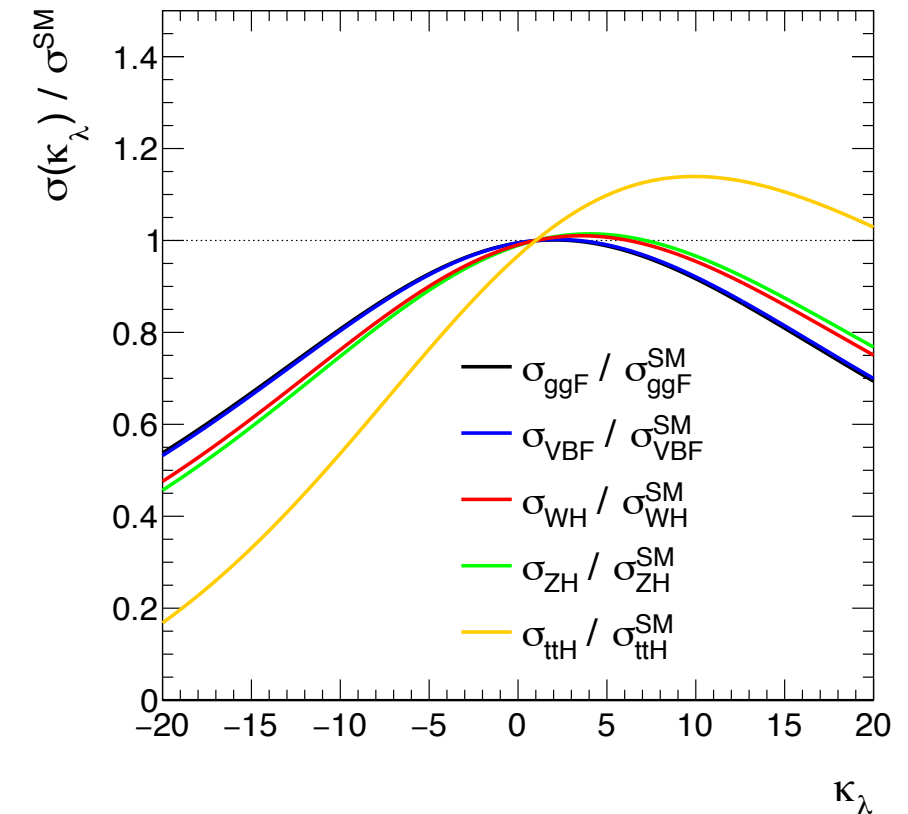
- Indirect constraint with comparing NLO EW dependant  $\lambda_{HHH}$  effects

# Di-Higgs production

- Modified Higgs production cross section and branching ratios to account for NLO EW corrections ( $K_{EW}^i$  and  $C_1^f$ )

$$\mu_i(\kappa_\lambda, \kappa_i) = \frac{\sigma^{\text{BSM}}}{\sigma^{\text{SM}}} = Z_H^{\text{BSM}}(\kappa_\lambda) \left[ \kappa_i^2 + \frac{(\kappa_\lambda - 1)C_1^i}{K_{EW}^i} \right]$$

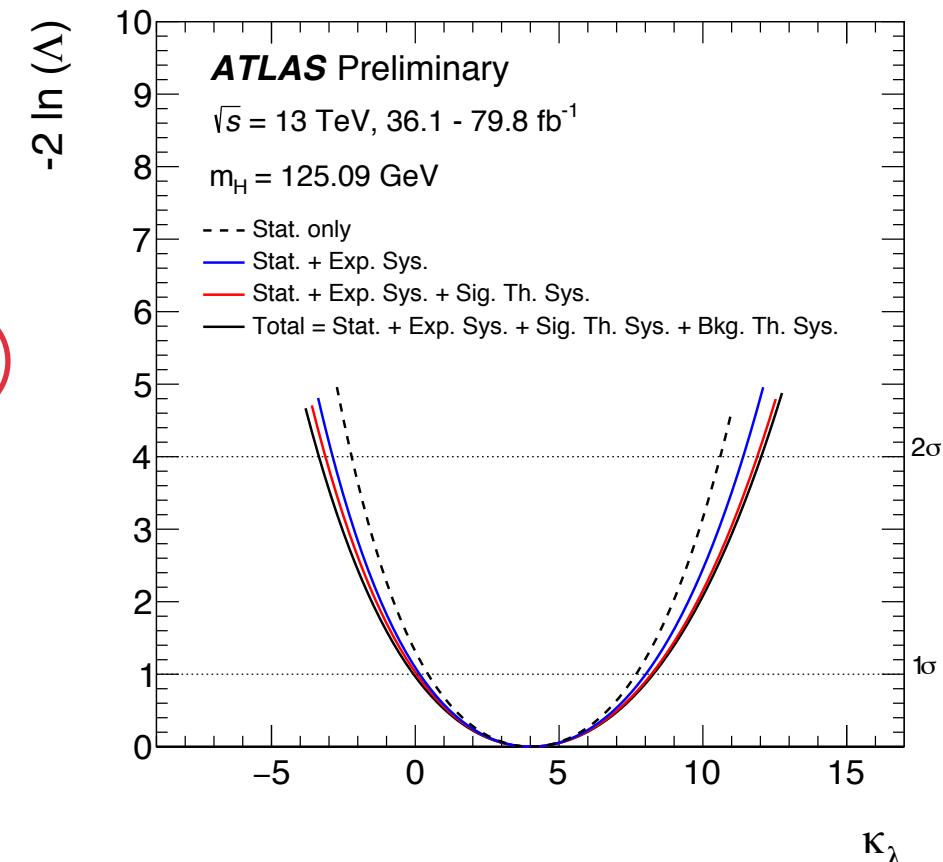
$$\mu_f(\kappa_\lambda, \kappa_f) = \frac{\text{BR}_f^{\text{BSM}}}{\text{BR}_f^{\text{SM}}} = \frac{\kappa_f^2 + (\kappa_\lambda - 1)C_1^f}{\sum_j \text{BR}_j^{\text{SM}} \left[ \kappa_j^2 + (\kappa_\lambda - 1)C_1^j \right]}$$



- Combined fit over Higgs combination

$$\kappa_\lambda = 4.0^{+4.3}_{-4.1} = 4.0^{+3.7}_{-3.6} (\text{stat.})^{+1.6}_{-1.5} (\text{exp.})^{+1.3}_{-0.9} (\text{sig. th.})^{+0.8}_{-0.9} (\text{bkg. th.})$$

- 95% C.L.  $-3.2 < \kappa_\lambda < 11.9$  comparable over direct HH searches ( $-5.0 < \kappa_\lambda < 12.1$ )



- Importance of  $m_H$  in several aspects of our understanding of fundamental physics.

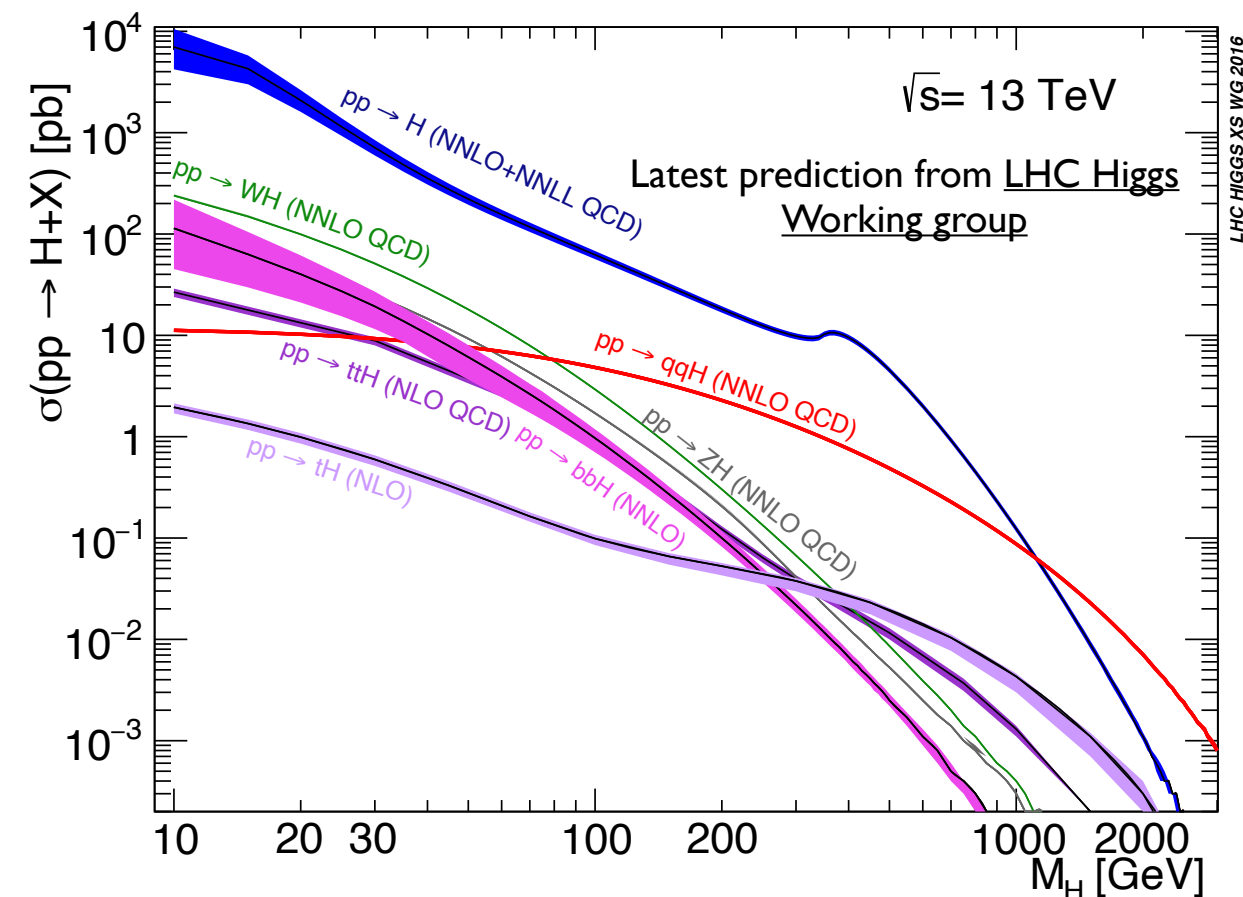
$$\mathcal{L} = -\frac{1}{4}F_{\mu\nu}F^{\mu\nu} + i\bar{\Psi}\not{D}\psi + D_{\mu}\Phi^{\dagger}D^{\mu}\Phi - \boxed{V(\Phi)} + \bar{\Psi}_L\hat{Y}\Phi\Psi_R + h.c.$$

Power law expansion of the potential

$$V(h) = \frac{1}{4}\lambda h^4 + \lambda v h^3 + \lambda v^2 h^2$$

- Understanding the perturbative expansion of its potential ( $\lambda v^2 h^2$ ).
- Precise higher order corrections to the theory predictions of the Higgs interactions depend on the value of  $m_H$ .
- Input to precision global fit of the Standard Model.

Aim at improving significantly on the experimental precision on  $m_H$



Prediction and uncertainties of Higgs production processes as a function of the  $m_H$

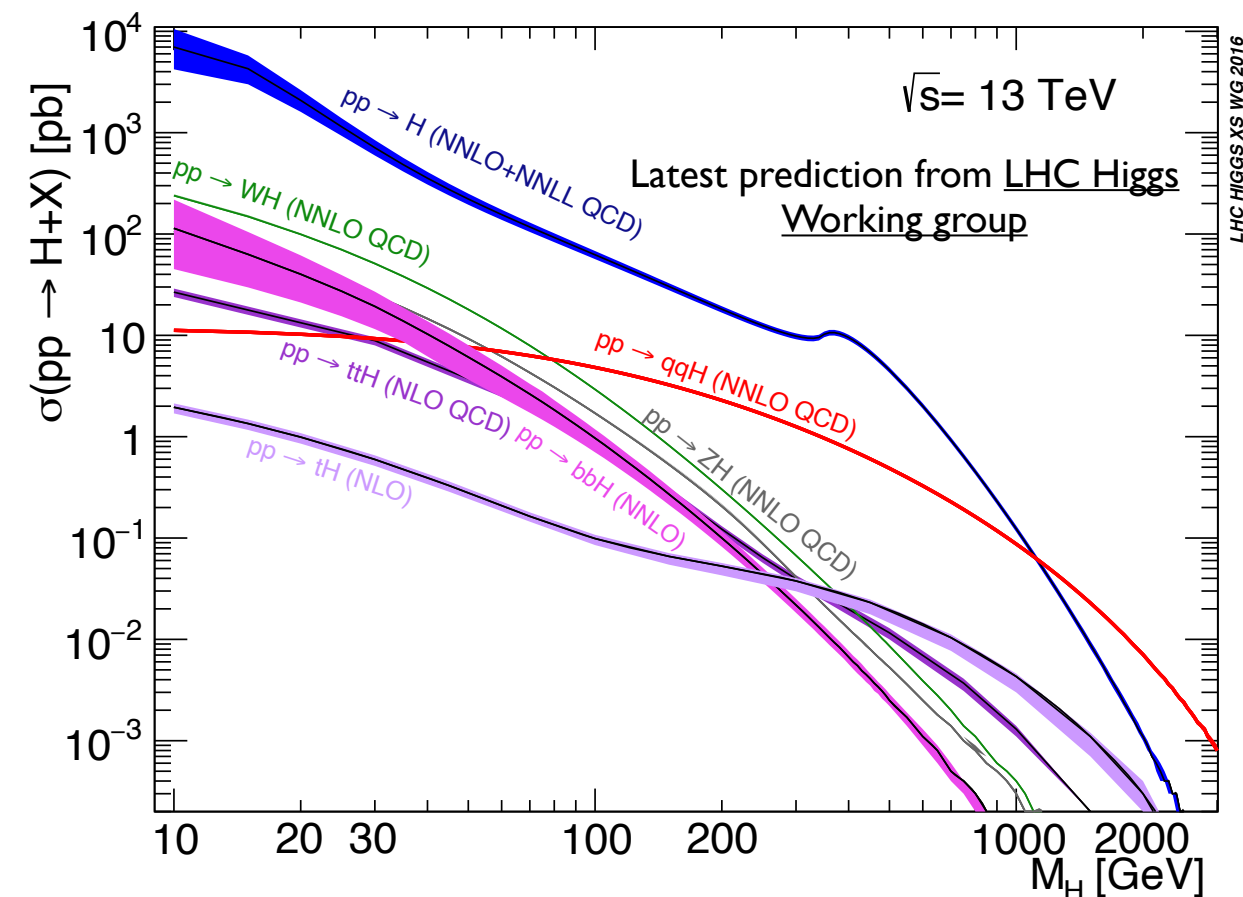
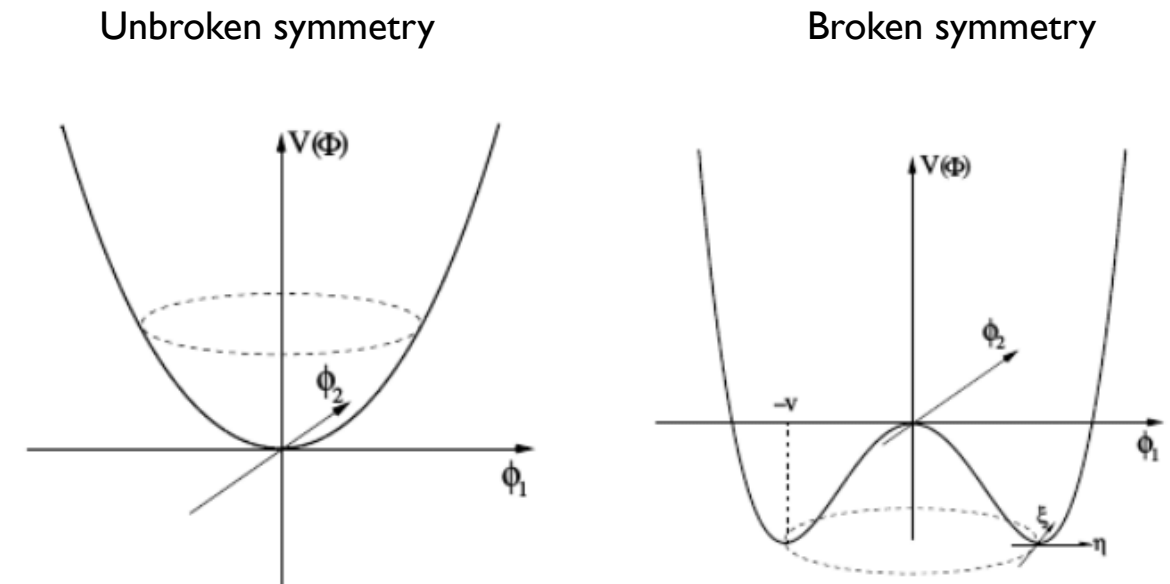
- Importance of  $m_H$  in several aspects of our understanding of fundamental physics.

Power law expansion of the potential

$$V(h) = \frac{1}{4}\lambda h^4 + \lambda v h^3 + \lambda v^2 h^2$$

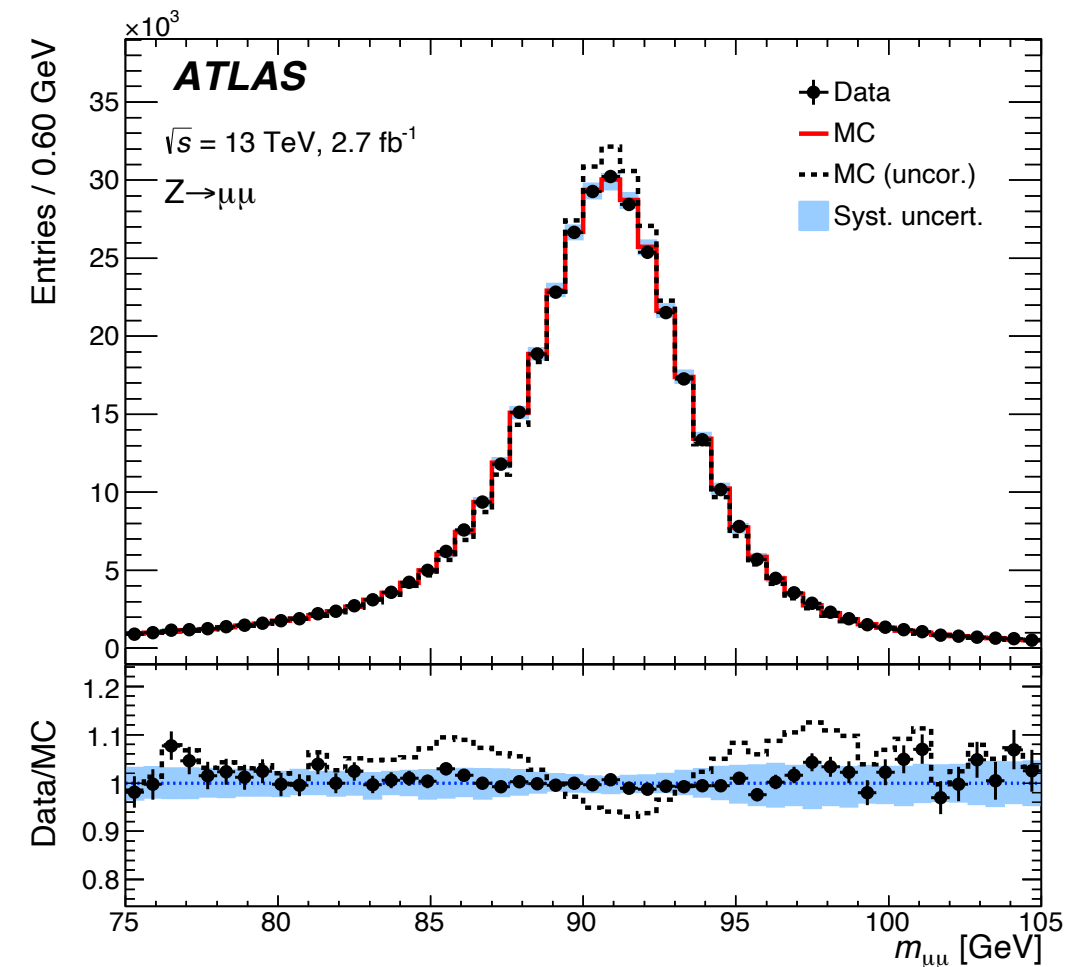
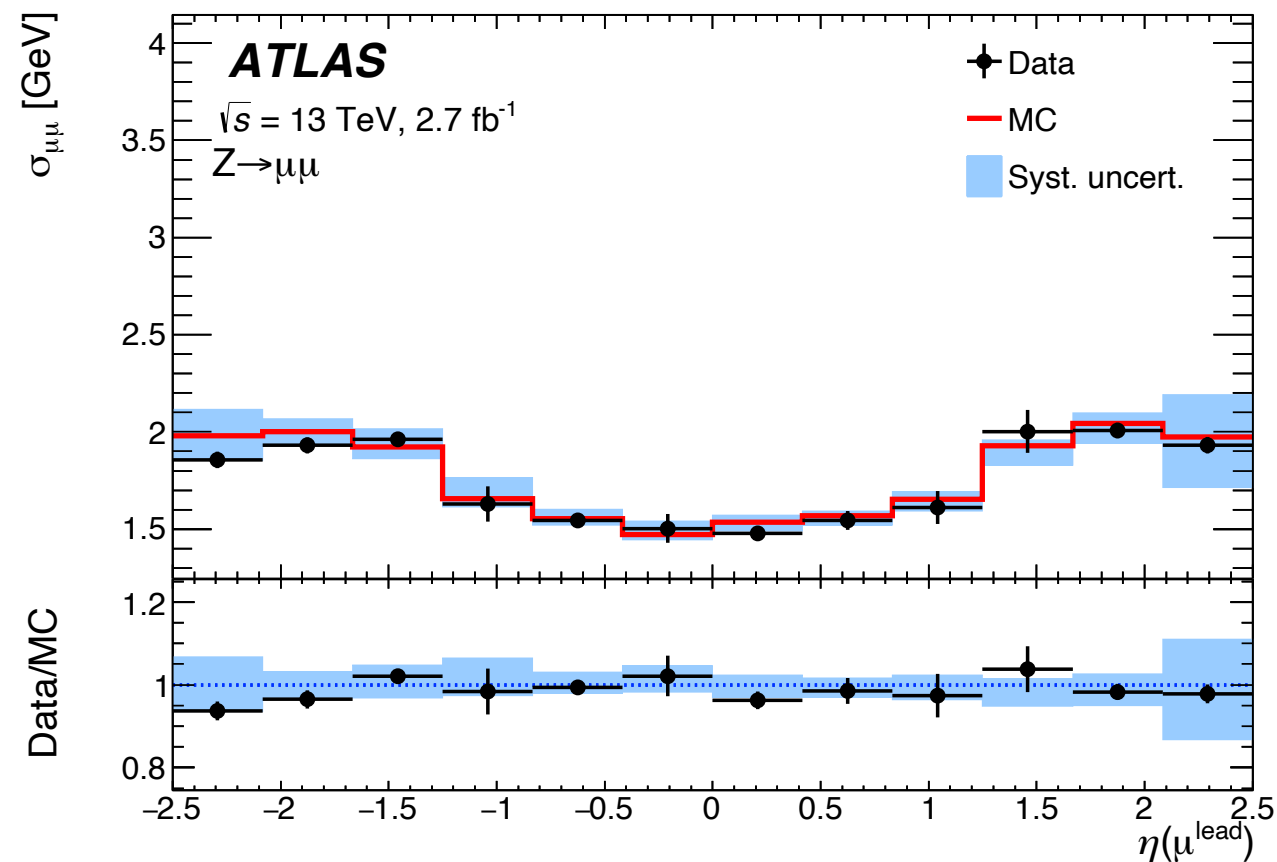
- Understanding the perturbative expansion of its potential ( $\lambda v^2 h^2$ ).
- Precise higher order corrections to the theory predictions of the Higgs interactions depend on the value of  $m_H$ .
- Input to precision global fit of the Standard Model.

Aim at improving significantly on the experimental precision on  $m_H$



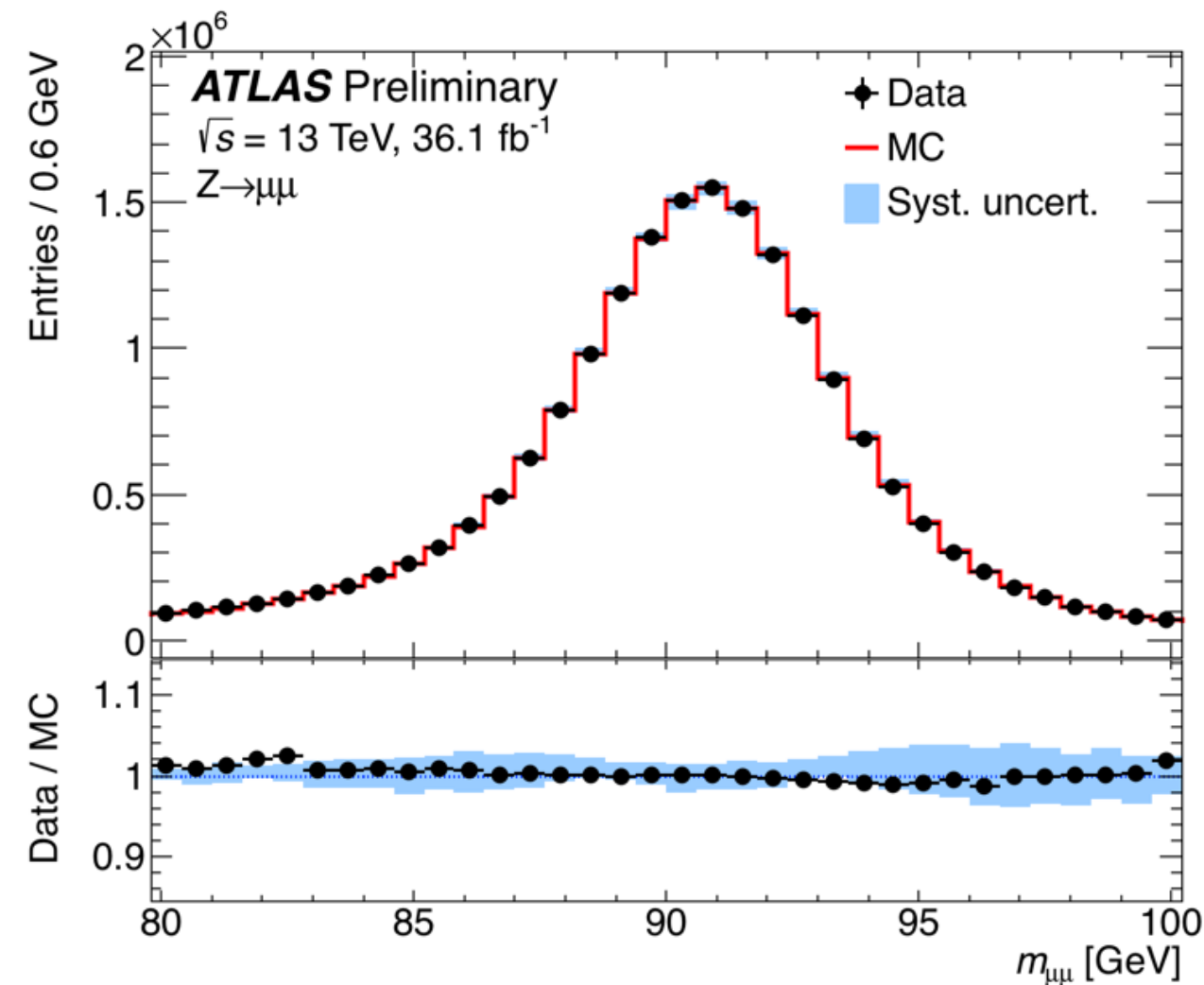
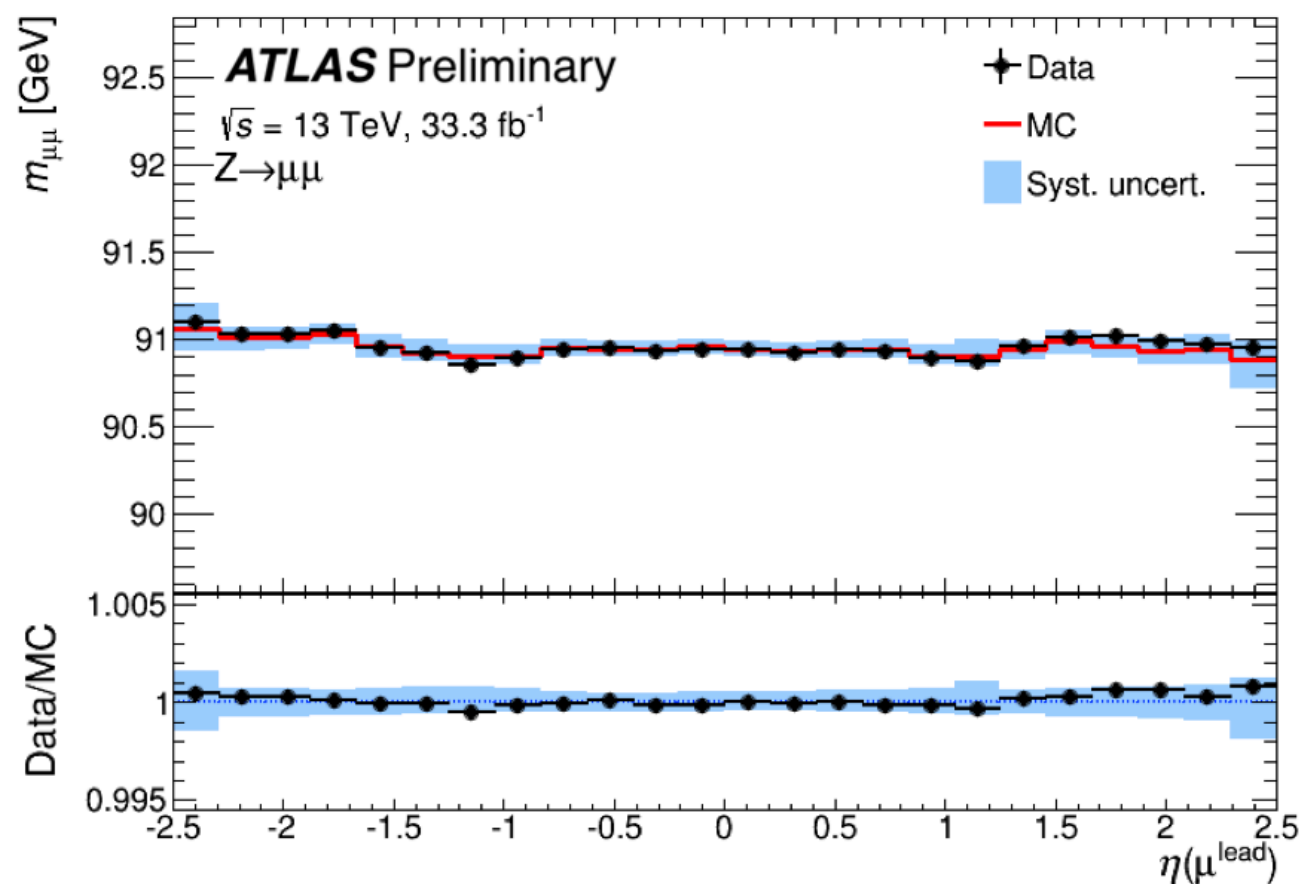
Prediction and uncertainties of Higgs production processes as a function of the  $m_H$

- Resolution muon channels ( $4\mu$ ,  $2e2\mu$  and  $4\mu$ ) crucial for  $m_H$  uncertainty:
  - ▶ Excellent momentum resolution of about 1% at about  $p_T$  45 ~GeV.
- Momenta calibrated to  $J/\psi$  and  $Z$  samples in data
  - ▶ for residual mis modelling of  $E^{\text{loss}}$  in calorimeters, alignment precision etc.
  - ▶ Including corrections to data accounting for alignment weak modes.
  - ▶ Precision down to 0.5 per mille for  $|\eta| < 1.0$





- Resolution muon channels ( $4\mu$ ,  $2e2\mu$  and  $4\mu$ ) crucial for  $m_H$  uncertainty:
  - ▶ Excellent momentum resolution of about 1% at about  $p_T$  45 ~GeV.
- Simulated momenta calibrated to  $J/\psi$  and  $Z$  samples in data
  - ▶ for residual mis modelling of  $E^{\text{loss}}$  in calorimeters, alignment precision etc.
  - ▶ Uncertainty of about 10% on the resolution and 0.5% on the momentum scale.

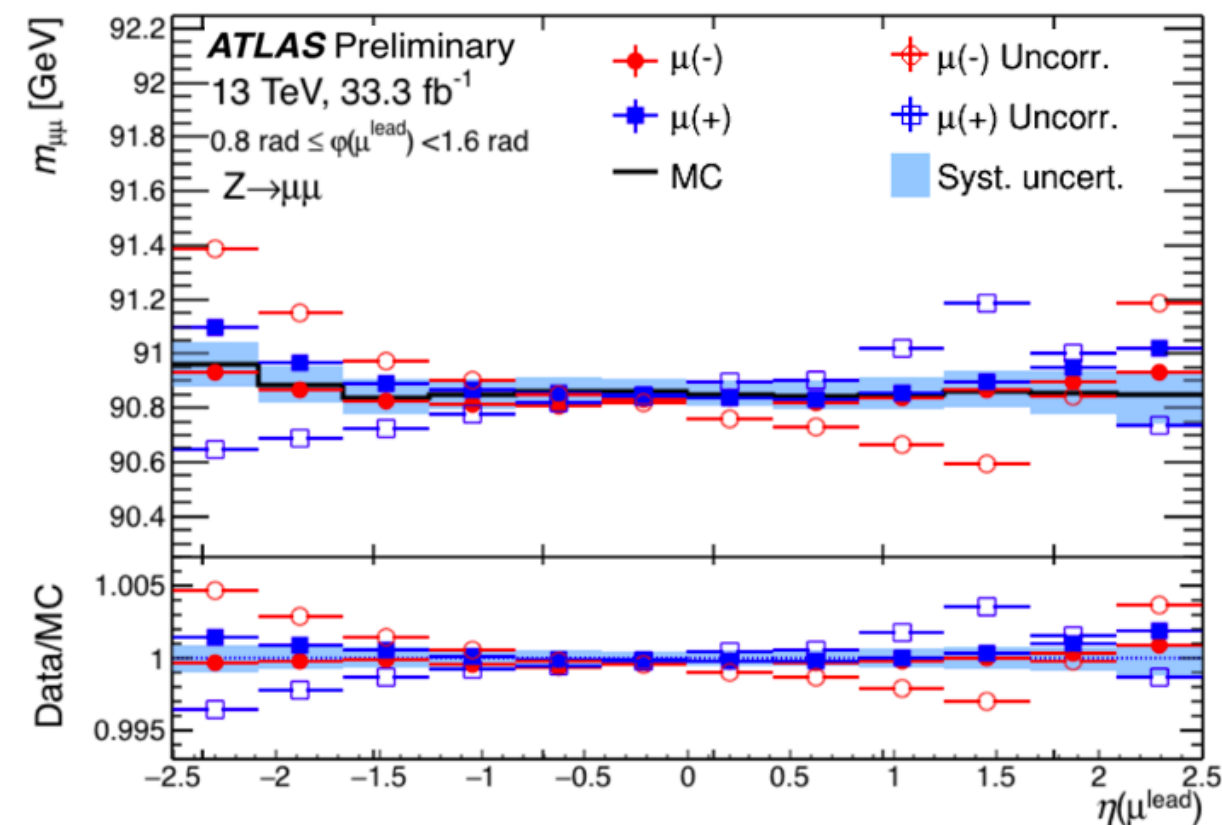
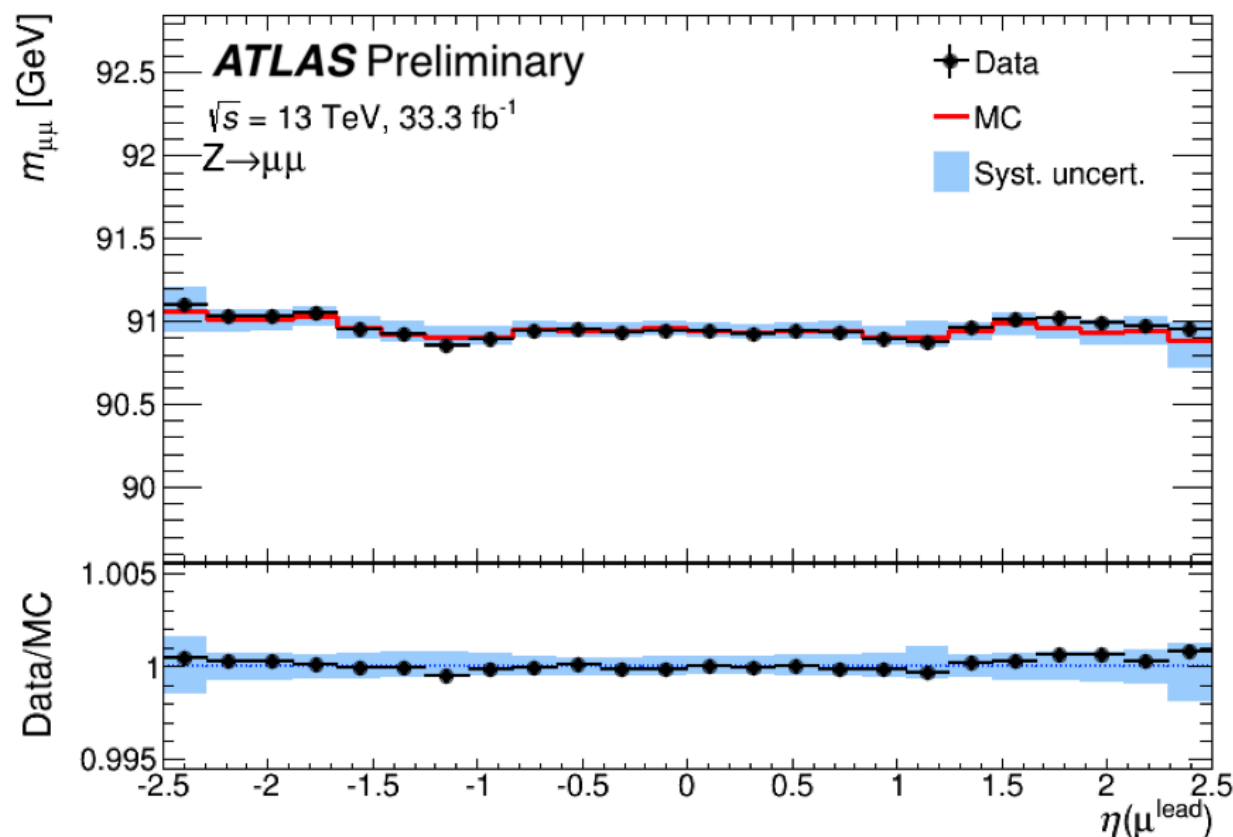
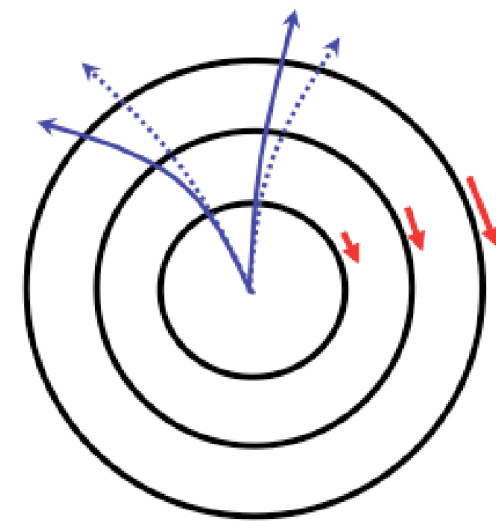


- Local misalignments and second order effects:

- Charge dependent sagitta bias, with net effect of worsening resolution
- In-situ correction based on  $Z \rightarrow \mu\mu$  data, **recovers up to 5% in resolution.**

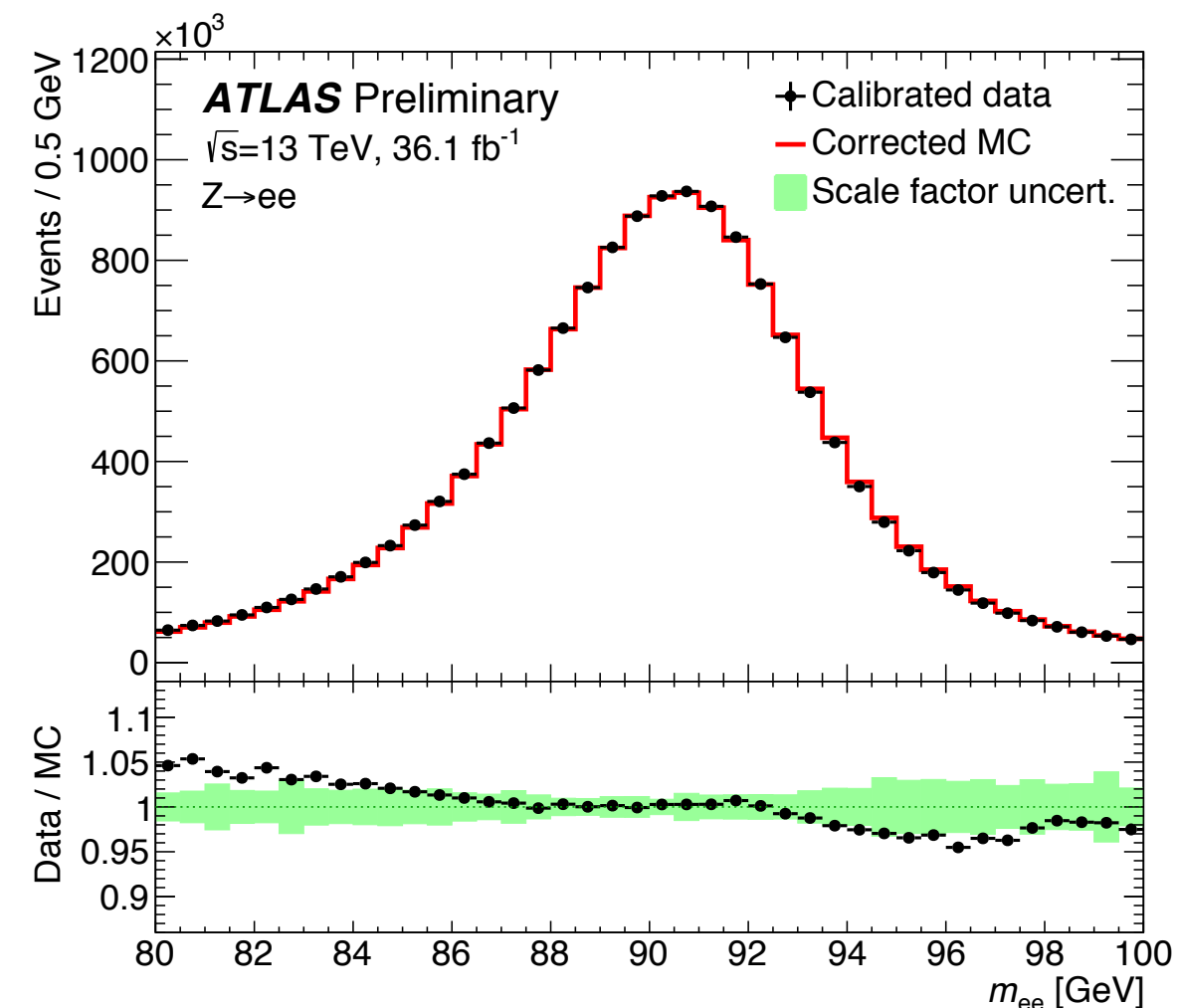
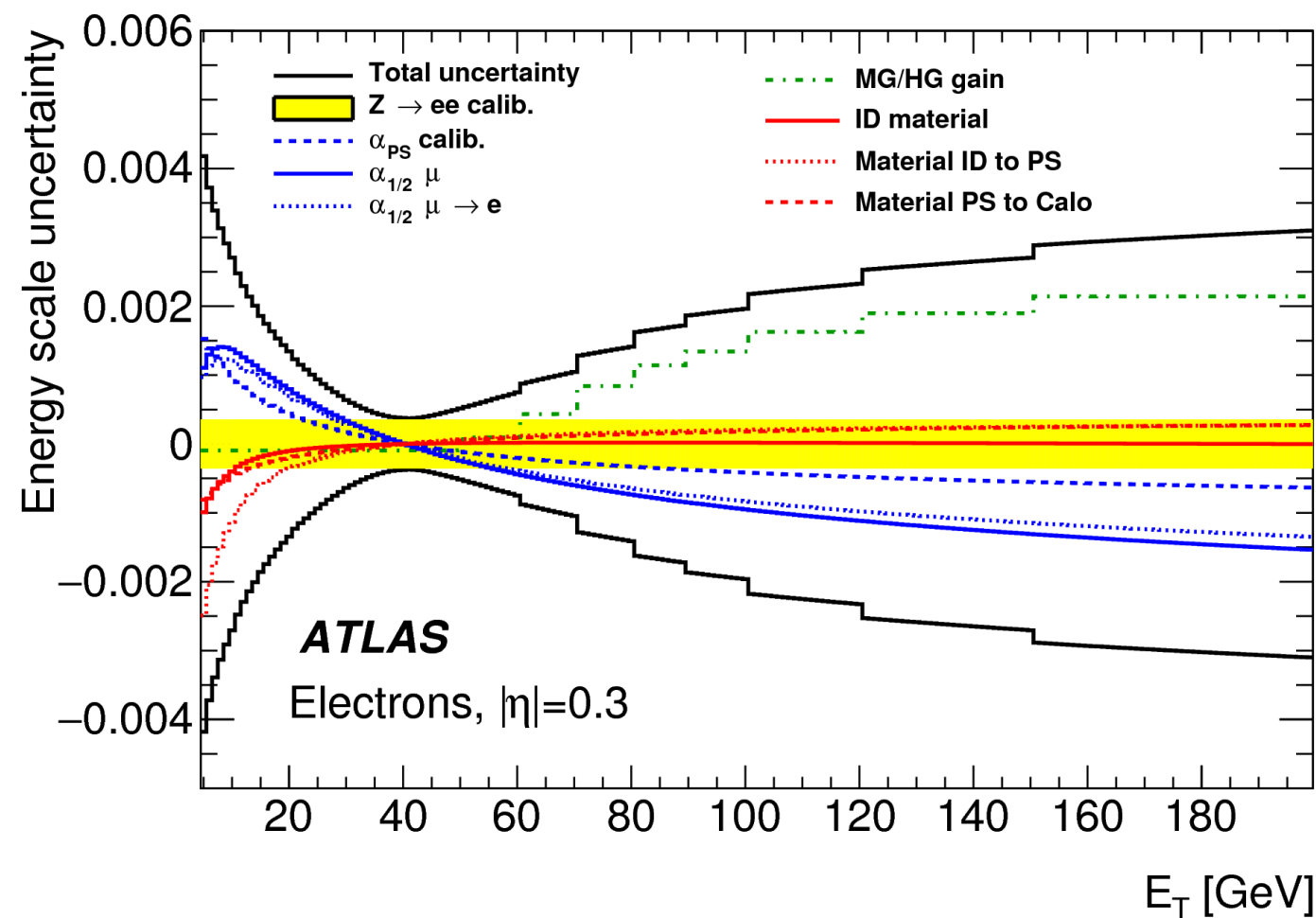
- Momentum scale understood down to the per mille level

- Precision down to 0.5 per mille for  $|\eta| < 1.0$

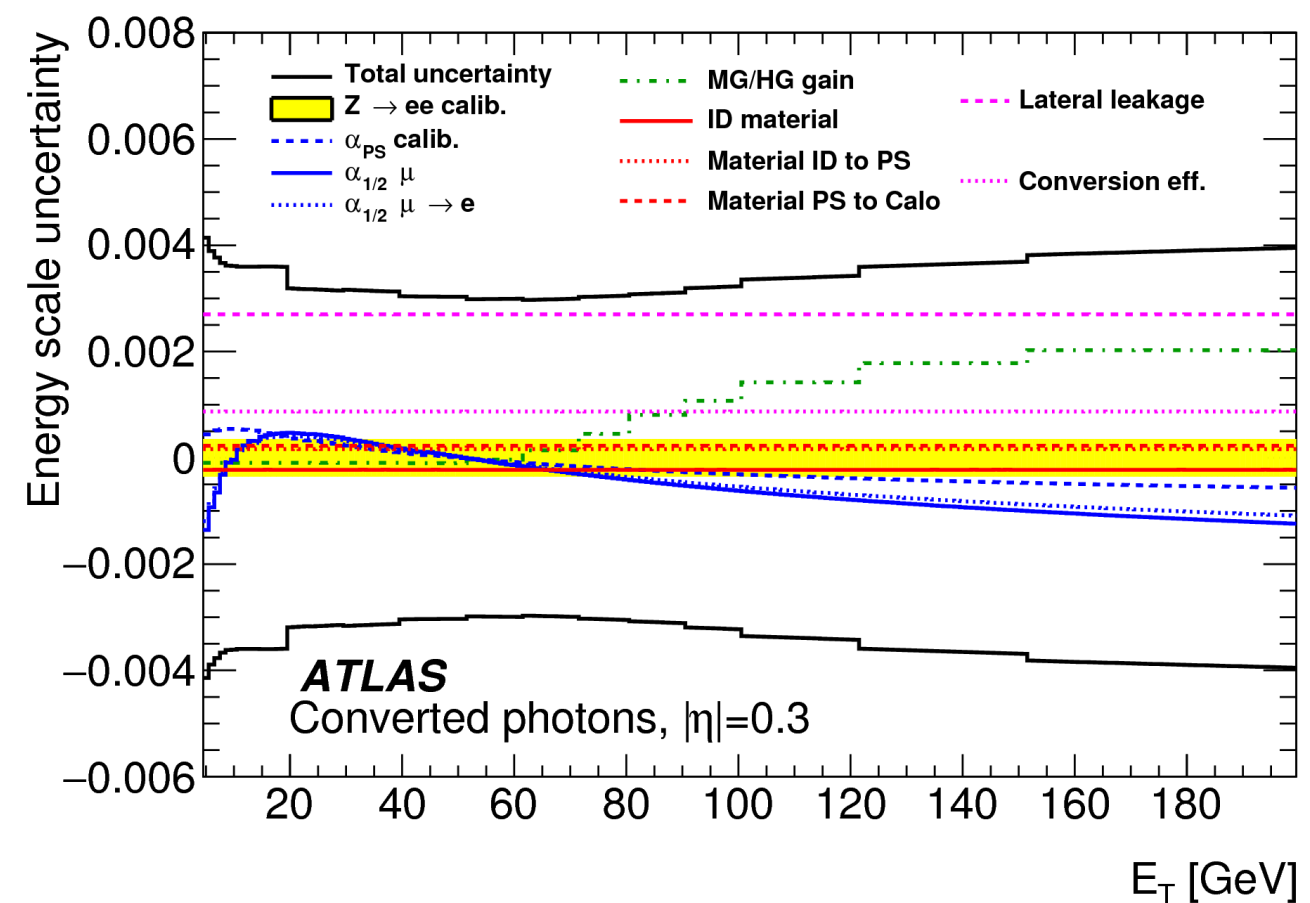
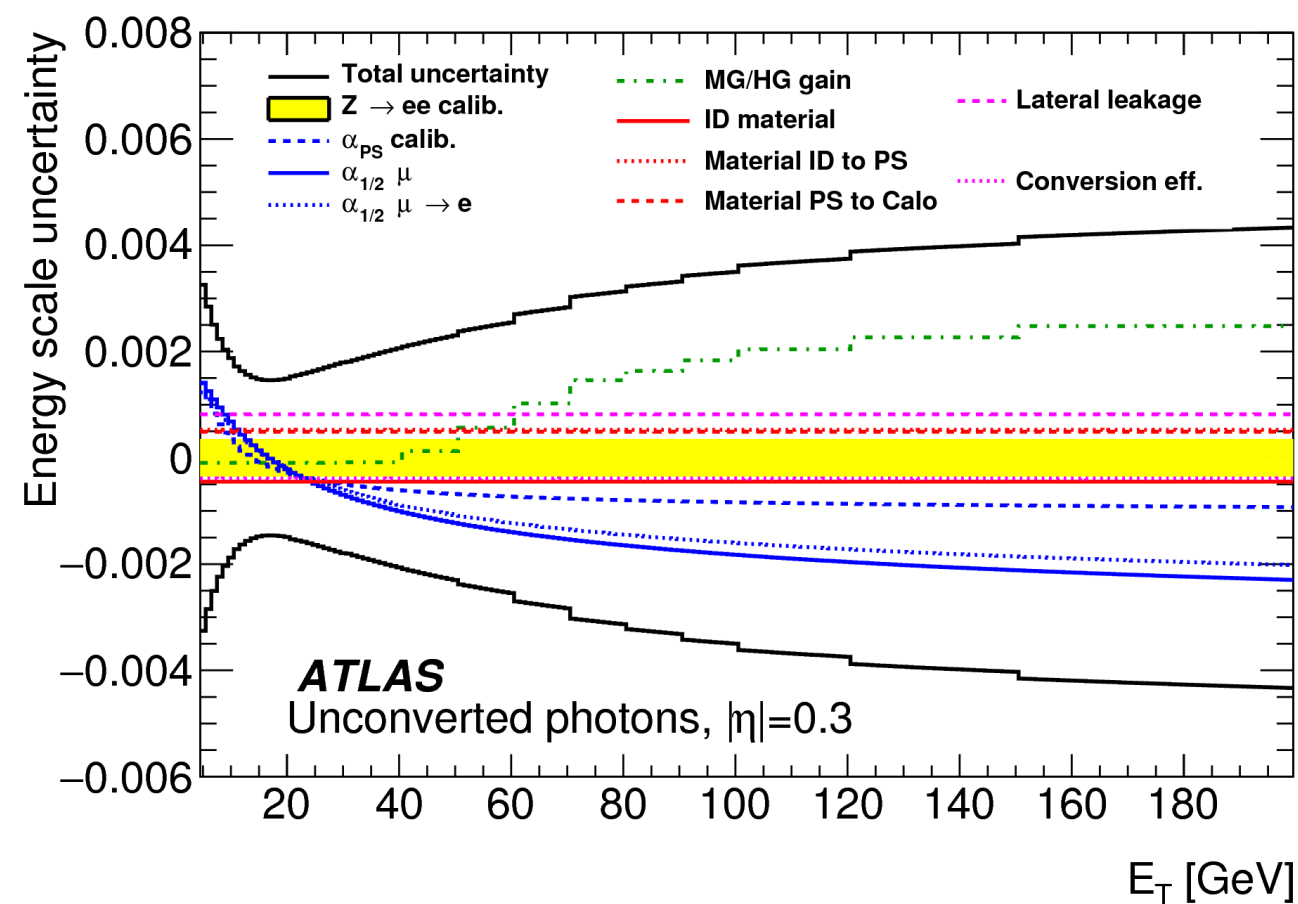




- Good energy calibration necessary for increased precision on  $m_H$ 
  - ▶ Two step approach: i) material energy loss and ii) global calorimetric scale from  $Z \rightarrow ee$  data
- Total scale uncertainty of at 40 GeV at the per-mille level.



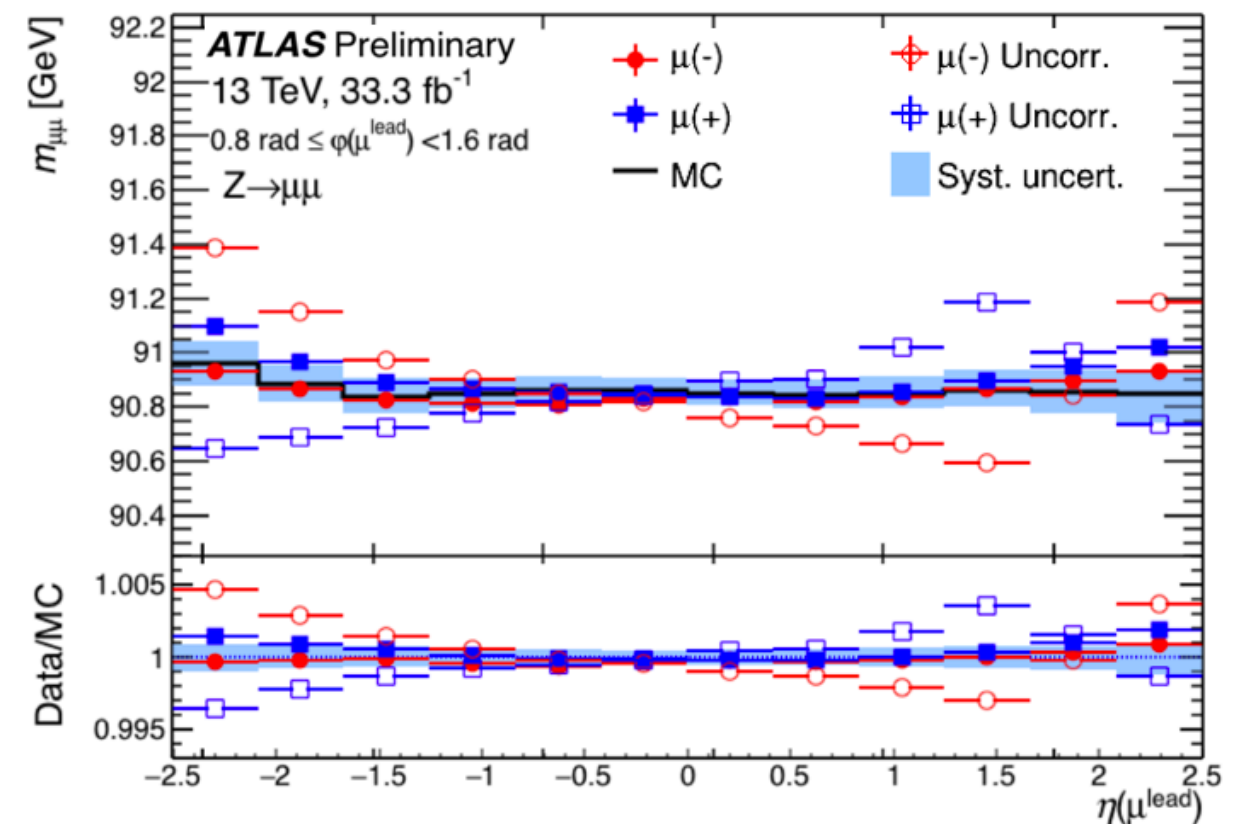
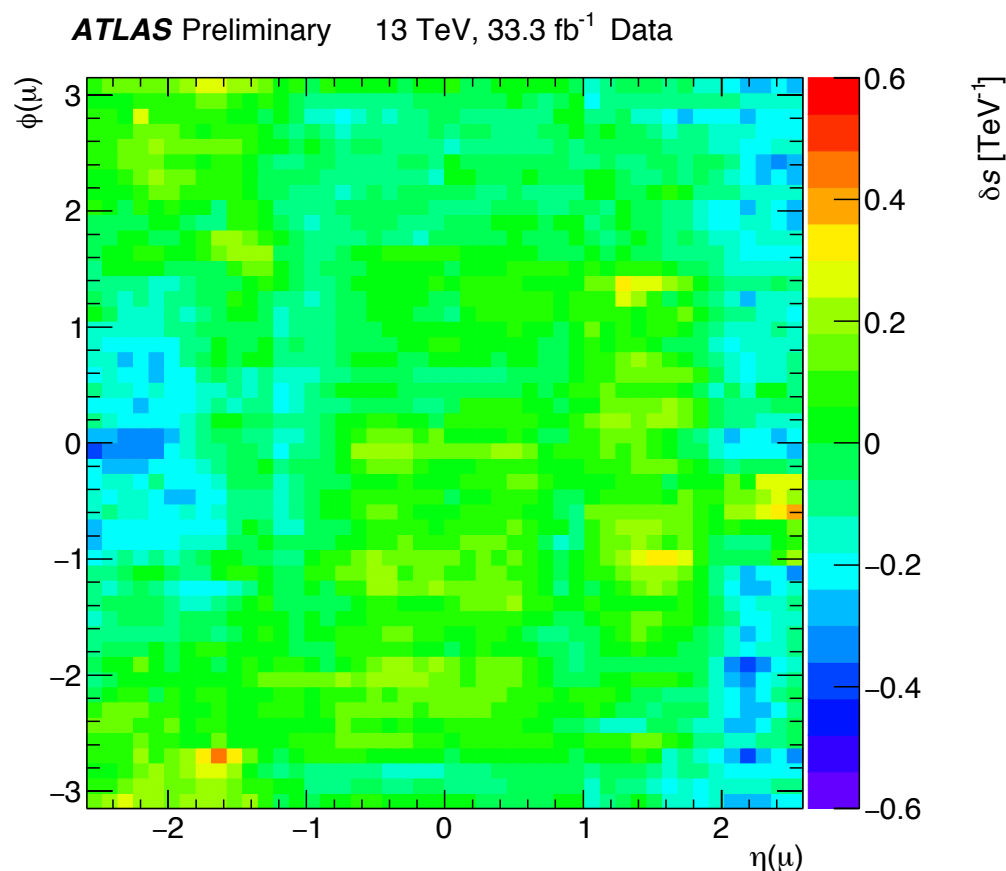
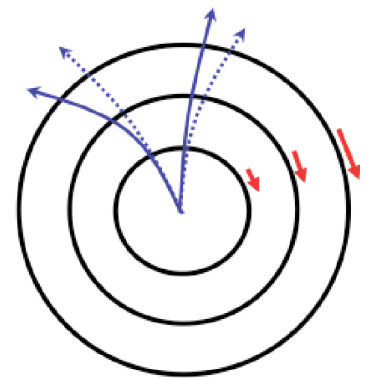
- Good energy calibration necessary for increased precision on  $m_H$ 
  - ▶ Two step approach: i) material energy loss and ii) global calorimetric scale from  $Z \rightarrow ee$  data
- Total scale uncertainty of at 40 GeV at the per-mille level.



## ● Correction for local misalignments

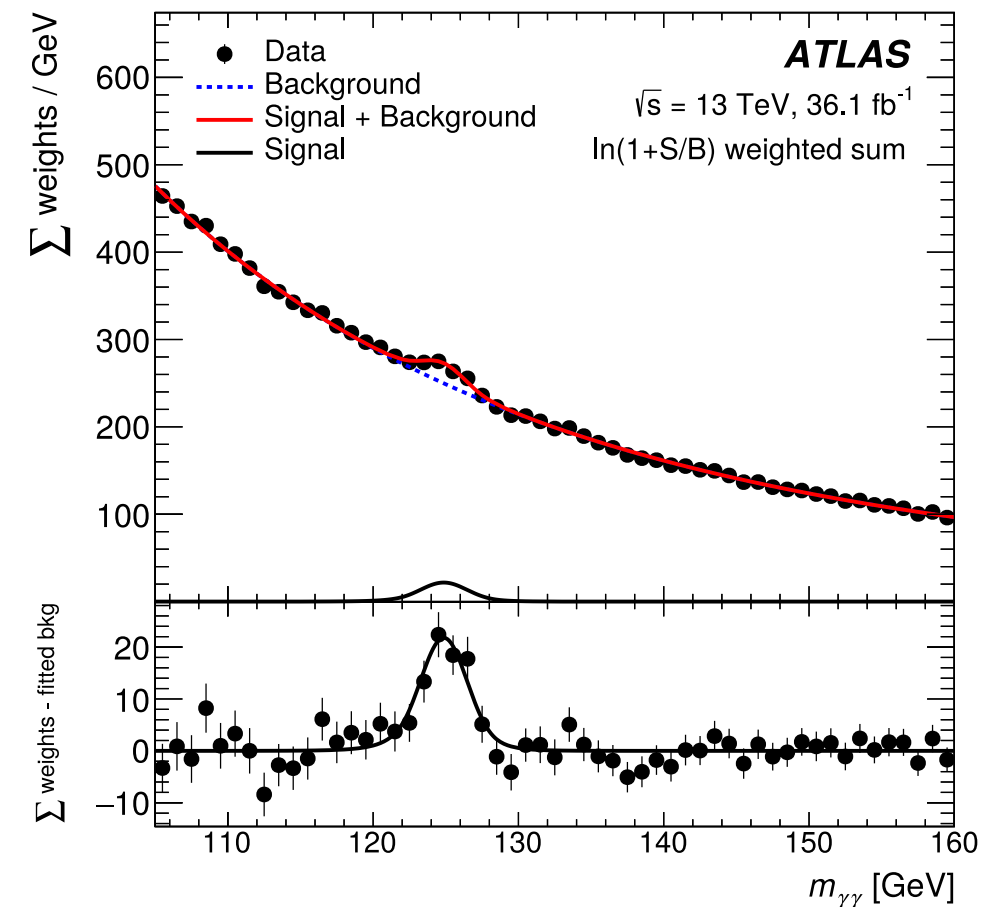
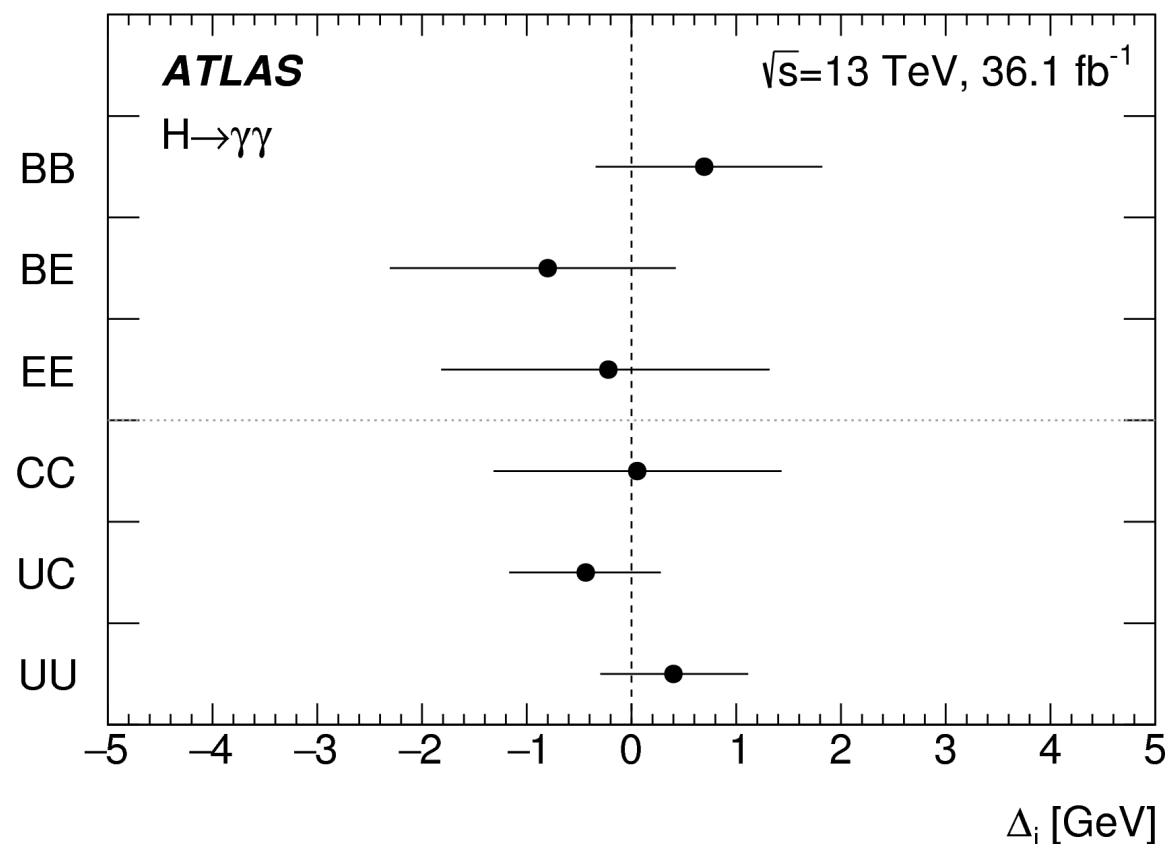
- ▶ Charge dependent bias, with net effect of worsening resolution
- ▶ In-situ correction based on  $Z \rightarrow \mu\mu$  data, recovers up to 5% in resolution.
- ▶ Iteratively removing the bias  $\delta_s$ :

$$p_T^{\text{corr}}(\mu) = \frac{p_T^{\text{bias}}(\mu)}{1 - q(\mu)\delta_s(\eta, \phi)p_T^{\text{bias}}(\mu)}$$



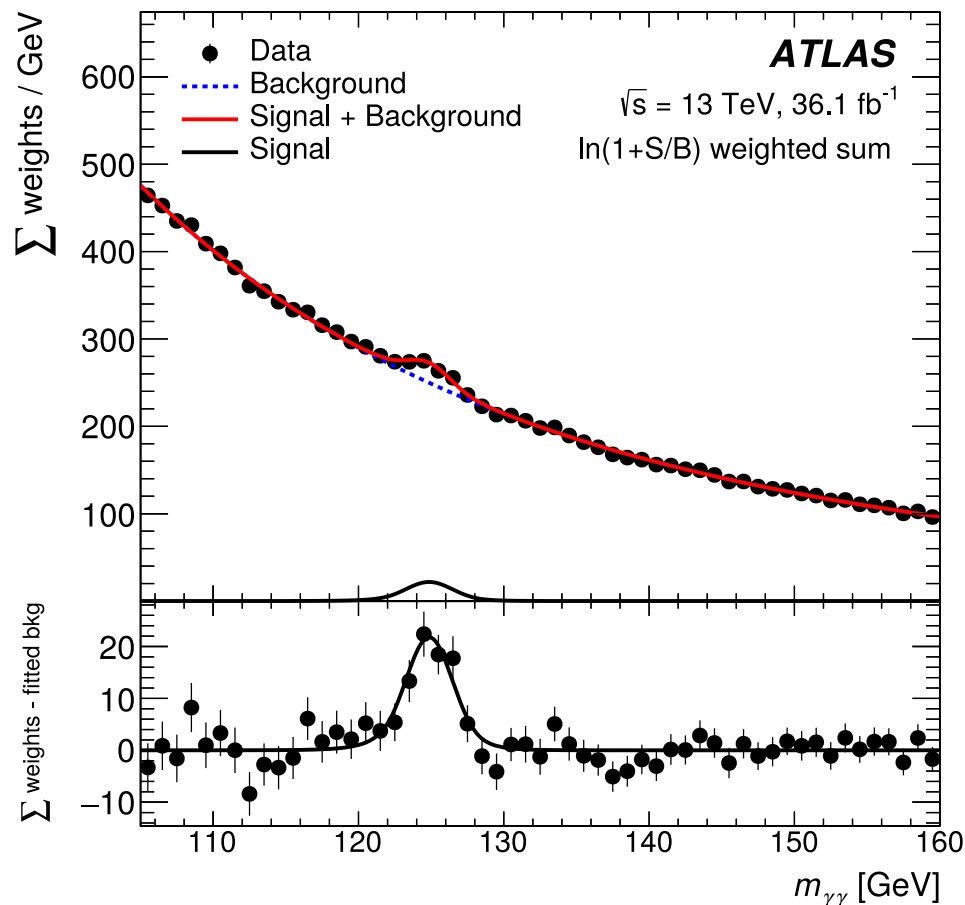
- $H \rightarrow \gamma\gamma$  updated result at Run II.
  - ▶ Analytical function in kinematic and detector categories.
  - ▶ Reduction of uncertainty through categorisation of events as a function of resolution and signal significance.
- Expected statistical uncertainty of **0.21 GeV** and **0.34 GeV** systematic uncertainty

$$m_H^{\gamma\gamma} = 124.93 \pm 0.40 (\pm 0.21 \text{ stat only}) \text{ GeV}$$



- $H \rightarrow \gamma\gamma$  updated result at Run II.
  - ▶ Analytical function in kinematic and detector categories.
  - ▶ Reduction of uncertainty through categorisation of events as a function of resolution and signal significance.
- Expected statistical uncertainty of **0.21 GeV** and **0.34 GeV** systematic uncertainty

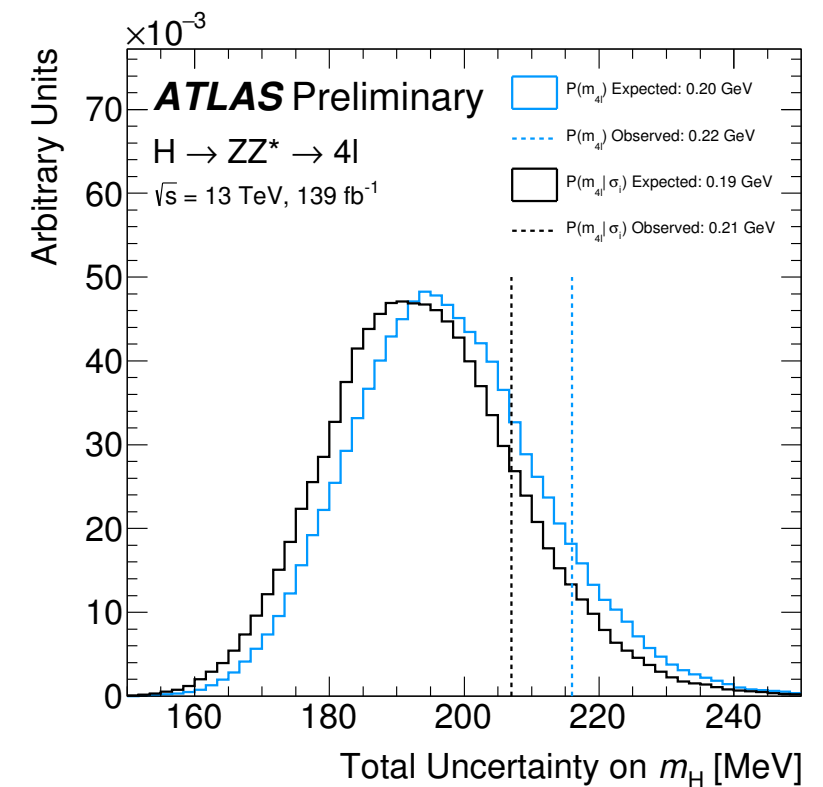
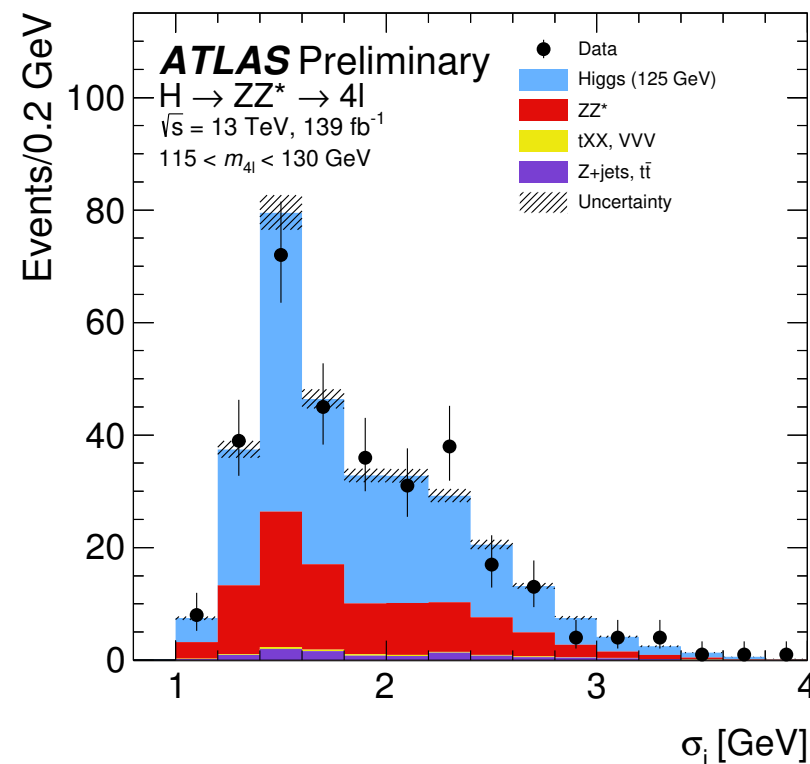
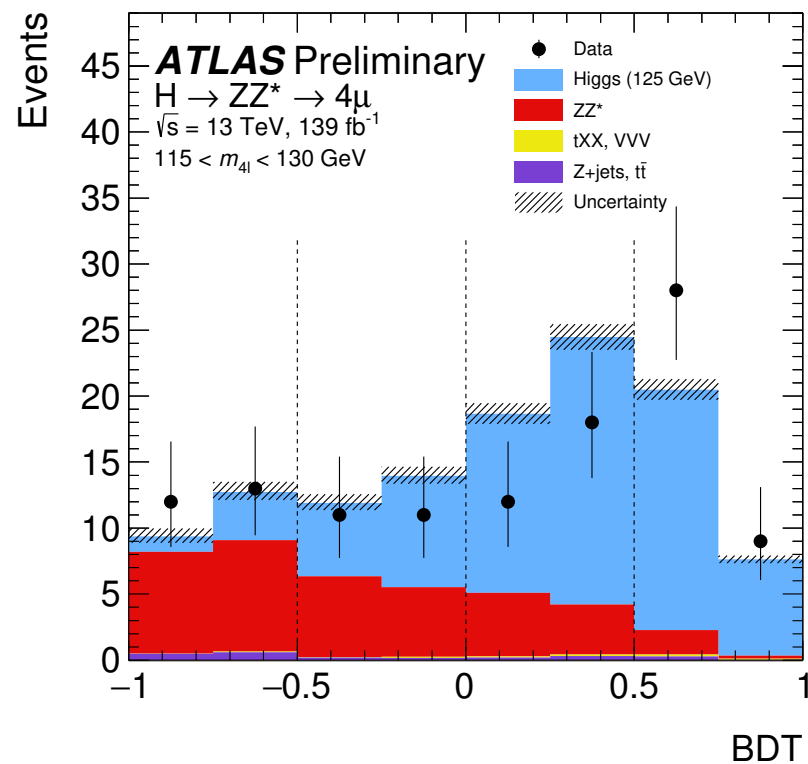
$$m_H^{\gamma\gamma} = 124.93 \pm 0.40 \text{ (}\pm 0.21 \text{ stat only) GeV}$$



Source	Systematic uncertainty in $m_H$ [MeV]
EM calorimeter response linearity	60
Non-ID material	55
EM calorimeter layer intercalibration	55
$Z \rightarrow ee$ calibration	45
ID material	45
Lateral shower shape	40
Muon momentum scale	20
Conversion reconstruction	20
$H \rightarrow \gamma\gamma$ background modelling	20
$H \rightarrow \gamma\gamma$ vertex reconstruction	15
$e/\gamma$ energy resolution	15
All other systematic uncertainties	10

## ● Three-prong approach to reduce uncertainty at analysis level:

- (i) ~15% from  $m_{12}$  constraint to  $m_Z$  with kinematic fit and  $m_Z$  constraints on alignment weak modes.
- (i) ~2% from **kinematic discriminant** selecting signal and background events
  - ▶ Boosted Decision Tree on  $p_T(4\ell)$ ,  $y(4\ell)$  and  $\log(|\mathcal{M}_H|^2/|\mathcal{M}_{ZZ^*}|^2)$
- (ii) ~5% from multivariate **per-event resolution likelihood**.
  - ▶ Neural network to solve uncertainty correlations induced by kinematic discriminant.



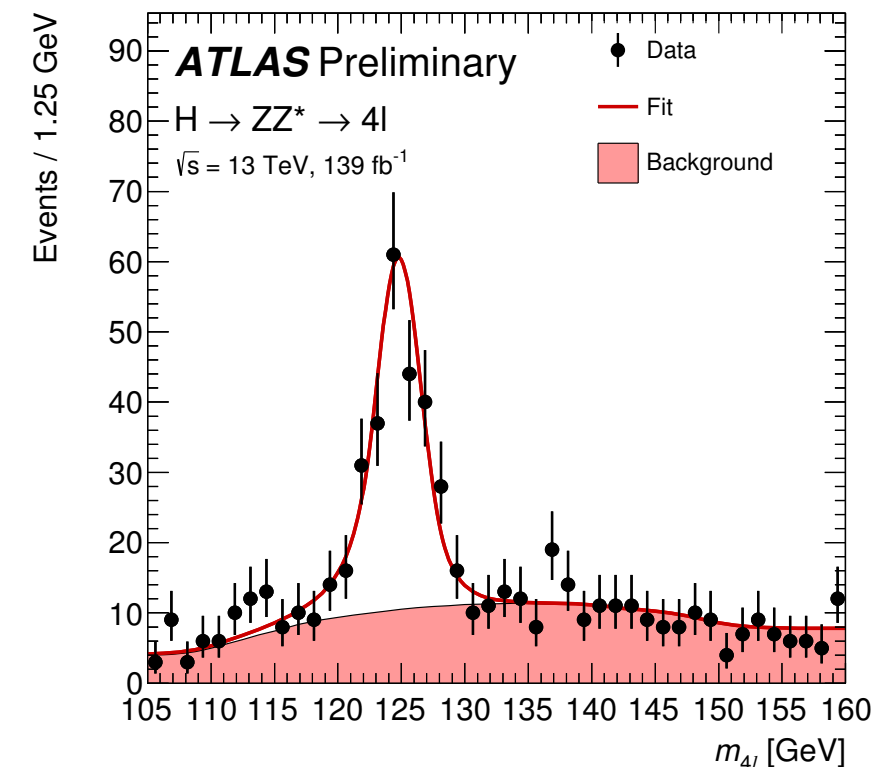
## ● Three-prong approach to reduce uncertainty at analysis level:

- (i) ~15% from  $m_{12}$  constraint to  $m_Z$  with kinematic fit and  $m_Z$  constraints on alignment weak modes.
- (i) ~2% from kinematic discriminant selecting signal and background events
  - ▶ Boosted Decision Tree on  $p_T(4\ell)$ ,  $y(4\ell)$  and  $\log(|\mathcal{M}_H|^2/|\mathcal{M}_{ZZ^*}|^2)$
- (ii) ~2% from multivariate per-event resolution likelihood.
  - ▶ Neural network to solve uncertainty correlations induced by kinematic discriminant.

## ● Systematic uncertainty of ~70 MeV

Systematic Uncertainty	Impact (GeV)
Muon momentum scale	+0.08, -0.06
Electron energy scale	$\pm 0.02$
Muon momentum resolution	$\pm 0.01$
Muon sagitta bias correction	$\pm 0.01$

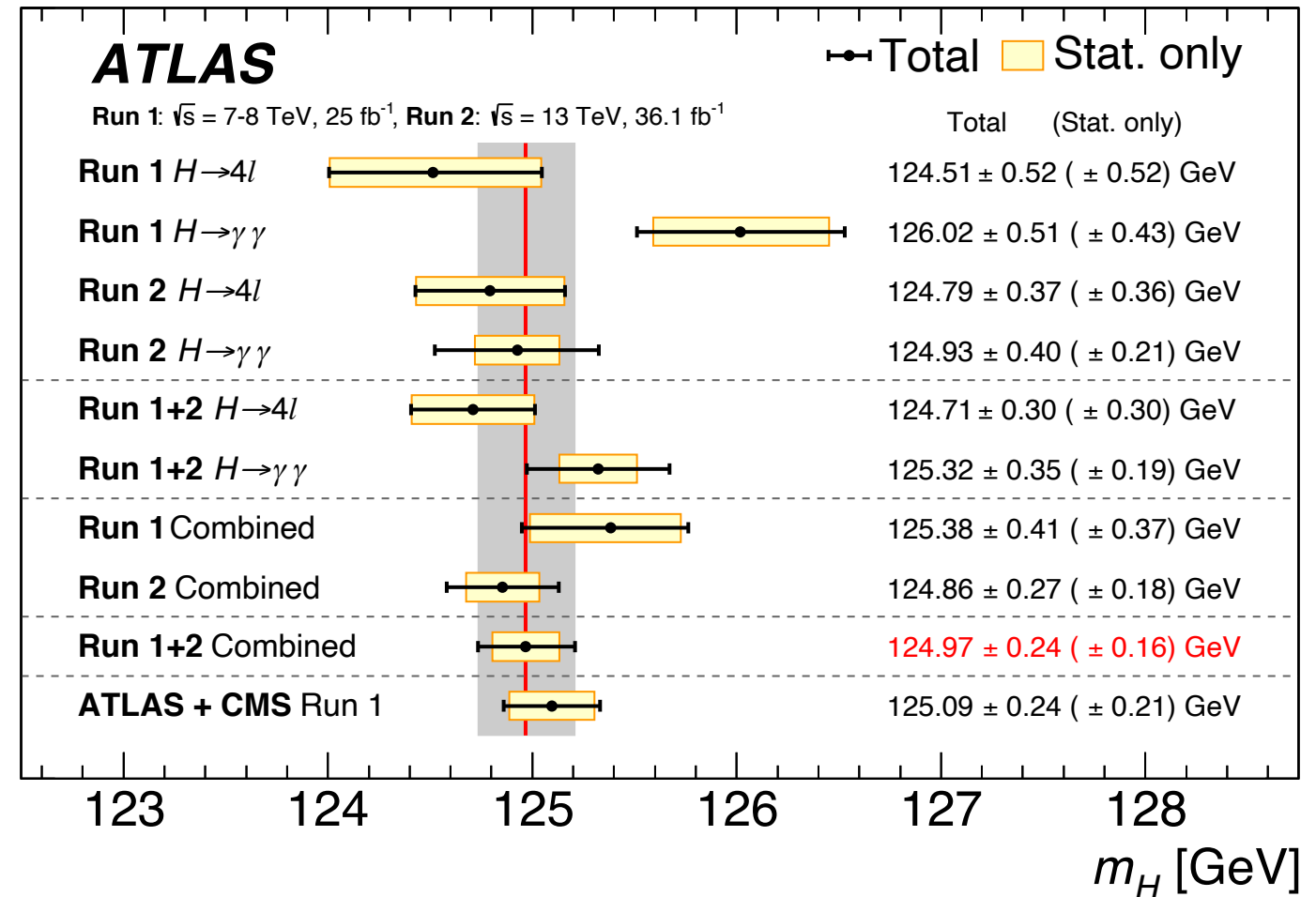
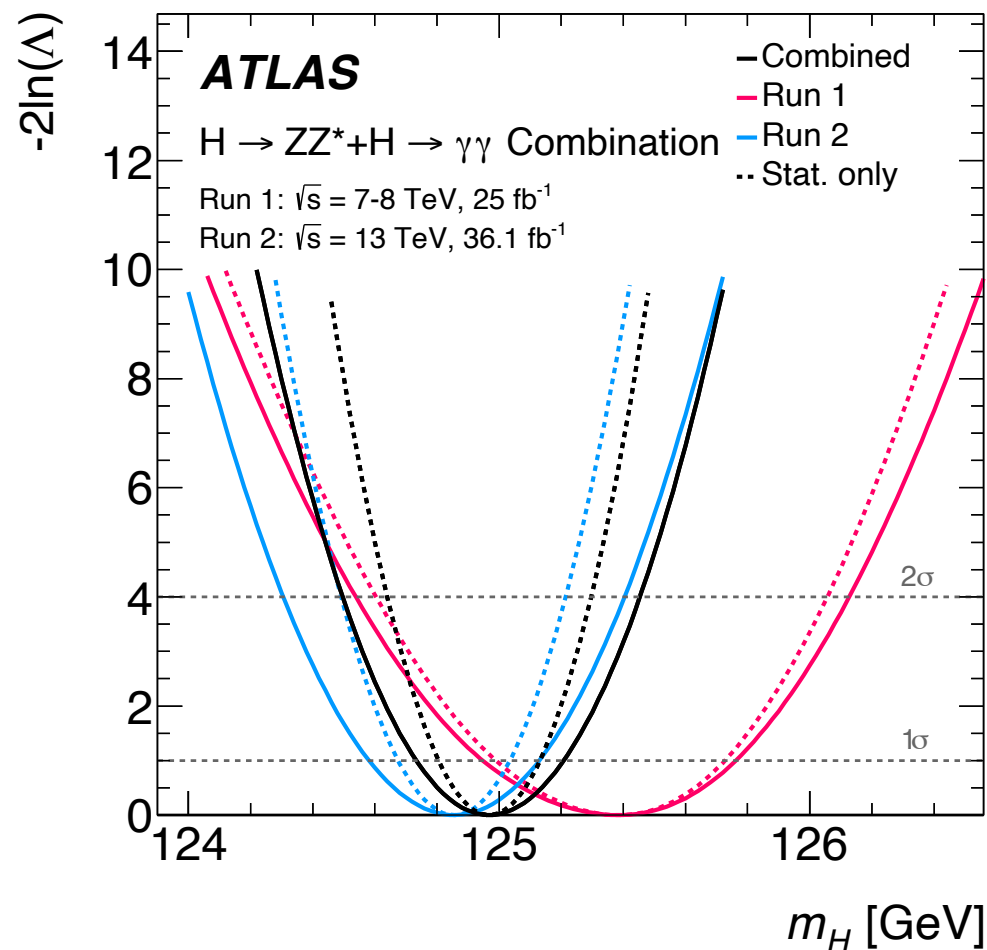
- ▶ 61% improvement w.r.t  $m_H^{H \rightarrow ZZ, \text{Run I}}$
- ▶ 15% improved precision w.r.t  $m_H^{\text{ATLAS+CMS, Run I}}$



$$m_H = 124.92^{+0.21}_{-0.20} \text{ GeV}$$



- $4\ell$  and  $\gamma\gamma$  measurements are combined with ATLAS Run I result [arXiv:1806.00242](https://arxiv.org/abs/1806.00242)



- Run 2 precision improved w.r.t Run I.

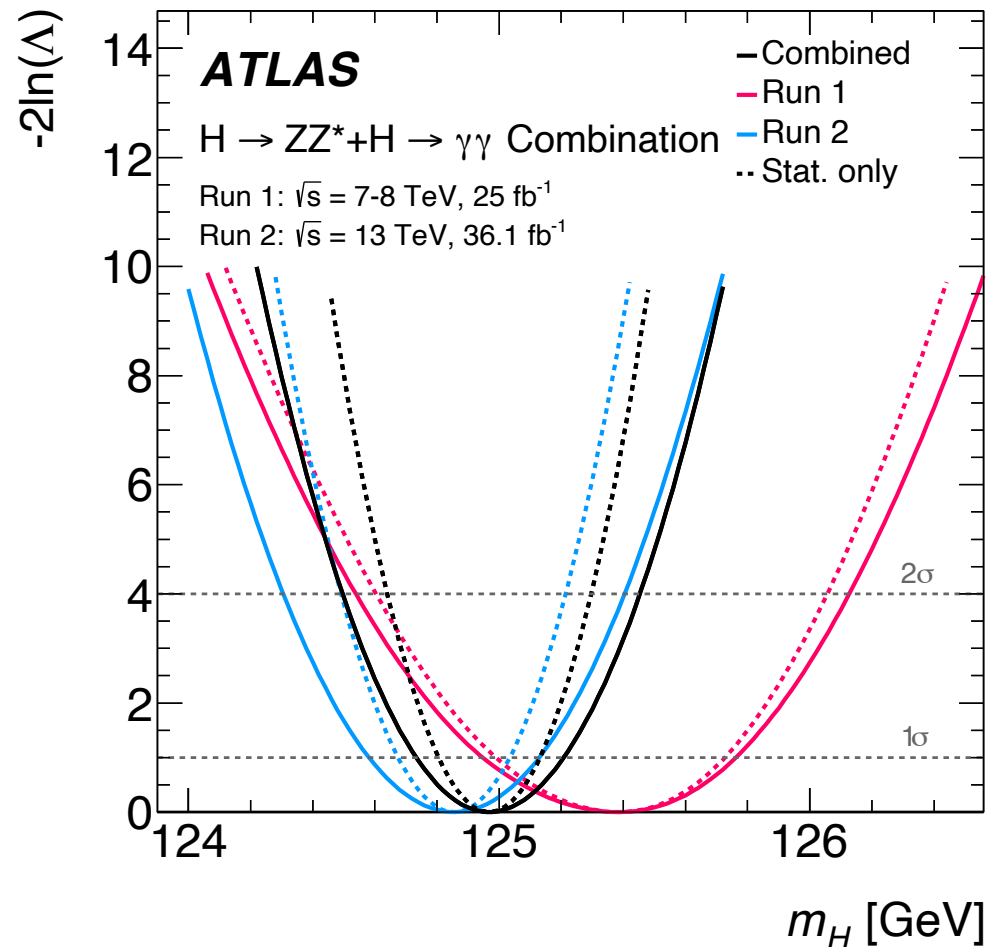
$$m_H = 124.86 \pm 0.27 (\pm 0.18 \text{ stat only}) \text{ GeV}$$

- ATLAS Run I + 2 comparable precision to LHC Run I combination.

$$m_H = 124.97 \pm 0.24 (\pm 0.16 \text{ stat only}) \text{ GeV}$$



- $4\ell$  and  $\gamma\gamma$  measurements are combined with ATLAS Run I result



Source	Systematic uncertainty in $m_H$ [MeV]
EM calorimeter response linearity	60
Non-ID material	55
EM calorimeter layer intercalibration	55
$Z \rightarrow ee$ calibration	45
ID material	45
Lateral shower shape	40
Muon momentum scale	20
Conversion reconstruction	20
$H \rightarrow \gamma\gamma$ background modelling	20
$H \rightarrow \gamma\gamma$ vertex reconstruction	15
$e/\gamma$ energy resolution	15
All other systematic uncertainties	10

- Run 2 precision improved w.r.t Run I.

$$m_H = 124.86 \pm 0.27 (\pm 0.18 \text{ stat only}) \text{ GeV}$$

- ATLAS Run I + 2 comparable precision to LHC Run I combination.

$$m_H = 124.97 \pm 0.24 (\pm 0.16 \text{ stat only}) \text{ GeV}$$

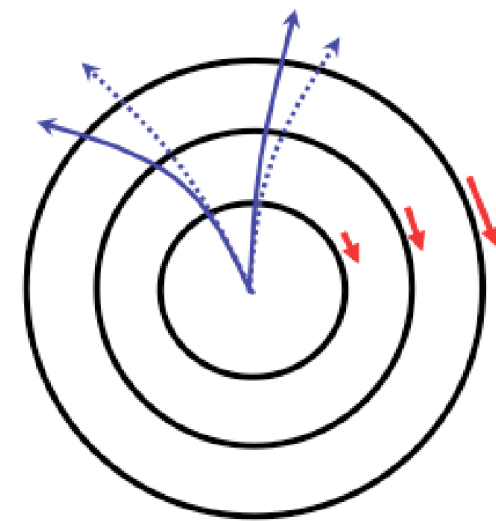
# Muon $p_T$ resolution

- Local misalignments and second order effects:

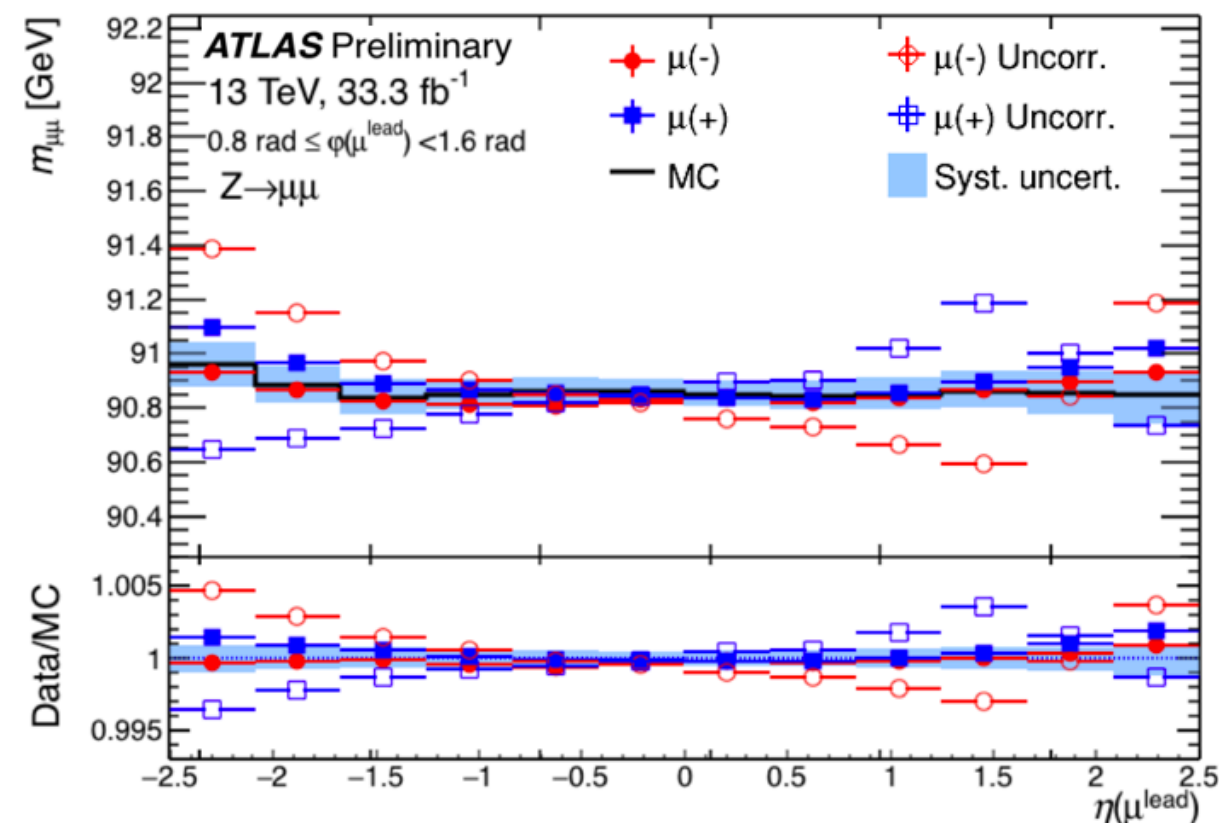
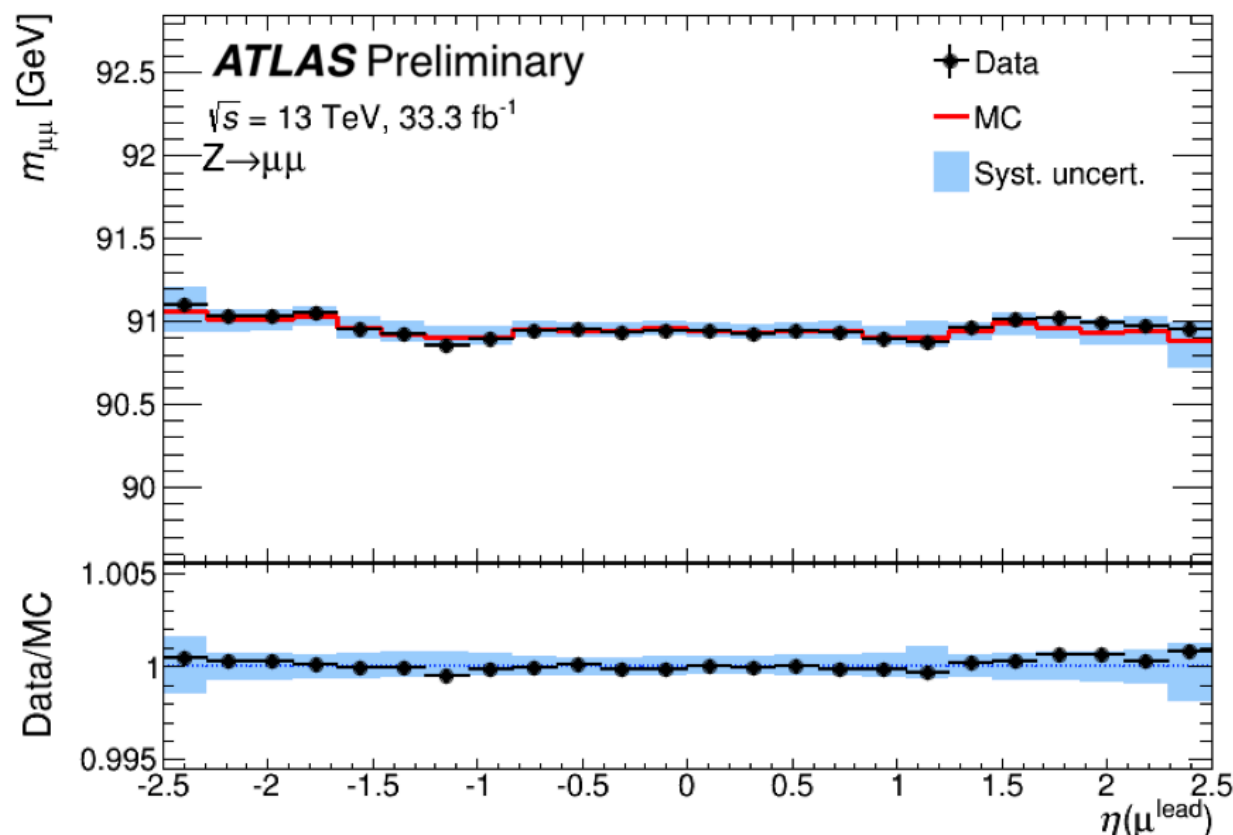
- ▶ Charge dependent sagitta bias, with net effect of worsening resolution
- ▶ *In-situ* correction based on  $Z \rightarrow \mu\mu$  data, **recovers up to 5% in resolution.**

- Momentum scale understood down to the per mille level

- ▶ Precision down to 0.5 per mille for  $|\eta| < 1.0$



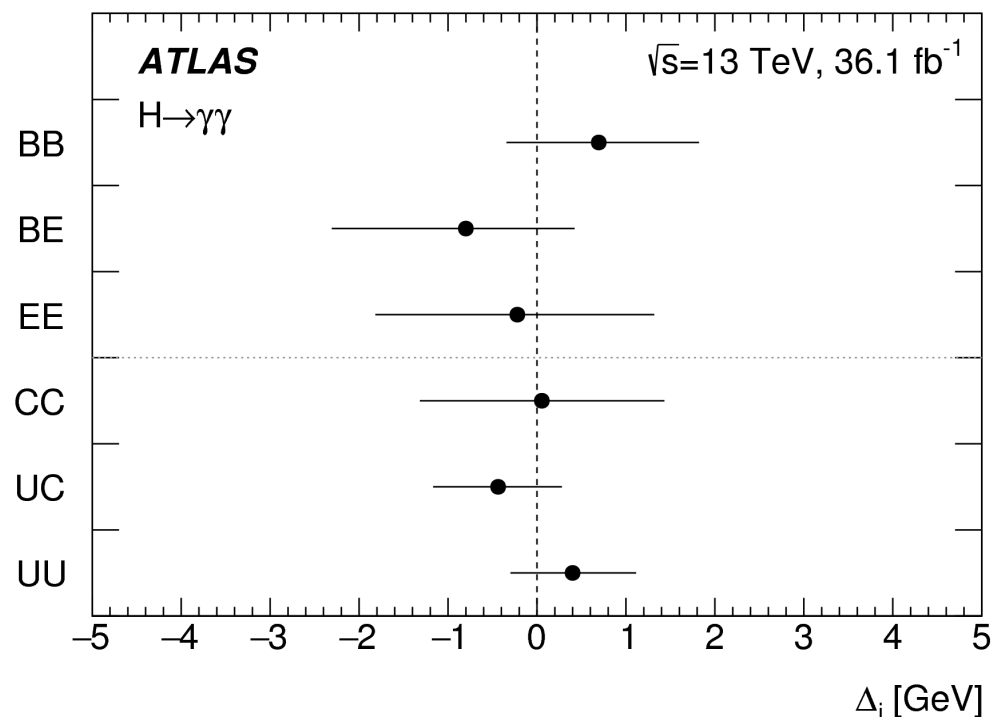
Detector layer movements biasing the measurement of the bending of the particle



Biased positive and negative tracks (red and blue symbols with crosses)  
 Corrected positive and negative tracks (red and blue symbols)

- $H \rightarrow \gamma\gamma$  updated result at Run II with 36.1 fb<sup>-1</sup>.
  - ▶ Analytical  $m_{\gamma\gamma}$  background functions in kinematic and detector related categories.
  - ▶ Reduction of uncertainty through categorisation of events as a function of:
    - ▶ resolution and signal significance.
    - ▶ Systematic uncertainties.
- Expected statistical uncertainty of **0.21 GeV** and **0.34 GeV** systematic uncertainty

$$m_H^{\gamma\gamma} = 124.93 \pm 0.40 (\pm 0.21 \text{ stat only}) \text{ GeV}$$

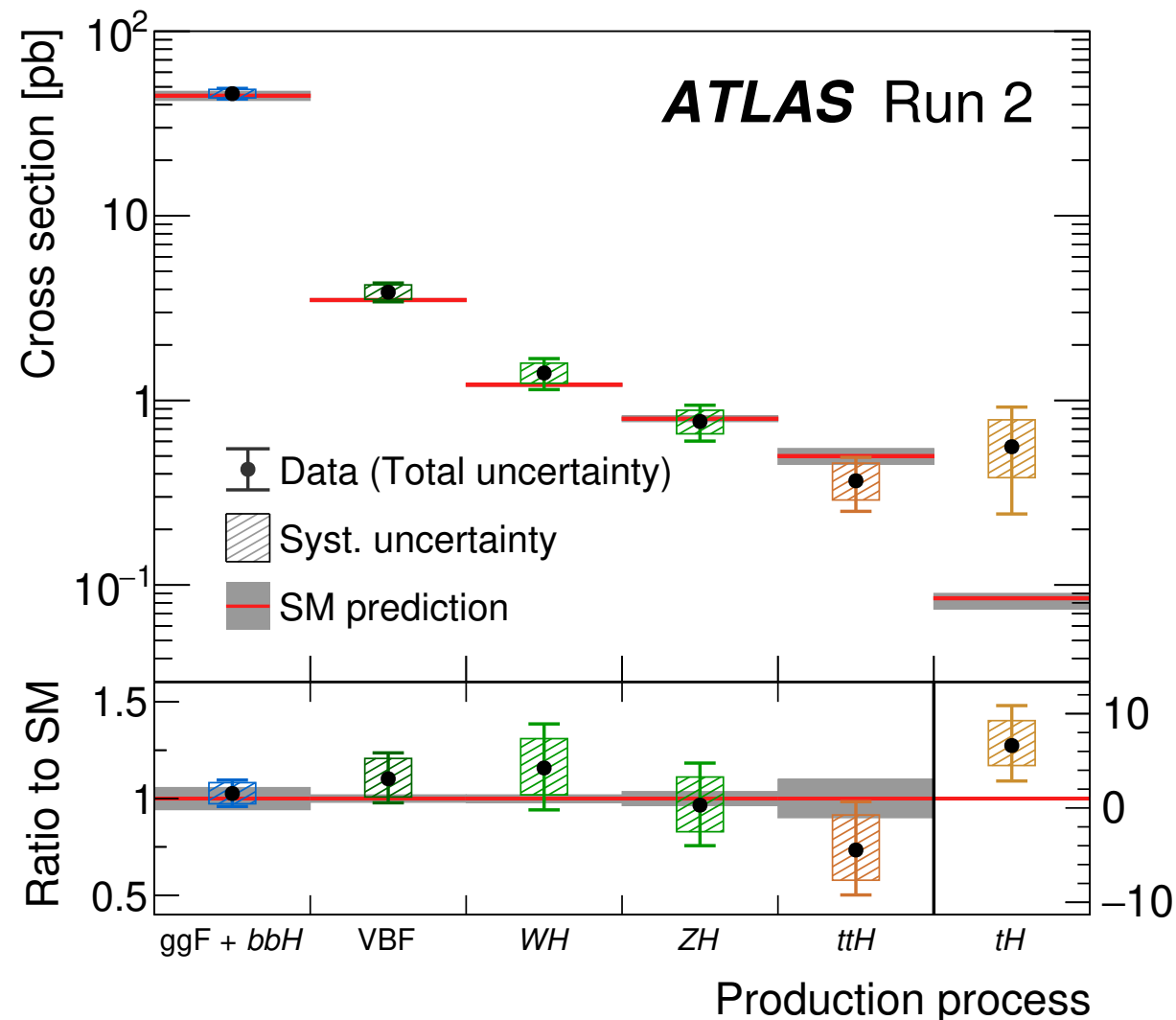


Source	Systematic uncertainty on $m_H^{\gamma\gamma}$ [MeV]
EM calorimeter cell non-linearity	$\pm 180$
EM calorimeter layer calibration	$\pm 170$
Non-ID material	$\pm 120$
ID material	$\pm 110$
Lateral shower shape	$\pm 110$
$Z \rightarrow ee$ calibration	$\pm 80$
Conversion reconstruction	$\pm 50$
Background model	$\pm 50$
Selection of the diphoton production vertex	$\pm 40$
Resolution	$\pm 20$
Signal model	$\pm 20$

- Simultaneous fit to all template cross sections

- ▶ Extraction of global signal strength ( $\mu = \sigma^{\text{obs}} / \sigma^{\text{exp}}$ ).
- ▶ Experimental sensitivity of the same order as of theory (up to N<sup>3</sup>LO for ggF)

$$\mu = 1.05 \pm 0.06 = 1.05 \pm 0.03 \text{ (stat.)} \pm 0.03 \text{ (exp.)} \pm 0.04 \text{ (sig. th.)} \pm 0.02 \text{ (bkg. th.)}$$



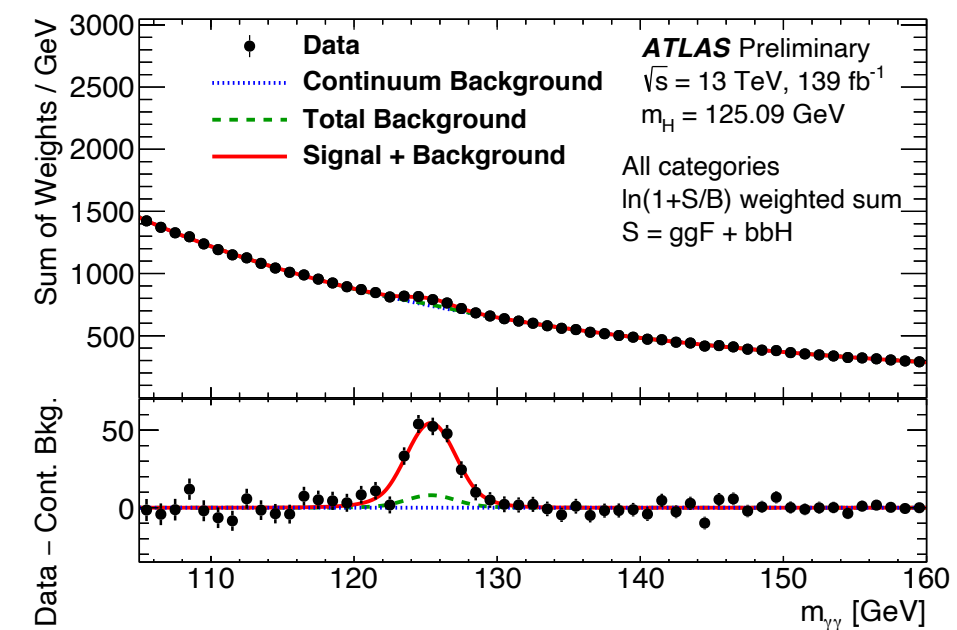
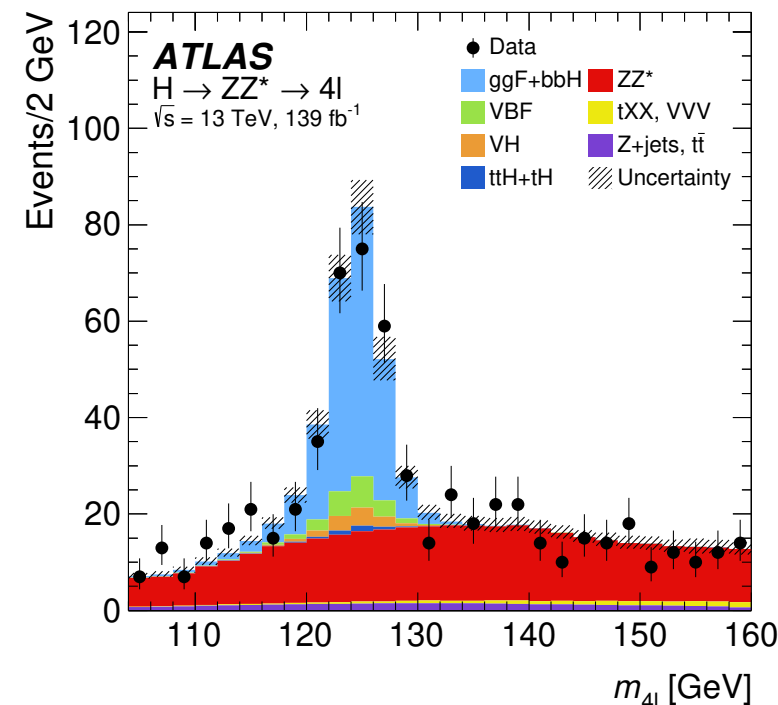
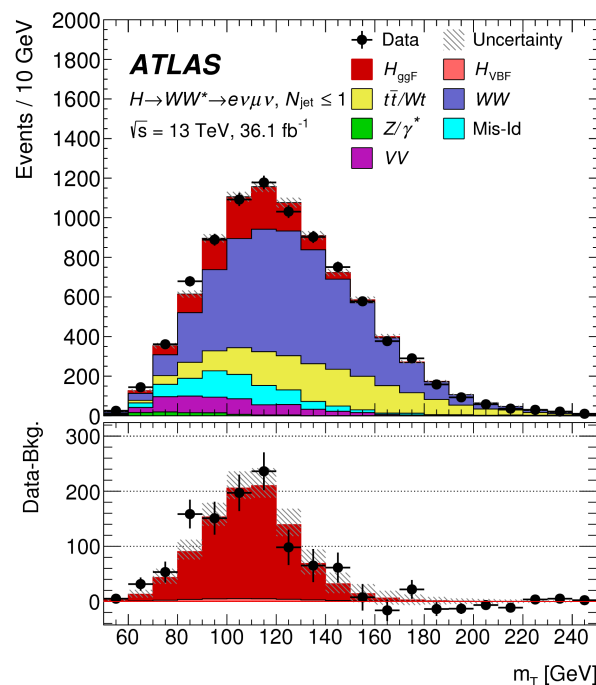
ATLAS-CONF-2021-053

Uncertainty source	$\Delta\mu/\mu$ [%]
Luminosity	2.0
Background modeling	1.6
Jets, $E_T^{\text{miss}}$	1.4
Flavour tagging	1.1
Electrons, photons	2.2
Muons	0.2
$\tau$ -lepton	0.4
Other	1.6
MC statistical uncertainty	1.7

## ● ATLAS full Run-2 combination

- Combined sensitivity of all channels to increase the precision of the Higgs productions.

Decay mode	Targeted production processes	$\mathcal{L}$ [fb $^{-1}$ ]
$H \rightarrow \gamma\gamma$	ggF, VBF, WH, ZH, $t\bar{t}H$ , $tH$	139
$H \rightarrow ZZ$	ggF, VBF, WH + ZH, $t\bar{t}H$ + $tH$	139
	$t\bar{t}H$ + $tH$ (multilepton)	36.1
$H \rightarrow WW$	ggF, VBF	139
	WH, ZH	36.1
	$t\bar{t}H$ + $tH$ (multilepton)	36.1
$H \rightarrow Z\gamma$	inclusive	139
$H \rightarrow b\bar{b}$	WH, ZH	139
	VBF	126
	$t\bar{t}H$ + $tH$	139
	inclusive	139
$H \rightarrow \tau\tau$	ggF, VBF, WH + ZH, $t\bar{t}H$ + $tH$	139
	$t\bar{t}H$ + $tH$ (multilepton)	36.1
$H \rightarrow \mu\mu$	ggF + $t\bar{t}H$ + $tH$ , VBF + WH + ZH	139
$H \rightarrow c\bar{c}$	WH + ZH	139
$H \rightarrow \text{invisible}$	VBF	139
	ZH	139

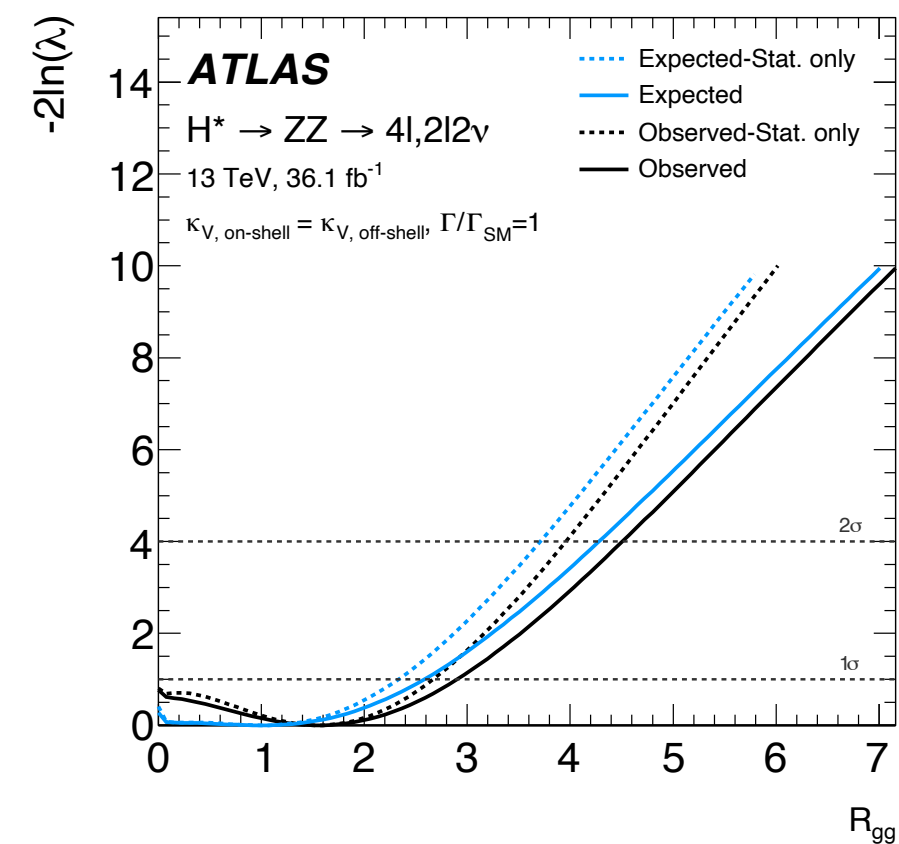
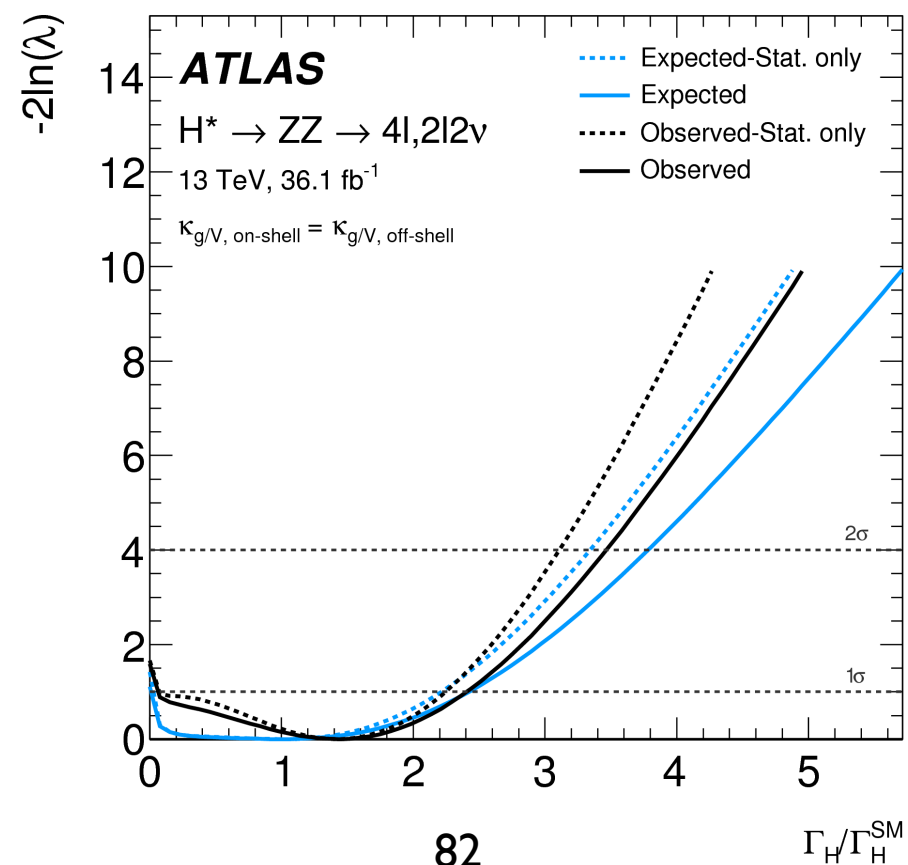
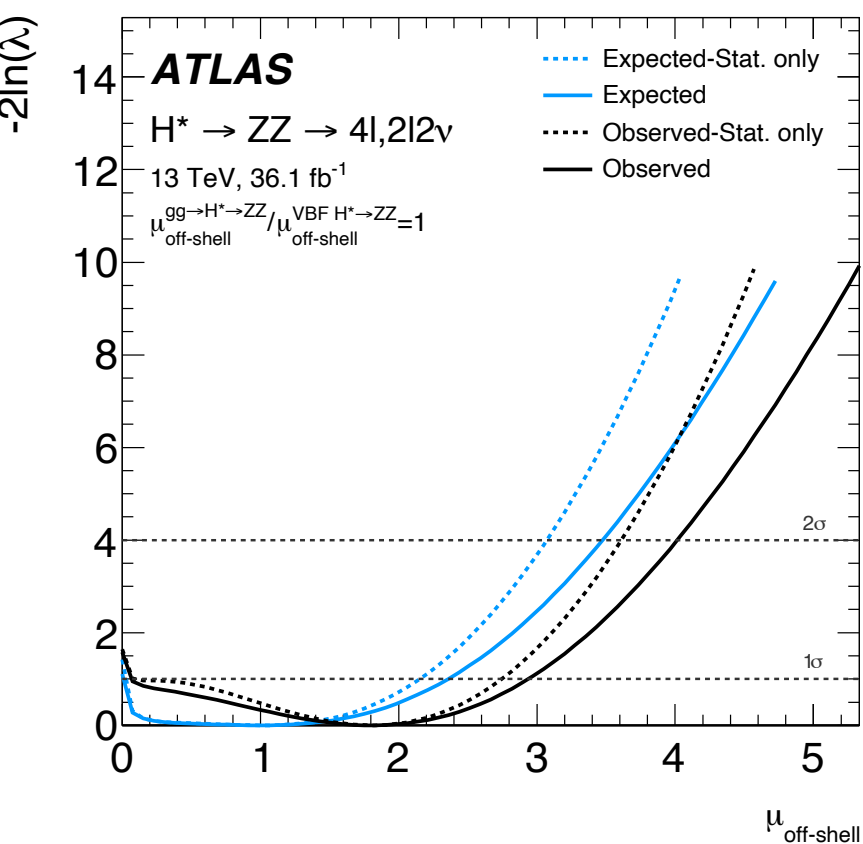


# Higgs width

## ● Study of the the $m_{4\ell}$ spectrum and off-shell $H$ production

[JHEP 04 \(2019\) 048](#),  
[Phys. Lett. B 786 \(2018\) 223](#)

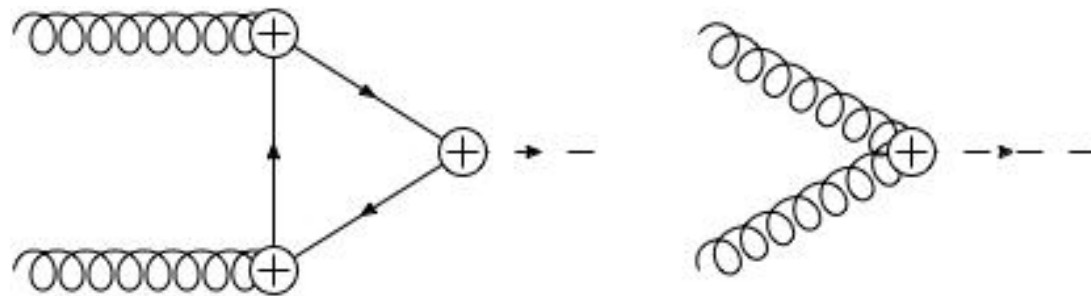
- ▶ Measured upper limit on width combining  $4\ell$  and  $\ell\bar{\ell}\nu\bar{\nu}$
- ▶ Limit  $\Gamma_H$  possible from the off-shell to on-shell event yield ratio  $R_{gg}$ 
  - ◆ on-shell event yields  $\sim k_{g,\text{on-shell}}^2 / \Gamma_H$ , while off-shell  $\sim k_{g,\text{off-shell}}^2$
- ▶ Observed (expected) upper limit on  $\Gamma_H$  14.4 (15.2) MeV





- Higgs boson kinematics:

- $p_{T,4\ell}$ : Lagrangian structure of H interactions.



- Sensitivity to phenomena resonant at higher energies  $\rightarrow$  changes in observables at lower energies.

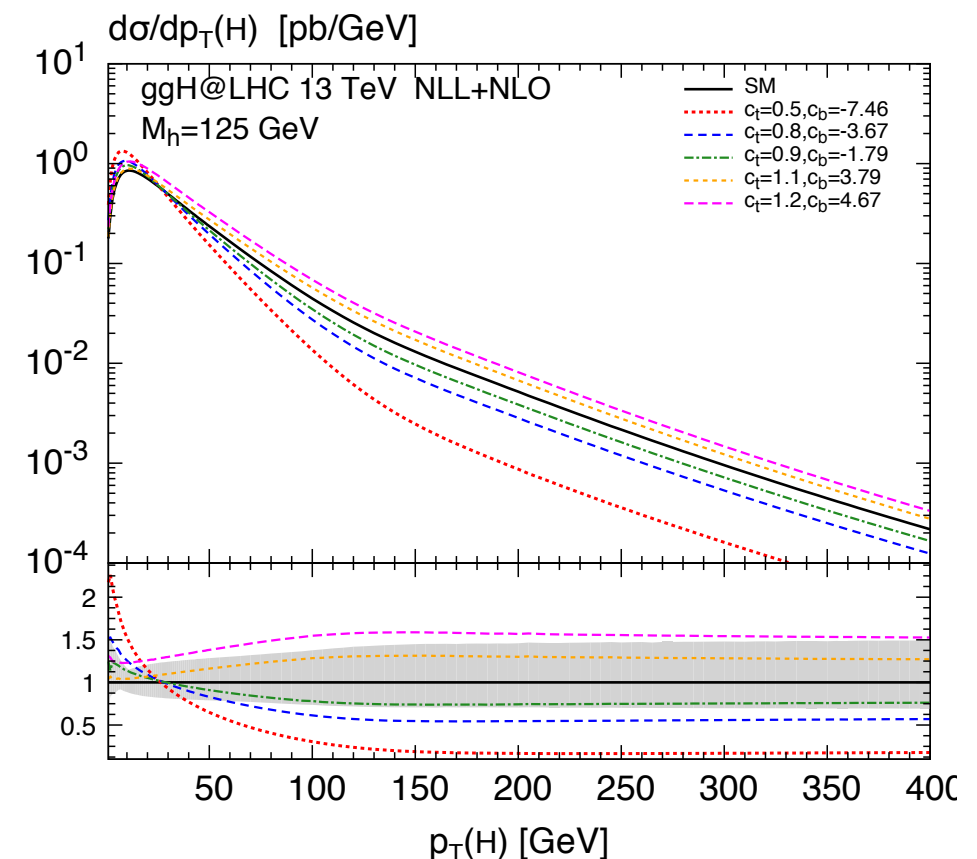
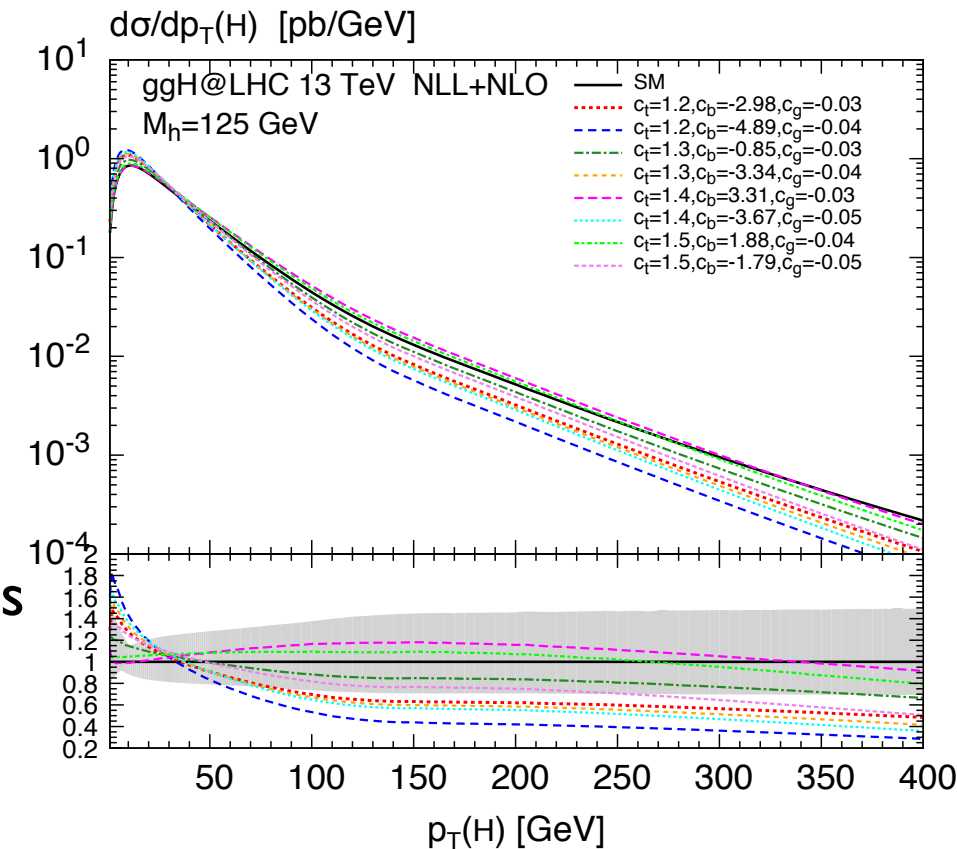
$$\frac{c_1}{\Lambda^2} \mathcal{O}_1 \rightarrow \frac{\alpha_S}{\pi v} c_g h G_{\mu\nu}^a G^{a,\mu\nu}, \quad \left. \vphantom{\frac{c_1}{\Lambda^2} \mathcal{O}_1} \right\} c_g: ggH \text{ contact interaction}$$

$$\frac{c_2}{\Lambda^2} \mathcal{O}_2 \rightarrow \frac{m_t}{v} c_t h \bar{t} t, \quad \left. \vphantom{\frac{c_2}{\Lambda^2} \mathcal{O}_2} \right\} c_t: t \text{ and } b \text{ Yukawa couplings}$$

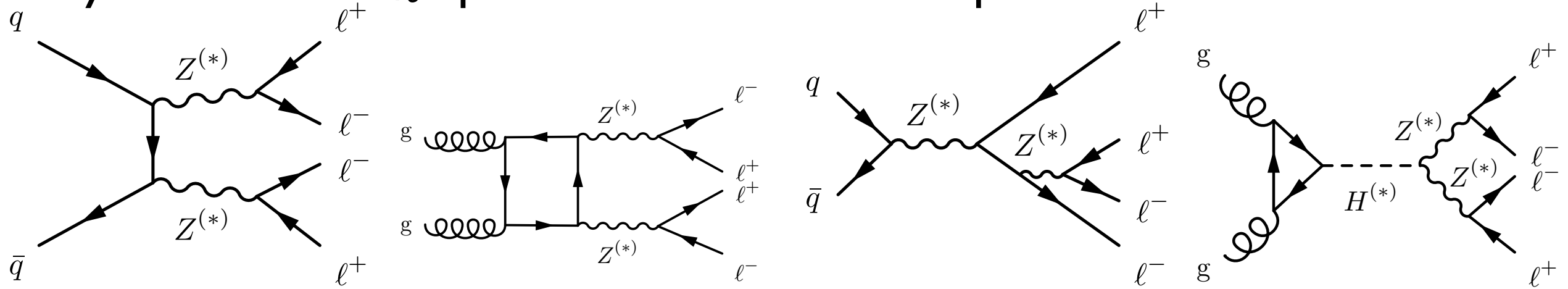
$$\frac{c_3}{\Lambda^2} \mathcal{O}_3 \rightarrow \frac{m_b}{v} c_b h \bar{b} b,$$

$$\frac{c_4}{\Lambda^2} \mathcal{O}_4 \rightarrow c_{tg} \frac{g_S m_t}{2v^3} (v + h) G_{\mu\nu}^a (\bar{t}_L \sigma^{\mu\nu} T^a t_R + h.c.)$$

$c_{tg}$ : dipole-moment,  $g$ - $t$  interaction



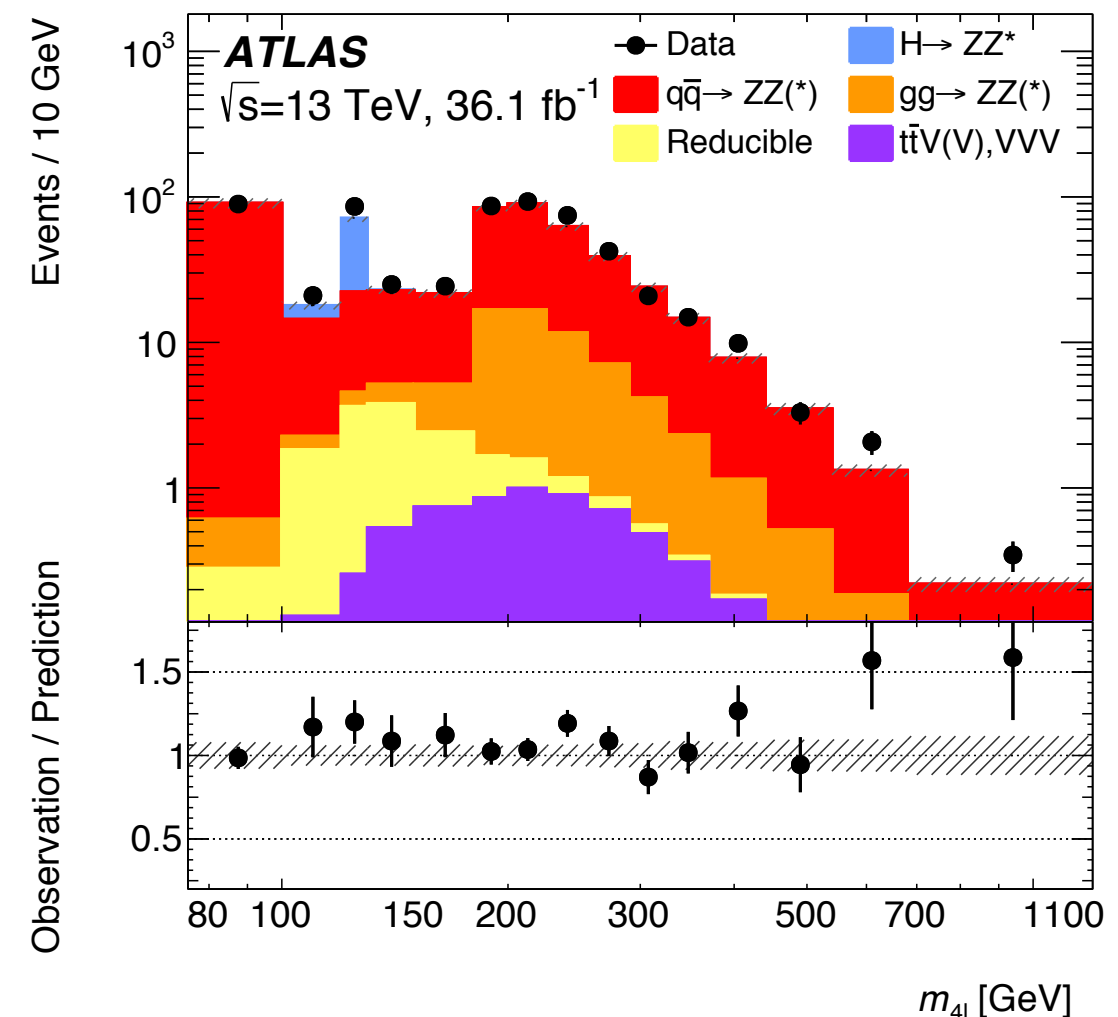
## ● Study of the the $m_{4\ell}$ spectrum and Offshell $H$ production



- ▶  $m_{4\ell}$  ranges from single  $Z$  resonance, including  $H$  production up to  $ZZ$  production
- ▶ Extraction of the  $\text{BR}(Z \rightarrow 4\ell)$

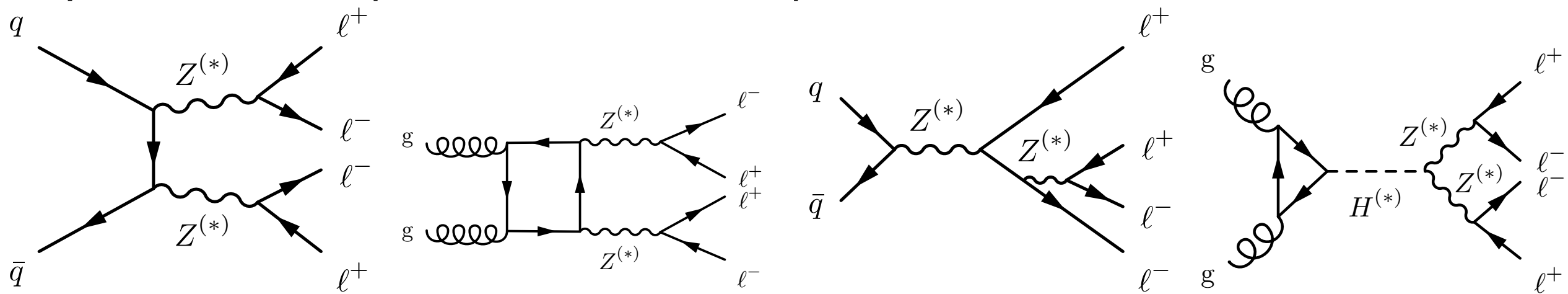
Measurement	$\mathcal{B}_{Z \rightarrow 4\ell} / 10^{-6}$
ATLAS, $\sqrt{s} = 7$ TeV and 8 TeV [8]	$4.31 \pm 0.34(\text{stat}) \pm 0.17(\text{syst})$
CMS, $\sqrt{s} = 13$ TeV [6]	$4.83^{+0.23}_{-0.22}(\text{stat})^{+0.32}_{-0.29}(\text{syst}) \pm 0.08(\text{theo}) \pm 0.12(\text{lumi})$
ATLAS, $\sqrt{s} = 13$ TeV	$4.70 \pm 0.32(\text{stat}) \pm 0.21(\text{syst}) \pm 0.14(\text{lumi})$

- ▶ Offshell Higgs production, enhanced at 350 GeV because of top-quark loops in  $ggF$ 
  - ◆ Including interference between  $H$  and  $ZZ$  productions.
- ▶ Above  $\sim 2m_Z$  enhancements of  $qq \rightarrow ZZ$  and  $gg \rightarrow ZZ$ .

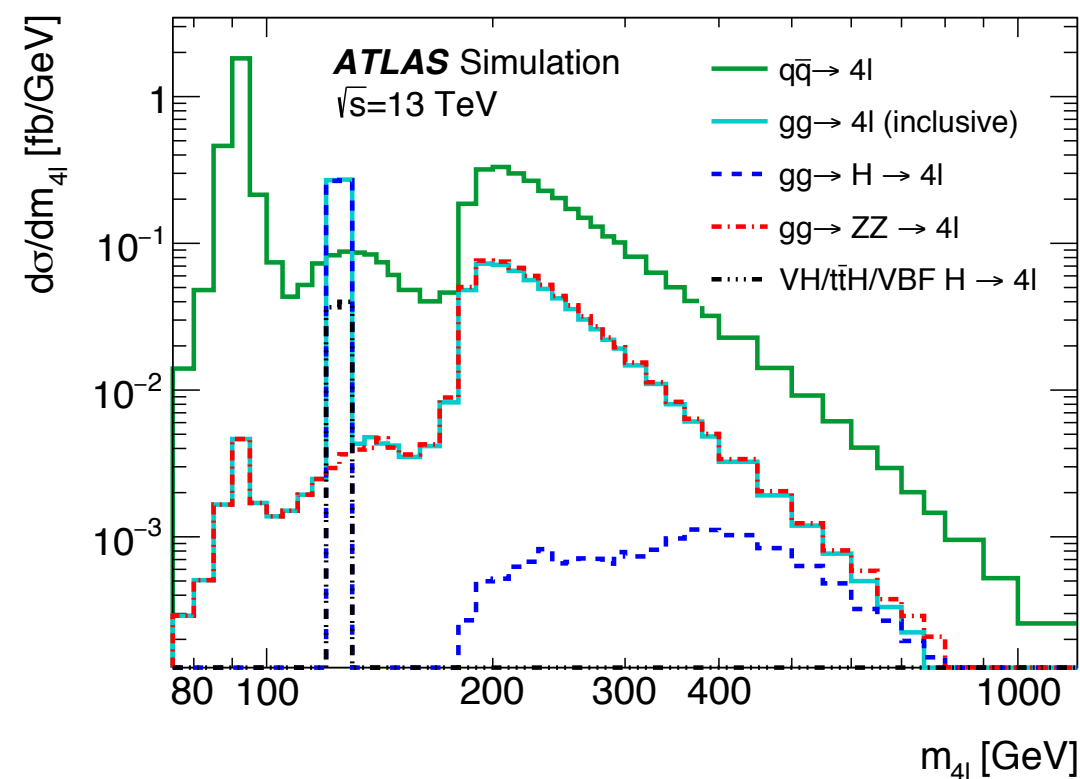




- Study of the the  $m_{4\ell}$  spectrum and Offshell  $H$  production

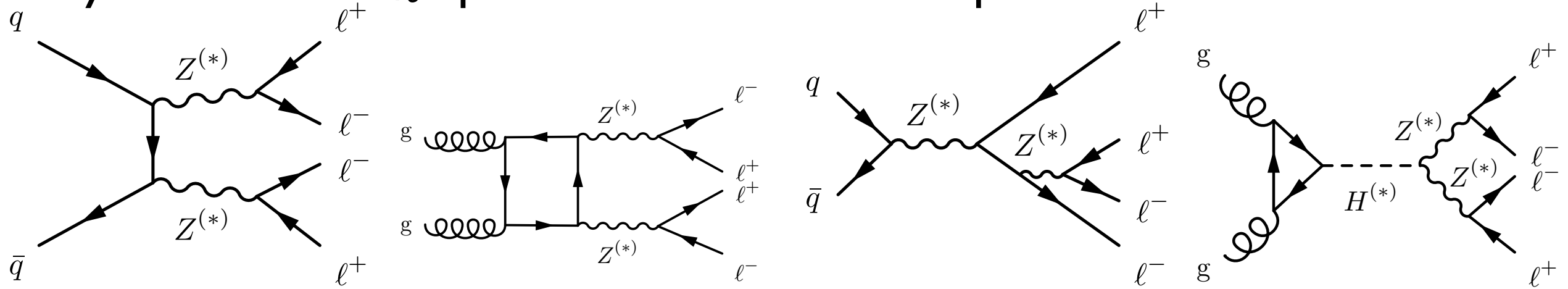


- $m_{4\ell}$  ranges from single  $Z$  resonance, including  $H$  production up to  $ZZ$  production



- Offshell Higgs production, enhanced at 350 GeV because of top-quark loops in  $ggF$ 
  - Including interference between  $H$  and  $ZZ$  productions.
- Above  $\sim 2m_Z$  enhancements of  $qq \rightarrow ZZ$  and  $gg \rightarrow ZZ$ .

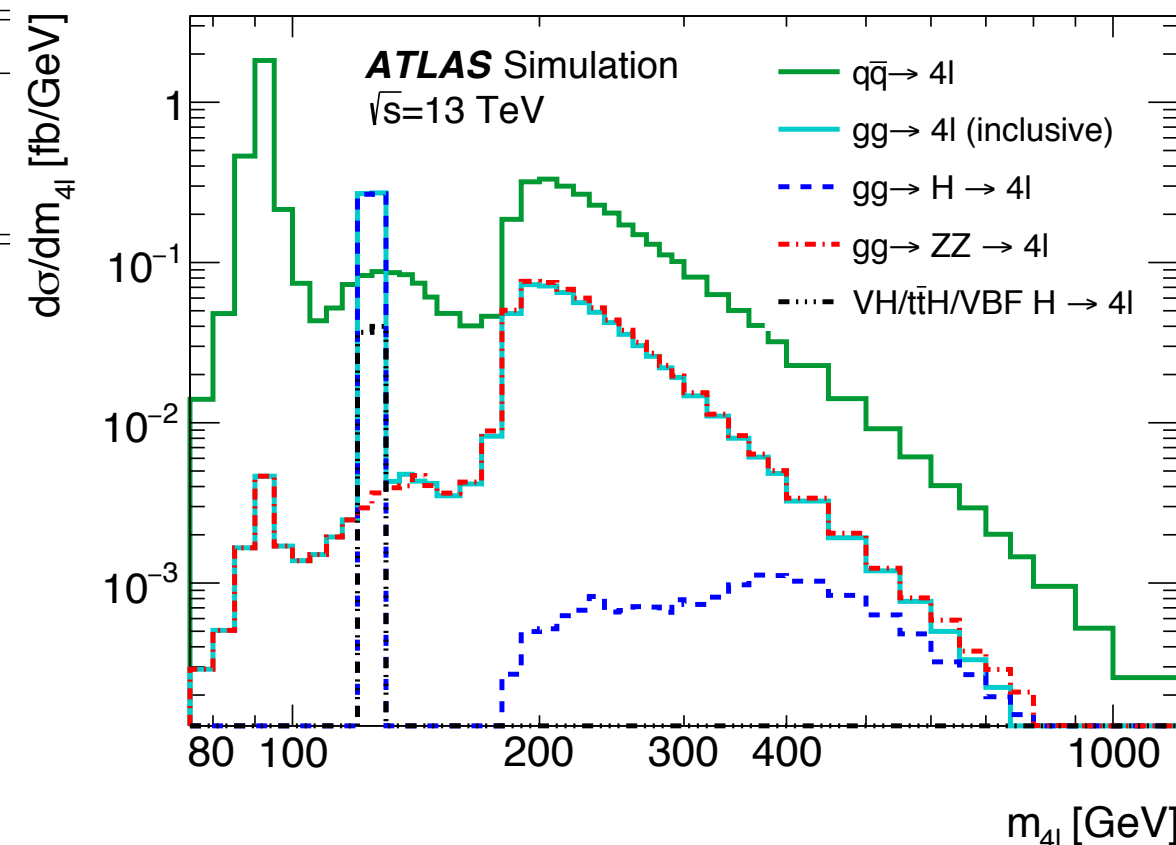
## ● Study of the the $m_{4\ell}$ spectrum and Offshell $H$ production



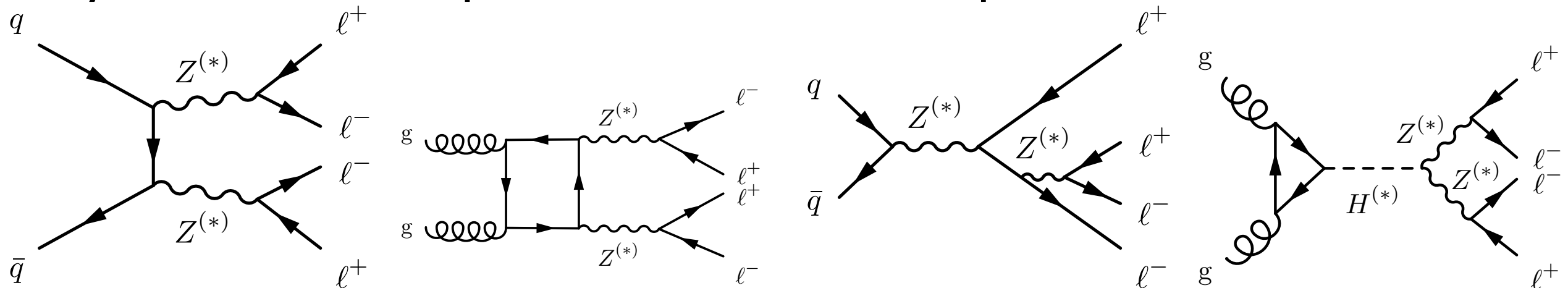
- ▶  $m_{4\ell}$  ranges from single  $Z$  resonance, including  $H$  production up to  $ZZ$  production
- ▶ Extraction of the  $\text{BR}(Z \rightarrow 4\ell)$

Measurement	$\mathcal{B}_{Z \rightarrow 4\ell} / 10^{-6}$
ATLAS, $\sqrt{s} = 7$ TeV and 8 TeV [8]	$4.31 \pm 0.34(\text{stat}) \pm 0.17(\text{syst})$
CMS, $\sqrt{s} = 13$ TeV [6]	$4.83^{+0.23}_{-0.22}(\text{stat})^{+0.32}_{-0.29}(\text{syst}) \pm 0.08(\text{theo}) \pm 0.12(\text{lumi})$
ATLAS, $\sqrt{s} = 13$ TeV	$4.70 \pm 0.32(\text{stat}) \pm 0.21(\text{syst}) \pm 0.14(\text{lumi})$

- ▶ Offshell Higgs production, enhanced at 350 GeV because of top-quark loops in  $ggF$ 
  - ◆ Including interference between  $H$  and  $ZZ$  productions.
- ▶ Above  $\sim 2m_Z$  enhancements of  $qq \rightarrow ZZ$  and  $gg \rightarrow ZZ$ .



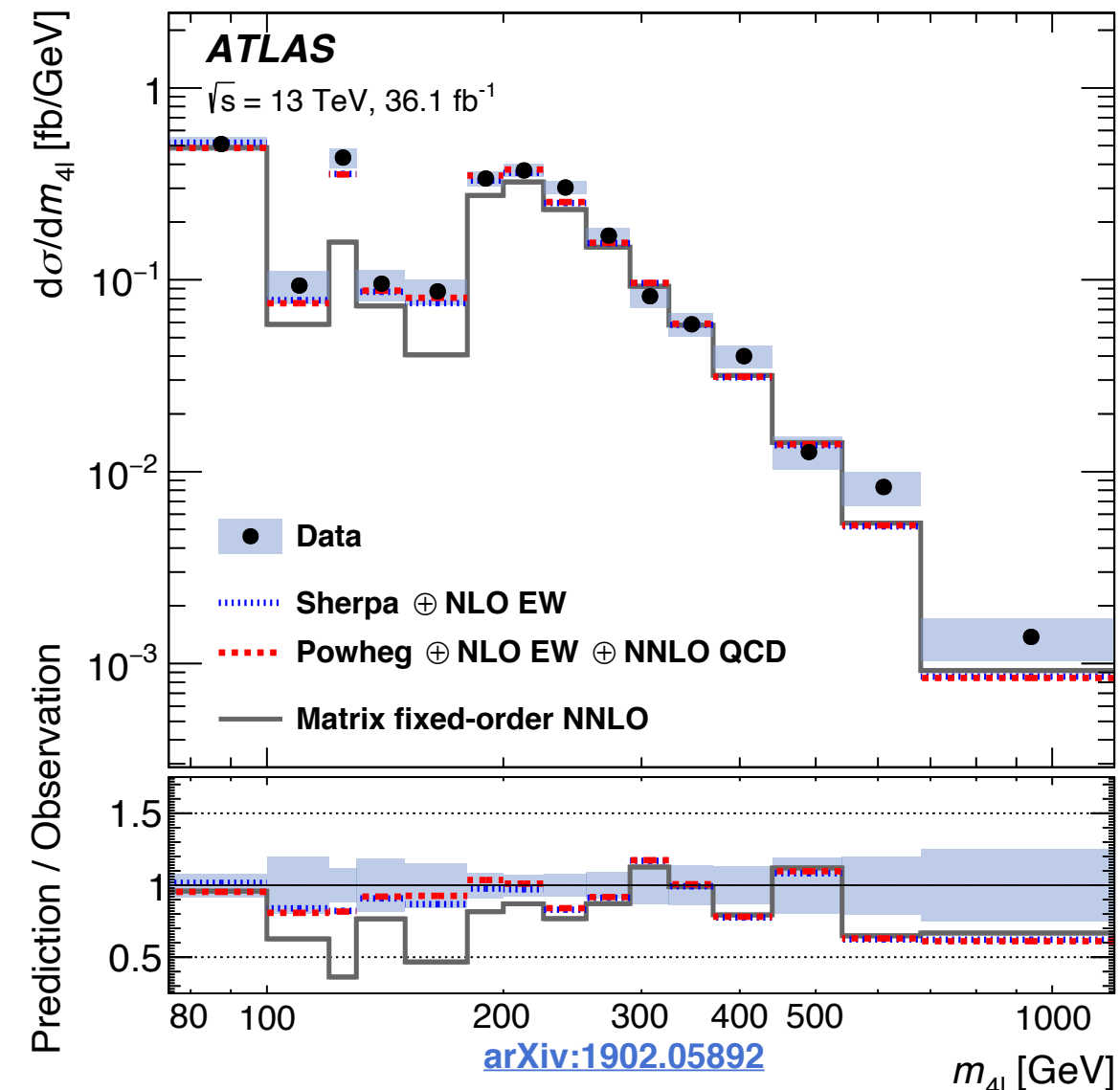
## ● Study of the the $m_{4\ell}$ spectrum and Offshell $H$ production



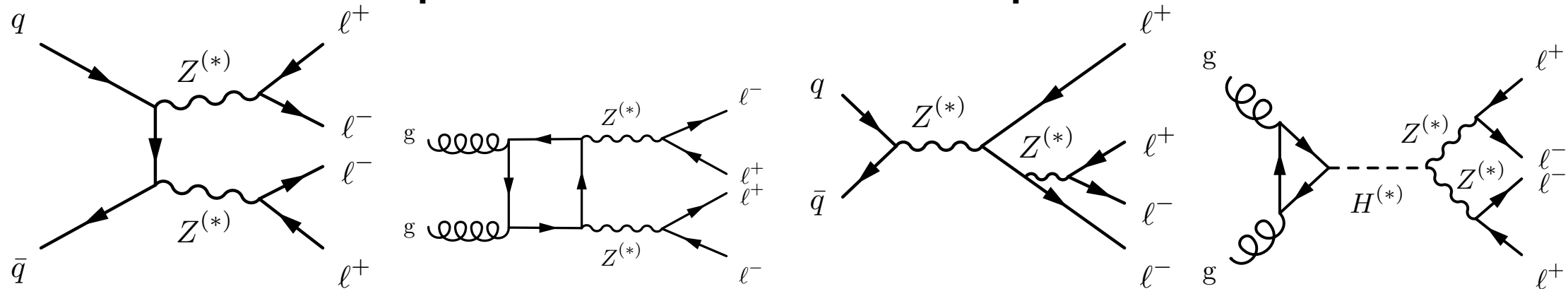
- ▶  $m_{4\ell}$  ranges from single  $Z$  resonance, including  $H$  production up to  $ZZ$  production
- ▶ Extraction of the  $\text{BR}(Z \rightarrow 4\ell)$

Measurement	$\mathcal{B}_{Z \rightarrow 4\ell} / 10^{-6}$
ATLAS, $\sqrt{s} = 7$ TeV and 8 TeV [8]	$4.31 \pm 0.34(\text{stat}) \pm 0.17(\text{syst})$
CMS, $\sqrt{s} = 13$ TeV [6]	$4.83^{+0.23}_{-0.22}(\text{stat})^{+0.32}_{-0.29}(\text{syst}) \pm 0.08(\text{theo}) \pm 0.12(\text{lumi})$
ATLAS, $\sqrt{s} = 13$ TeV	$4.70 \pm 0.32(\text{stat}) \pm 0.21(\text{syst}) \pm 0.14(\text{lumi})$

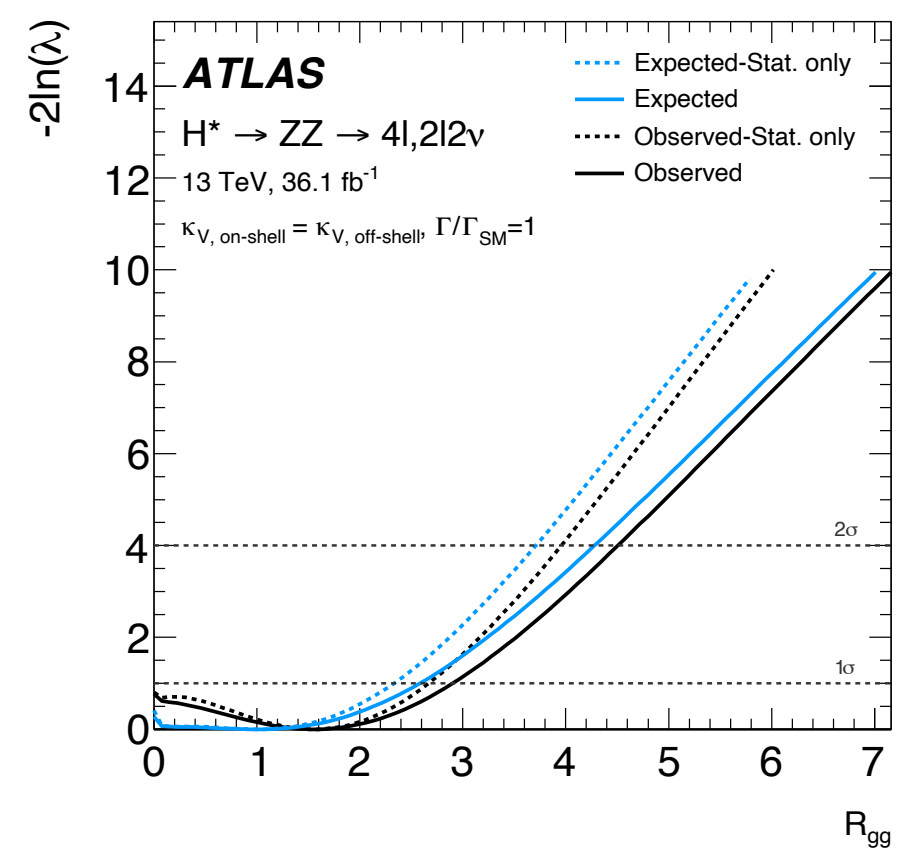
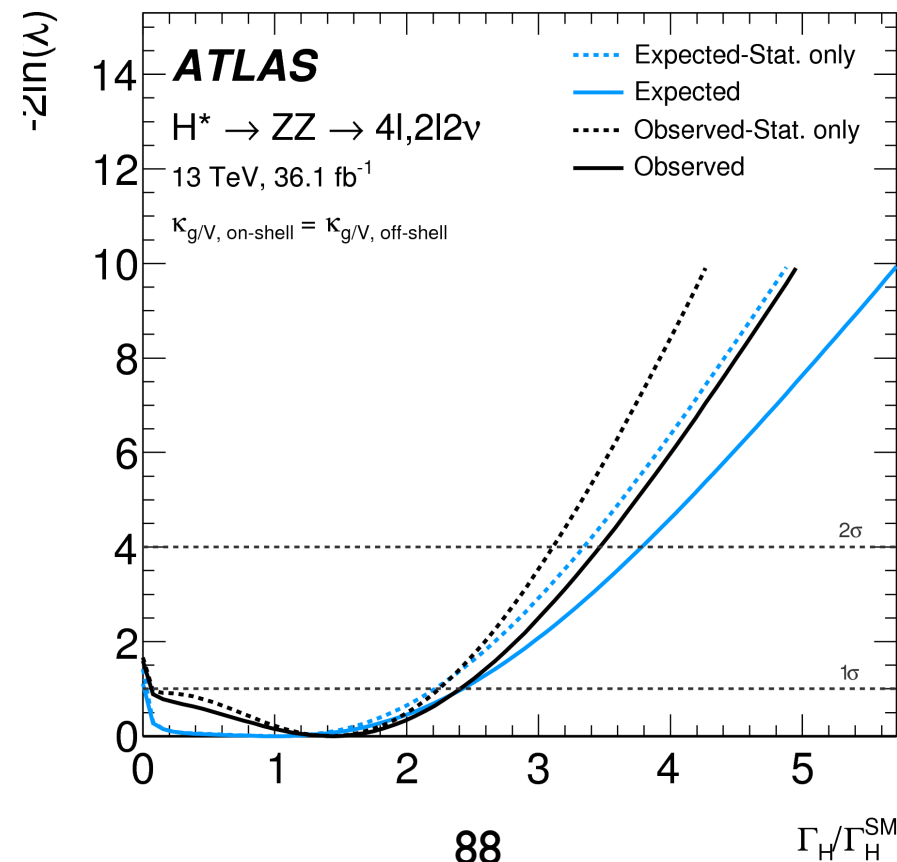
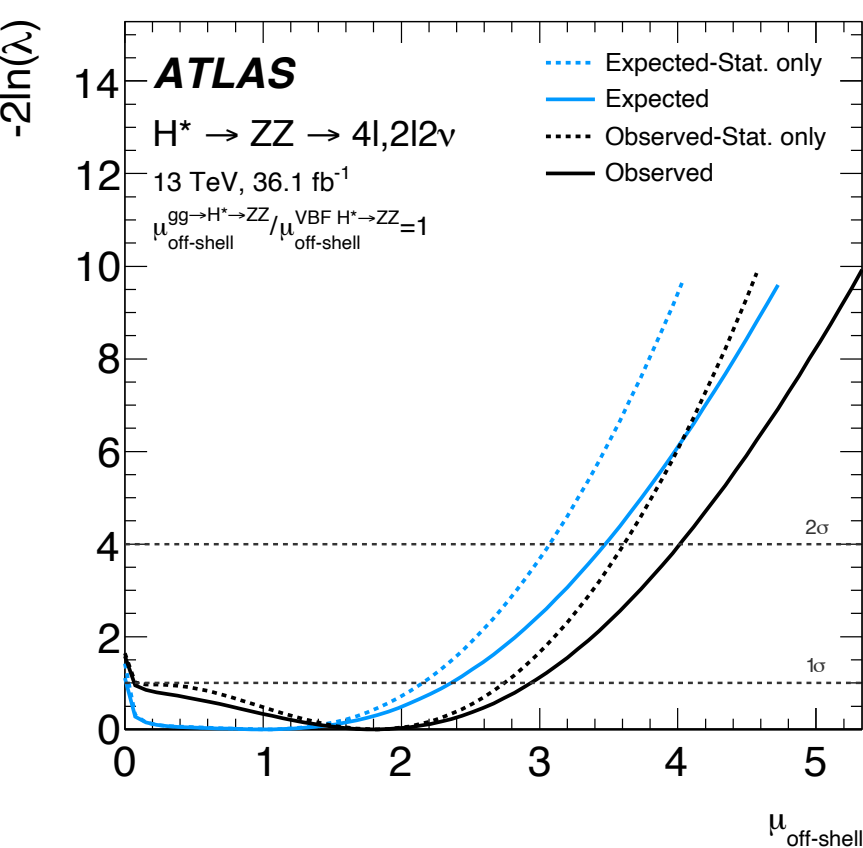
- ▶ Offshell Higgs production, enhanced at 350 GeV because of top-quark loops in  $ggF$ 
  - ◆ Including interference between  $H$  and  $ZZ$  productions.
- ▶ Above  $\sim 2m_Z$  enhancements of  $qq \rightarrow ZZ$  and  $gg \rightarrow ZZ$ .



## ● Study of the the $m_{4\ell}$ spectrum and off-shell $H$ production

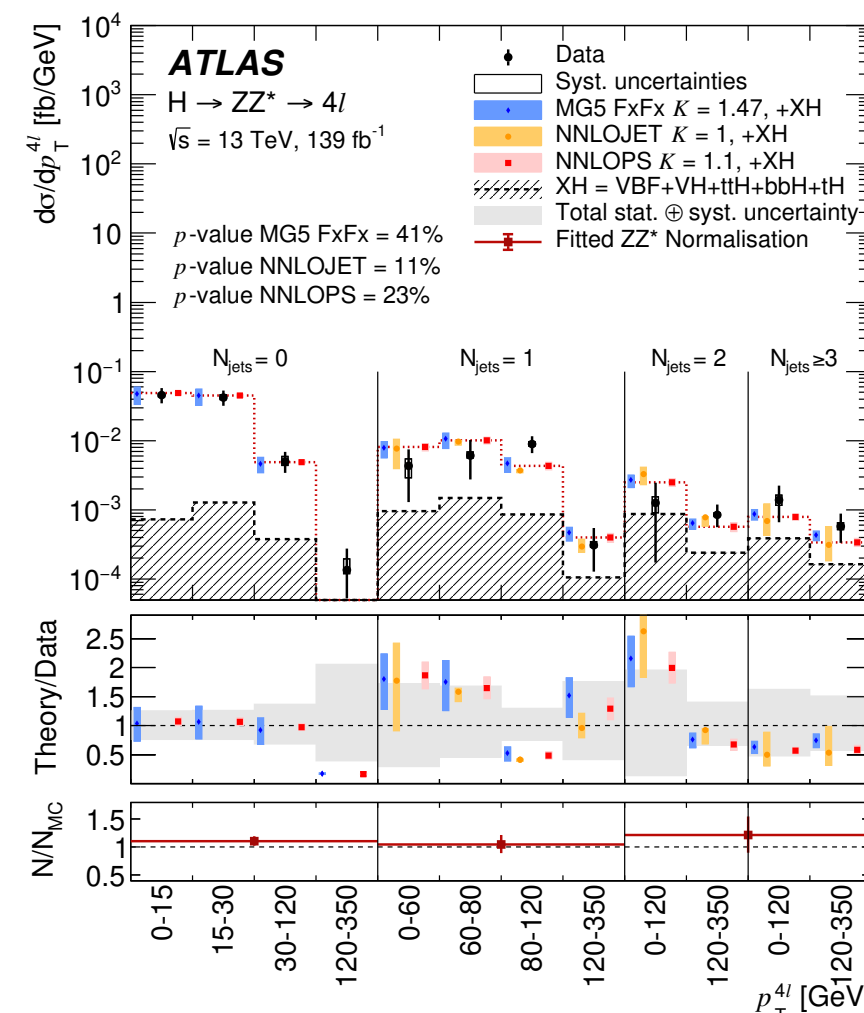
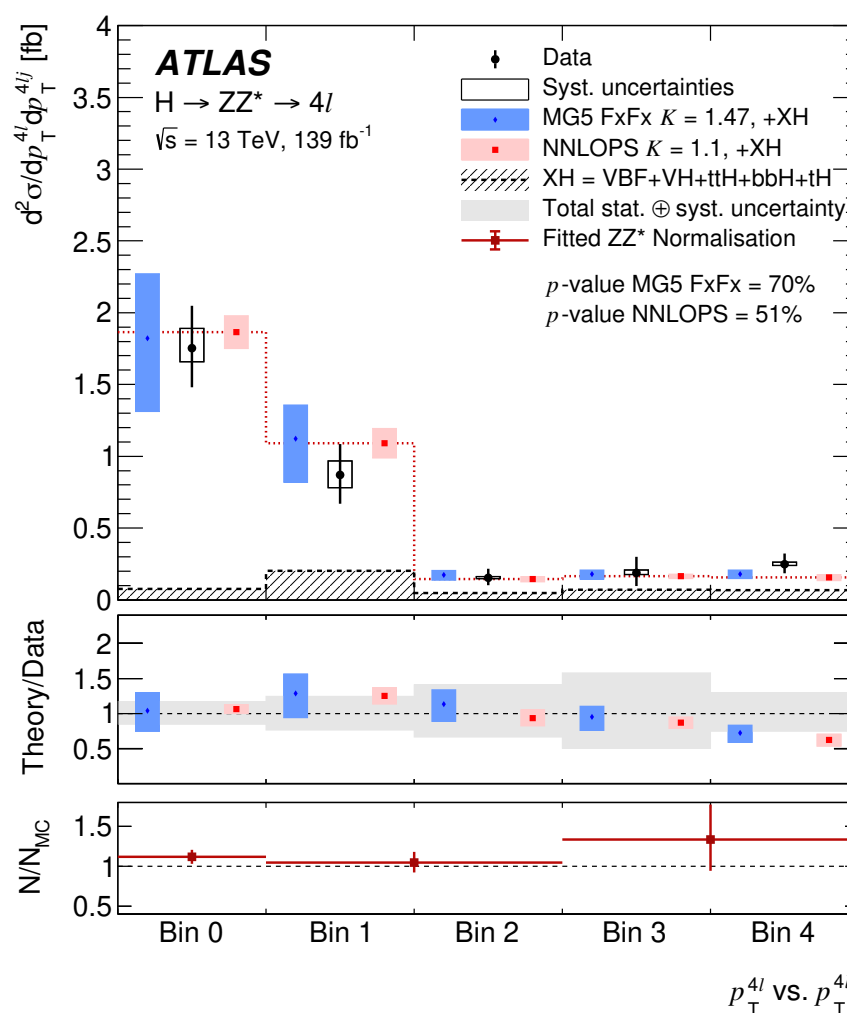
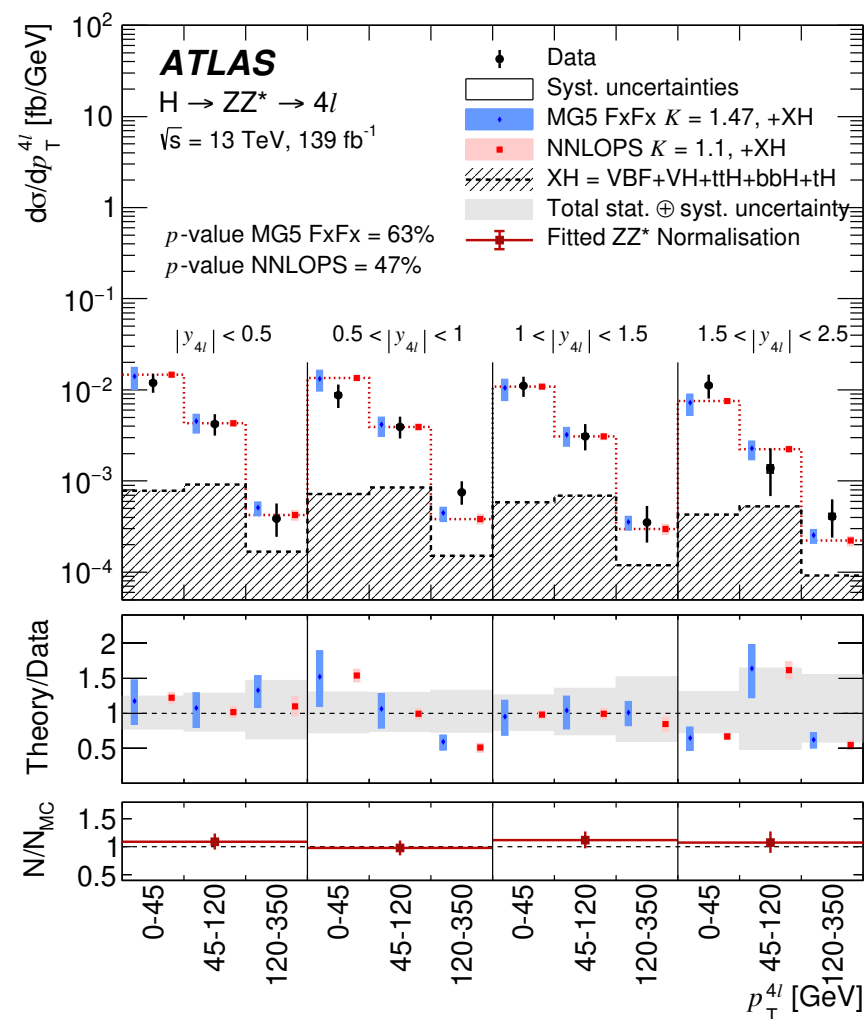
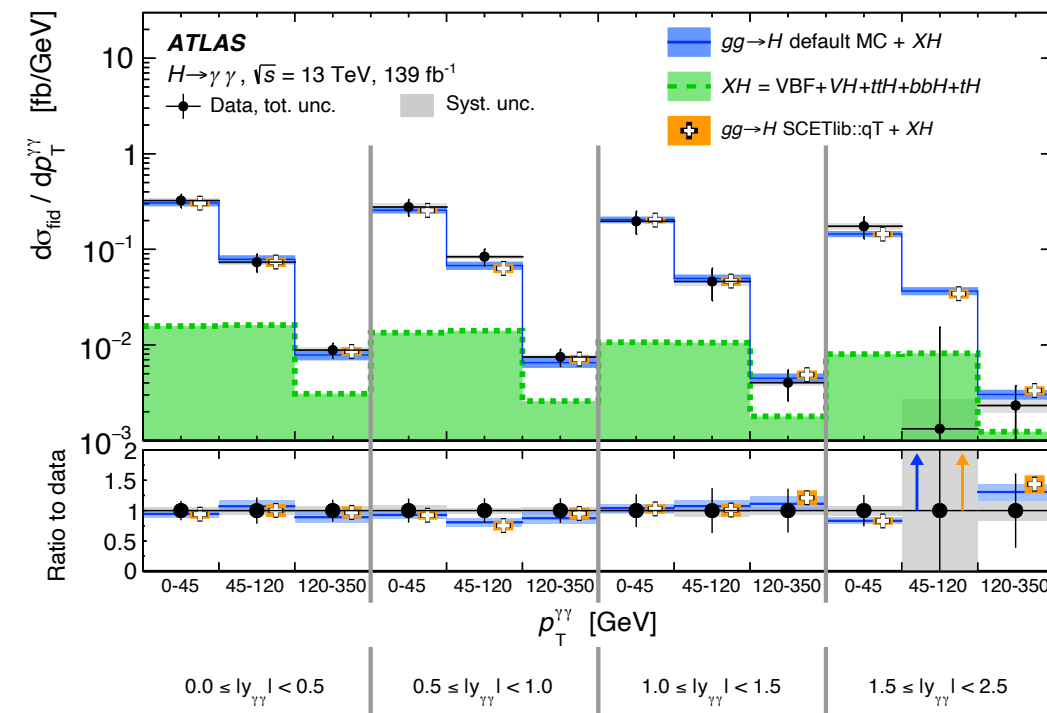


- ▶ Offshell Higgs production, enhanced at 350 GeV because of top-quark loops in ggF
- ▶ Measured upper limit on width combining 4 $\ell$  and  $\ell\bar{\ell}\nu\bar{\nu}$
- ▶ Limit  $\Gamma_H$  possible from the off-shell to on-shell event yield ratio  $R_{gg}$ 
  - ◆ on-shell event yields  $\sim k_{g,\text{on-shell}}^2 / \Gamma_H$ , while off-shell  $\sim k_{g,\text{off-shell}}^2$



## ● Double differential $d^2\sigma/dp_T dN_J$ :

- ▶ Probe the Higgs production mode
- ▶  $N_J = 0$  dominated by  $ggF$  production
- ▶  $N_J > 1$  VBF enriched production

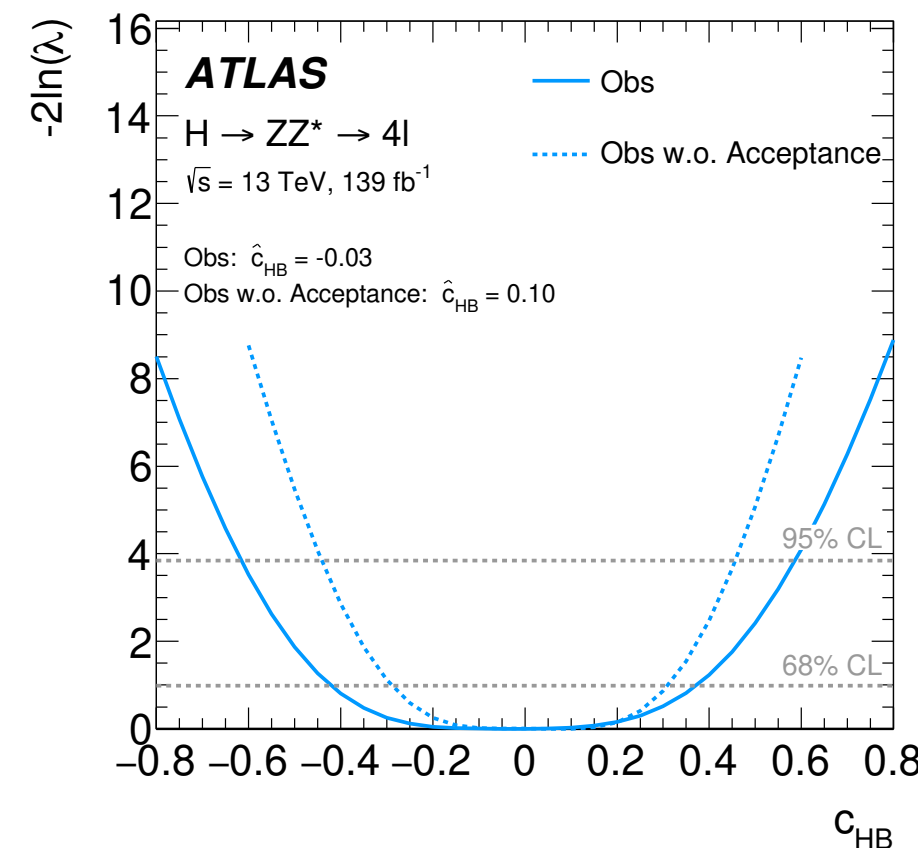
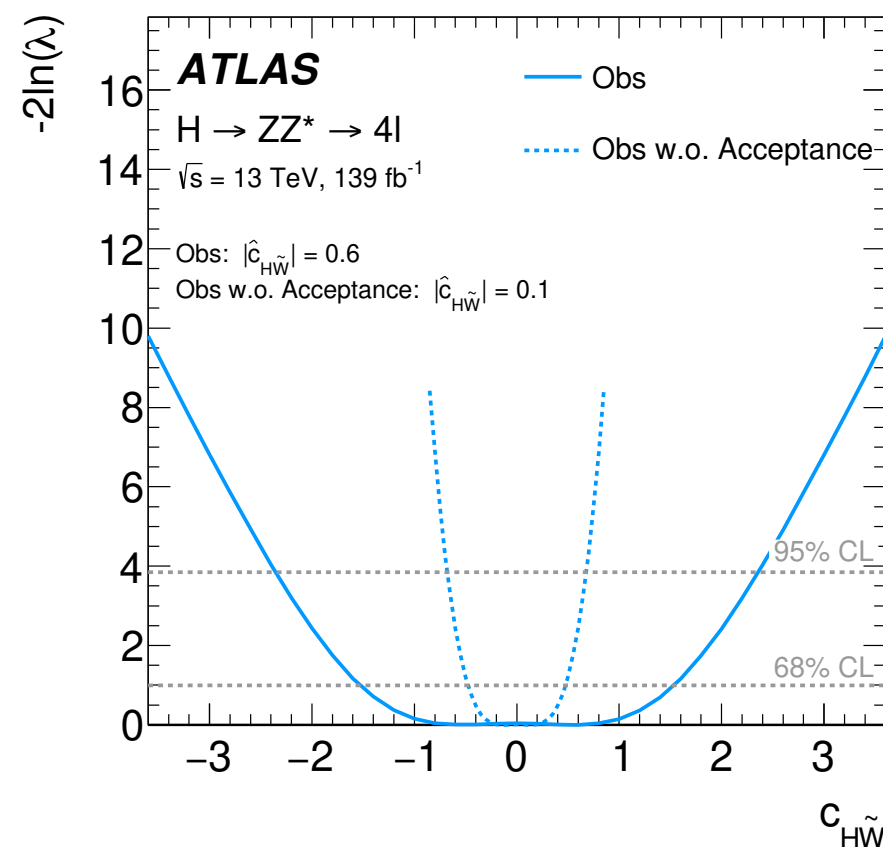
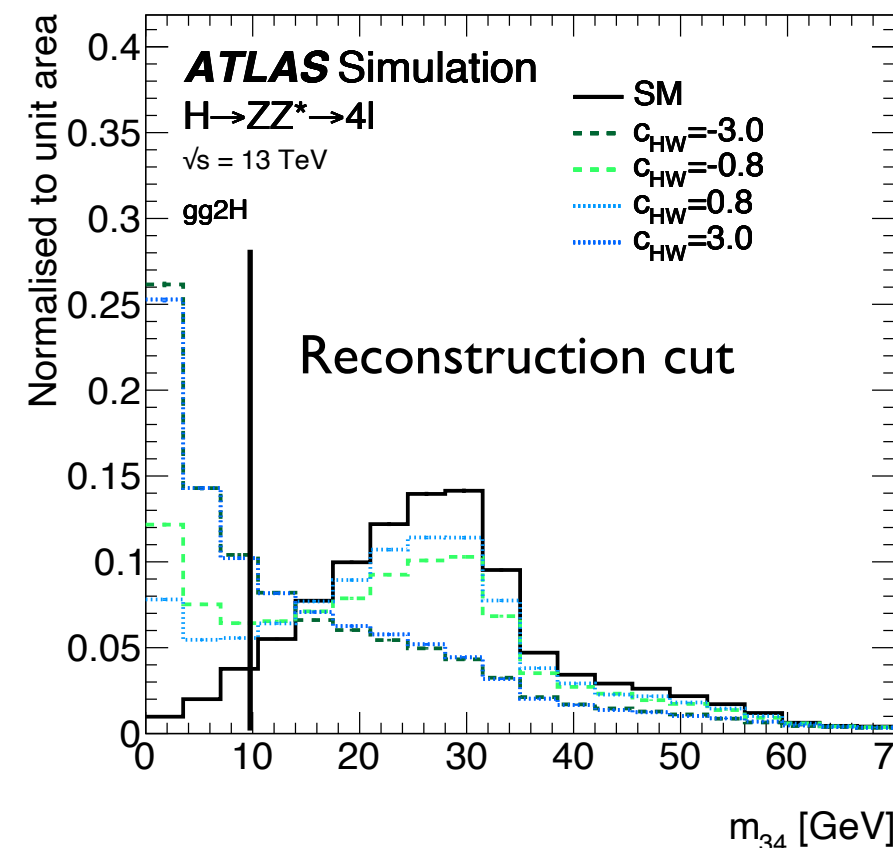


- Results interpreted in the context of new physics:

$$\mathcal{L}_{\text{SMEFT}} = \mathcal{L}_{\text{SM}} + \sum_i^{N_{d6}} \frac{c_i}{\Lambda^2} \mathcal{O}_i^{(6)} + \sum_j^{N_{d8}} \frac{b_j}{\Lambda^4} \mathcal{O}_j^{(8)} + \dots$$

- Standard Model Effective Field Theory as the standard candle.
- Probe for non-SM contributions to the tensor structure of the Higgs boson.

- Account for BSM acceptance effects in kinematic observables of decay products



# Couplings interpretations

- Interpretation of couplings cross sections in the context of new physics.
- Assuming production and decay are factorised

$$\sigma_i \times B_f = \frac{\sigma_i(\kappa) \times \Gamma_f(\kappa)}{\Gamma_H}$$

$$\kappa_V = 1.03 \pm 0.03$$

$$\kappa_F = 0.97 \pm 0.07.$$

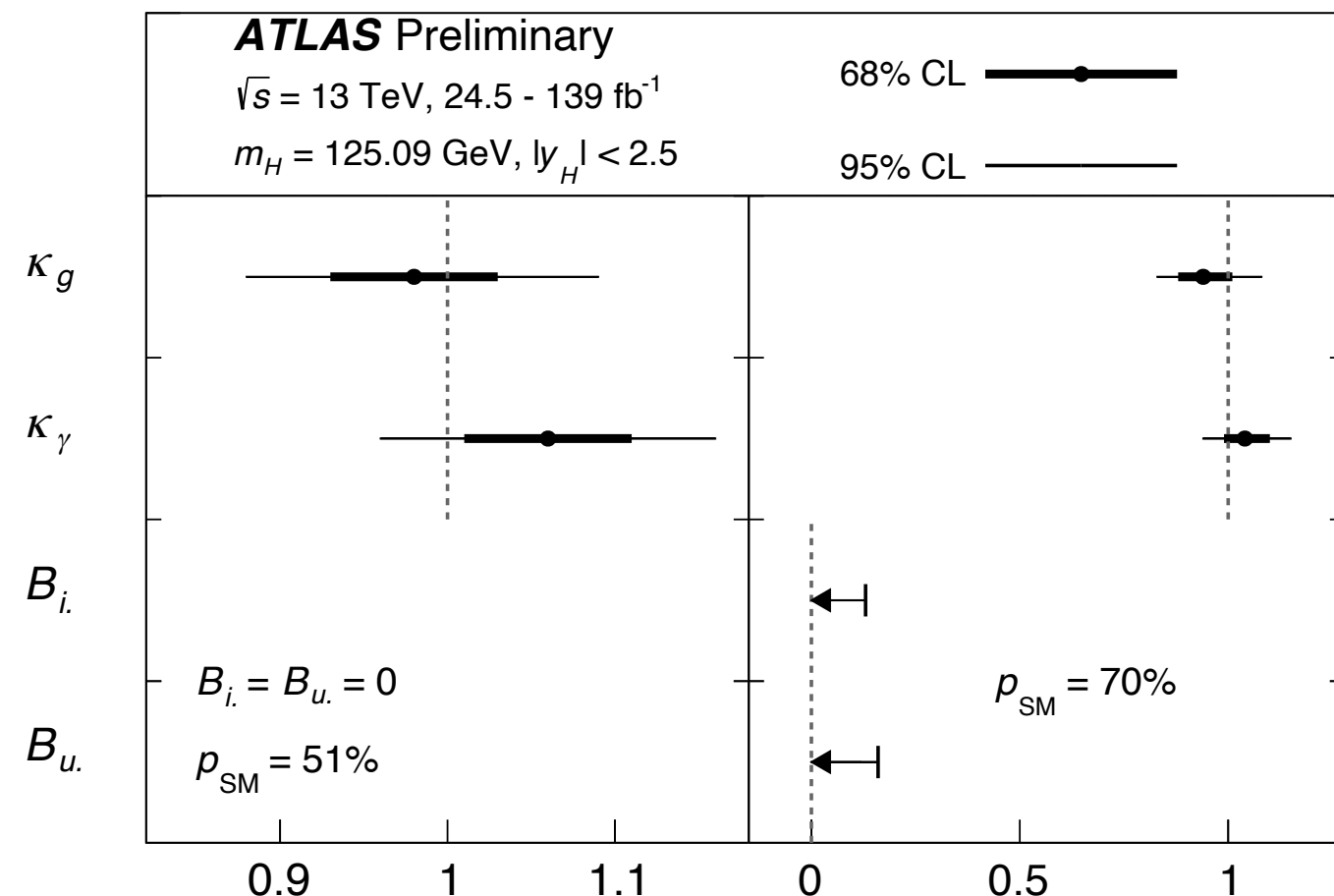
- Coupling strength modifiers

$$\kappa_j^2 = \frac{\sigma_j}{\sigma_j^{\text{SM}}}$$

$$\kappa_j^2 = \frac{\Gamma_j}{\Gamma_j^{\text{SM}}}$$

- BSM contributions in loops and decays

- ▶  $k_g$  and  $k_\gamma$  measured with all other modifiers fixed to SM value.
- ▶ Both hypotheses of invisible decays ( $B_{\text{inv}}$  and  $B_{\text{und}}$  floating, with  $k_F=k_V=1$ ) and no invisible decays ( $B_{\text{inv}}=B_{\text{und}}=0$ ).



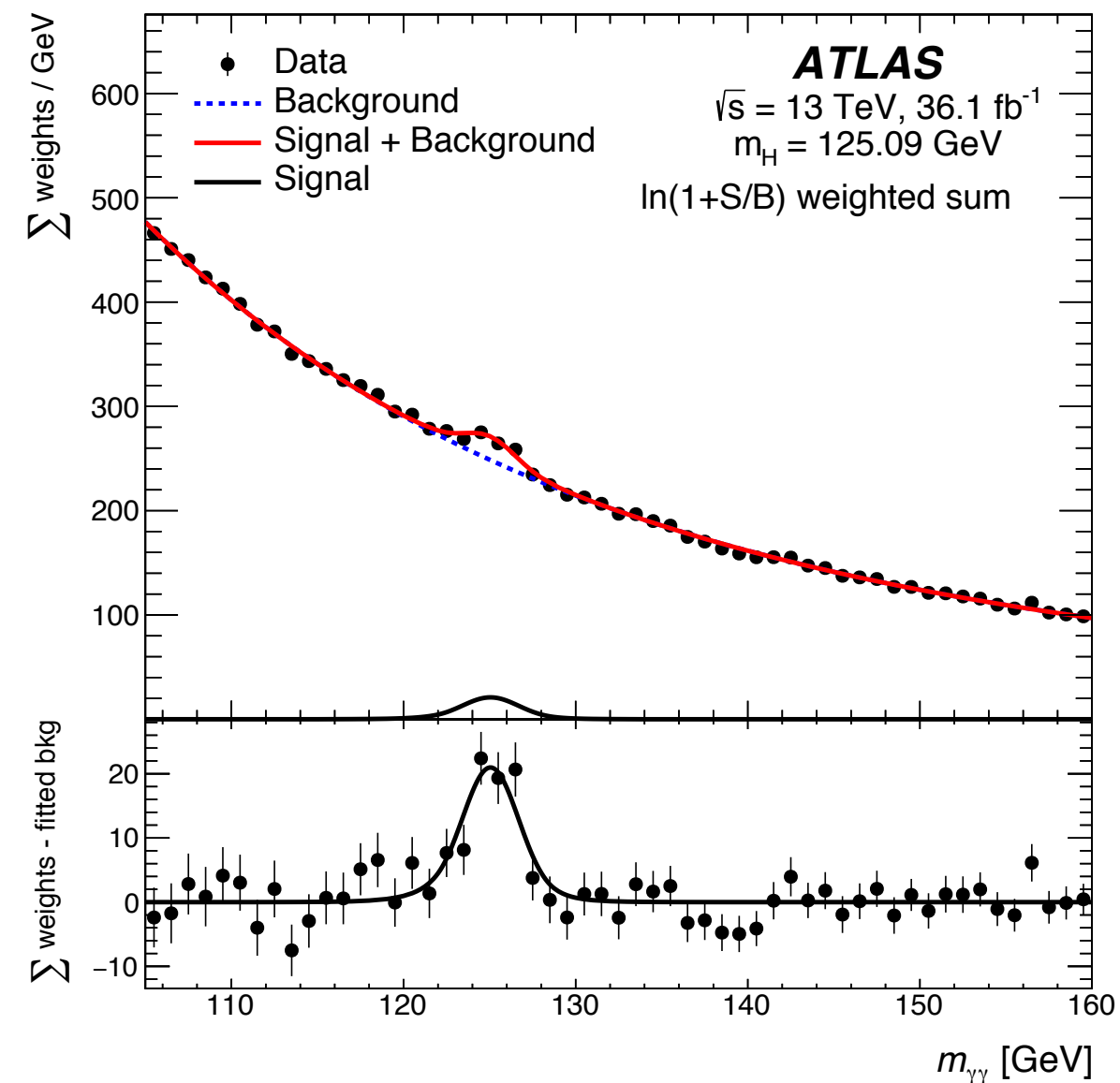


## ● Diphoton event selection

- ▶ At least two photon with  $E_T > 25$  GeV
- ▶ Highest  $E_T$  pair forms candidate.
- ▶ Vertex identification with Neural Network
  - ◆ Vertex within 0.3 mm for 79% of ggH events.

## ● Background estimation

- ▶ Entirely estimated from data
- ▶ Prompt photons: maximum likelihood fit to  $m_{\gamma\gamma}$  spectrum
- ▶ Jets misidentified as photons: from control sample





- $4\ell$ : isolate signal under the Higgs resonant peak ( $115 < m_{4\ell} < 130$ ).
- $\gamma\gamma$  cross section extracted from resonant peak over the  $\gamma\gamma$  continuum.
- Higgs boson  $p_{T,4\ell(\gamma\gamma)}$  and rapidity ( $y_{4\ell(\gamma\gamma)}$ ) probe.
  - ▶  $p_{T,4\ell(\gamma\gamma)}$ : Lagrangian structure of  $H$  interactions, Yukawa couplings
  - ▶  $y_{4\ell(\gamma\gamma)}$ : Sensitivity to proton's parton density functions.

